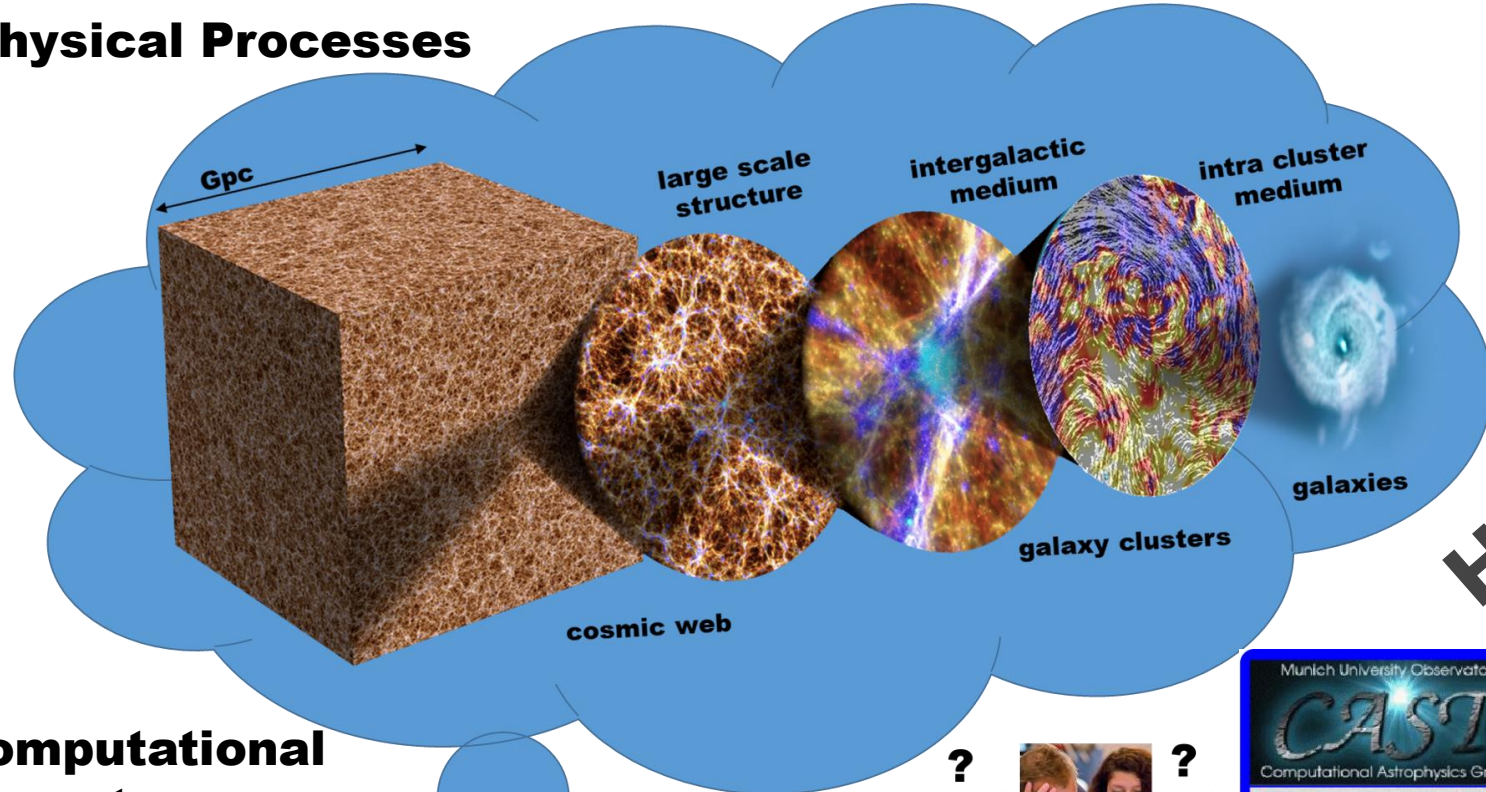


Physical Processes

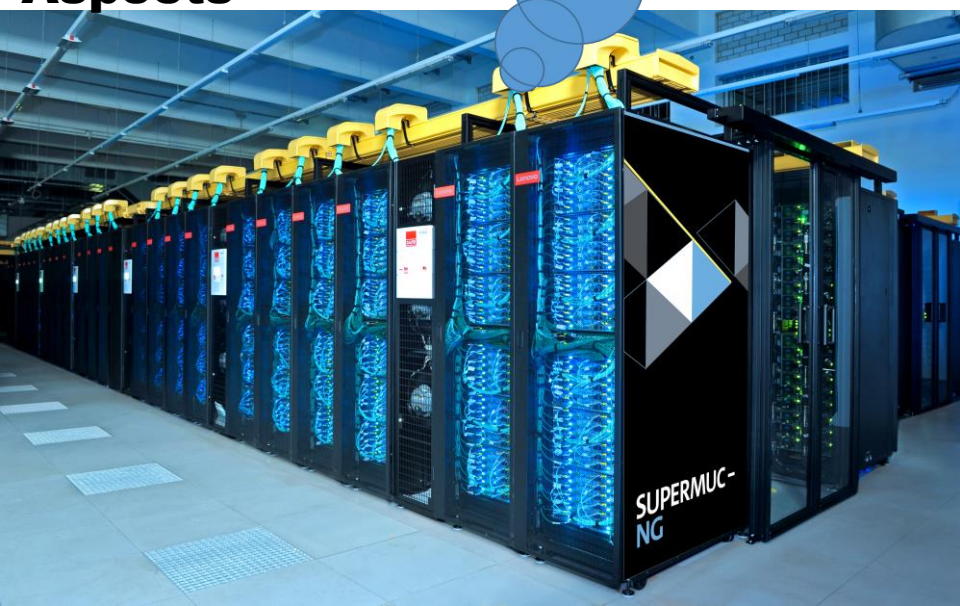


HPC Challenges in Astrophysics

CAST@USM



Computational Aspects



Astro Quiz



Historical Aspects

Munich University Observatory
CAST
Computational Astrophysics Group

Research:

- Star Formation / ISM
- ISM / Molecular Clouds
- Galactic Dynamics
- Galaxy Formation and Evolution
- Active Galactic Nuclei
- Cosmology
- Galaxy Clusters
- Cosmic Magnetism
- Planet and Star Formation

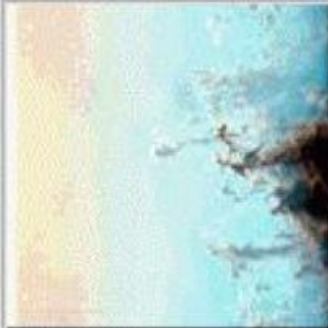
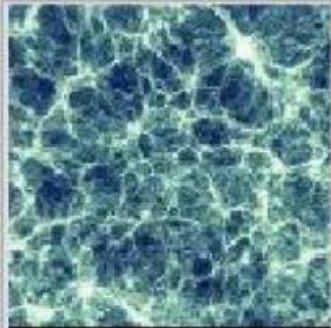
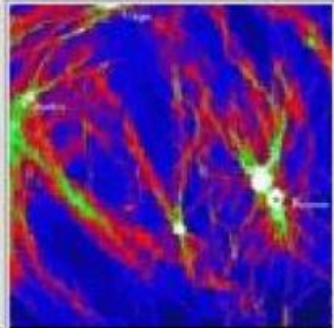
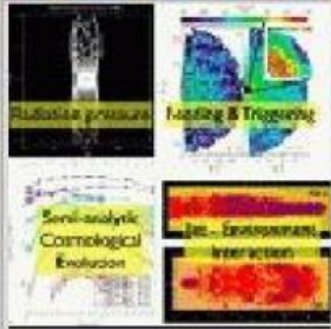
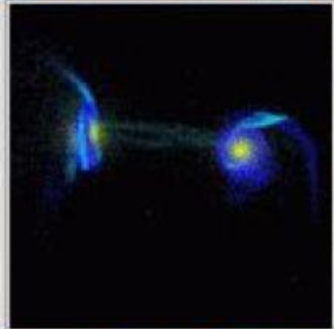
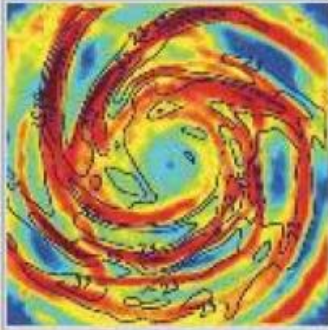
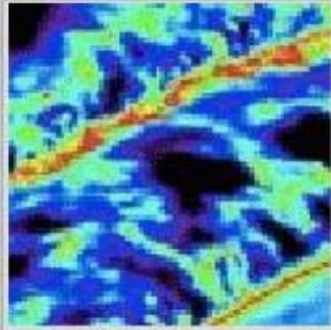
www.usm.uni-muenchen.de/CAST

The Computational Astrophysics Group

Munich University Observatory

CAST

Computational Astrophysics Group



Research:

Star Formation / ISM

ISM / Molecular Clouds

Galactic Dynamics

Galaxy Formation and Evolution

Active Galactic Nuclei

Cosmology

Galaxy Clusters

Cosmic Magnetism

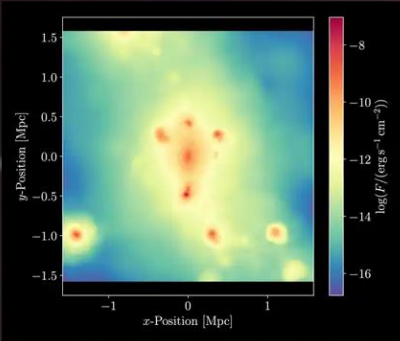
Planet and Star Formation

www.usm.uni-muenchen.de/CAST

Some exemplary past Master Projects:

I: Analyzing Simulations

Axion Quark Nuggets – Testing a Novel Dark Matter Model using the Cosmological Simulation ‘SLOW’ and Inferring its Observational Detectability



Here, we analyze a novel, promising Dark Matter candidate called Axion Quark Nuggets (AQNs) in the context of traceable electromagnetic signatures in galaxy clusters after interactions with baryonic matter. We use a cosmological simulation called "Simulation of the LOcal Web (SLOW)", which simulates the local universe and therefore contains galaxy clusters that resemble digital twins of their real counterparts. We propose that the Fornax and Virgo clusters are the most promising candidates hosting detectable AQN signatures.

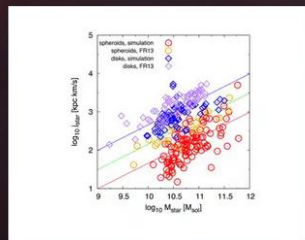


Julian Sommer



Adelheid Teklu

Angular Momentum Distribution in Galactic Halos

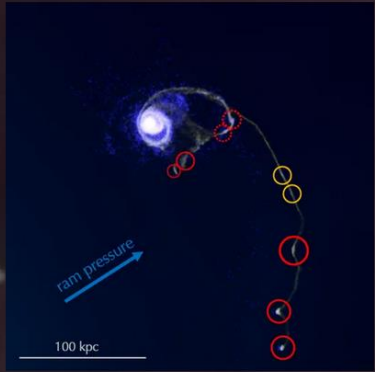


The evolution and distribution of the angular momentum (AM) of dark matter (DM) halos have been discussed in several studies over the past decades. To understand the connection between the AM of the DM halo and its galaxy, we extract in total more than 2,000 individual galaxies from the uhr run of Box4 of the Magneticum Pathfinder simulations at different redshifts. In these simulations we are able to split the galaxies into disk and spheroidal systems. Our simulations reproduce well the observed scaling relations between the stellar mass and the stellar specific angular momentum. We find that disk galaxies preferentially reside in halos where the AM vector of the DM in the center is better aligned with the AM vector of the whole DM halo. The distribution of the spin parameter λ also shows a separation of disk and spheroidal galaxies.

Some exemplary past Master Projects:

II: Performing Simulations

Collecting Shells in the Tides: Formation of Dwarf Galaxies From Mergers Inside Galaxy Clusters



Although galaxy interactions are thought to provide a possible cradle for low-mass objects, environmental influence could still be a crucial driver for their formation and evolution. This hypothesis is stimulated by observations of star forming knots inside extended tidal tails of ongoing galaxy mergers in clusters. Such an arrangement prompts the intriguing question as to whether cluster environments could support tidal dwarf formation. I test this evolutionary channel by performing hydrodynamical simulations of galaxy mergers inside clusters. I demonstrate that environments indeed are capable of stripping tidal dwarf galaxies. Exposed to ram pressure, these gas dominated objects exhibit high star formation rates, while also losing gas at the high-mass end. With



Anna Ivleva

Simulated Galaxy Interactions In Cosmological and Idealized Environments



Most of all galaxies are not field galaxies but are accompanied by other galaxies in groups or clusters. A special case of these galaxy gatherings are compact galaxy groups, which are extremely dense accumulations of galaxies in which galaxy interactions occur very frequently. These interactions have a huge impact on the corresponding galaxies and are a fundamental part of galaxy evolution. The information about the merging events are stored in the outer stellar halo of a galaxy or in the intra group light (IGL) respectively. In this thesis cosmological zoom simulations of compact groups as well as a parameter study using high-resolution isolated galaxy merger simulations covering a large bandwidth of orbit parameters and mass-

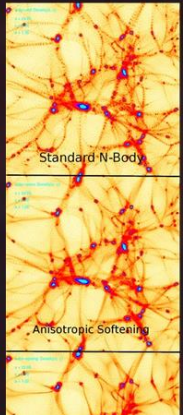


Geray Karademir

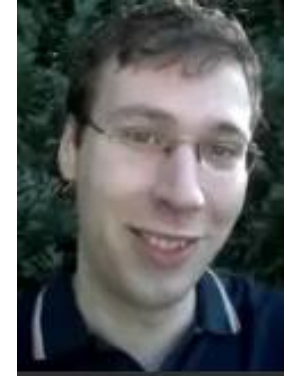
Some exemplary past Master Projects:

III: Developing Simulations

Modelling Warm Dark Matter in Cosmological Simulations



The standard Λ CDM model of cosmology postulates that the formation of structures in the universe is driven by a largely unknown component of dark matter. It is one of the most important projects of modern physics to find out what dark matter is. Cosmological simulations are an important tool to predict the effects of different dark matter models, and to constrain properties of dark matter by the comparison with observations of our universe. We attempt to simulate different warm dark matter scenarios in cosmological “zoom-in” simulations (which allow the investigation of a single object in high resolution), and cosmological boxes (which exhibit low resolution, but good statistics). However, N-Body

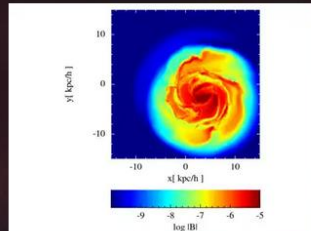


Jens Stücker



Eirini Batziou

The Interplay of Magnetic Fields and Star Formation Processes Using SPMHD Simulations

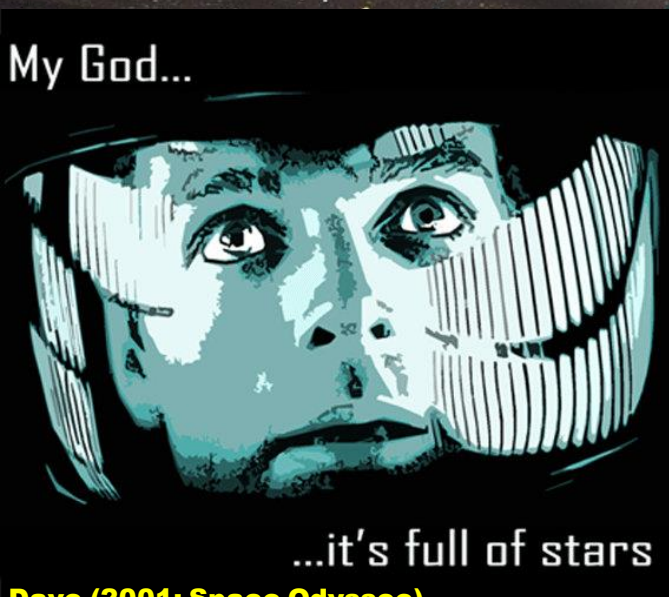


Cosmological simulations deal with very large structures and there is not enough resolution to couple all the dynamical range of processes taking place, so it is very important to model consistently phenomena that occur in unresolved scales. One example of subresolution model is proposed by [Springel and Hernquist, 2003] in which the star formation and the supernova feedback can be modeled by a multiphase structure of the Interstellar Medium (ISM). In their approach, the ISM consists of cold and hot gas and includes radiative heating, cooling, star formation and feedback from supernova. This model predicts a self-regulated star formation quiescent mode for the gaseous part of disk galaxies and has only one free parameter: the overall time-scale for star formation. First improvement of this model is to express the star formation rate in terms of external pressure, which allows to include further physical processes such as

HPC Challenges in Astrophysics

I) The Universe

What is the universe?



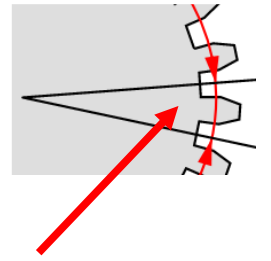
Dave (2001: Space Odyssee)

Bild: APOD 23. Aug 2010, Alex Cherney, Terrastro

Astro Quiz !



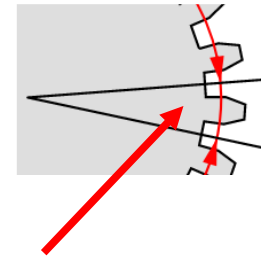
I) Warmup



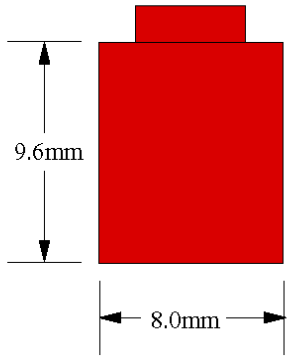
How big is the gear spacing for this LEGO gear ?



I) Warmup



Note 6:5 ratio of unit height to unit length.

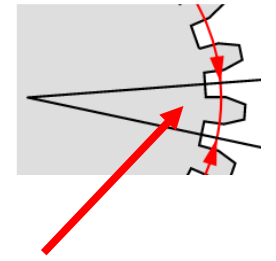


Full Height	One-Third	Horizontal	
Units	Units	Units	
1	2	2	
3	1	4	
5		6	
6	2	8	
8	1	10	

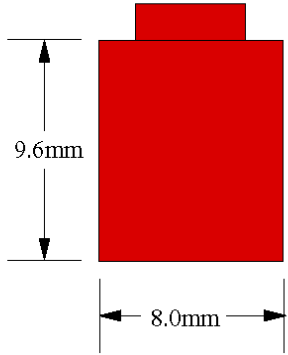
How big is the gear spacing for this LEGO gear ?



I) Warmup



Note 6:5 ratio of unit height to unit length.



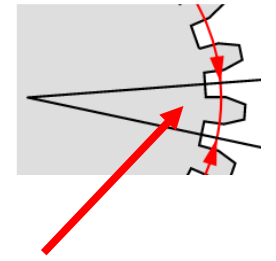
Full Height	One-Third	Horizontal	
Units	Units	Units	
1	2	2	
3	1	4	
5		6	
6	2	8	
8	1	10	

How big is the gear spacing for this LEGO gear ?

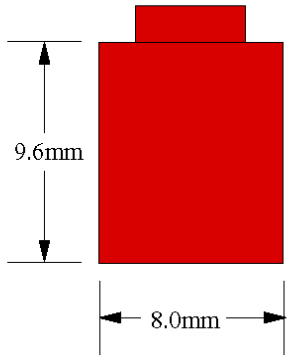
Basic gears: T8, T24, T40



I) Warmup

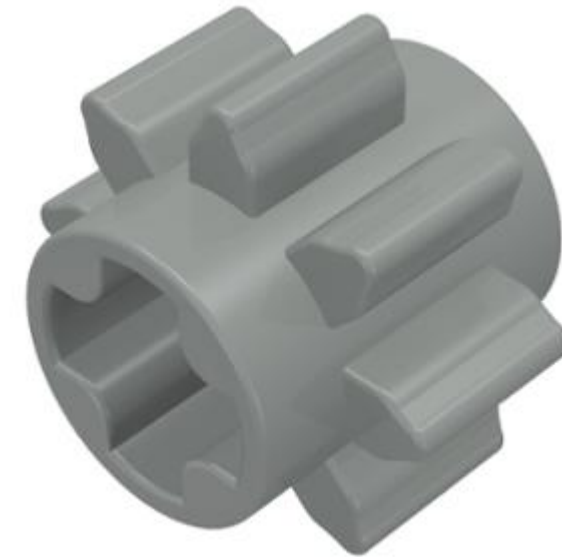


Note 6:5 ratio of unit height to unit length.

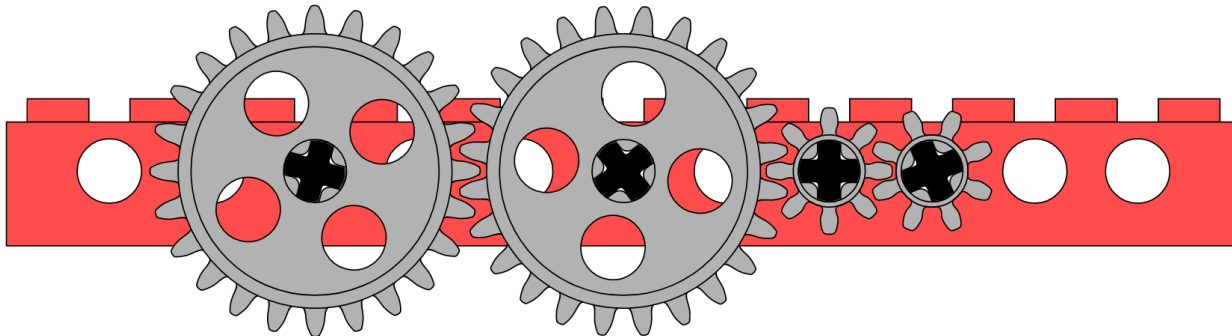


Full Height	One-Third	Horizontal
Units	Units	Units
1	2	2
3	1	4
5		6
6	2	8
8	1	10

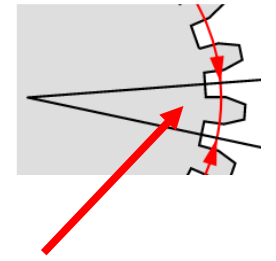
How big is the gear spacing for this LEGO gear ?



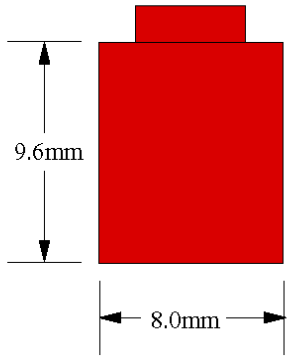
Basic gears: T8, T24, T40



I) Warmup



Note 6:5 ratio of unit height to unit length.



Full Height	One-Third	Horizontal
Units	Units	Units
1	2	2
3	1	4
5		6
6	2	8
8	1	10

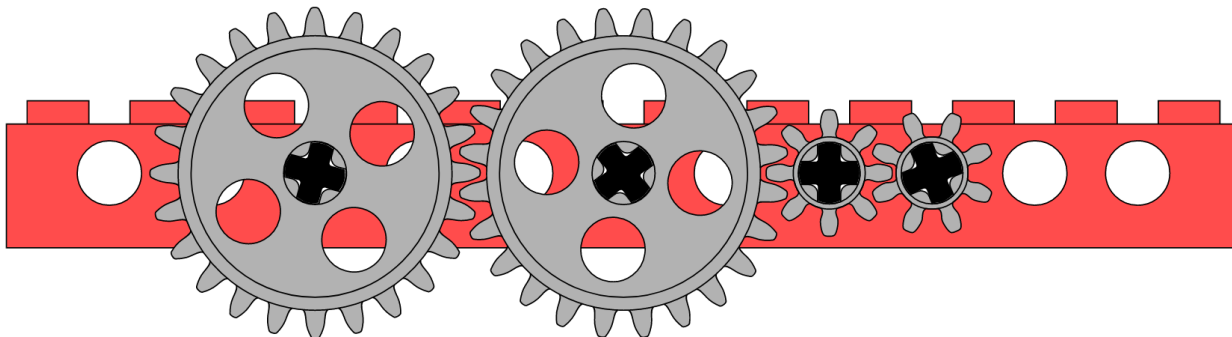
How big is the gear spacing for this LEGO gear ?



N = 8 24 40

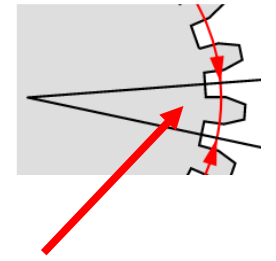
Basic gears: T8, T24, T40

r = 0.5 1.5 2.5 x 8mm

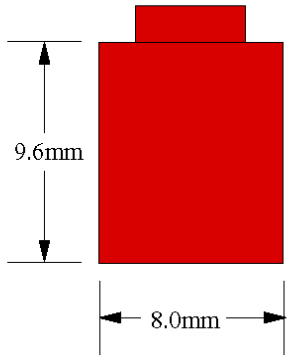


$$S = \frac{2r\pi}{N} = ???$$

I) Warmup



Note 6:5 ratio of unit height to unit length.



Full Height	One-Third	Horizontal
Units	Units	Units
1	2	2
3	1	4
5		6
6	2	8
8	1	10

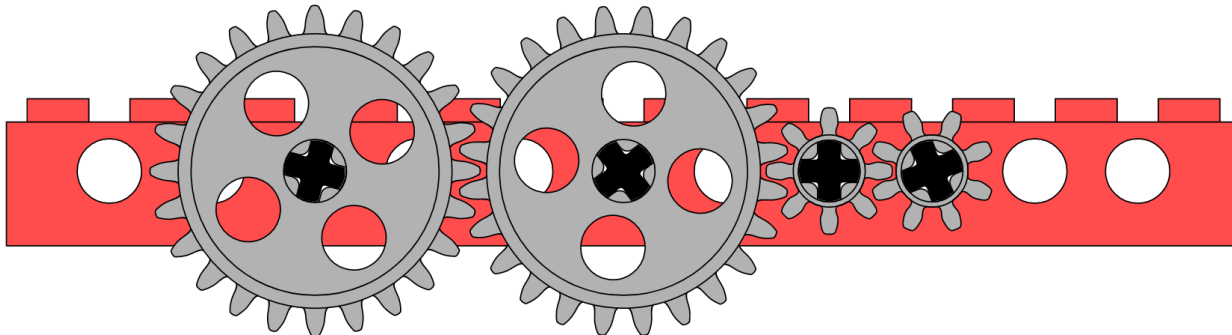
How big is the gear spacing for this LEGO gear ?



N = 8 24 40

Basic gears: T8, T24, T40

r = 0.5 1.5 2.5 x 8mm



$$S = \frac{2r\pi}{N} = \pi !!!$$

II) The search

What did these people searched there around 1900 ?



Jones, 2017



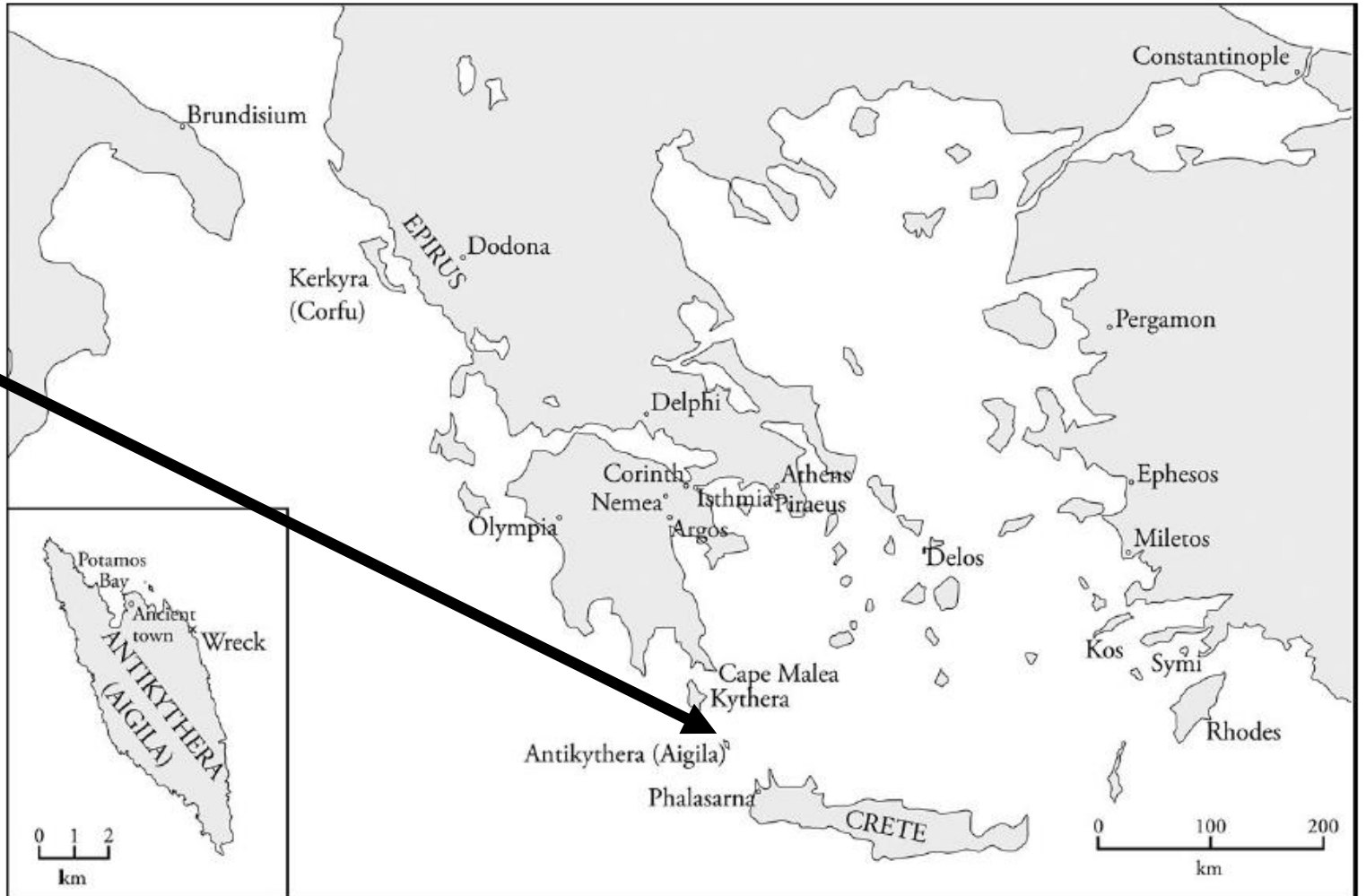
II) The search

What did these people searched there around 1900 ?

Jones, 2017



Sponges !

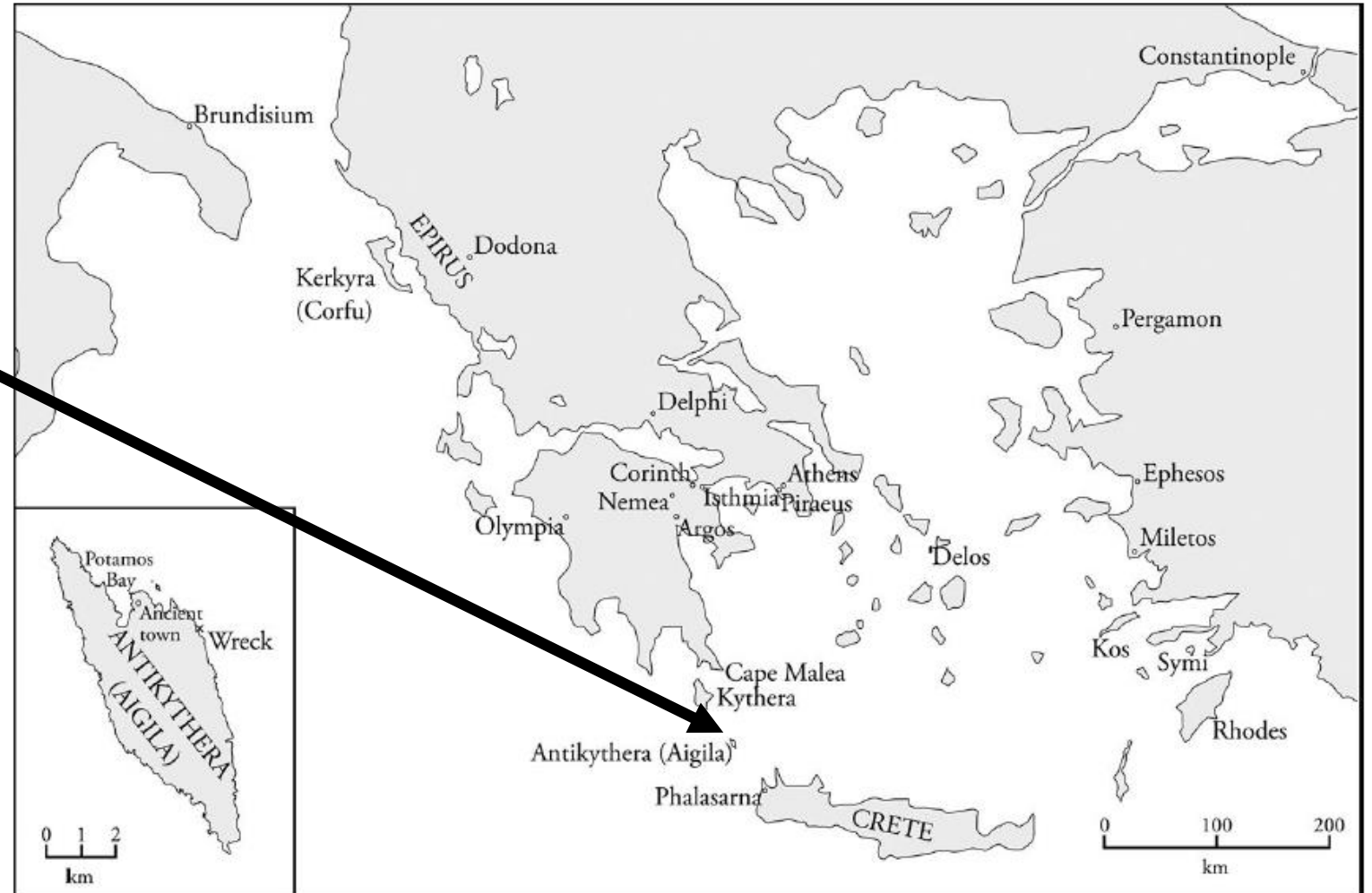


III) The discovery

What did these people found instead ?



Jones, 2017



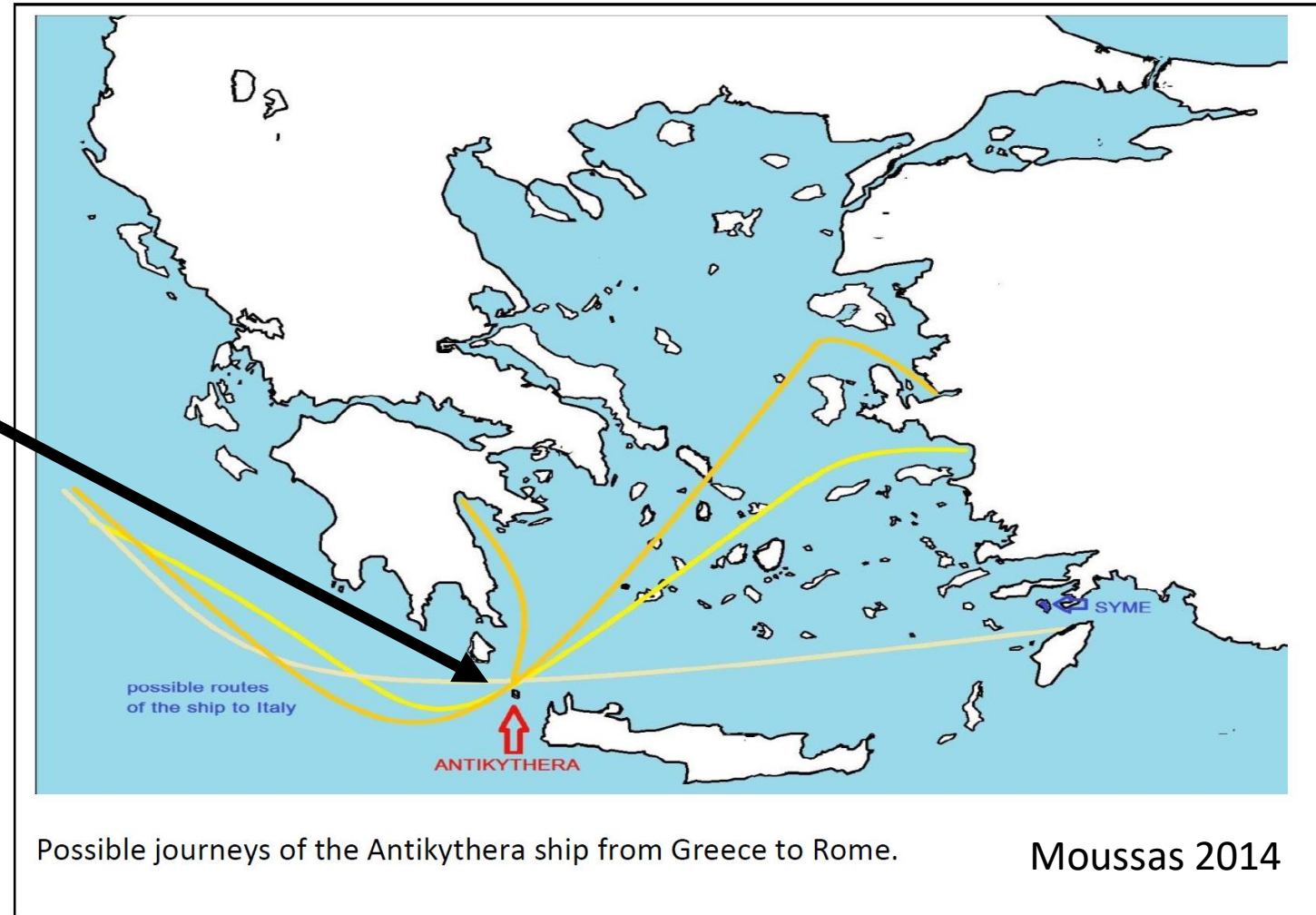
III) The discovery

What did these people found instead ?



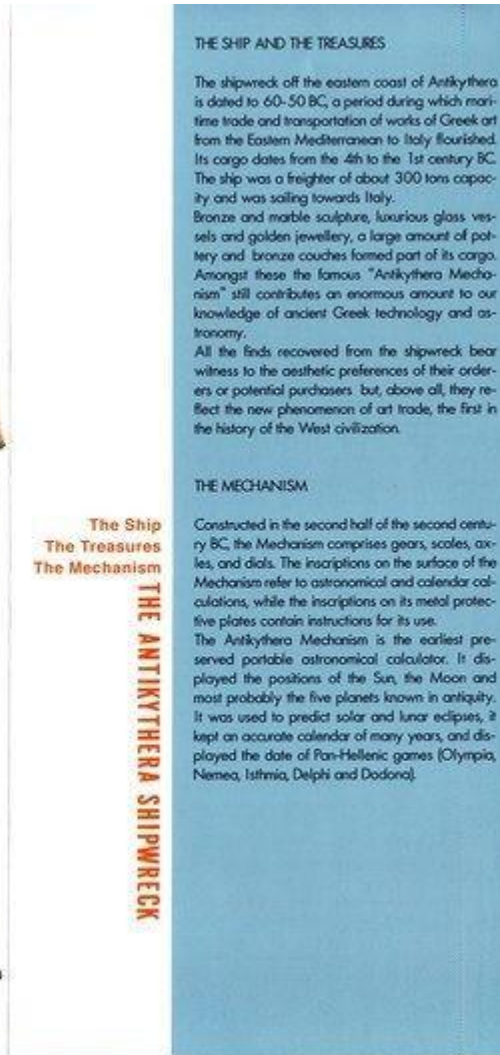
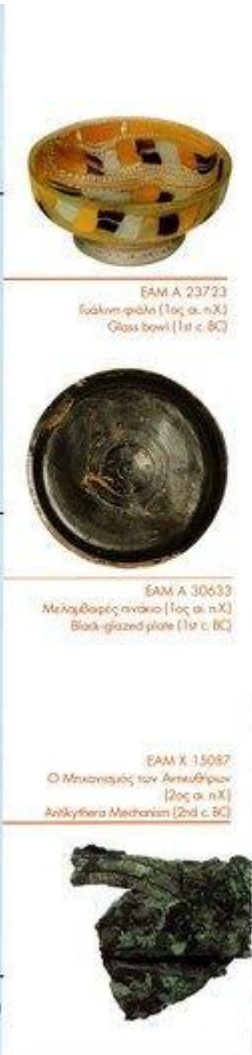
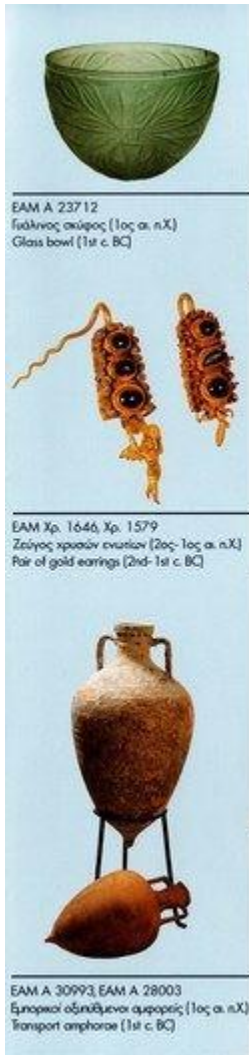
Jones, 2017

**Roman ship wreck
from 1st century BC**



III) The real discovery

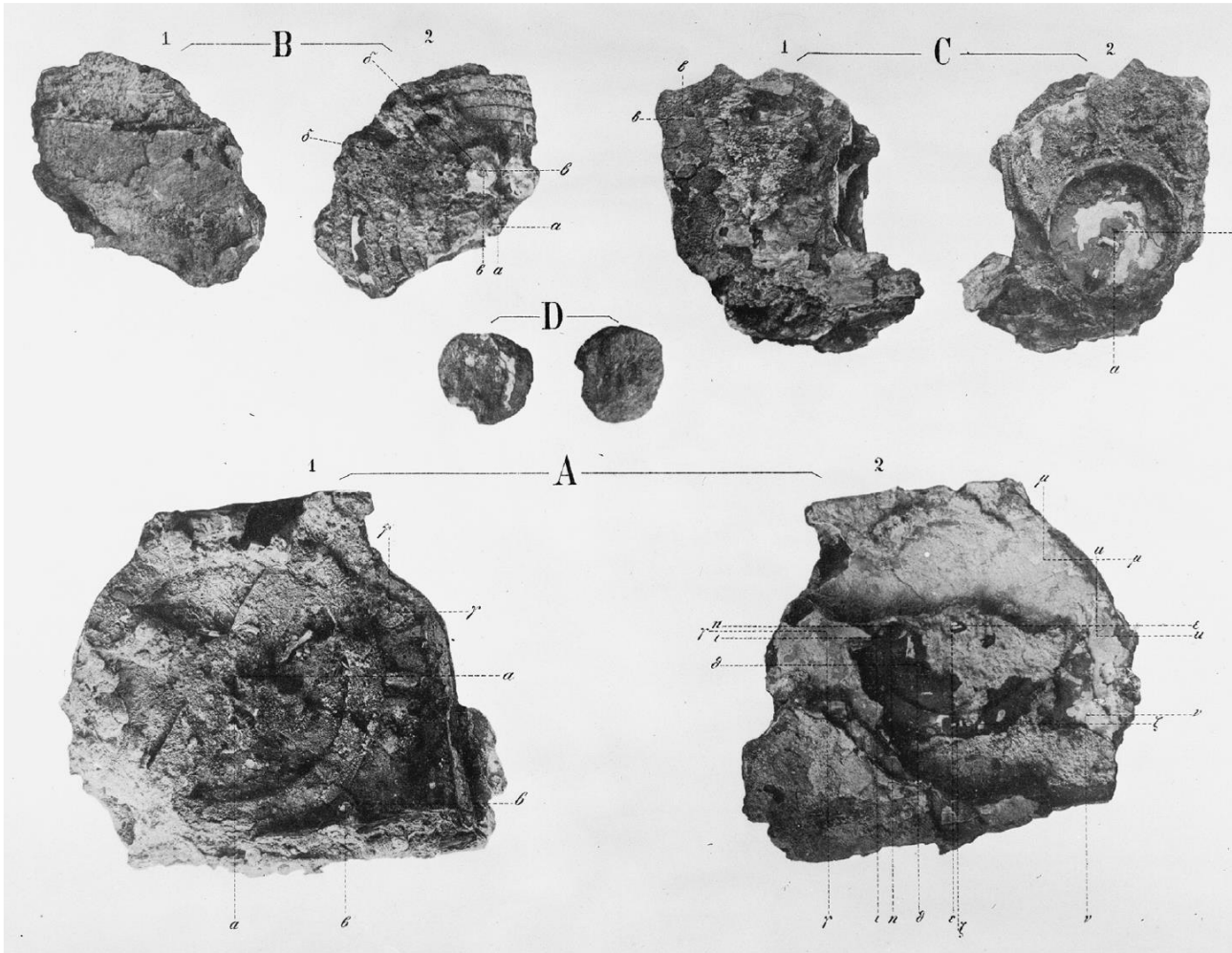
What was the real discovery ?



- ca. 100 marble statues
- several bronze statues
- amphorae and ceramics
- silver coins
- fragmented lump corroded bronze
- sofas with bronze ornaments
- bronze lyre
- few bronze statuettes
- golden earrings

III) The real discovery

What was the real discovery ?



- ca. 100 marble statues
- several bronze statues
- amphorae and ceramics
- silver coins
- **fragmented lump corroded bronze**
- sofas with bronze ornaments
- bronze lyre
- few bronze statuettes
- golden earrings

IV) Unveiling

What was discovery by X-Ray scans of the fragments?

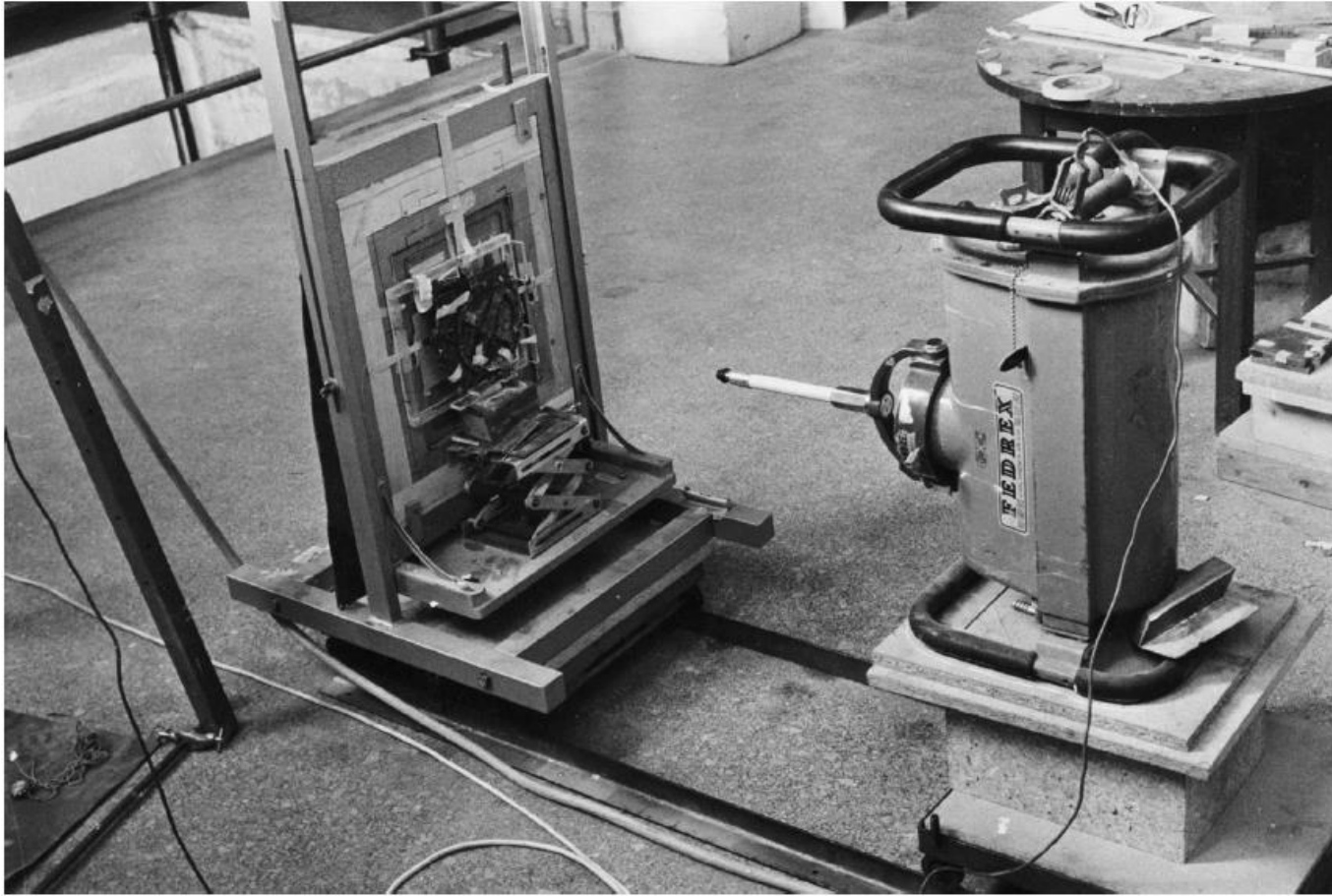


FIG. 2.7. Karakalos's 1971 X-ray setup with Fragment A. (Adler Planetarium, © Derek de Solla Price heirs) Jones, 2017



Figure 2. X-Tek's Bladerunner 450kV microfocus X-ray CT system

2005

Ramsey, 2007

IV) Unveiling

What was discovery by X-Ray scans of the fragments?

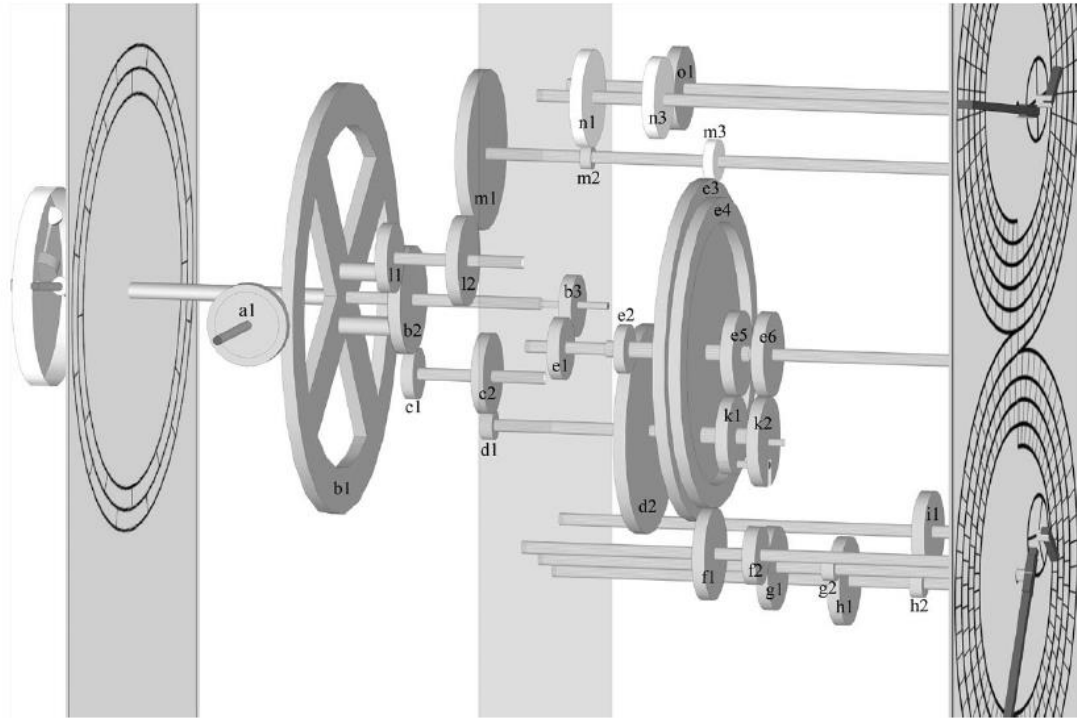


FIG. 8.8. Exploded view of the gearwork driving the solar, lunar, and calendrical outputs of the Mechanism. The base plate is represented by the transparent rectangle in the middle. Gears shown in dark gray are at least partly extant, while those in pale gray are restored completions of the trains; the conjectured Callippic dial and the four conjectural gears that would have driven it are omitted. (image by and copyright of M. G. Edmunds)

- **39 (or 42) gears (29 identifiable)**
- **19 (or 21) shafts and axis**
- **7 (or 8) pointers**
- **instruction manual**
- **3 deals**
- **Thousands of tiny text characters**

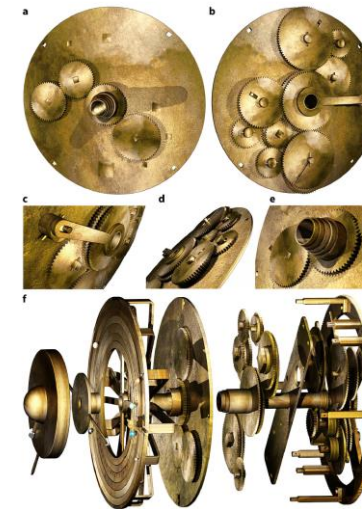
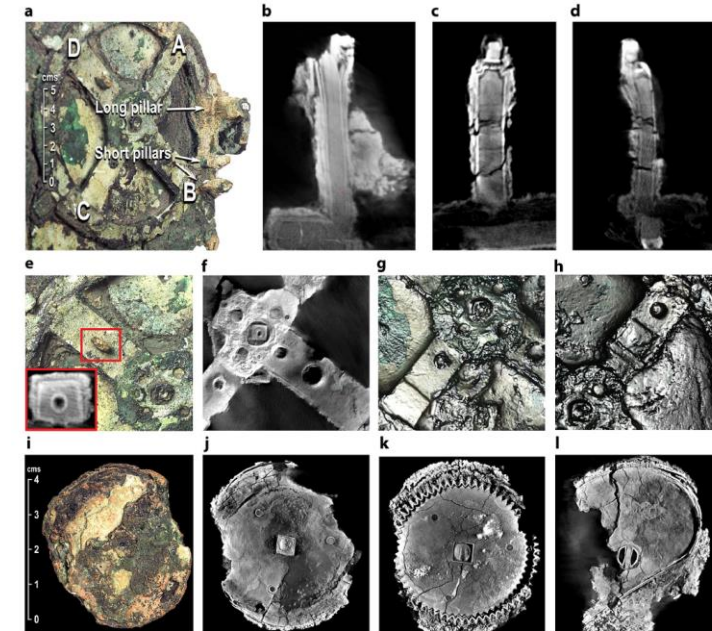


Figure 6. True Sun, Superior Planets and exploded Cosmos gearing. (a) The gears at the front of the CP. Center (c) Fixed gear 26, riveted to a subsidiary plate (not seen). Bottom right in (a) 64, shared between Mars and Jupiter. Top left in (a) 52, shared between the true Sun and Saturn. Left in (a) 56 is the epicyclic gear for the true Sun gearing. (b) The mechanisms seen from the back of the CP. Clockwise from the top: Saturn, true Sun, Mars, Jupiter. (c) Close-up of true Sun mechanism. (d) Close-up of gears showing interlaced layers. (e) Close-up of output tubes. (f) Exploded model of Cosmos gearing. From right to left: h1, mean Sun, Solis, Mercury, Venus, true Sun and superior planets gearing, CP and shared gears, Ring Display, Dragon Hand, Moon position and phase mechanism.



V) The display

What did the Antikythera Mechanism show?

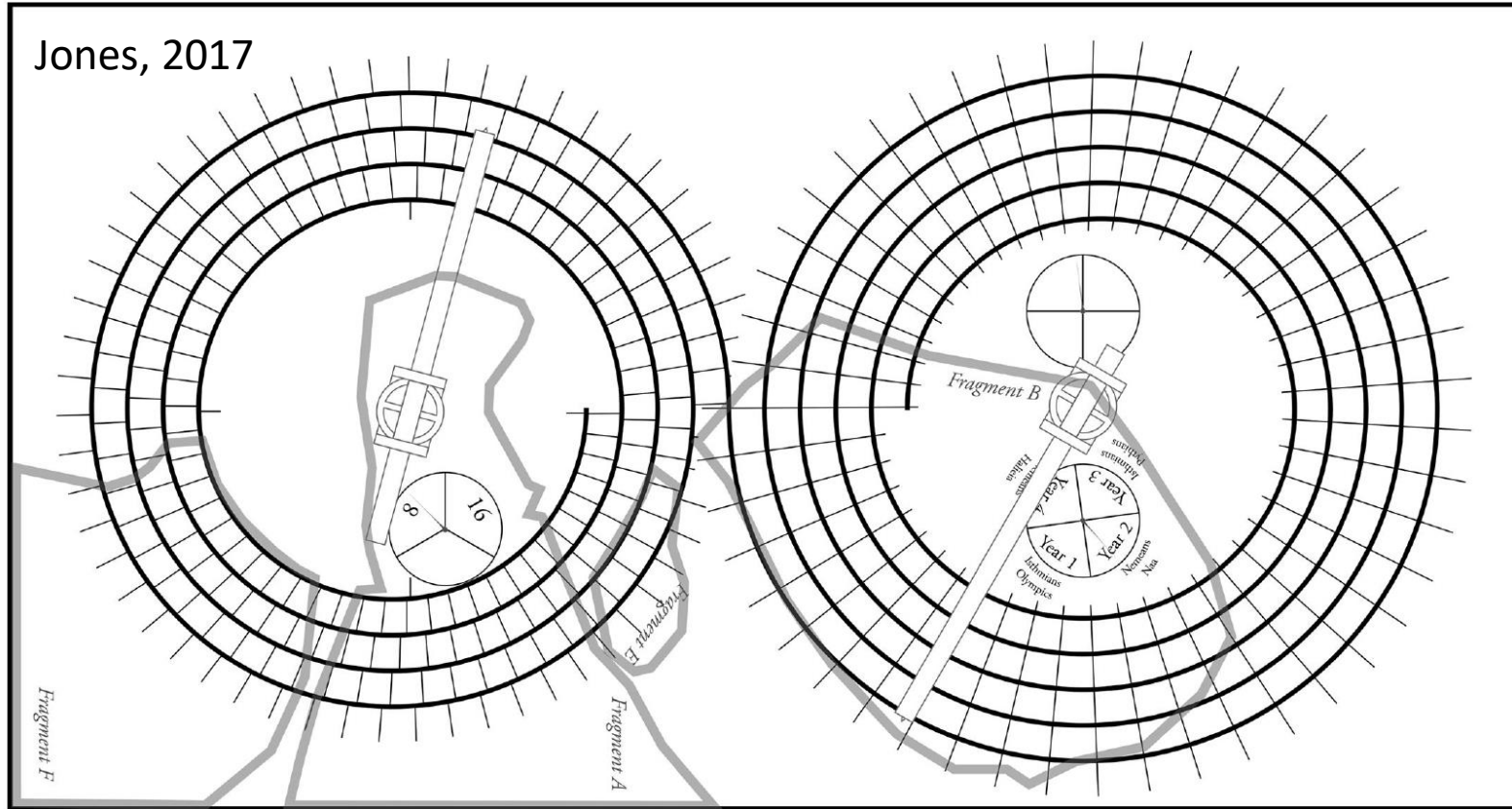
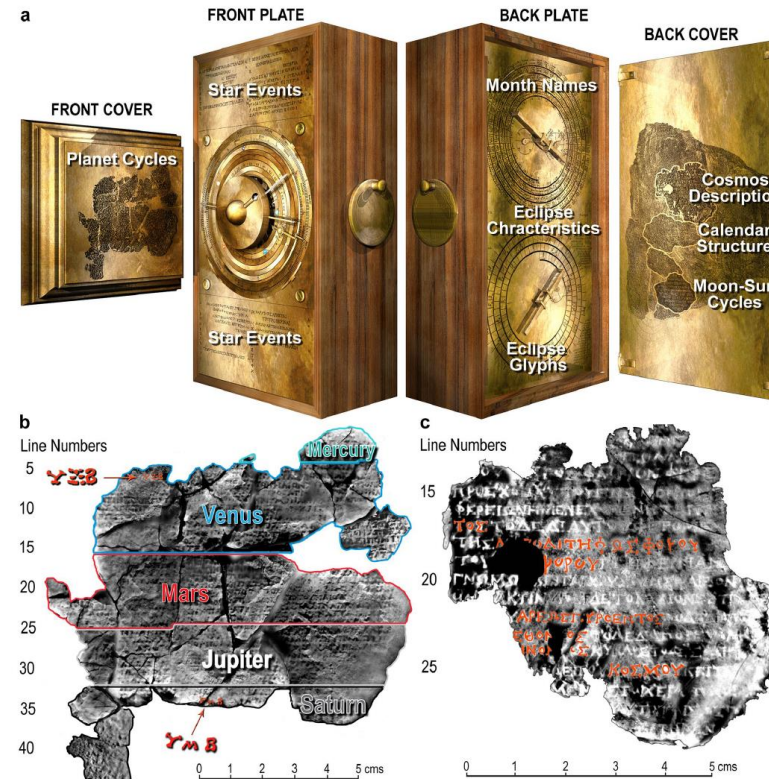
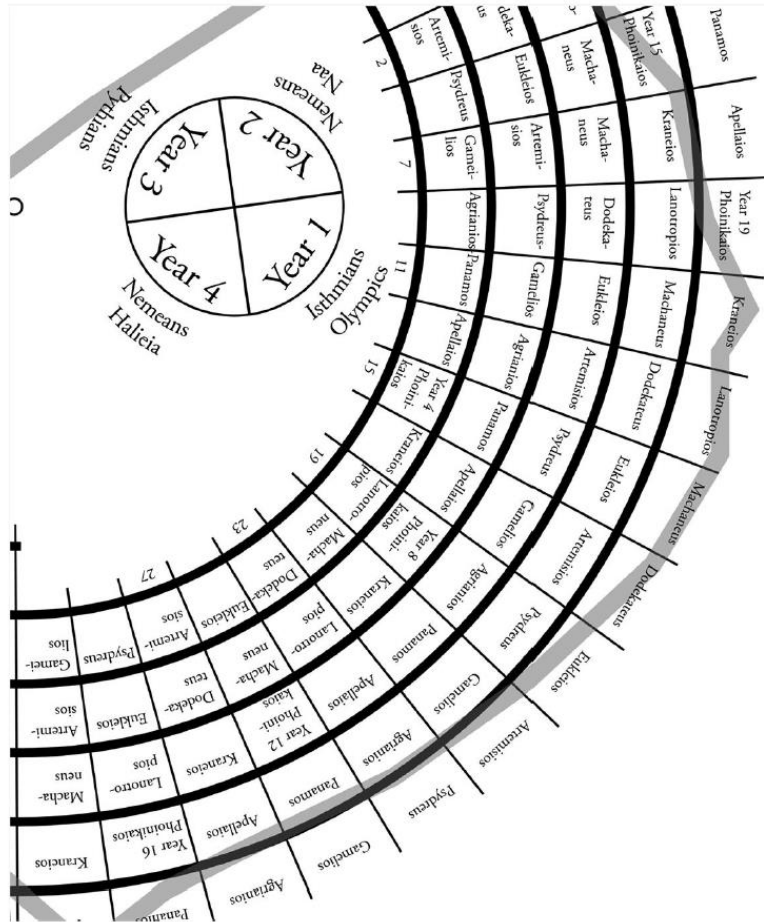


FIG. 3.1. Dial layout of the back plate with its pointers, omitting the inscriptions of the spiral scales, and with the subsidiary dial inscriptions in translation. *Top*, the spiral Metonic dial enclosing the Callippic dial on the left and the Games dial on the right. *Bottom*, the spiral Saros dial enclosing the Exeligmos dial. Gray outlines roughly indicate preserved portions in Fragments B, E, A, and F.

V) The display

What did the Antikythera Mechanism show?



- Position of the Sun
- Position of Moon (incl. phase)
- Predicts solar/lunar eclipse
- Dates of Games and Festivities
- Planetarium

As complex as clocks from 14th century!

Gears with up to 223 teeth!

Up to 8 overlapping axis/shafts!

Figure 1. Inscriptions on the Antikythera mechanism. (a) FRONT COVER: Planet cycles^{8,12}, framed by moulding from Fragment 3 (Supplementary Fig. S5). FRONT PLATE: *Paraegma*^{12,25}, above and below the Cosmos Display, indexed to the Zodiac Dial. BACK PLATE: Month names on the Metonic Calendar^{4,8}, Eclipse characteristics, round Metonic Calendar and Saros Eclipse Prediction Dials^{7,8}—indexed to the latter. Eclipse glyphs indexed to the Saros Dial⁸. BACK COVER: *User Manual*, including Cosmos description¹³ (Supplementary Discussion S2), Calendar Structure⁸ and Moon-Sun Cycles¹². (b) Front Cover Inscription (FCI): composite X-ray CT from Fragments G, 26 and 29 and other small fragments^{8,12}. The FCI describes synodic cycles of the planets and is divided into regions for each planet in the CCO (Supplementary Discussion S2). The numbers ΨEB (462) in the Venus section and ΨMB (442) in the Saturn section are highlighted¹² (Supplementary Fig. S4). (c) Back Cover Inscription (BCI)¹³ (Supplementary Discussion S2): composite X-ray CT from Fragments A and B. A *User Manual*: the upper part is a description of the front Cosmos Display⁸ with planets in the CCO; in red are the planet names as well as the word ΚΟΣΜΟΥ—“of the Cosmos”.

FIG. 3.3. Detail of the Metonic dial with translated calendar inscriptions.

Jones, 2017

Freth 2021, Science Reports, Nature

Side node: approximation to an approximation:

Freth 2021, Science Reports, Nature

a: Combinations of Period Relations

VENUS (5, 8) + 2 x (720, 1151) = (1445, 2310) = 5 x (289, 462) \equiv (289, 462)
 SATURN -1 x (29, 30) + 8 x (57, 59) = (427, 442)
 3 x (57, 59) + (256, 265) = (427, 442)

b: Constrained Parmenides Process

VENUS				SATURN			
Under	New	Over		Under	New	Over	
(5, 8)	(725, 1159)	(720, 1151)		(57, 59)	(313, 324)	(256, 265)	
(725, 1159)	(1445, 2310)	(720, 1151)		(57, 59)	(370, 383)	(313, 324)	
	\equiv (289, 462)			(57, 59)	(427, 442)	(370, 383)	

c: Unconstrained Parmenides Process

Iteration 1: (p + r, q + s)
 Iteration 2: (2p + r, 2q + s), (p + 2r, q + 2s)
 Iteration 3: (3p + r, 3q + s), (p + 3r, q + 3s)
 Iteration 4: (4p + r, 4q + s), (3p + 2r, 3q + 2s), (2p + 3r, 2q + 3s), (p + 4r, q + 4s)

d: Unconstrained Parmenides Process

MERCURY				VENUS			
p	q	r	s	p	q	r	s
145	46	684	217	5	8	720	1151
p+r	q+s			p+r	q+s		
829	263			725	1159		
2p+r	2q+s	p+2r	q+2s	2p+r	2q+s	p+2r	q+2s
974	309	1513	480	730	1167	1445	2310
3p+r	3q+s	p+3r	q+3s	3p+r	3q+s	p+3r	q+3s
1119	355	2197	697	735	1175	2165	3461

MARS				JUPITER				SATURN			
p	q	r	s	p	q	r	s	p	q	r	s
22	47	37	79	76	83	87	95	57	59	256	265
p+r	q+s			p+r	q+s			p+r	q+s		
59	126			163	178			313	324		
2p+r	2q+s	p+2r	q+2s	2p+r	2q+s	p+2r	q+2s	2p+r	2q+s	p+2r	q+2s
81	173	96	205	239	261	250	273	370	383	569	589
3p+r	3q+s	p+3r	q+3s	3p+r	3q+s	p+3r	q+3s	3p+r	3q+s	p+3r	q+3s
103	220	133	284	315	344	337	368	427	442	825	854

e: Period Relations for the Antikythera Mechanism

Planet	Syn.	Years	Factors	Factors	Error ϵ_s/y	Error ϵ_r^2/syn
MERCURY	1513	480	17 x 89	2 ⁵ x 3 x 5	-0.005022	-0.001593
VENUS	289	462	17 ²	2 x 3 x 7 x 11	0.008576	0.013710
MARS	133	284	7 x 19	2 ² x 71	0.003089	0.006596
JUPITER	315	344	3 ² x 5 x 7	2 ² x 43	0.000802	0.000876
SATURN	427	442	7 x 61	2 x 13 x 17	0.004208	0.004509

Figure 2. Finding period relations. Blue numbers refer to synodic cycles; red numbers refer to years. All the seed periods for these processes are known from Babylonian astronomy (Supplementary Tables S5, S6). (a) Linear combinations of Babylonian period relations, which give those for Venus and Saturn from the FCI. (b) Period relations generated by a conventional Parmenides Process, which also give those for Venus and Saturn from the FCI. (c) Iterations of an Unconstrained Parmenides Process. (2p+2r, 2q+2s) is omitted from Iteration 3 because it is the same as 2 x (p+r, q+s). (d) Three iterations of the Unconstrained Parmenides Process. The pairs in colour are those that are factorizable with prime factors < 100. The grey-shaded periods are those that are known from the FCI. Note that for Venus: (1445, 2310) \equiv (289, 462) and (735, 1175) \equiv (147, 235). The same table with errors is shown in Supplementary Table S5. (e) Periods derived from the Unconstrained Parmenides Process for our model of the Antikythera Mechanism and their errors, using our three criteria of accuracy, factorizability and economy. Except for the periods for Venus and Saturn, all the final periods were already known in Babylonian astronomy. The error parameters are defined in Supplementary Discussion S3.

A dialogue of Plato (fifth-fourth century BC) was named after the philosopher Parmenides of Elea (sixth-fifth century BC). This describes **Parmenides Proposition**:

In approximating θ , suppose rationales, p/q and r/s , satisfy $p/q < \theta < r/s$. Then $(p + r)/(q + s)$ is a new estimate between p/q and r/s :
 If it is an underestimate, it is a better underestimate than p/q .
 If it is an overestimate, it is a better overestimate than r/s .

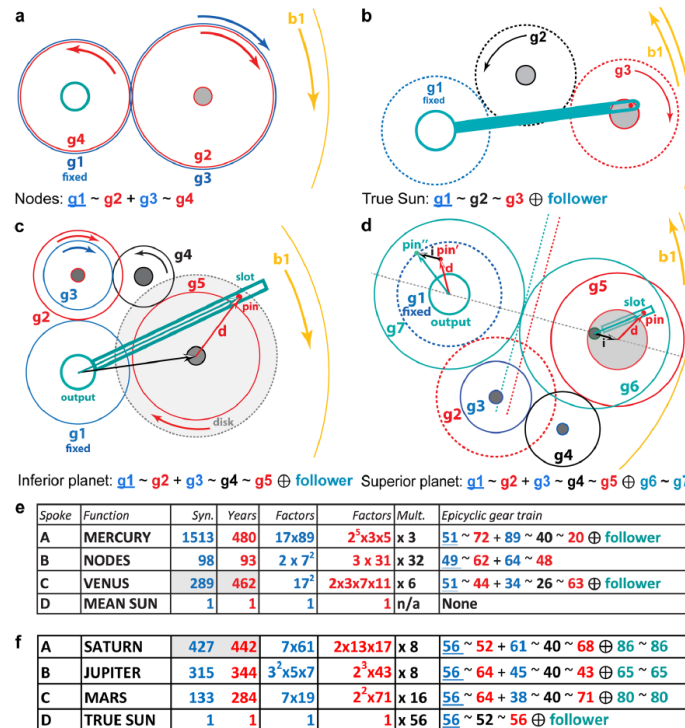


Figure 3. Epicyclic Mechanisms for the Cosmos. Fixed gears are underlined; blue gears calculate synodic cycles; red gears calculate years; black gears are idler gears; all designated by their tooth counts. “~” means “meshes with”; “+” means “fixed to the same arbor”; “⊕” means “with a pin-and-follower, turning on the central axis” or “with a pin-and-slot on eccentric axes”—creating variable motion (turquoise). Followers are slotted rods that follow a pin on the epicyclic gear and turn on the central axis. For each mechanism, there is a fixed gear at the centre, meshing with the first epicyclic gear, which is forced to rotate by the rotation of b1 or the CP. (a) 4-gear epicyclic system for the Line of Nodes. (b) 3-gear direct model for the true Sun. (c) 5-gear direct model for an inferior planet for complex period relations, with variable motion calculated by a pin and slotted follower. (d) 7-gear indirect model for a superior planet for complex period relations, with variable motion calculated by a pin-and-slot on eccentric axes. (e) Period relations and gear trains on the Main Drive Wheel, b1; Mercury & Venus share fixed 51. (f) Period relations and gear trains on the Circular Plate, CP, sharing fixed 56; gears also shared between Saturn/true Sun and Mars/Jupiter (Supplementary Discussion S4).

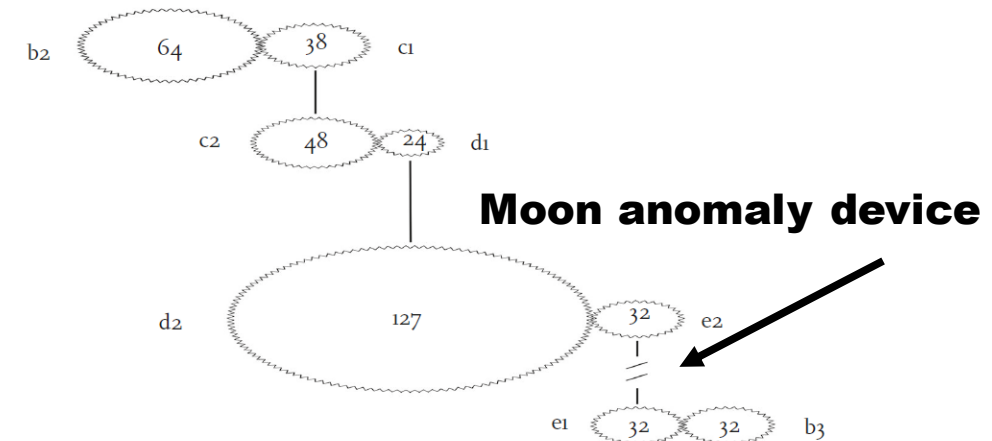
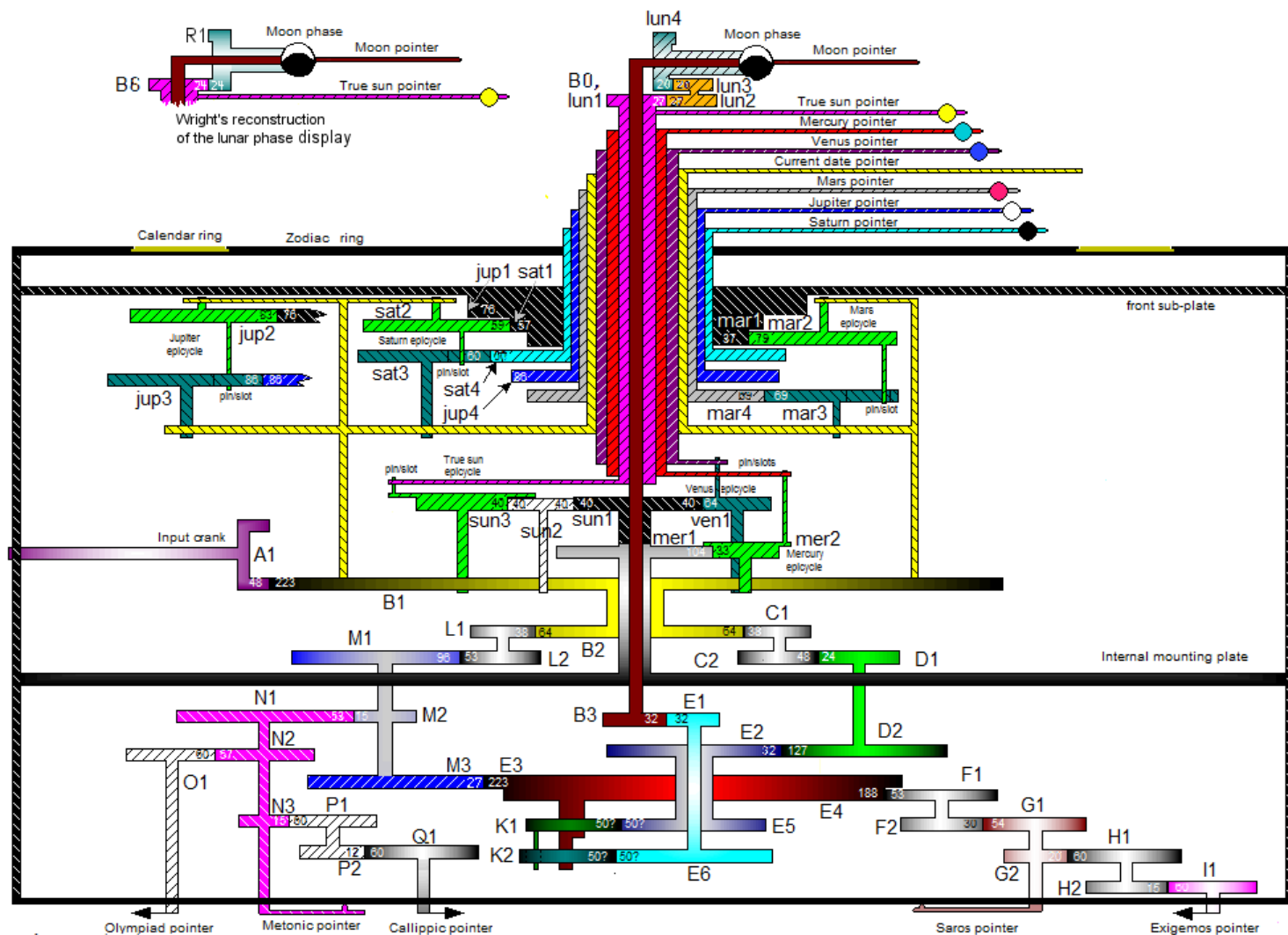


FIG. 8.11. Gear train for the Moon's pointer, omitting the lunar anomaly device between e2 and e1.

Jones, 2017

VI) Origin

From Syracuse or Rhodos (and why)?



VI) Origin

From Syracuse or Rhodes (and why)?

Syracuse:

Archimedes (287-212 BC)

Based on mechanical inventions of Archimedes

Month names agreed with used in that city

Number of identified solar eclipses good for Syracuse but bad for Athens and Rhodes

Machines for predicting celestial motions associated to Archimedes mentioned in ancient literature (e.g. Cicero's *De re publica*, 1st century BC)

Rhodes:

Hipparchus (190-125 BC)

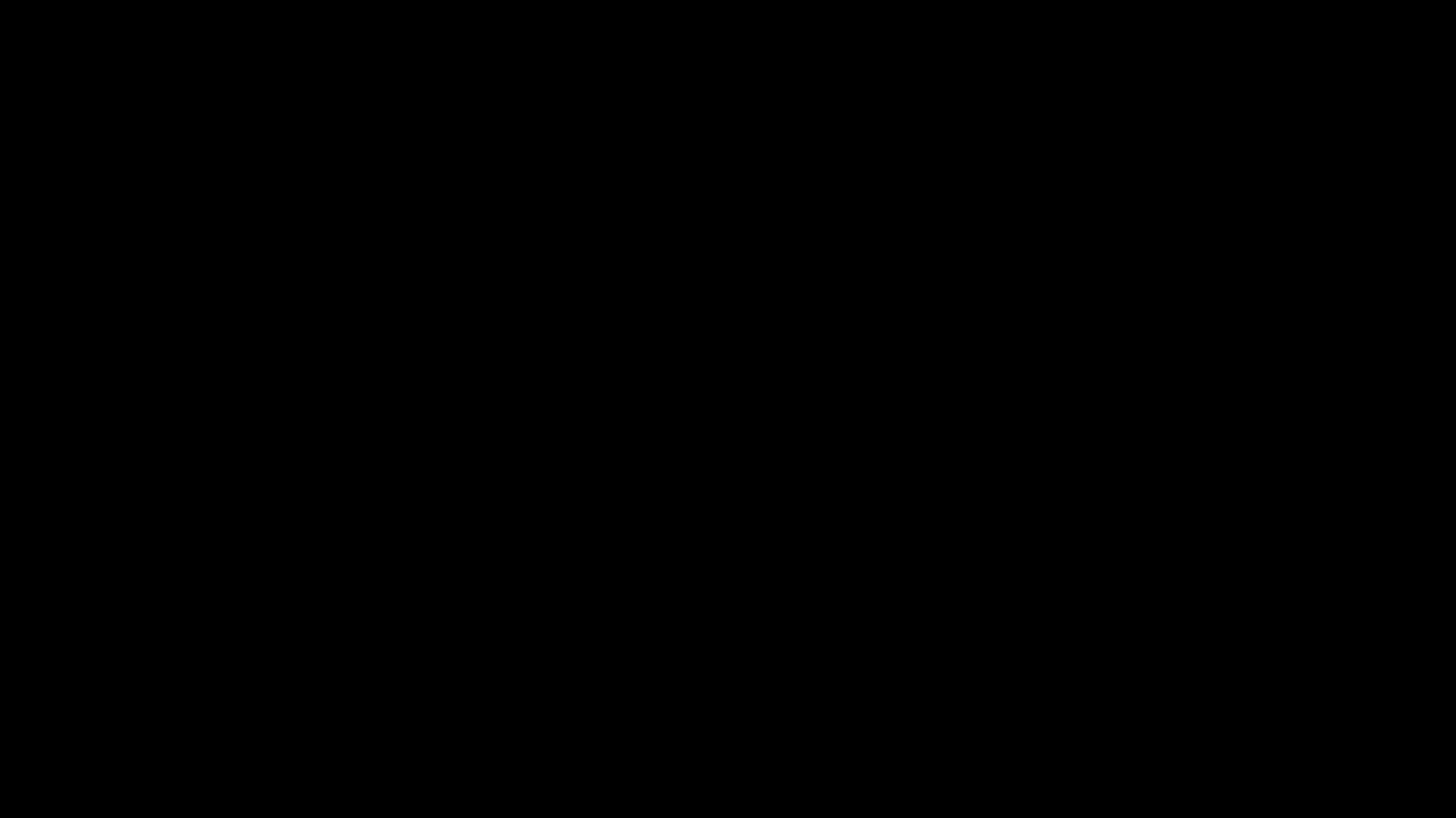
Lunar anomaly fits best to Hipparchus theory

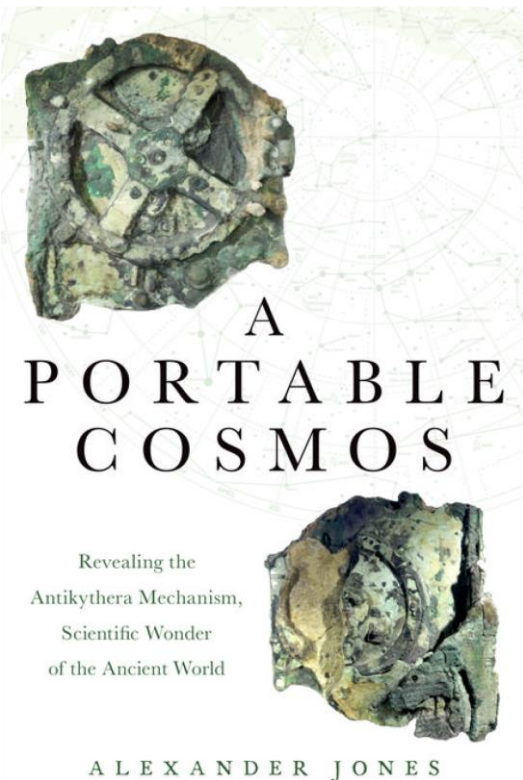
Ship had cargo from Rhodes

Style of writing points to 100-150 BC

Reconstruction: best fitted Saros cycle starts with new moon on 29 April 205 BC

Most likely was useless for predictions at the time the ship sunk (e.g. 70-60 BC)





Vol 444/30 November 2006

nature

NEWS & VIEWS

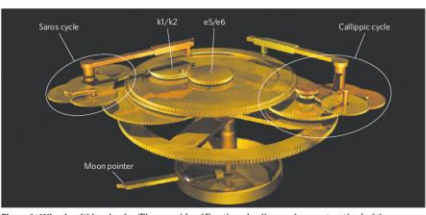
ARCHAEOLOGY

High tech from Ancient Greece

François Charette

The Antikythera Mechanism, salvaged 100 years ago from an ancient shipwreck, was long known to be some sort of mechanical calendar. But modern analysis is only now revealing just how sophisticated it was.

During renovation work in a northern Italian palazzo, an enigmatic artefact comes to light, dated to the late fifteenth century. After intensive analysis, it is identified as a complex steam engine — constructed 200 years before French inventor Denis Papin's pioneering experiments, and 300 years before the Industrial Revolution. Our view of the technical achievements of the Renaissance is completely changed. The reverberations are felt far beyond just scholarly circles. True, this hasn't happened. But a century-old archaeological find is continuing to force a comparable rethink of the technology of classical antiquity. In this issue, Freeth *et al.* (page 587) present the most up-to-



And many more...



15 Intriguing Facts About the Antikythera Mechanism

BY KRISTINA KILGROVE

JUNE 10, 2014



The Antikythera mechanism on display at the National Archaeological Museum, Athens. Photo: Wikimedia Commons (CC BY 2.0)

This week, researchers from the Antikythera Mechanism announced new insights about the mysterious Antikythera Mechanism, an unusual artifact that has intrigued archaeologists, classicists and the public for decades. Here are 15 facts about the mechanism, sometimes called "the world's first computer." Jump right to #14 for the latest interpretations of this singular object.

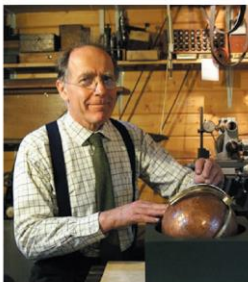
ANCIENT TECHNOLOGY

Archimedes' fabled sphere brought to life

Curator recreates a 2,000-year-old model of the Universe.

BY JO MARCHANT

A mechanical model of the Universe attributed to the ancient Greek mathematician and polymath Archimedes has been reconstructed after more than two millennia. The metallic globe, which reproduces the motions of the Sun, Moon and planets across the night sky, is on display for the first time, at a museum in Basel, Switzerland. The model, built by Michael Wright, a former curator at the Science Museum in London, is largely the product of erudite guesswork. But astrophysicist Mike Edmunds of Cardiff University, UK, says that it is a reminder that geared machines in antiquity were probably more complex than historians often assume. Several ancient writers and poets describe mechanical models of the heavens, which they



Michael Wright's machine models the heavens.

DIR 2007 - International Symposium on Digital Industrial Radiology and Computed Tomography, June 25-27, 2007, Lyon, France

The latest techniques reveal the earliest technology – A new inspection of the Antikythera Mechanism

Andrew T. Ramsey

X-Tek Systems Ltd., Tring, United Kingdom; Phone: +44 1442 828700, Fax: +44 1442 828118; andrew.ramsey@xtekxray.com

Abstract

In the National Archaeological Museum in Athens sit the remains of a remarkable machine, 1600 years ahead of its time. The Antikythera Mechanism, found on an ancient Greek shipwreck in 1901 is thought to date from the early second century BC. Early examination of the mechanism gave rise to theories that it was an astronomical computer. Later X-ray images revealed meticulous ancient workmanship not seen in bronze interlocking gears and inscriptions. Last year X-Tek was asked to use its CT system, originally developed to inspect aircraft turbine blades, to do a non-destructive examination of the mechanism, which revealed details of hidden text and symbols that confirmed the mechanism as a mechanical calculator, capable of predicting the motions of the sun, moon, and planets with remarkable accuracy, and could not only have been used to predict the occurrence of solar eclipses, but also to predict the occurrence of lunar eclipses. X-ray microfocus X-ray computed tomography (X-ray CT) revealed the internal structure of the mechanism, which revealed details of hidden text and symbols that confirmed the mechanism as a mechanical calculator, capable of predicting the motions of the sun, moon, and planets with remarkable accuracy, and could not only have been used to predict the occurrence of solar eclipses, but also to predict the occurrence of lunar eclipses.

scientific report

OPEN

A Model of the Cosmos in the ancient Greek Antikythera Mechanism

Tony Freeth^{1,2}, David Higgin¹, Aris Dacanalis¹, Lindsay MacDonald², Myrto Georgakopoulou^{1,3} & Adam Wojcik^{1,2,3}

The Antikythera Mechanism, an ancient Greek astronomical calculator, has challenged researchers since its discovery in 1901. Now split into 82 fragments, only a third of the original survives, including 30 corroded bronze gearwheels. Microfocus X-ray Computed Tomography (X-ray CT) in 2005 decoded the structure of the rear of the machine but the front remained largely unresolved. X-ray CT also revealed inscriptions describing the motions of the Sun, Moon and all five planets known in antiquity and how they were displayed at the front as an ancient Greek Cosmos. Inscriptions specifying complex planetary periods forced new thinking on the mechanization of this Cosmos, but no previous reconstruction has come close to matching the data. Our discoveries lead to a new model, satisfying and explaining the evidence. Solving this complex 3D puzzle reveals a creation of genius—combining cycles from Babylonian astronomy, mathematics from Plato's Academy and ancient Greek astronomical theories.



Journal of Earth Science and Engineering 4 (2014) 757-769
doi: 10.17265/2159-581X/2014. 12. 005

Thales of Miletus, Archimedes and the Solar Eclipses on the Antikythera Mechanism

Göran Henriksson

Department of Physics and Astronomy, Uppsala University, Uppsala SE 751 20, Sweden

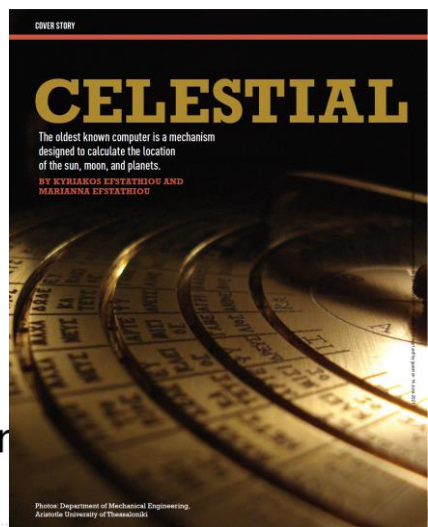
Received: November 06, 2014 / Accepted: November 28, 2014 / Published: December 25, 2014.

Abstract: Thales of Miletus (640?-546 BC) is famous for his prediction of the total solar eclipse in 585 BC. In this paper, the author demonstrate how Thales may have used the same principle for prediction of solar eclipses as that used on the Antikythera Mechanism. At the SEAC conference in Alexandria in 2009, the author presented the paper "Ten solar eclipses show that the Antikythera Mechanism was constructed for use on Sicily." The best defined series of exeligmos cycles started in 243 BC during the lifetime of Archimedes (287-212 BC) from Syracuse. The inscriptions on the Antikythera Mechanism were made in 100-150 BC and the last useful exeligmos started in 134 BC. The theory for the motion of the moon was from Hipparchus (ca 190-125 BC). A more complete investigation of the solar eclipses on the Antikythera Mechanism reveals that the first month in the first saros cycle started with the first new moon after the winter solstice in 542 BC. Four solar eclipses 537-528 BC, from the first saros cycle, and three one exeligmos cycle later, 487-478 BC, are preserved and may have been recorded in Croton by Pythagoras (ca 575-495 BC) and his school.

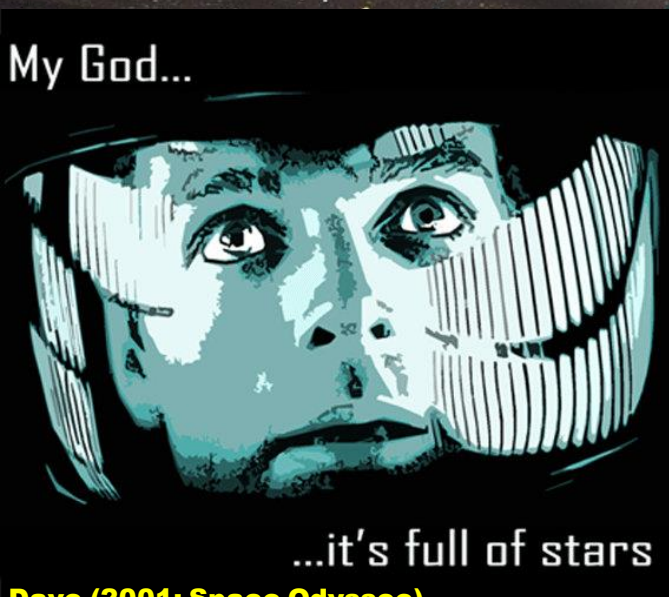
Key words: Solar eclipse, exeligmos cycle, saros cycle, seasonal hour, equinoctial hour.

hanical ation

sion of a geometrical me out of nowhere. I have been the internal mechanism?



What is the universe?



Dave (2001: Space Odyssee)

What is the universe?

Not only, but it is even full of galaxies ...

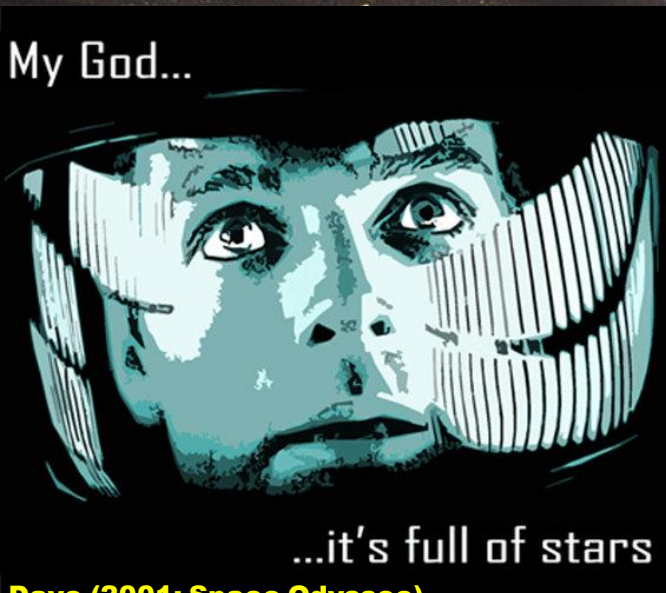
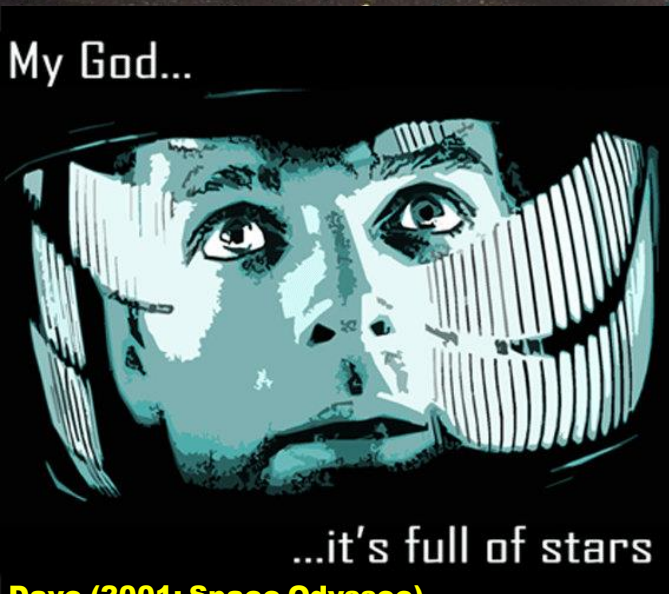


Bild: APOD 23. Aug 2010, Alex Cherney, Terrastro

What is the universe?

Not only, but it is even full of galaxies ...

So, how many stars in our galaxy and
how many galaxies in the Universe?



Dave (2001: Space Odyssee)

Bild: APOD 23. Aug 2010, Alex Cherney, Terraastro

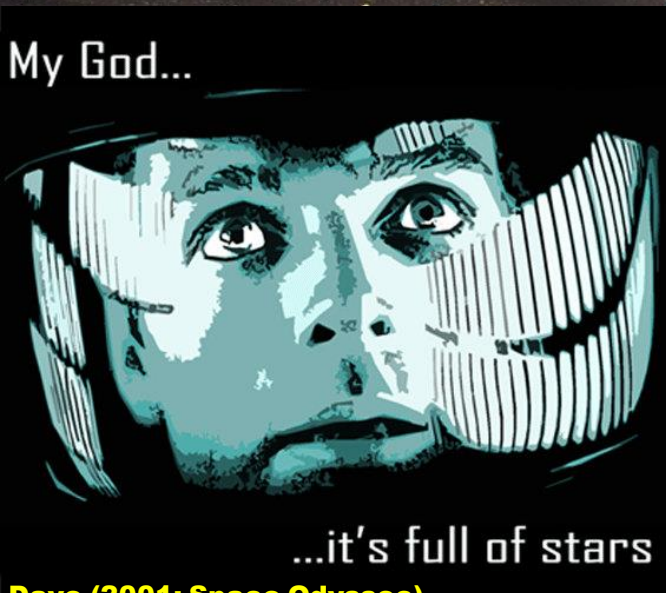
What is the universe?

Not only, but it is even full of galaxies ...

So, how many stars in our galaxy and
how many galaxies in the Universe?

Stars in our Galaxy: ~200.000.000.000
Galaxies in the Universe: ~100.000.000.000

~ 10^{22} (Impossible to directly simulate!)



Material Science:
ca. the numbers of atoms in a dice

Life Science:
7.9 billion humans (on earth)
10 quintillion (e.g. 10^{20}) insects

Meteorology:
~ 5×10^{46} water molecules (in the oceans)

What is the universe?

Not only, but it is even full of galaxies ...

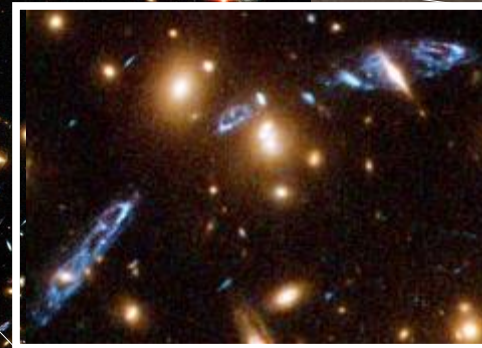
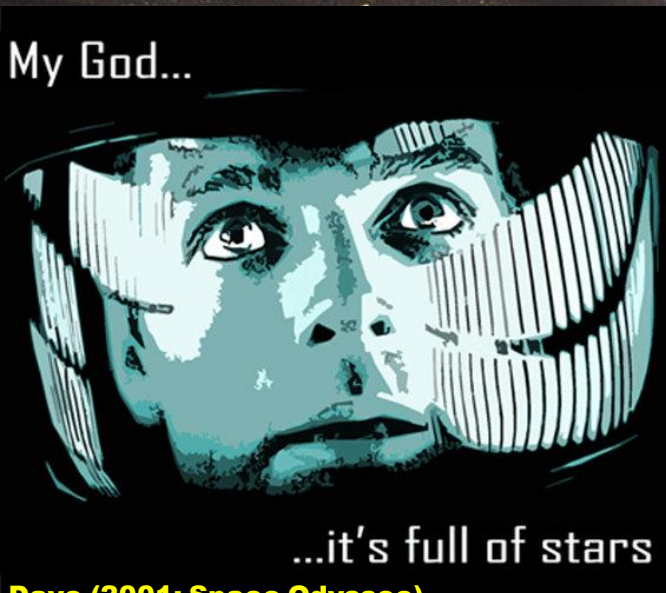
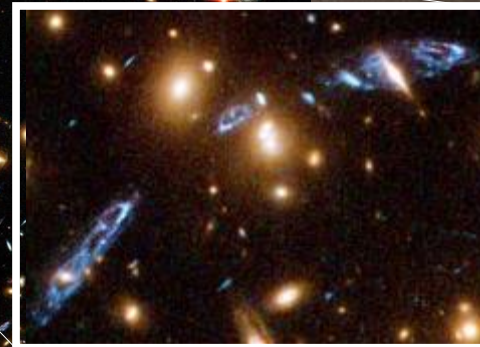


Bild: APOD 23. Aug 2010, Alex Cherney, Terrastro

What is the universe?

Not only, but it is even full of galaxies ...



Astro Quiz Again !



When was the first N-Body integration performed?

1941 with the help of light bulbs

A

1946 with the help of the ENIAC computer

B

1960 with the help of the "Siemens 2002" computer

C

1981 with one of the first IBM 5150 Models

D

1988 on the first Cray YMP super computer

E

2013 on SuperMUC at LRZ

F

**... and reveals us even the
dynamic of the universe !**

Bild: APOD 21. Juli 2008, Gemini Observatory

Bild: APOD 23. Aug 2010, Alex Cherney, Terrastro

THE ASTROPHYSICAL JOURNAL

AN INTERNATIONAL REVIEW OF SPECTROSCOPY AND
ASTRONOMICAL PHYSICS

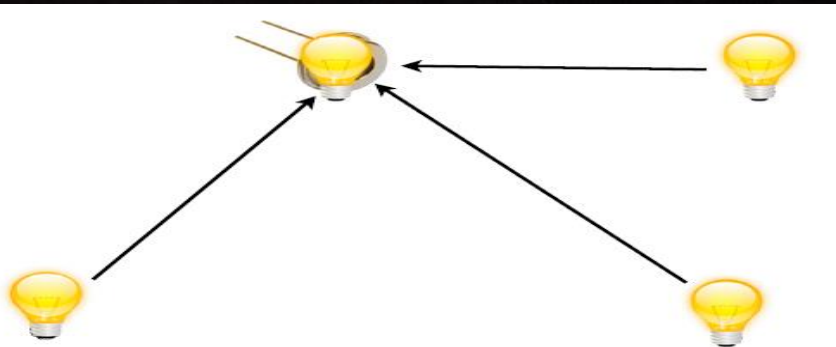
VOLUME 94

NOVEMBER 1941

NUMBER 3

ON THE CLUSTERING TENDENCIES AMONG THE NEBULAE
II. A STUDY OF ENCOUNTERS BETWEEN LABORATORY MODELS OF
STELLAR SYSTEMS BY A NEW INTEGRATION PROCEDURE

ERIK HOLMBERG



**Experiment with light bulbs and
photo-electric detector.**



**Experiment 1:
counter-rotating**

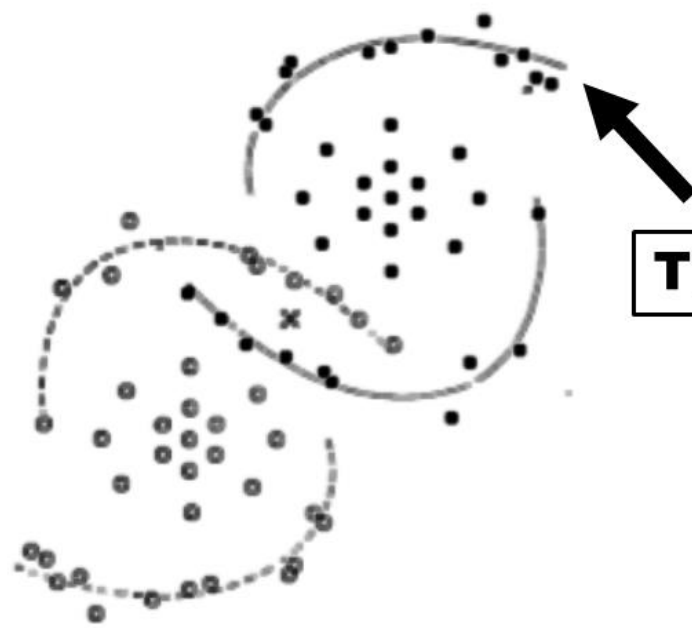


FIG. 4a

Time



**Experiment 2:
co-rotating**



FIG. 4b

Tidal arms !

**Experiment 1:
counter-rotating**

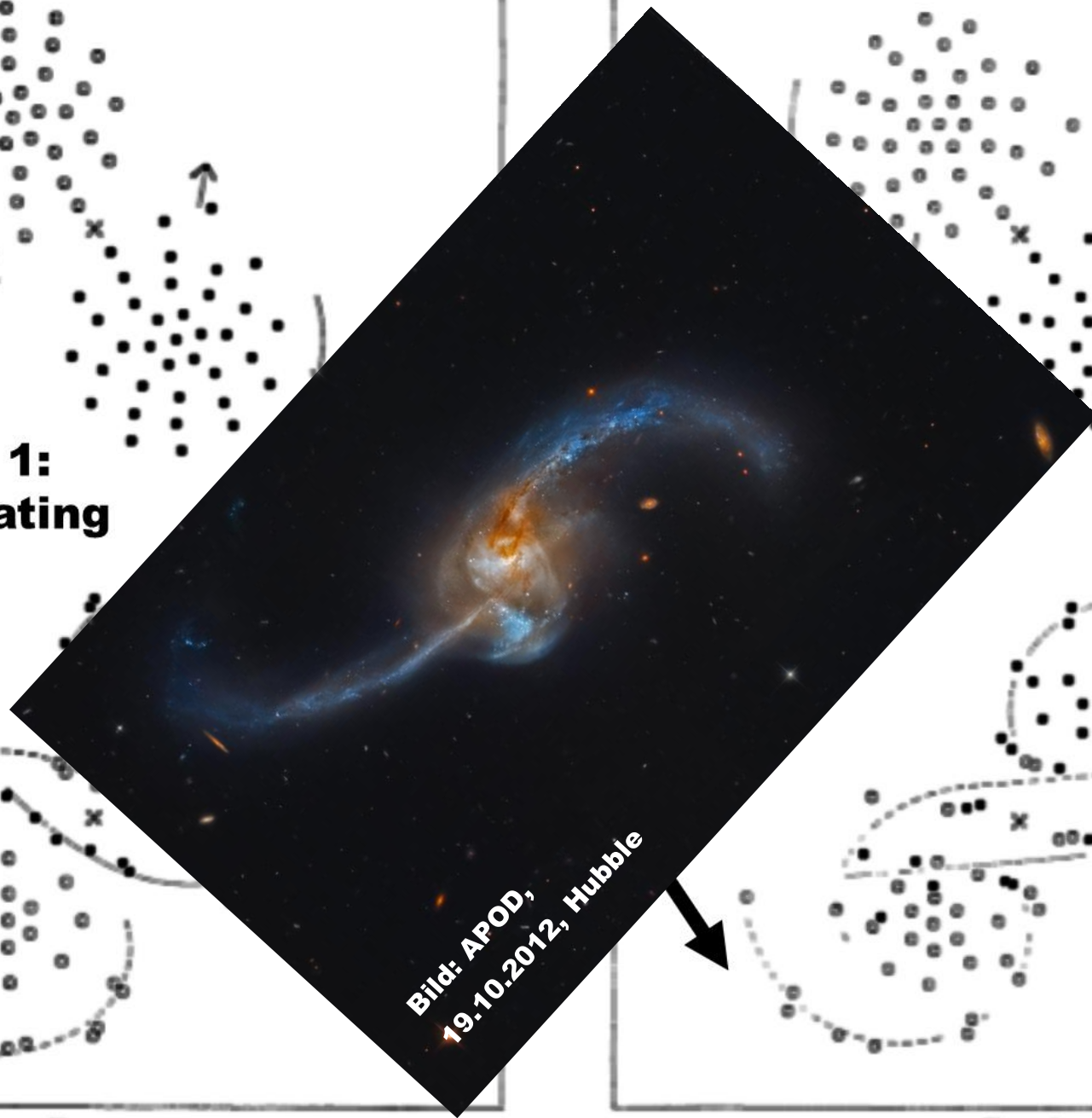


Bild: APOD,
19.10.2012, Hubble

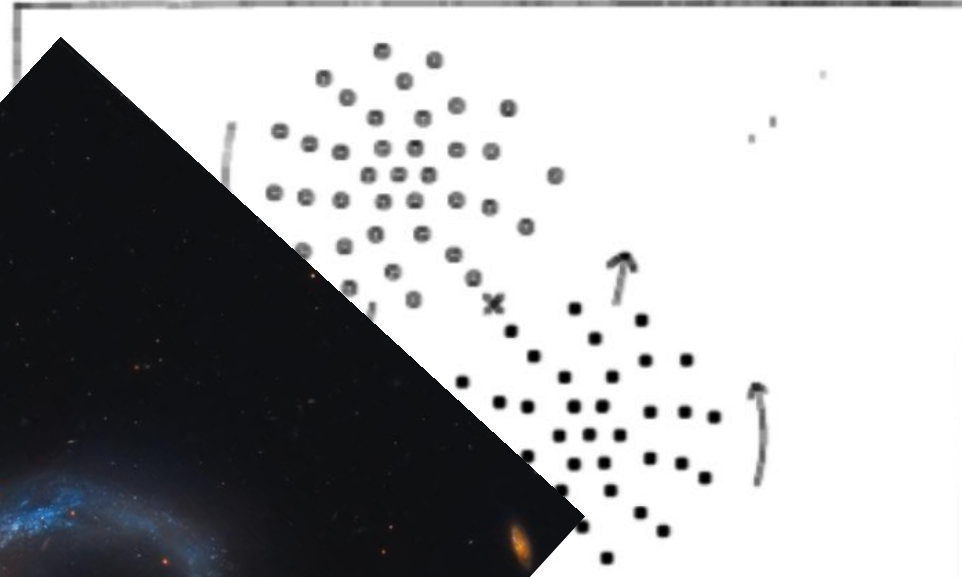
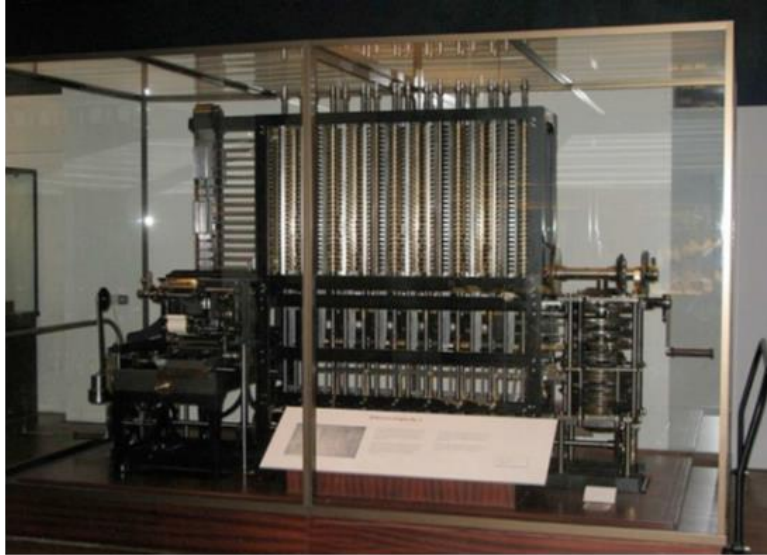


FIG. 4a

FIG. 4b

From Machines to Computers ...



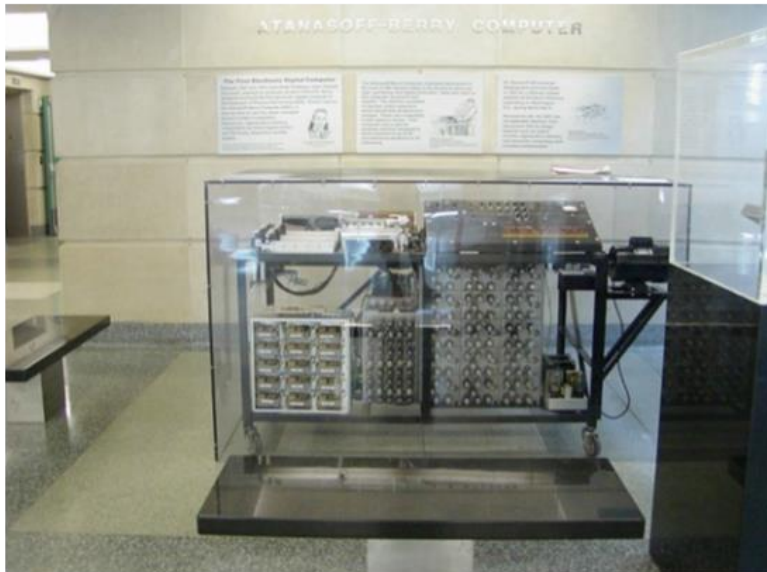
**Difference Engine
(1833; uncompleted)**



**Analytical Engine
(1838; uncompleted)**

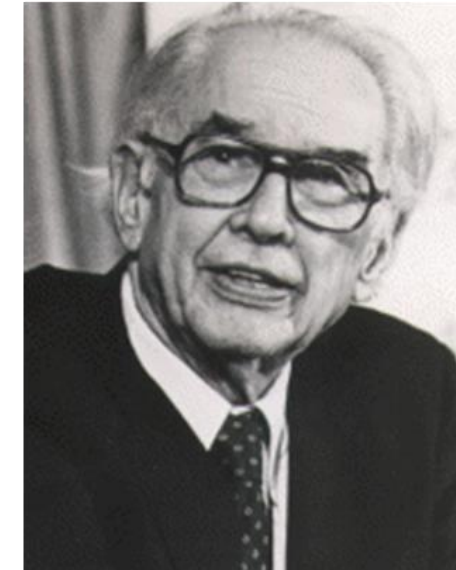


**Babbage
1791-1871**



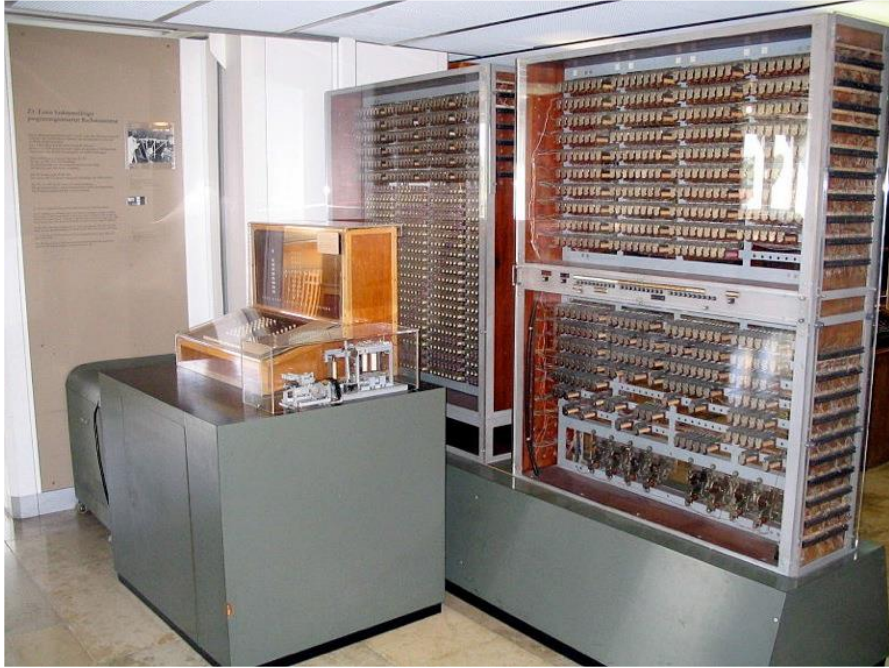
**Atanasoff-Berry Computer
1939-1942,
partially working**

**John Anasoff
1903-1995**



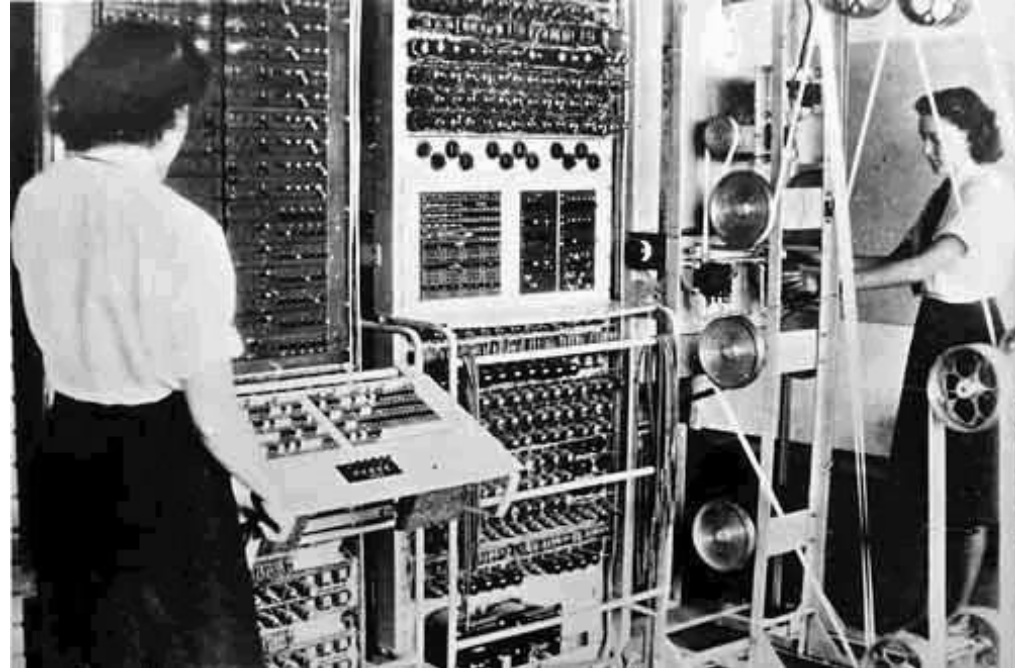
From Machines to Computers ...

**The first programmable computing facilities
where developed during second Word War:**



Z3, 1941-1943 (Germany)

- **Aerodynamic computations for airplane wings**
- **Destroyed in a bombing in 1943**
- **Reconstruction displayed in the German Museum here in Munich!**

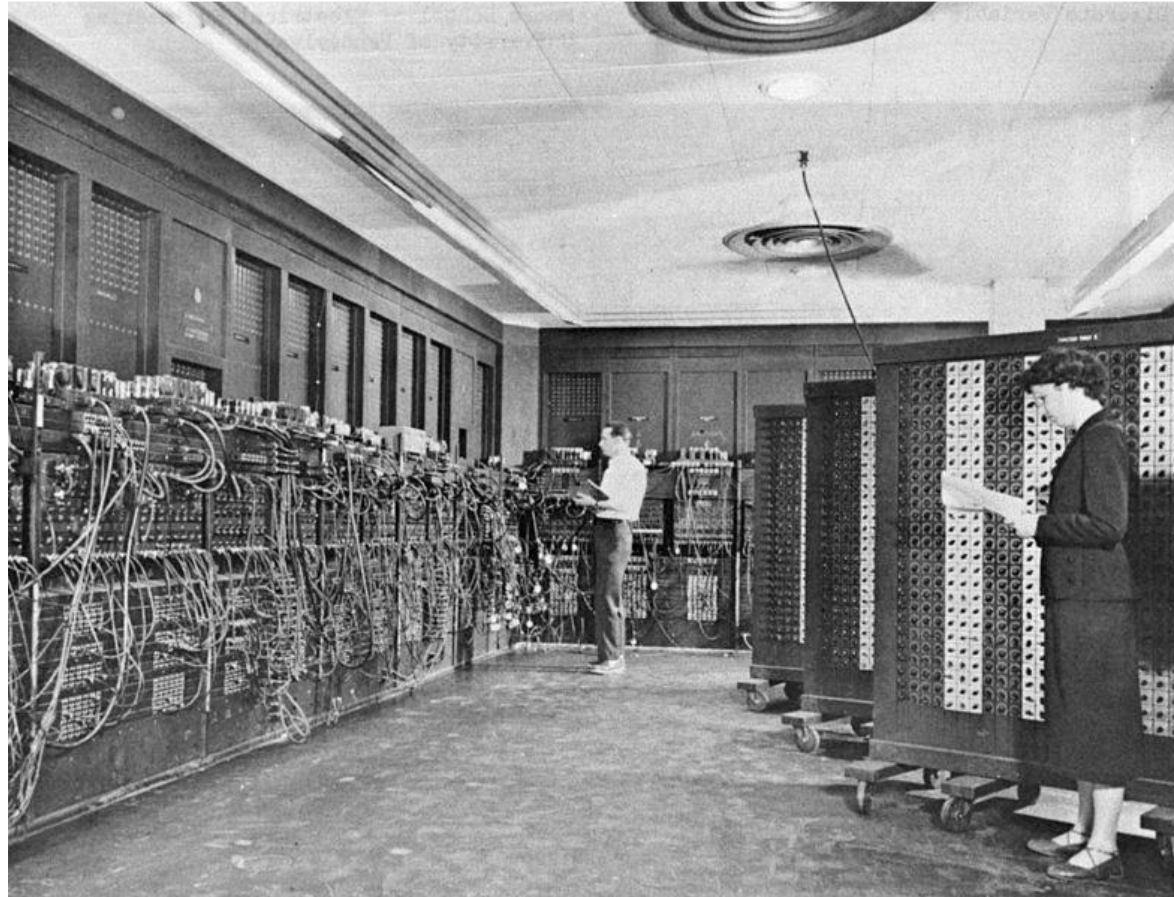


Colossus, 1944-1945 (England)

- **Was used to decipher the Enigma secret codes**
- **Was destroyed after second Word War (order by Churchill)**
- **Watch the movie, it's great!**

From Machines to Computers ...

Finally, ENIAC was declared to be the first programmable, electronic computer :



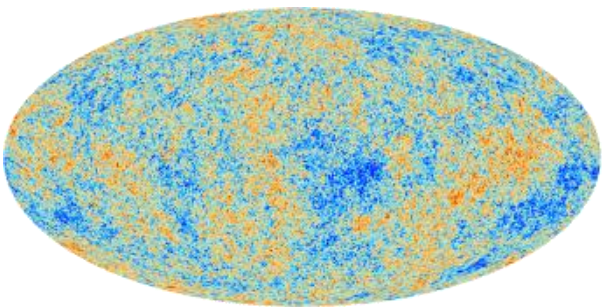
**ENIAC,
1946-1955
(USA)**

- **Computing of ballistic tables for the military**
- **After that, non military development started (IBM)**

HPC Challenges in Astrophysics

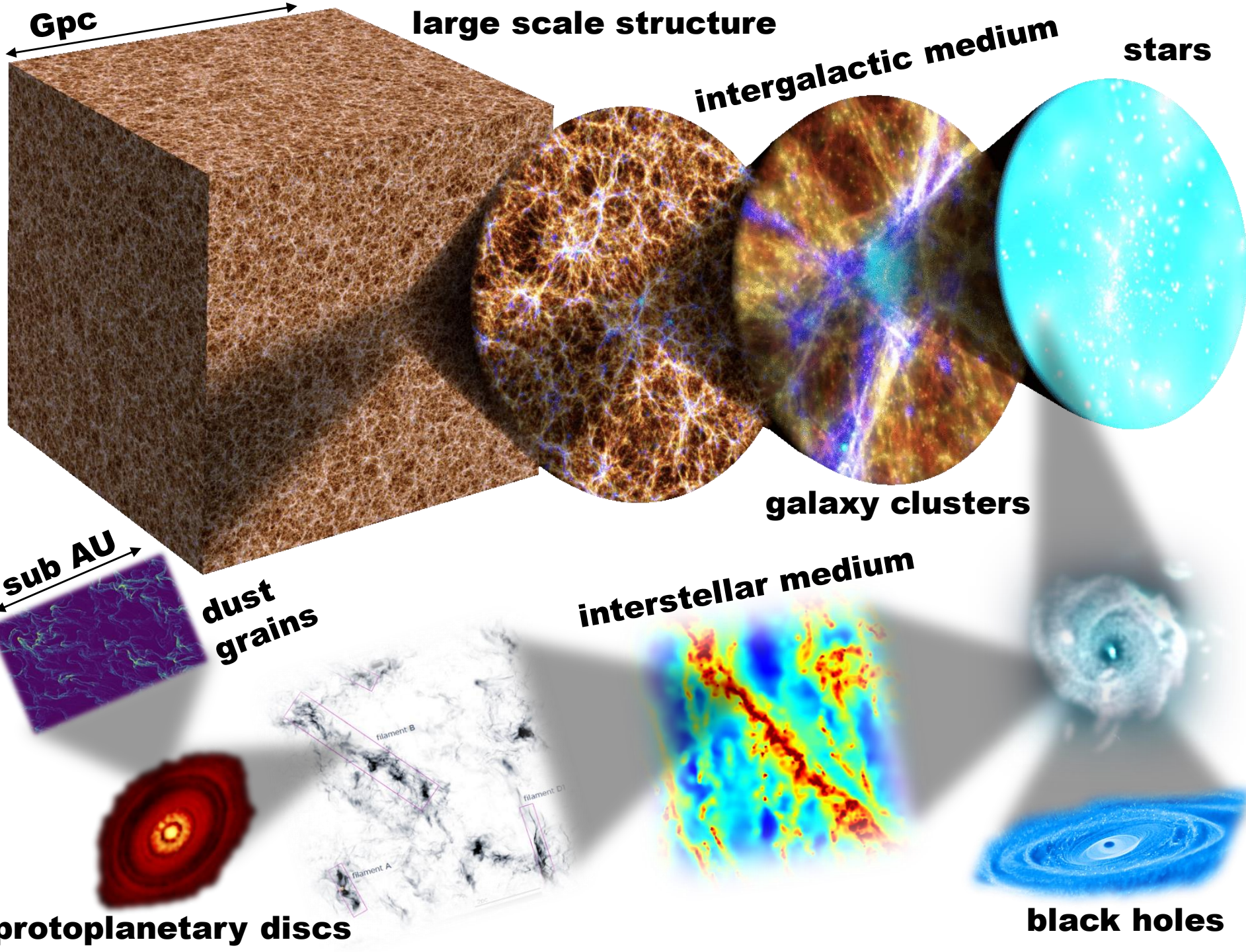
II) Simulating

The Computational Challenge



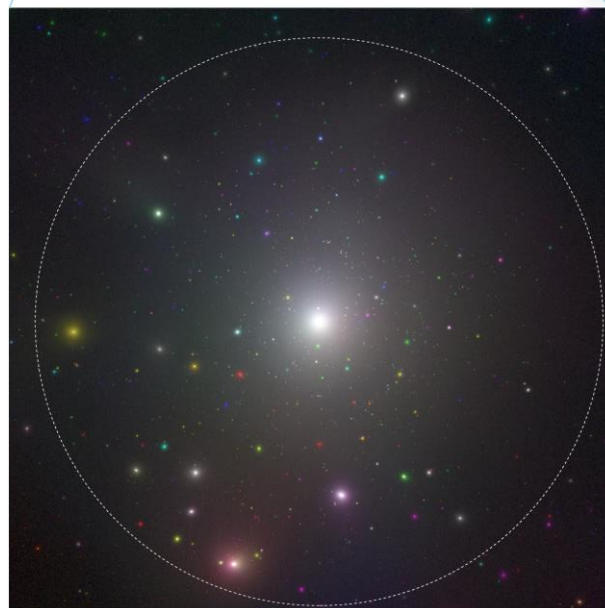
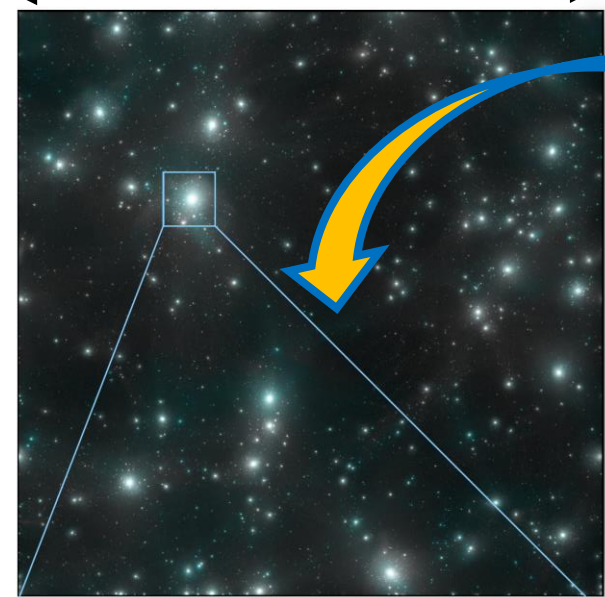
**multi-scale,
multi-physics**

Ω_{stars}	~ 0.002
Ω_{gas}	~ 0.04
Ω_{dm}	~ 0.23
Ω_{Λ}	~ 0.73



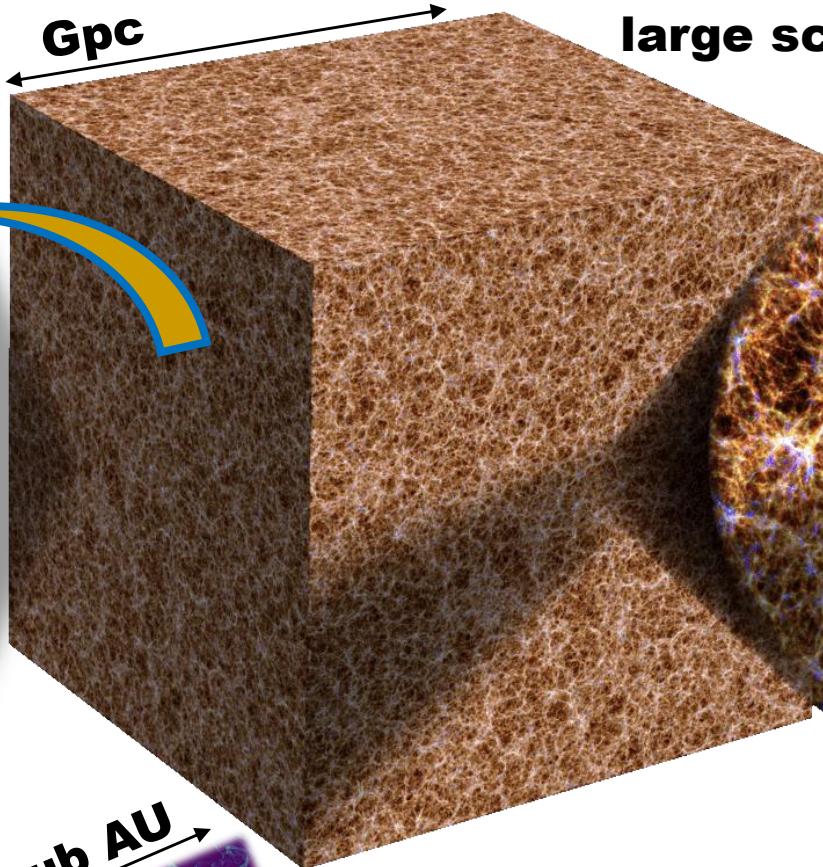
Dark Matter

0.864 pc



92.8 AU

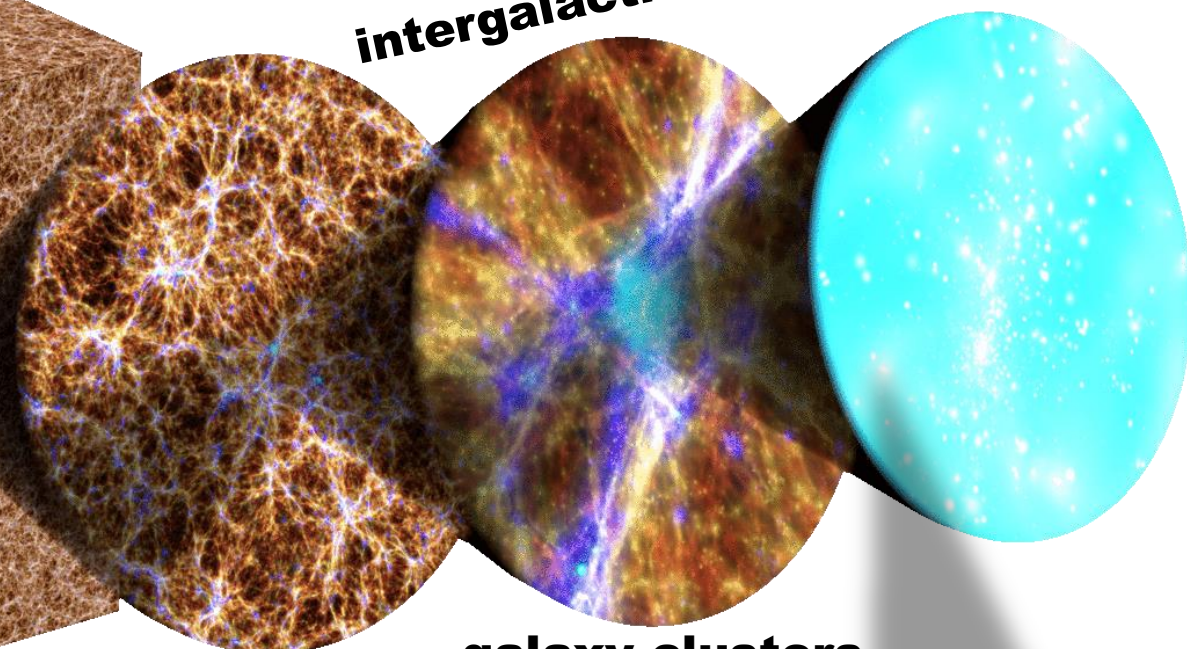
Gpc



large scale structure

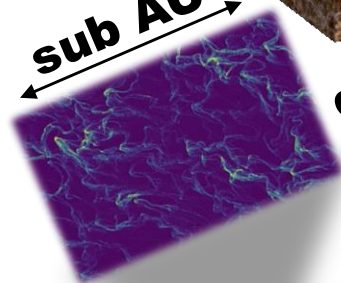
intergalactic medium

stars



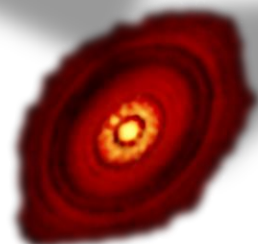
galaxy clusters

sub AU

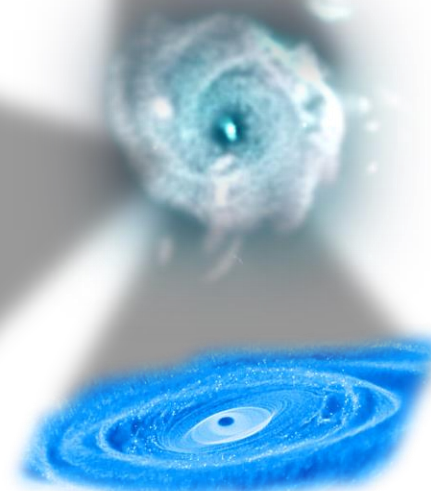
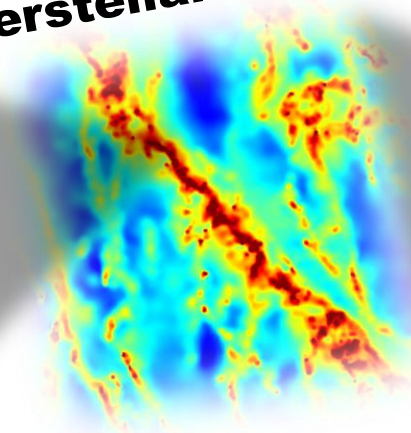
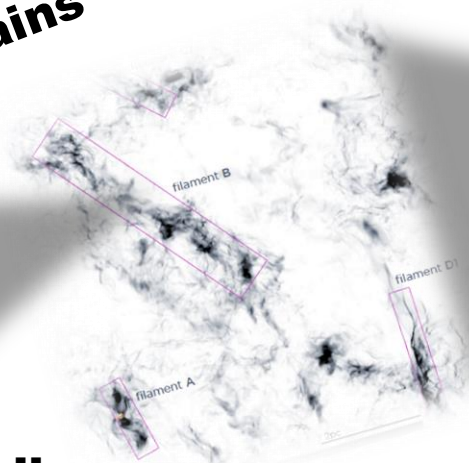


dust grains

interstellar medium



protoplanetary discs



black holes

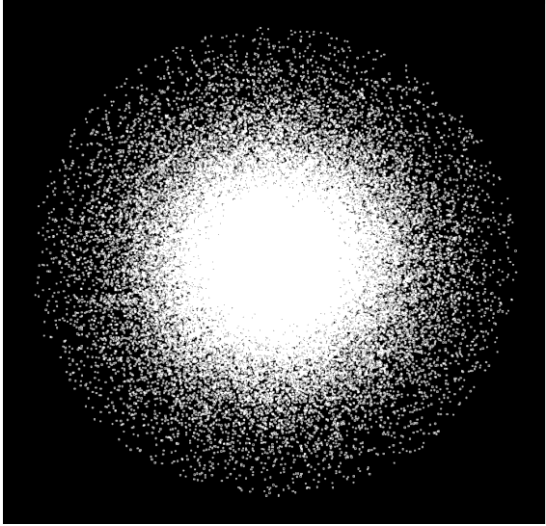
How to do simple an N-Body simulation:

$$\mathbf{F}_i = - \sum_{j=0, j \neq i}^{j=N} \frac{G m_i m_j}{r_{ij}^2} \hat{\mathbf{r}}_{ij}$$



How to do simple an N-Body simulation:

Particle distribution

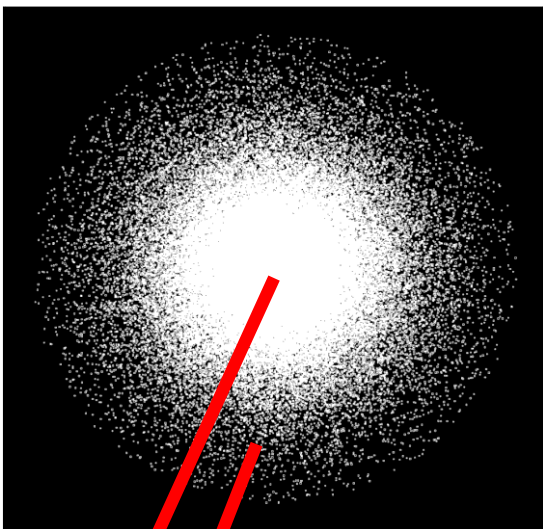


$$\mathbf{F}_i = - \sum_{j=0, j \neq i}^{j=N} \frac{G m_i m_j}{r_{ij}^2} \hat{\mathbf{r}}_{ij}$$



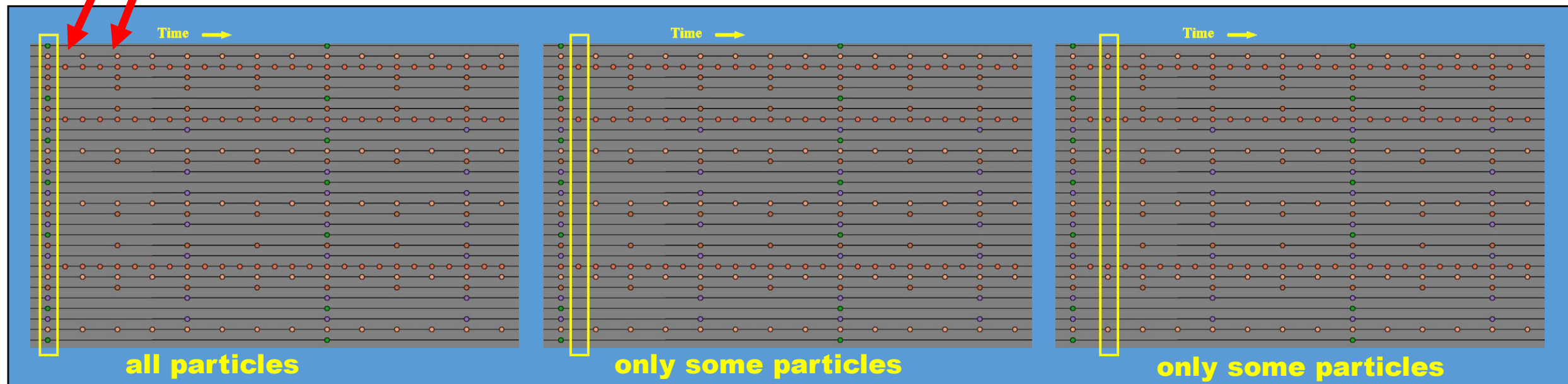
How to do simple an N-Body simulation:

Particle distribution



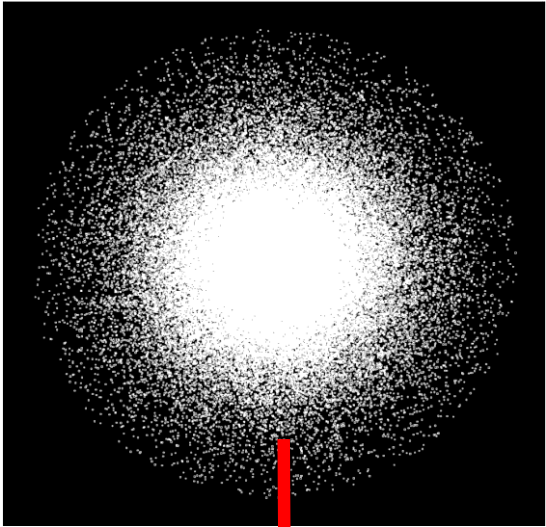
$$\mathbf{F}_i = - \sum_{j=0, j \neq i}^{j=N} \frac{G m_i m_j}{r_{ij}^2} \hat{\mathbf{r}}_{ij}$$

Using individual time-steps for the particles



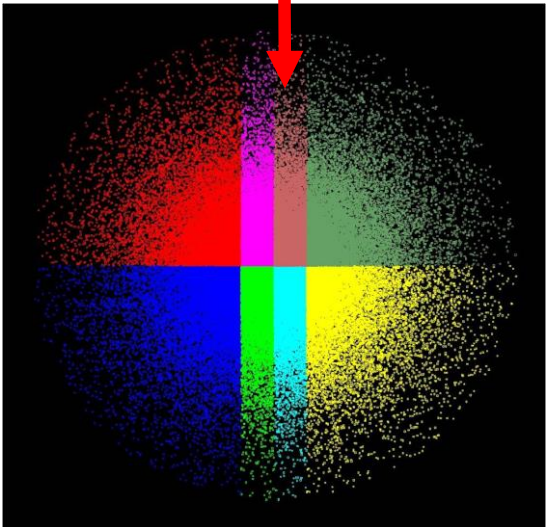
How to do simple an N-Body simulation:

Particle distribution



$$\mathbf{F}_i = - \sum_{j=0, j \neq i}^{j=N} \frac{G m_i m_j}{r_{ij}^2} \hat{\mathbf{r}}_{ij}$$

**Distributing the particles
across 8 computers**

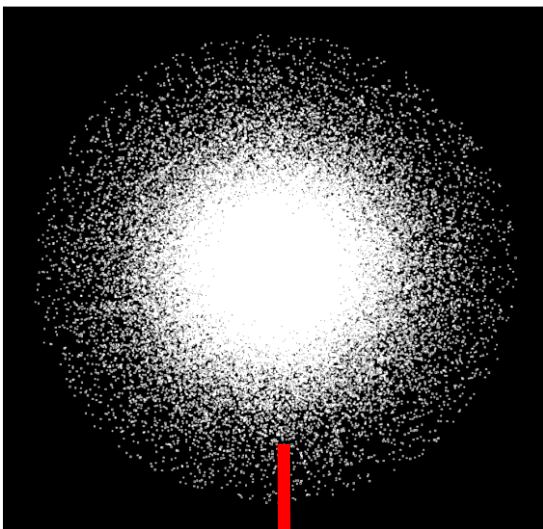


Equal number



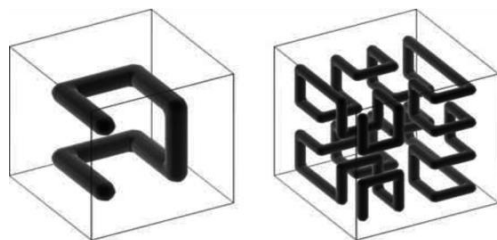
How to do simple an N-Body simulation:

Particle distribution

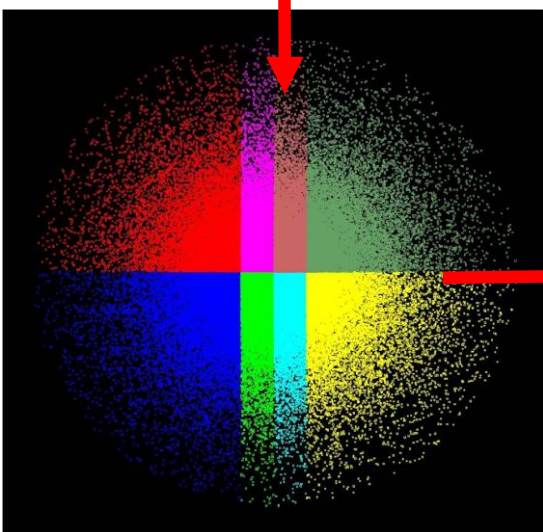


$$\mathbf{F}_i = - \sum_{j=0, j \neq i}^{j=N} \frac{G m_i m_j}{r_{ij}^2} \hat{\mathbf{r}}_{ij}$$

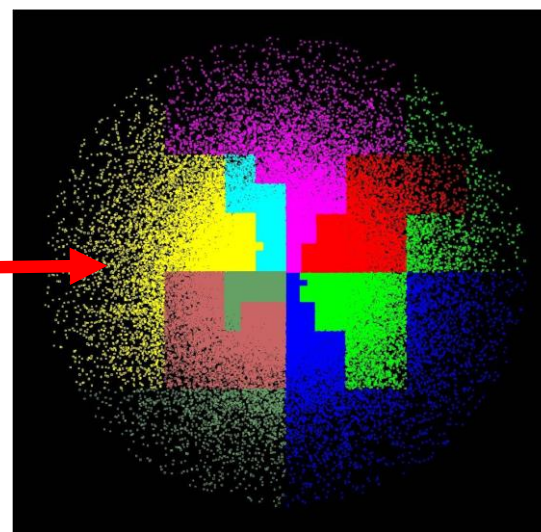
Distributing the particles
across 8 computers



Usage of space
filling curves!



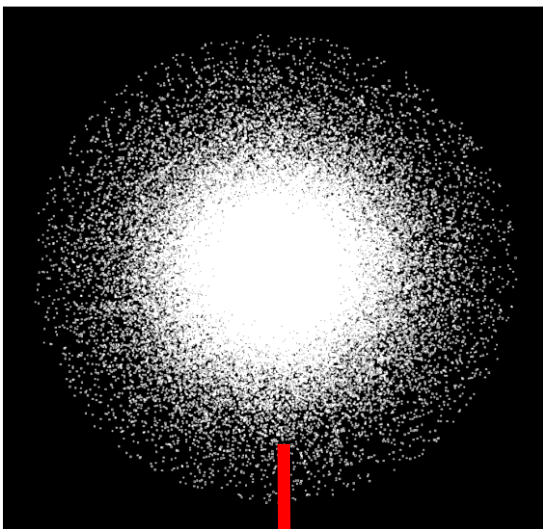
Equal number



Equal work

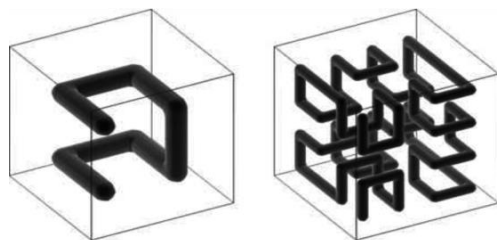
How to do simple an N-Body simulation:

Particle distribution

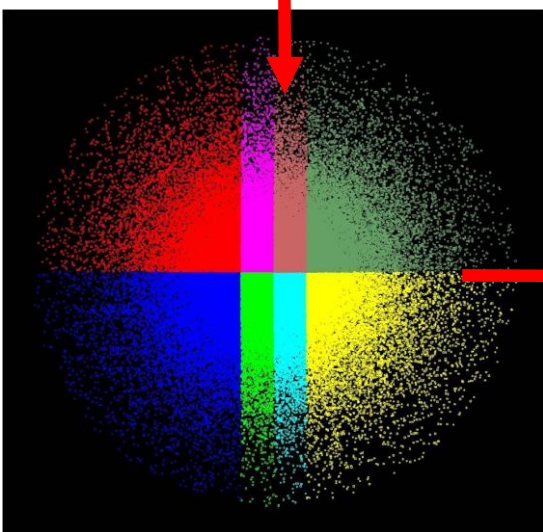


$$\mathbf{F}_i = - \sum_{j=0, j \neq i}^{j=N} \frac{G m_i m_j}{r_{ij}^2} \hat{\mathbf{r}}_{ij}$$

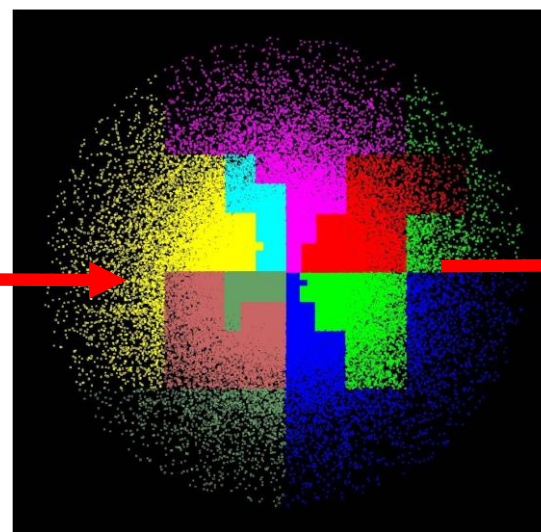
**Distributing the particles
across 8 computers**



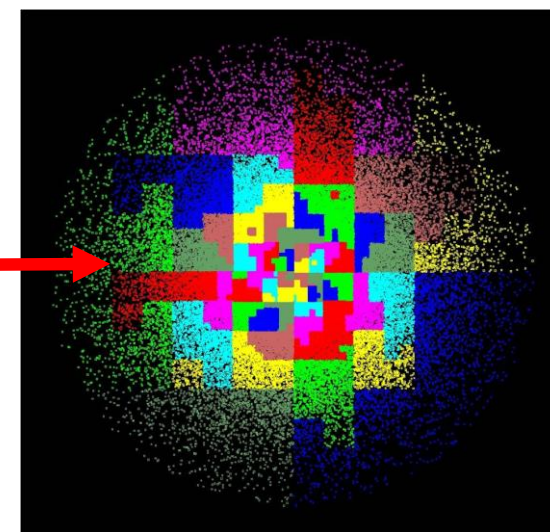
**Usage of space
filling curves!**



Equal number

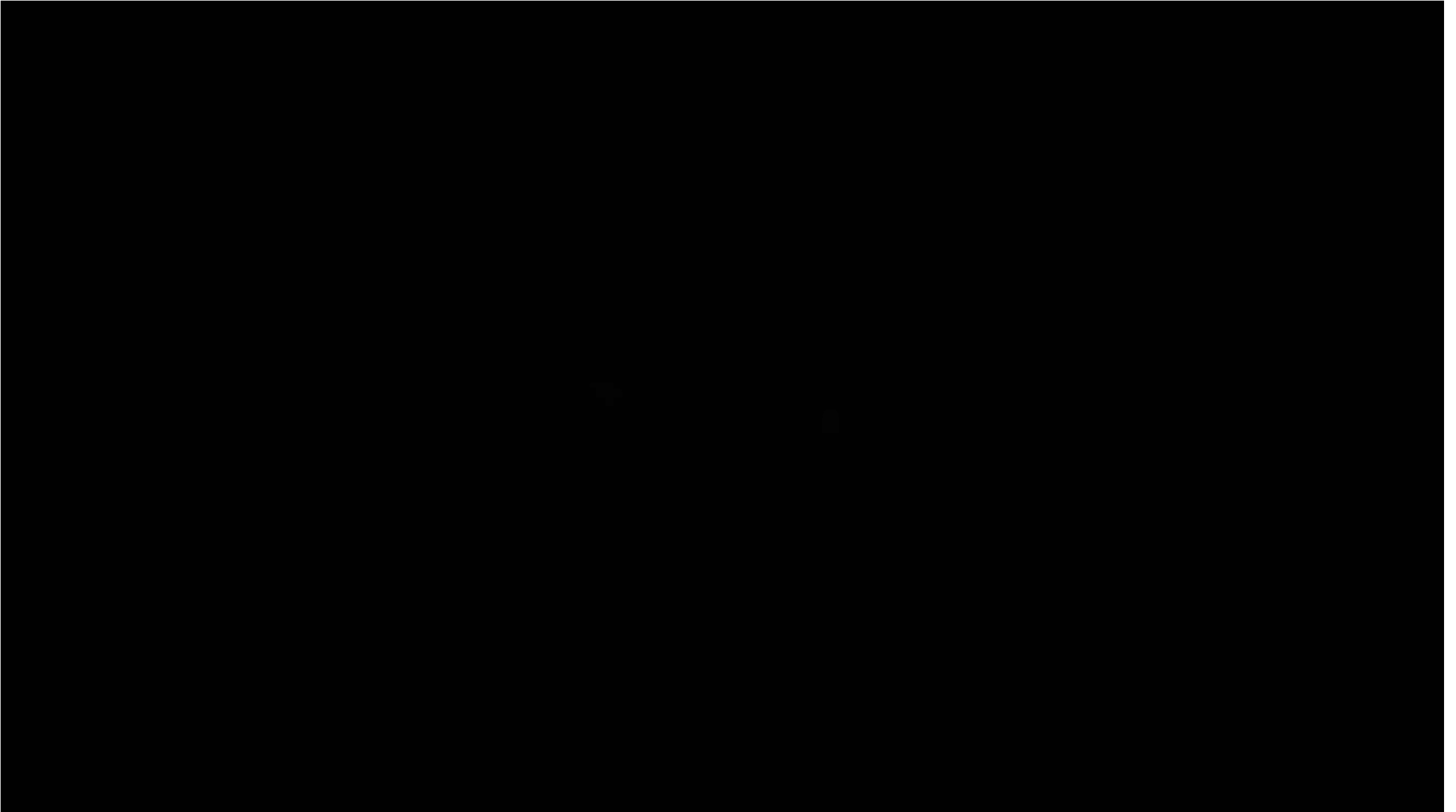


Equal work



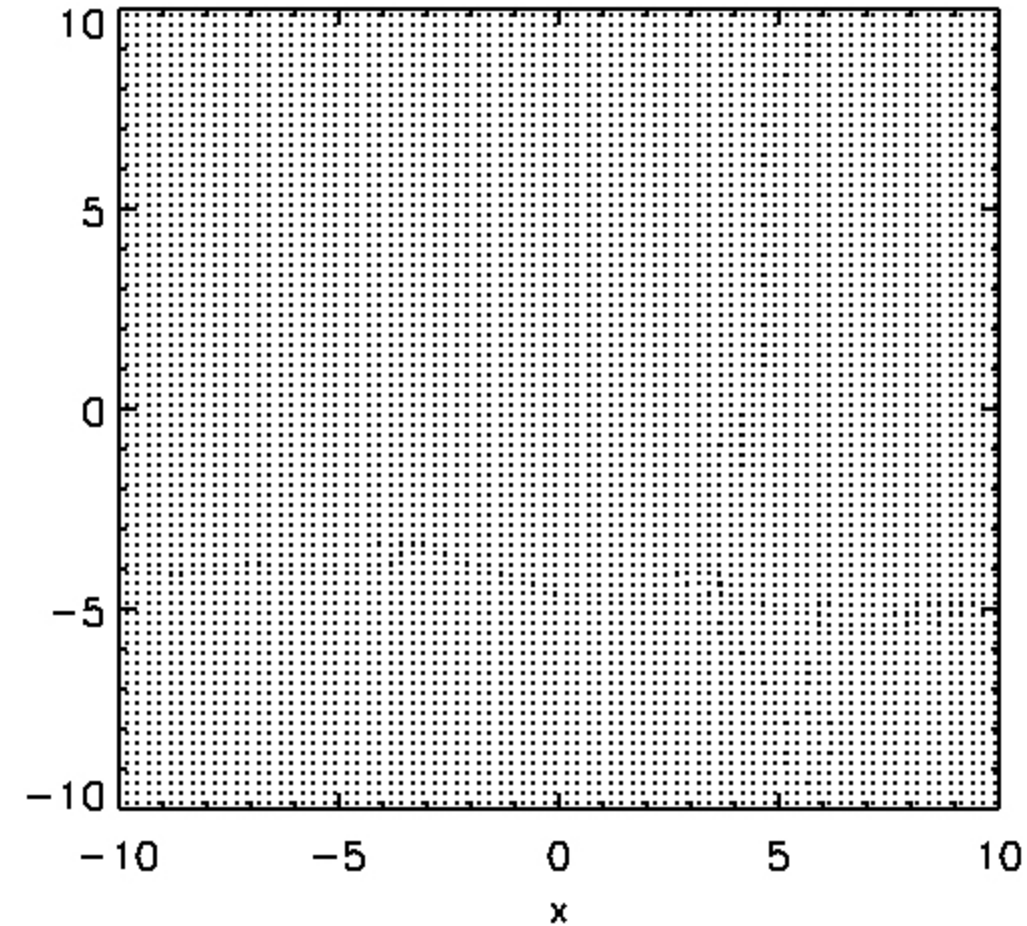
Equal number & work

Can we explain observations of merging galaxies?



How to do cosmological N-Body simulation:

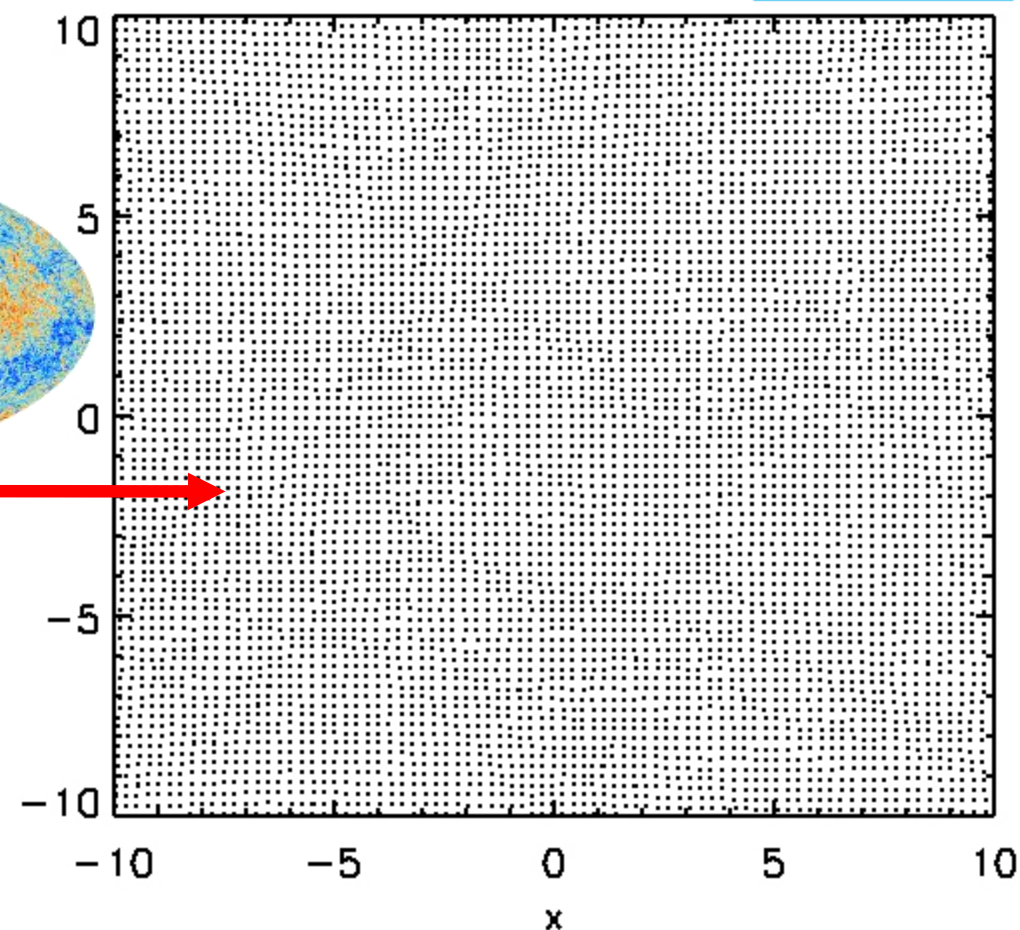
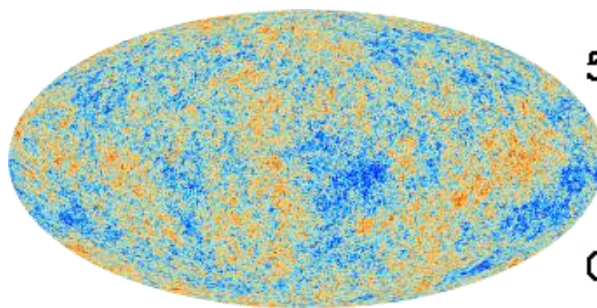
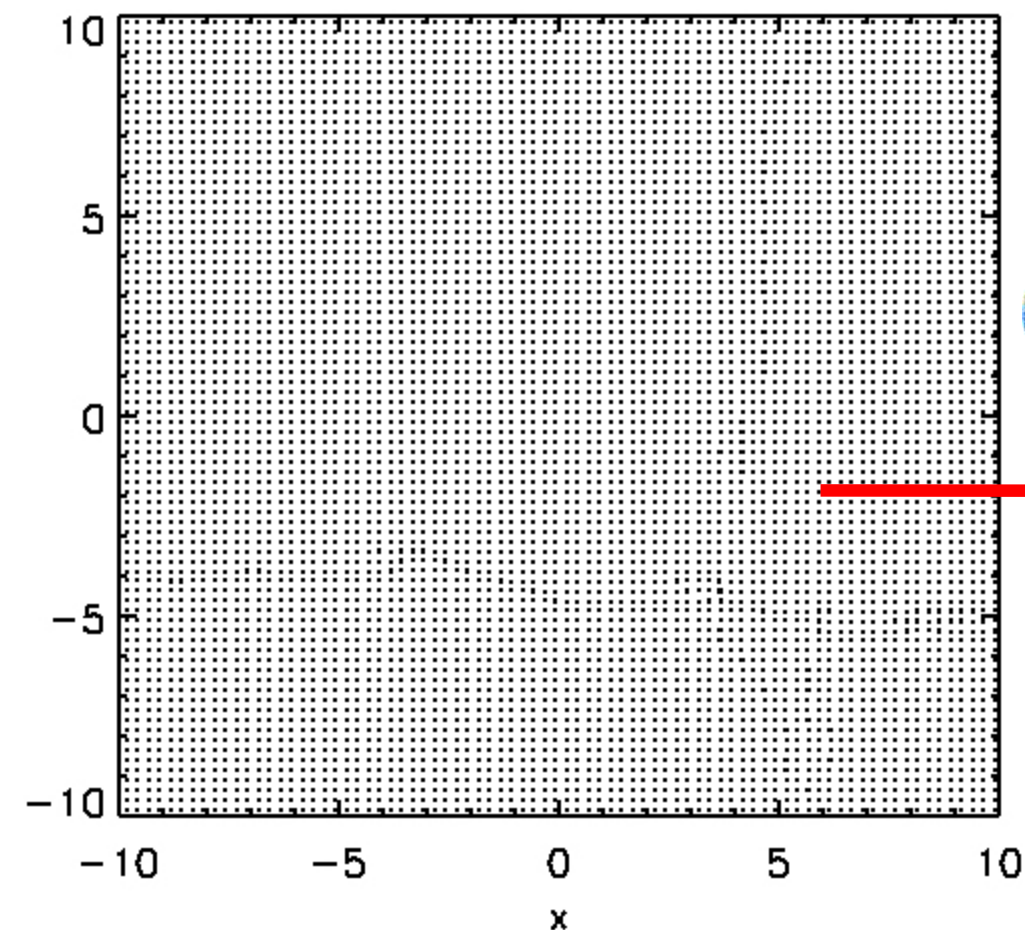
Ω_{stars}	~ 0.002
Ω_{gas}	~ 0.038
Ω_{dm}	~ 0.267
Ω_{Λ}	~ 0.693



1. Discretize the space

How to do cosmological N-Body simulation:

Ω_{stars}	~ 0.002
Ω_{gas}	~ 0.038
Ω_{dm}	~ 0.267
Ω_{Λ}	~ 0.693

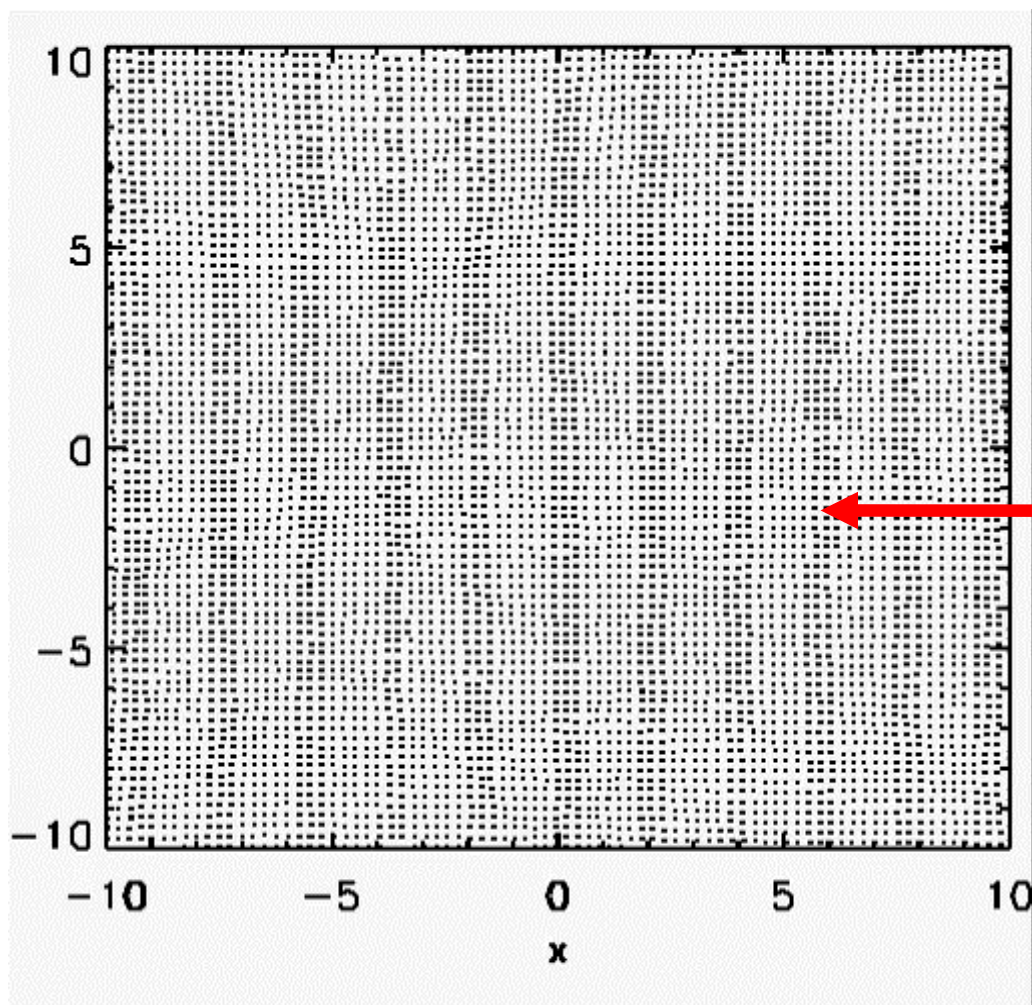


1. Discretize the space

2. Imprint of observed density fluctuations

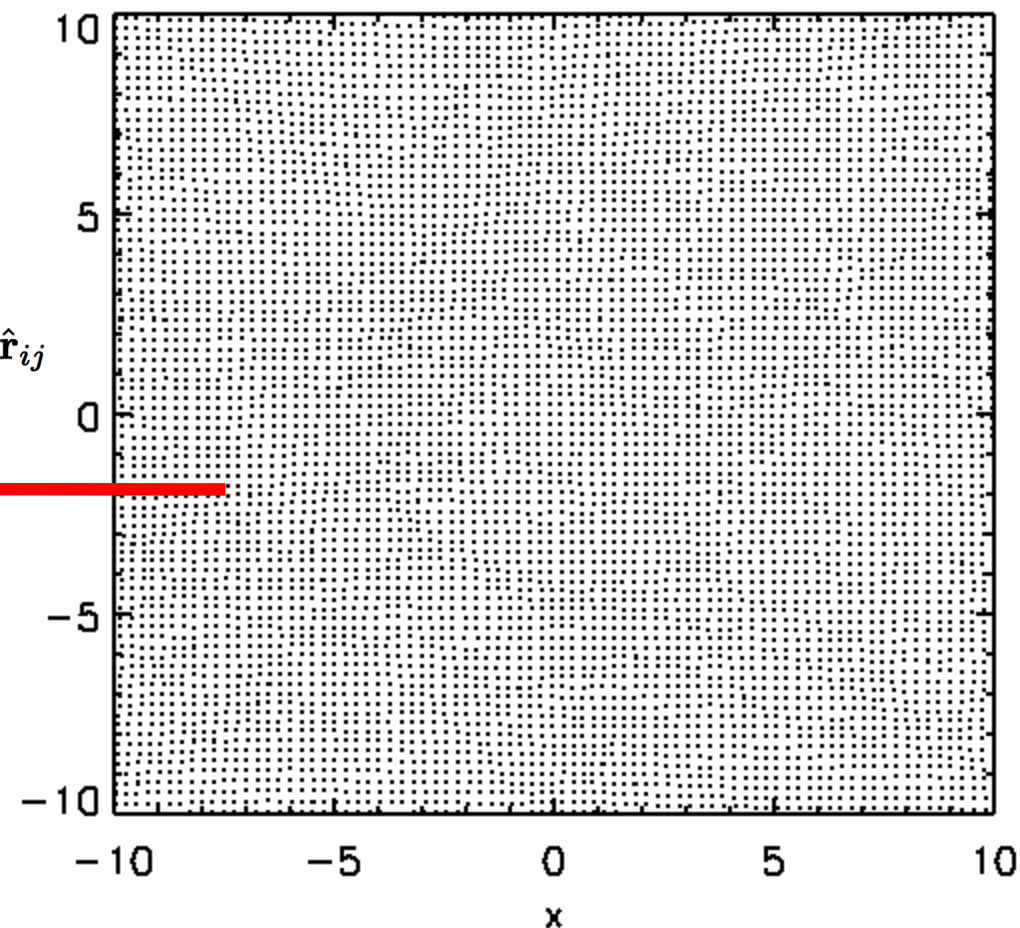
How to do cosmological N-Body simulation:

Ω_{stars}	~ 0.002
Ω_{gas}	~ 0.038
Ω_{dm}	~ 0.267
Ω_{Λ}	~ 0.693



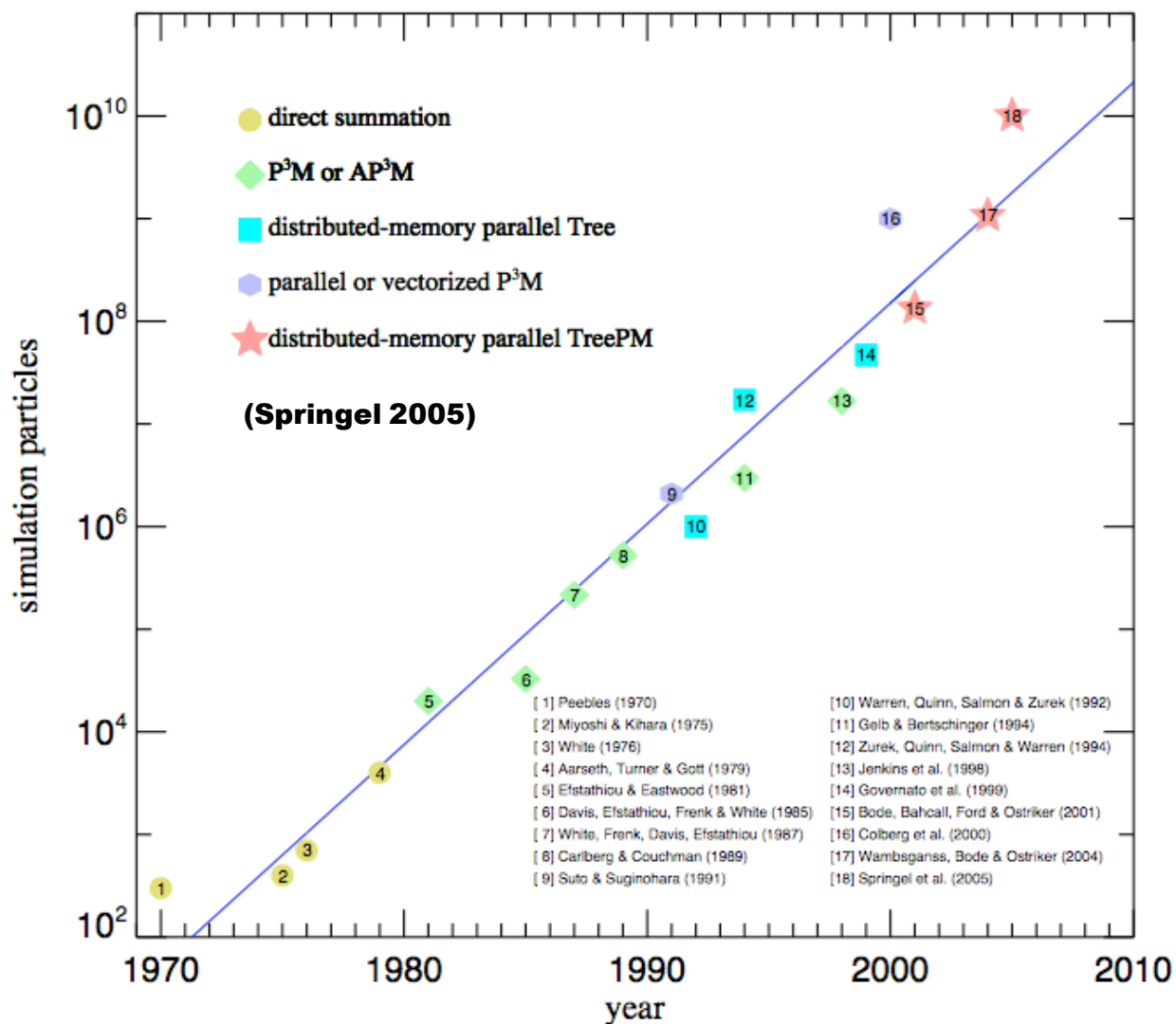
3. Solve the equations of motion

$$\mathbf{F}_i = - \sum_{j=0, j \neq i}^{j=N} \frac{G m_i m_j}{r_{ij}^2} \hat{\mathbf{r}}_{ij}$$

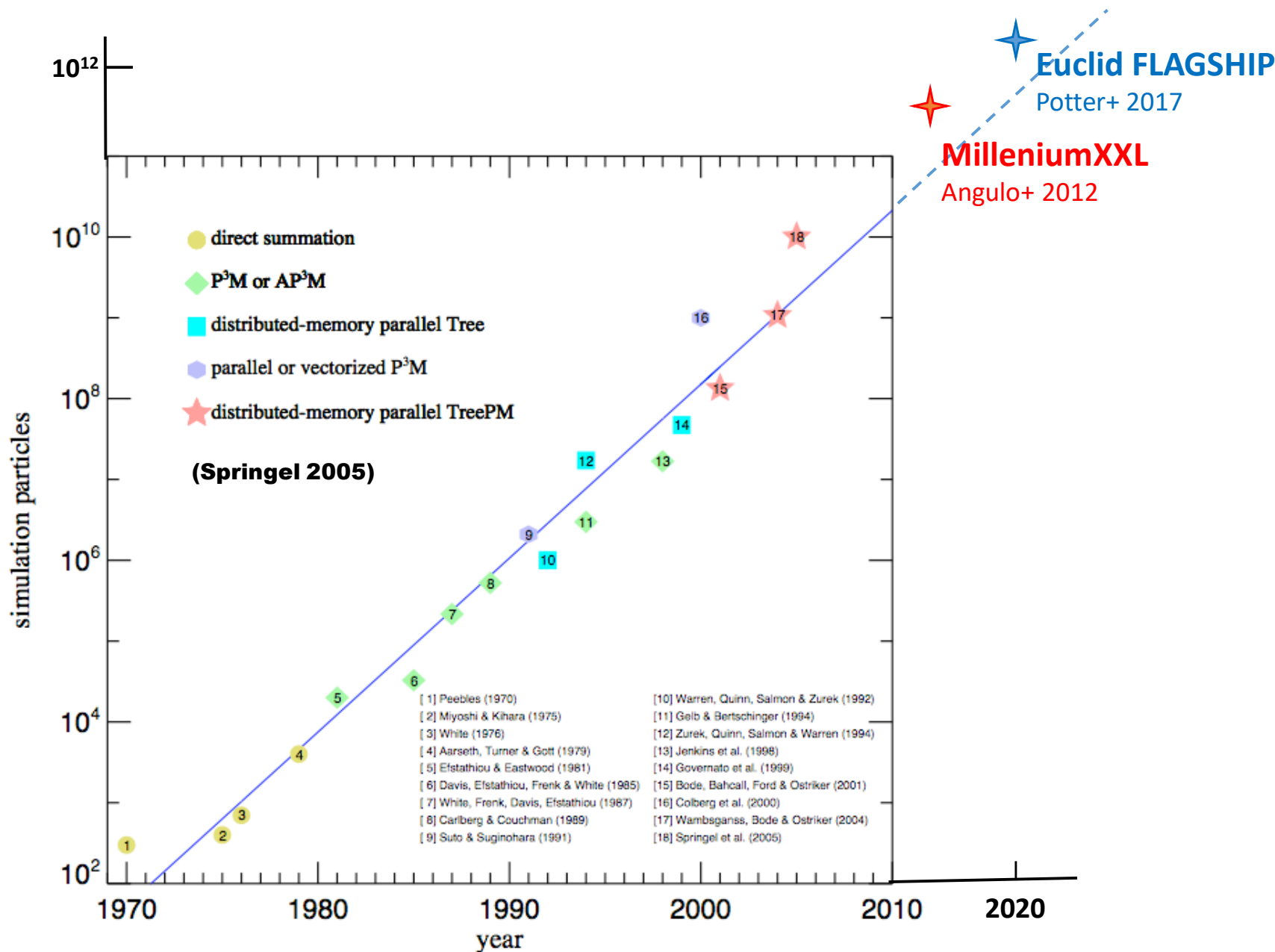


2. Imprint of observed density fluctuations

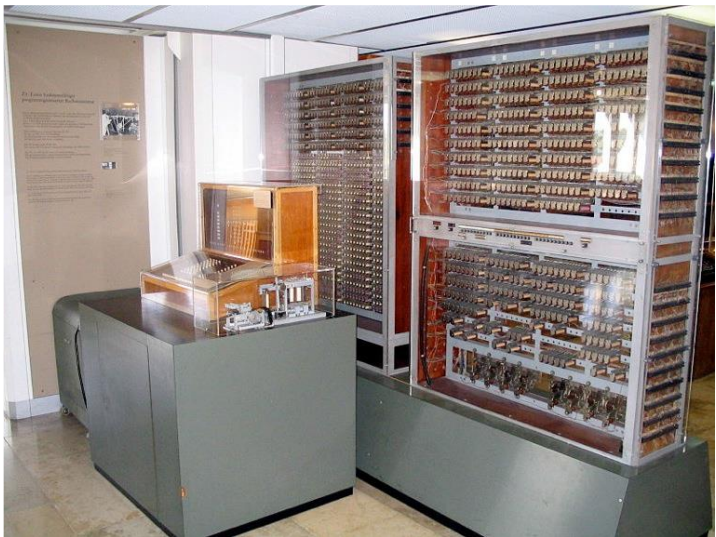
Growing computing power helps since then



Growing computing power helps since then



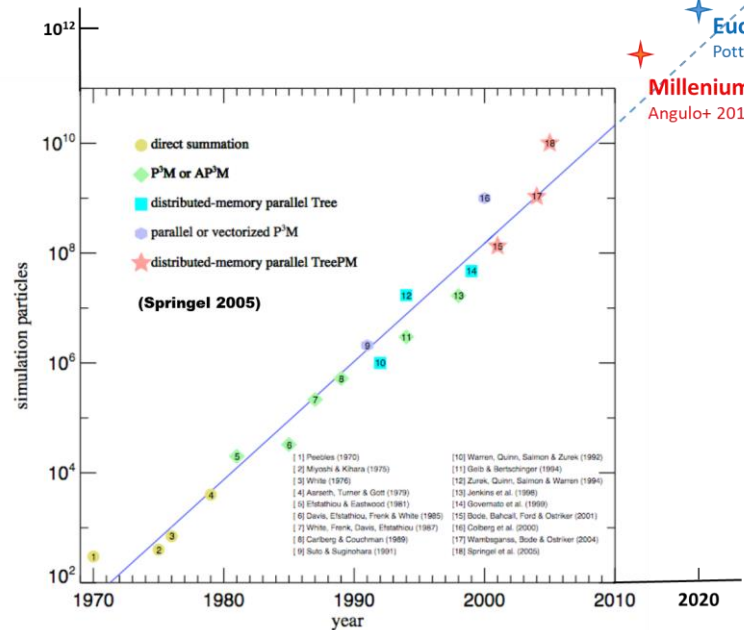
Growing computing power helps since then



Z3, 1941-1943 (Germany)
5 Computations per second



SuperMUC, 2013- (München)
3 Petaflops ($3 \cdot 10^{15}$ per second)



**Moore's Law: Doubles all 1.5 Years
(but see talk by Zhukov)**

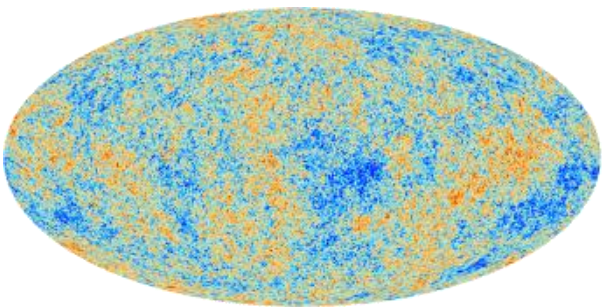
Z3 – SuperMUC: 1.4 Years

N-Body: 1970-2010: 1.3 Years

HPC Challenges in Astrophysics

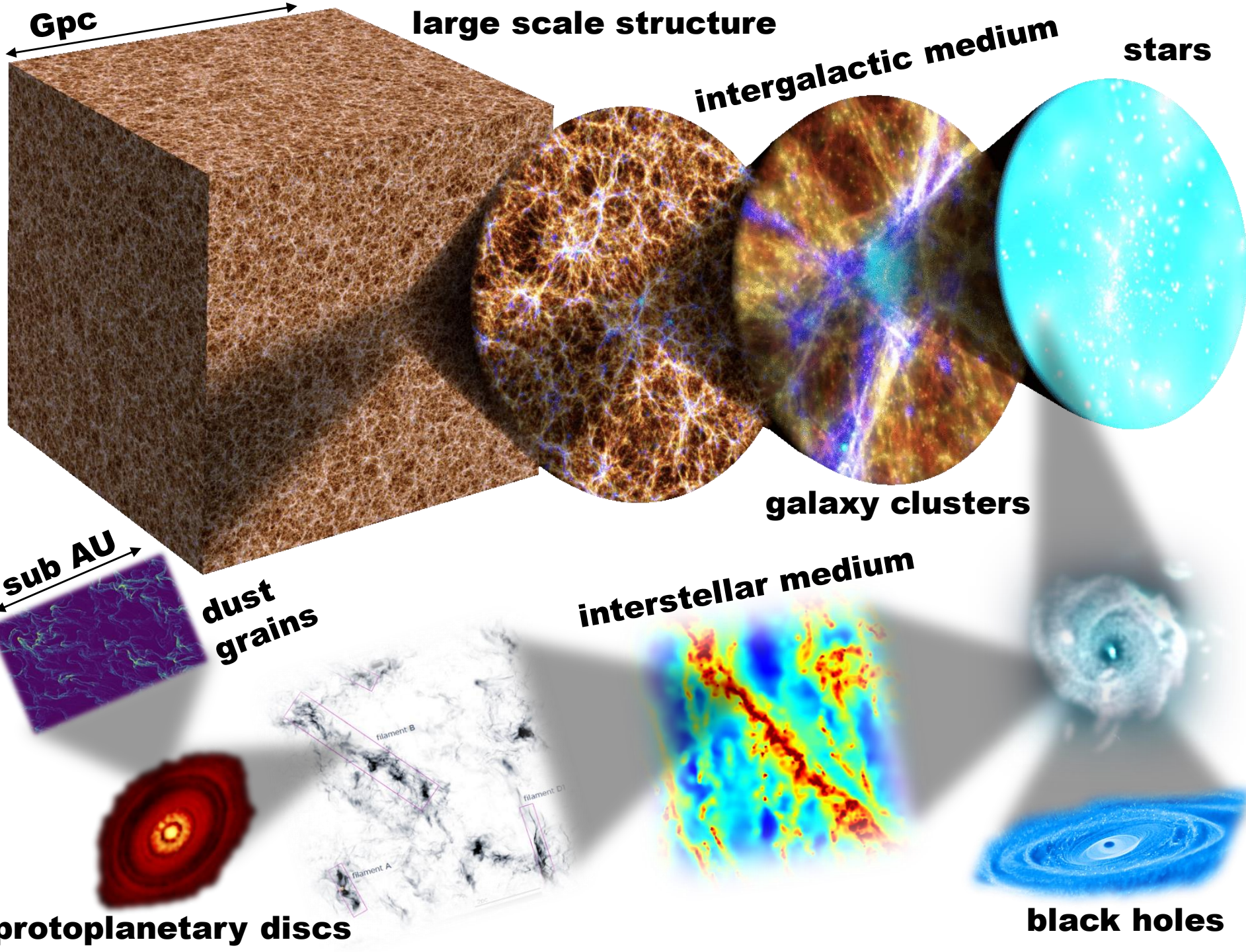
III) The Physics

The Computational Challenge

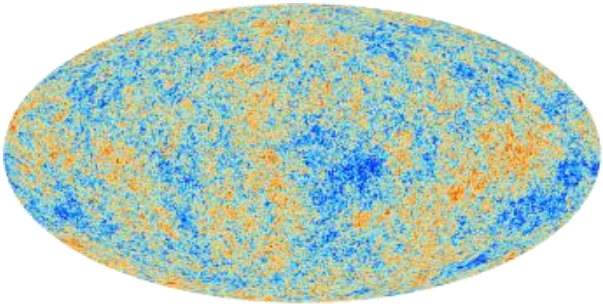


**multi-scale,
multi-physics**

Ω_{stars}	~ 0.002
Ω_{gas}	~ 0.04
Ω_{dm}	~ 0.23
Ω_{Λ}	~ 0.73



The Computational Challenge



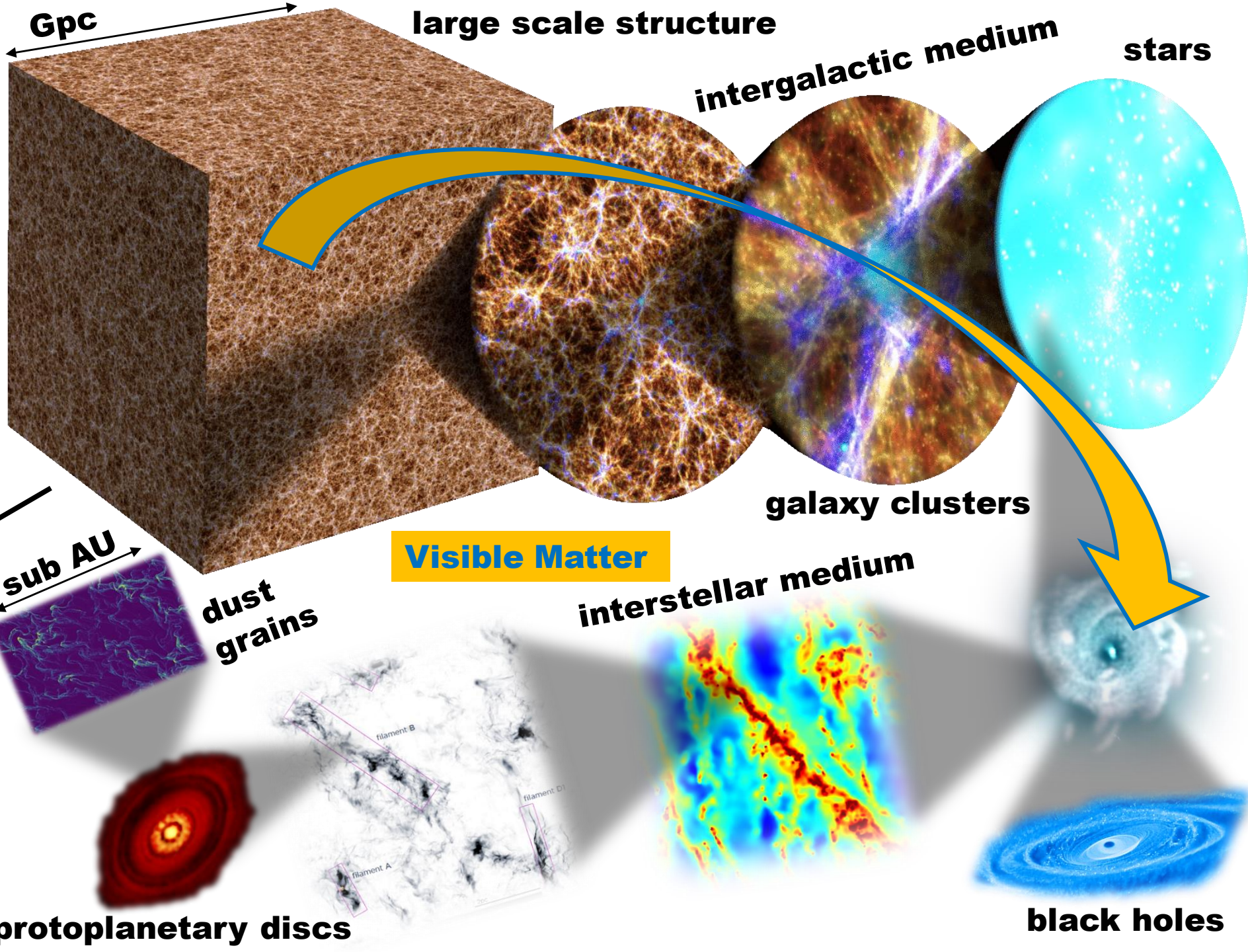
**multi-scale,
multi-physics**

$3 \cdot 10^{22} \text{ km}$



	λ_{mfp}	λ_{Lamor}	λ_{Debye}
electrons	1 kpc	700 km	6 km
protons		29000 km	

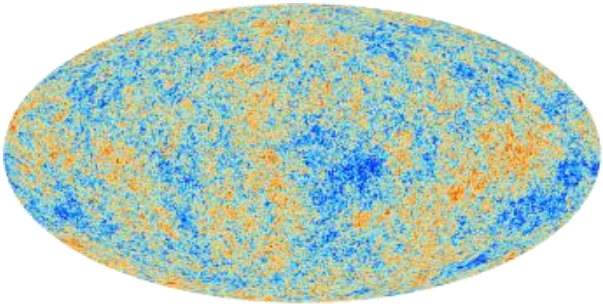
Plasma Physics!



protoplanetary discs

black holes

The Computational Challenge



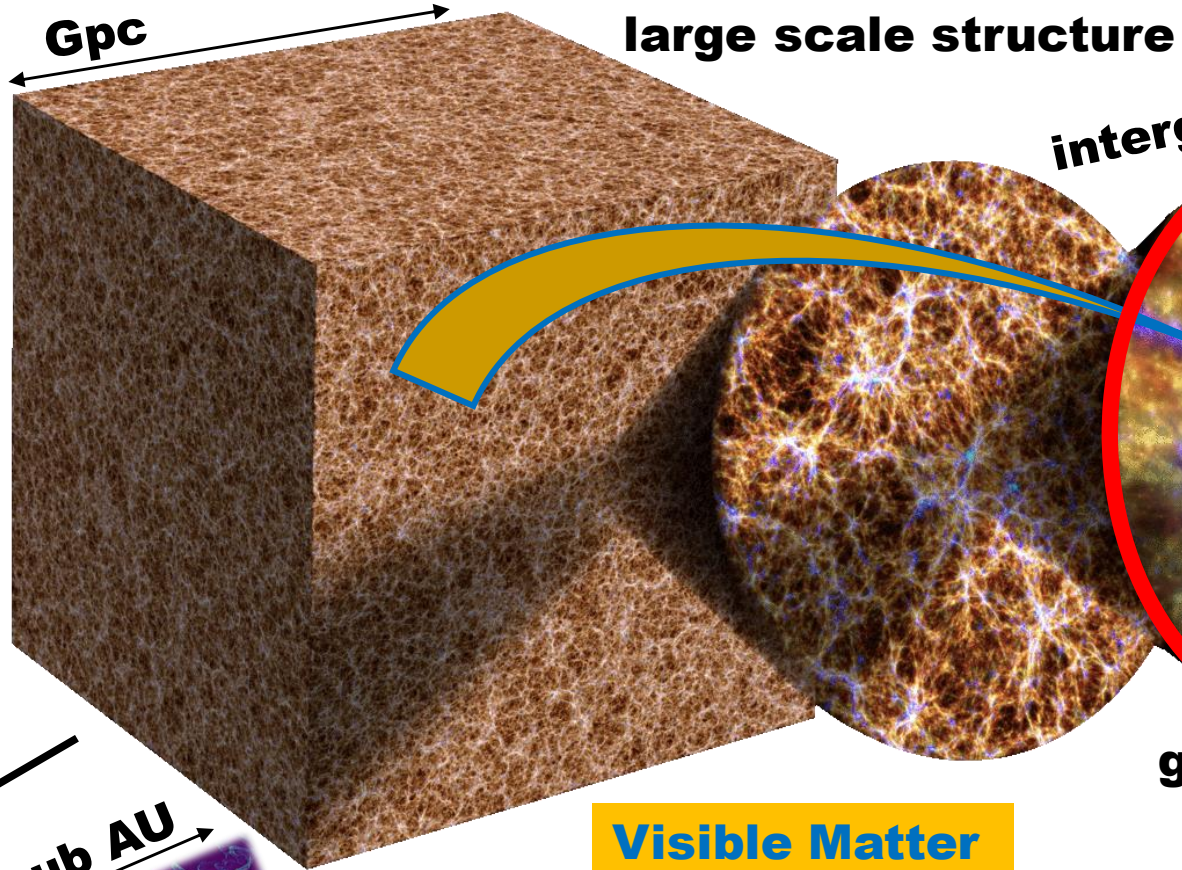
**multi-scale,
multi-physics**

$3 \cdot 10^{22} \text{ km}$

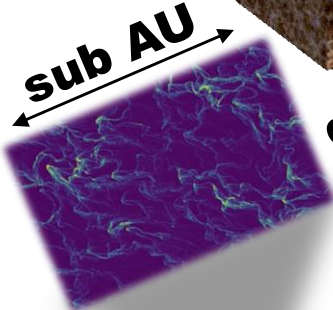


	λ_{mfp}	λ_{Lamor}	λ_{Debye}
electrons	1 kpc	700 km	6 km
protons		29000 km	

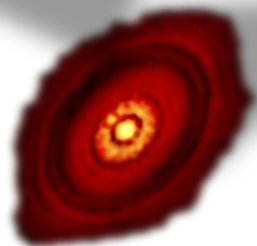
Plasma Physics!



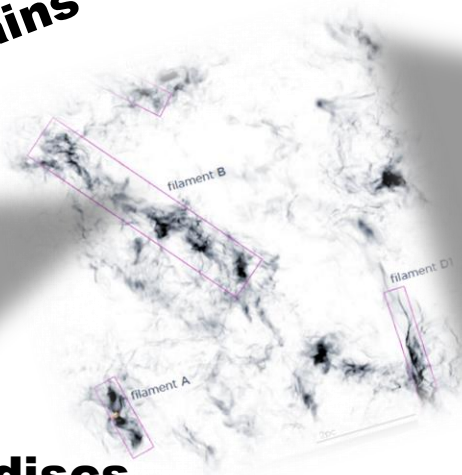
Visible Matter



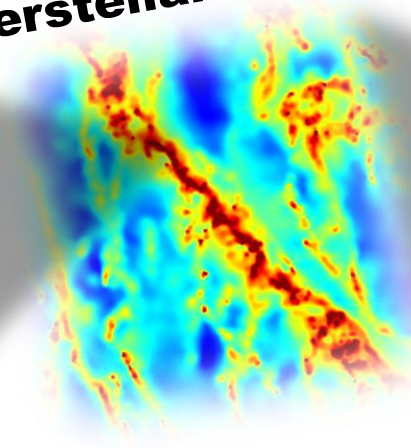
dust grains



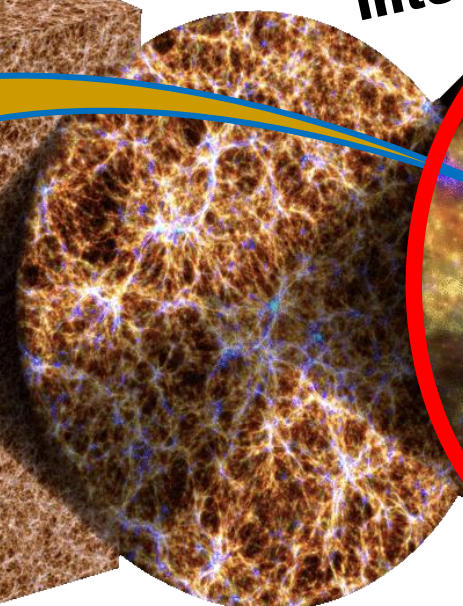
protoplanetary discs



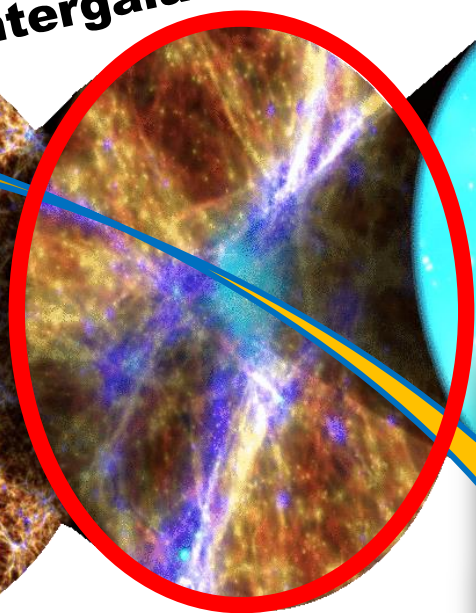
interstellar medium



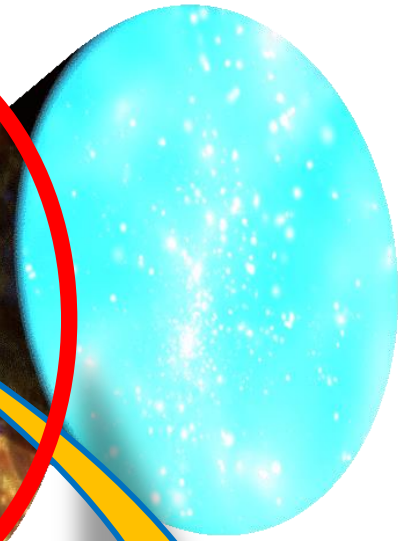
intergalactic medium



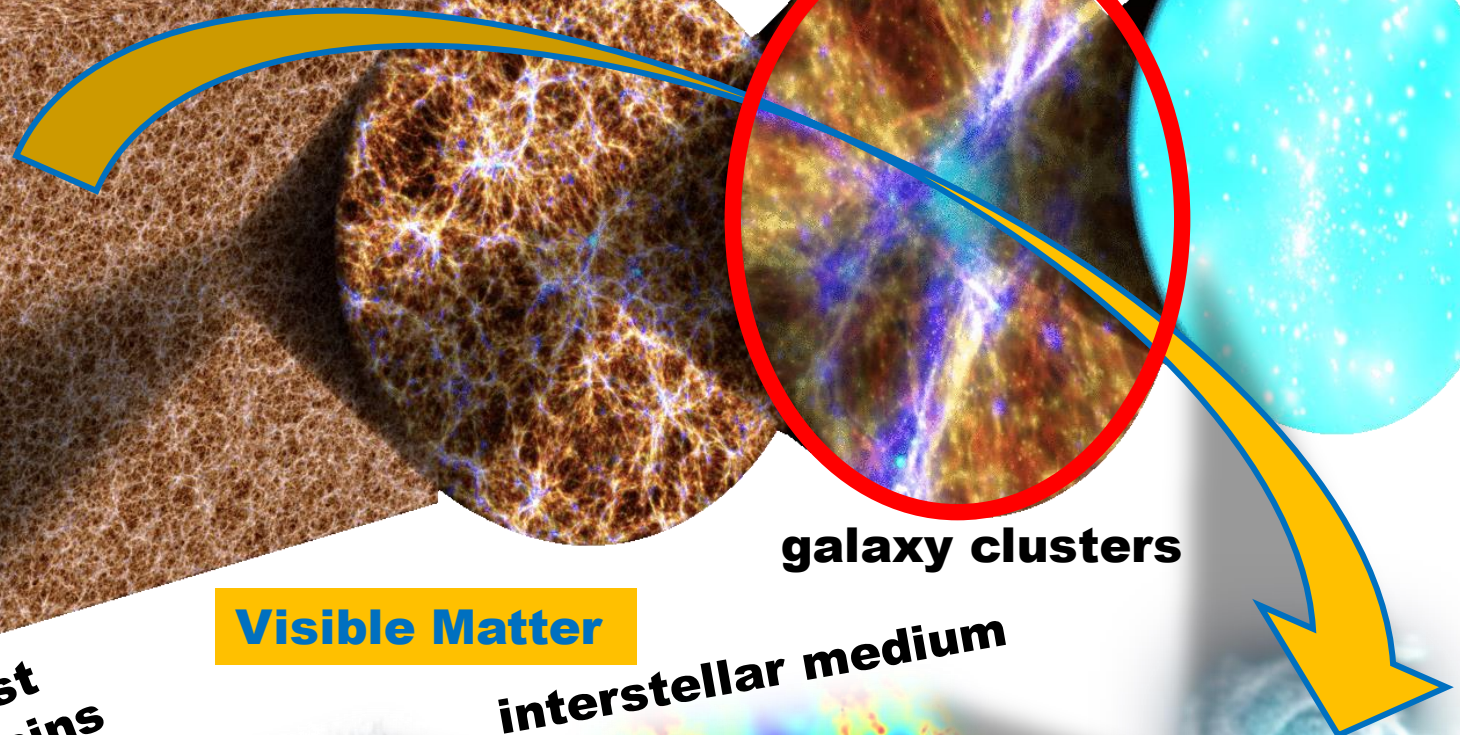
galaxy clusters



stars



black holes



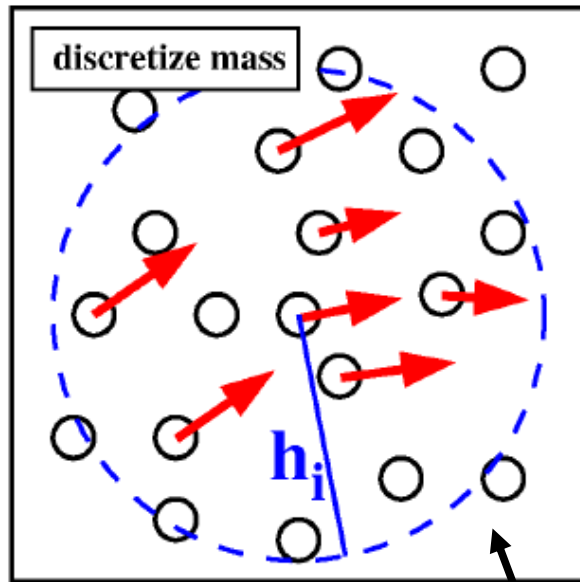
Basics: hydro-dynamics for simulations

Ω_{stars}	~ 0.002
Ω_{gas}	~ 0.038
Ω_{dm}	~ 0.267
Ω_{Λ}	~ 0.693

Hydrodynamic methods and
sub-resolution models
for cosmological simulations

Milena Valentini^{*,†,§} and Klaus Dolag^{*,†,§}

Lagrangian



$\underbrace{\frac{d}{dt}}_{\text{Lagrangian derivative}}$

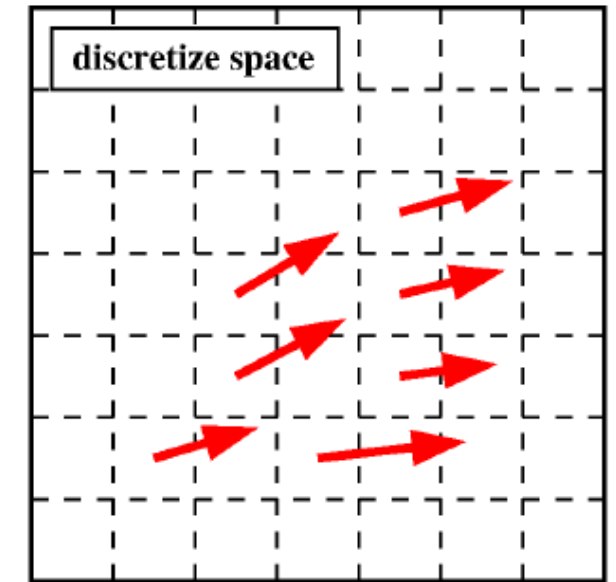
=

$\underbrace{\frac{\partial}{\partial t}}_{\text{Eulerian derivative}}$

+

$\underbrace{\vec{v} \cdot \vec{\nabla}}_{\text{convective derivative}}$

Eulerian



a) Discretize either mass or volume

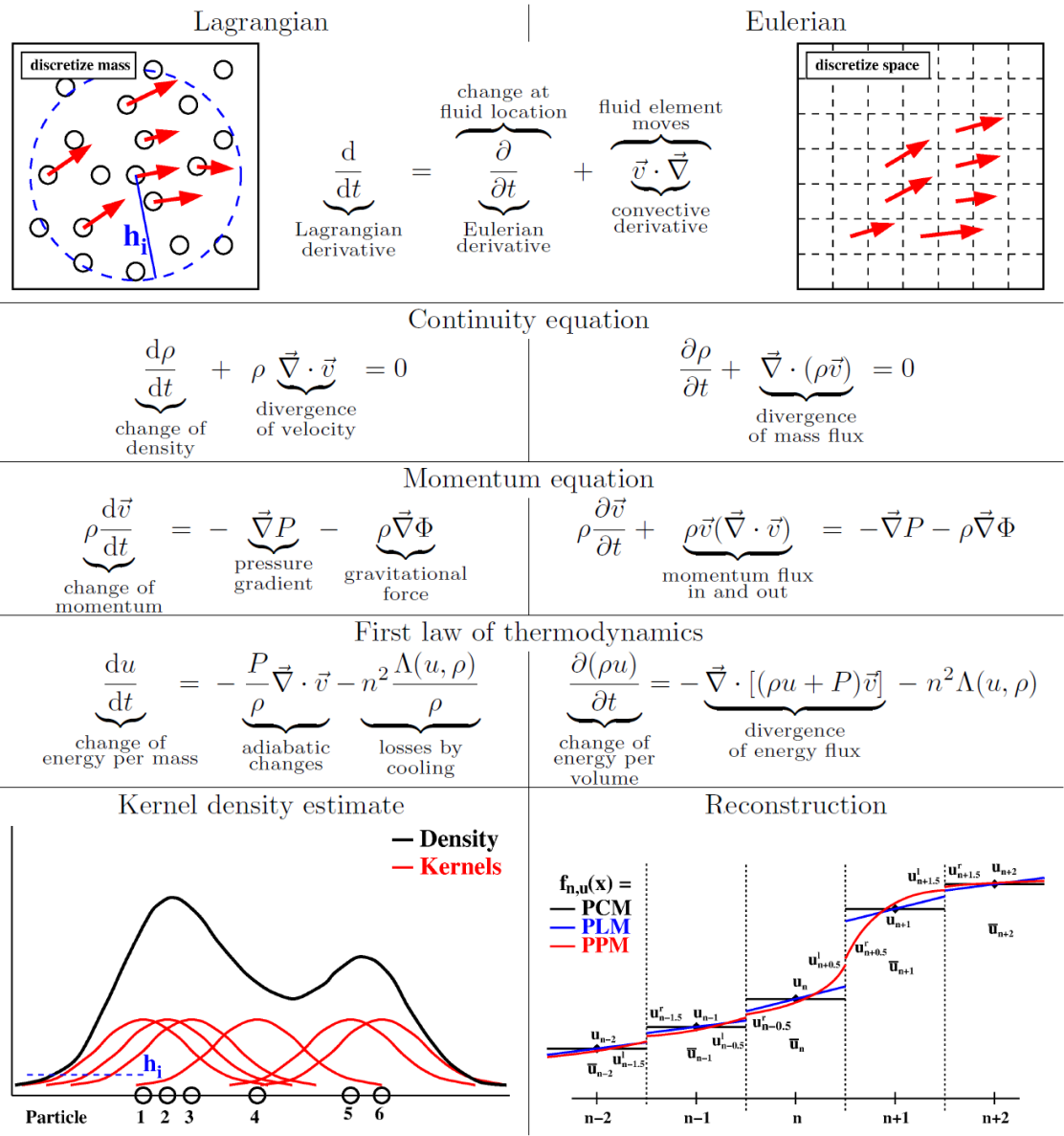
**Easy to couple to classical
N-body simulations.**

Basics: hydro-dynamics for simulations

Ω_{stars}	~ 0.002
Ω_{gas}	~ 0.038
Ω_{dm}	~ 0.267
Ω_{Λ}	~ 0.693

Hydrodynamic methods and
sub-resolution models
for cosmological simulations

Milena Valentini^{*,†,§} and Klaus Dolag^{*,†,§}

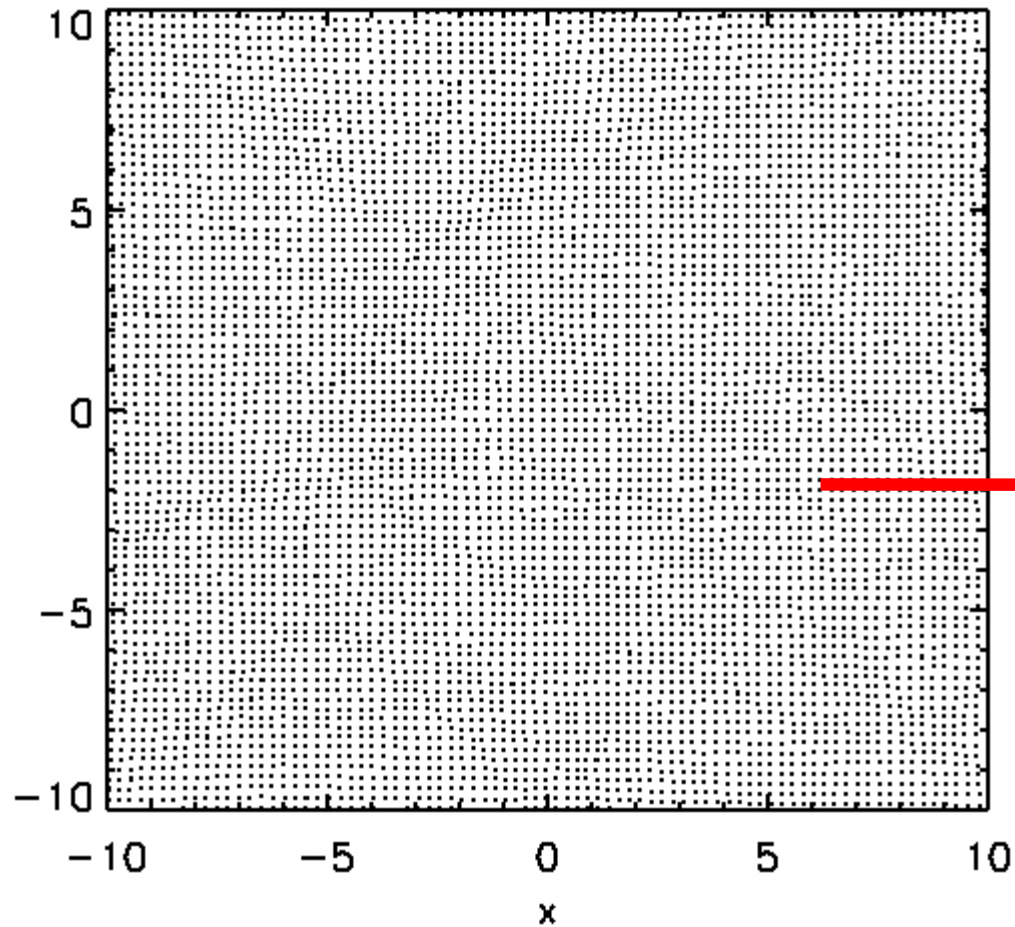


- a) Discretize either mass or volume
- b) Solve the Euler equations

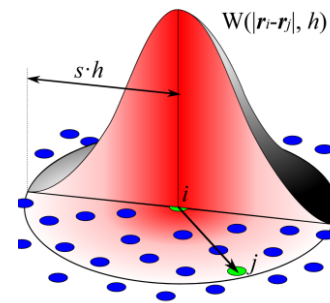
Fig. 3.2. Comparison of the concept of Lagrangian and Eulerian formulation of hydrodynamics and the resulting set of equations.

Basics: hydro-dynamics for simulations

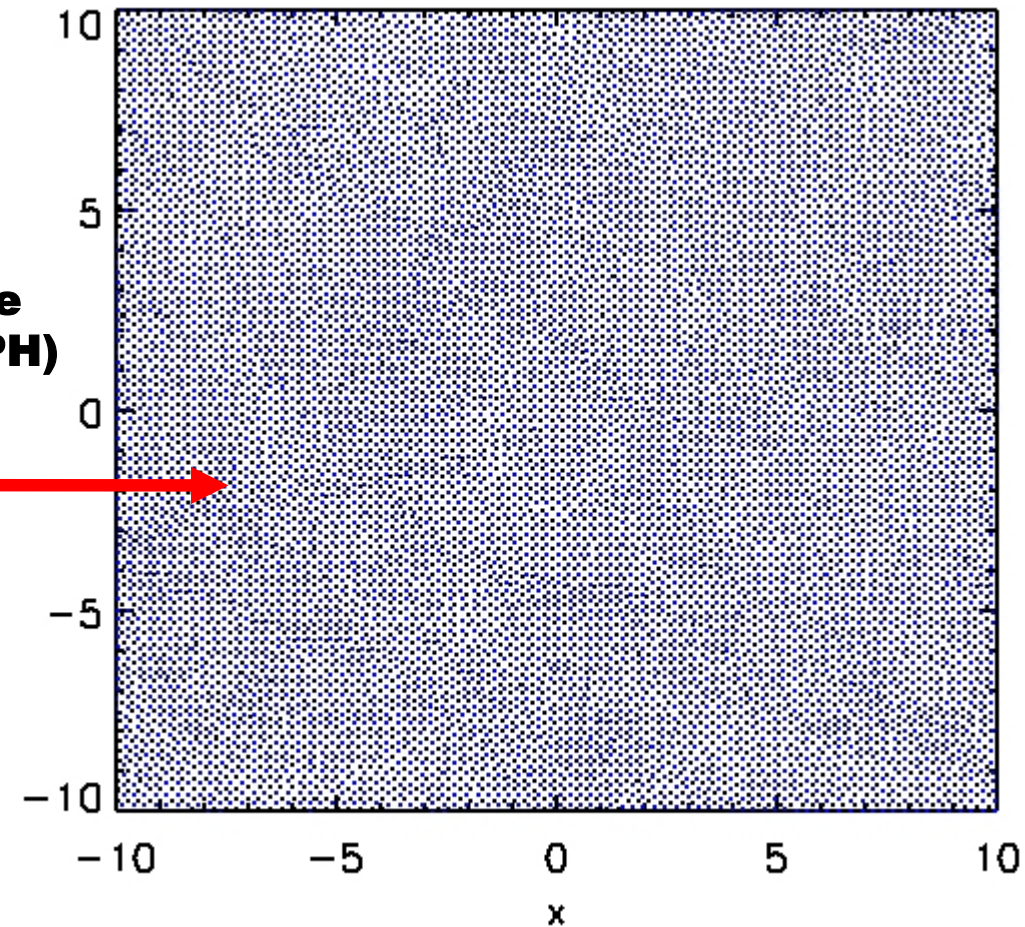
$\Omega_{\text{stars}} \sim 0.002$
 $\Omega_{\text{gas}} \sim 0.038$
 $\Omega_{\text{dm}} \sim 0.267$
 $\Omega_{\Lambda} \sim 0.693$



**Smoothed Particle
Hydrodynamics (SPH)**



by Jlcercos
wikipedia.org

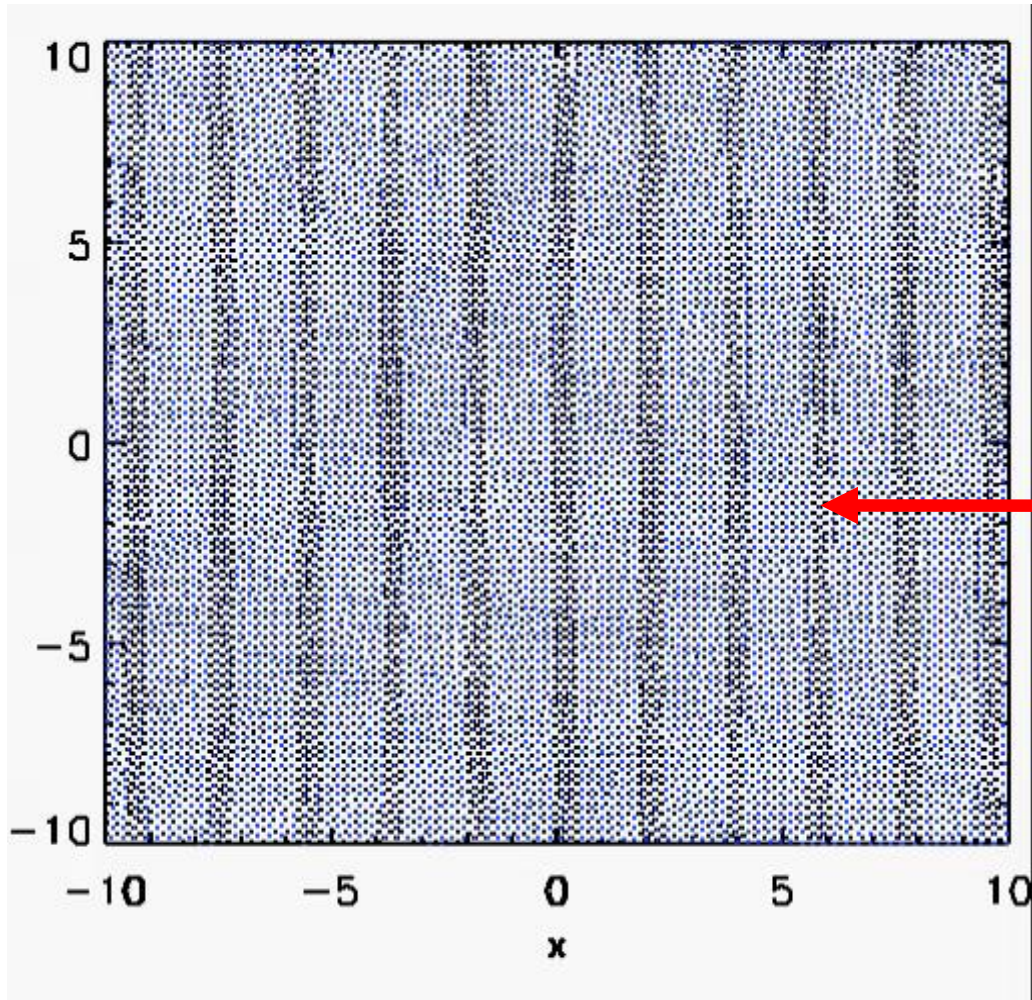


3. Solve the equations of motion

4. Add additional component to the fluid

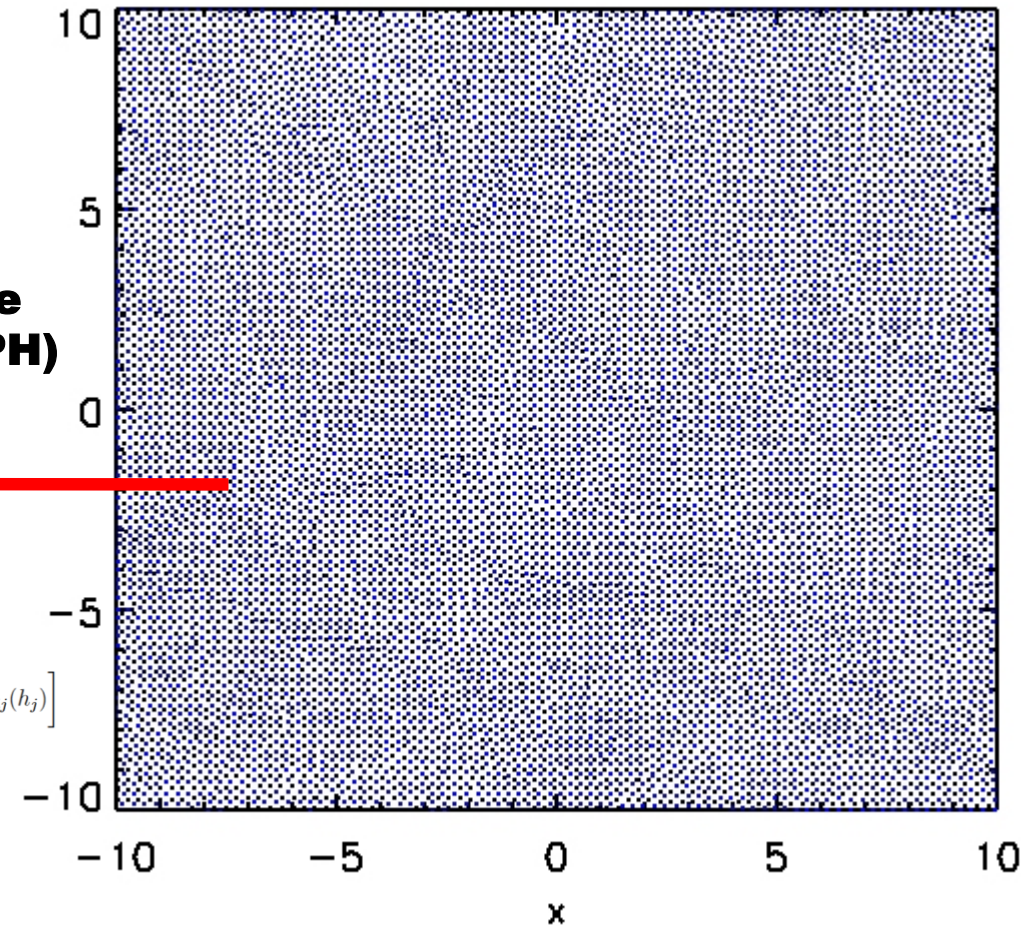
Basics: hydro-dynamics for simulations

$\Omega_{\text{stars}} \sim 0.002$
 $\Omega_{\text{gas}} \sim 0.038$
 $\Omega_{\text{dm}} \sim 0.267$
 $\Omega_{\Lambda} \sim 0.693$



Smoothed Particle Hydrodynamics (SPH)

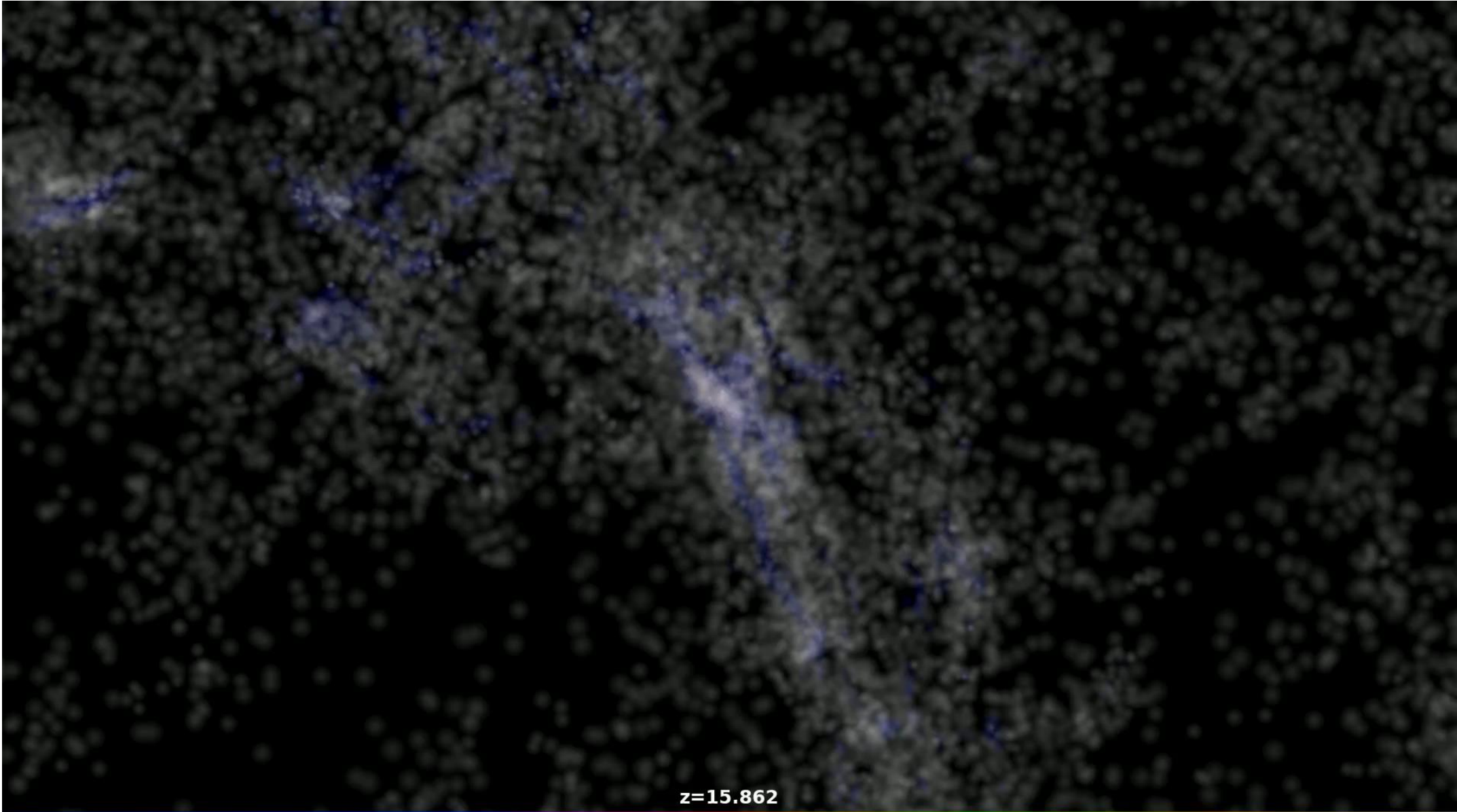
$$\frac{du_i}{dt} = f_i \frac{P_i}{\rho_i^2} \sum_j m_j (\mathbf{v}_i - \mathbf{v}_j) \cdot \nabla W_{ij}(h_i)$$
$$\frac{d\mathbf{v}_i}{dt} = - \sum_{j=1}^N m_j \left[f_i \frac{P_i}{\rho_i^2} \nabla_i W_{ij}(h_i) + f_j \frac{P_j}{\rho_j^2} \nabla_i W_{ij}(h_j) \right]$$



5. Solve the equations including motion for hydrodynamics

4. Add additional component to the fluid

Galaxy clusters, the hot atmosphere of massive galaxies

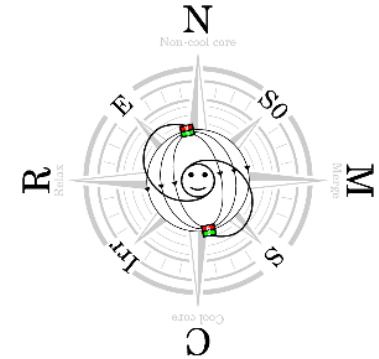
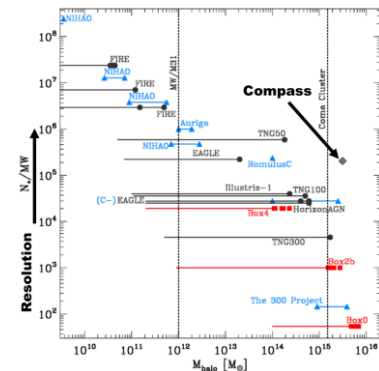


Galaxy Clusters:

$M \sim 2 \times 10^{15} M_{\text{sol}}$

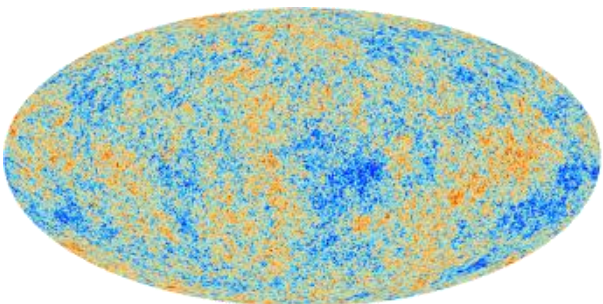
almost 10^9 part in R_{vir}
 ~ 90.000 galaxies
 ~ 250.000 timesteps

$\epsilon_{\text{gas/stars}} \sim 240 \text{ pc/h}$



Mach number: **2** **3** **4** **>5**

The Computational Challenge



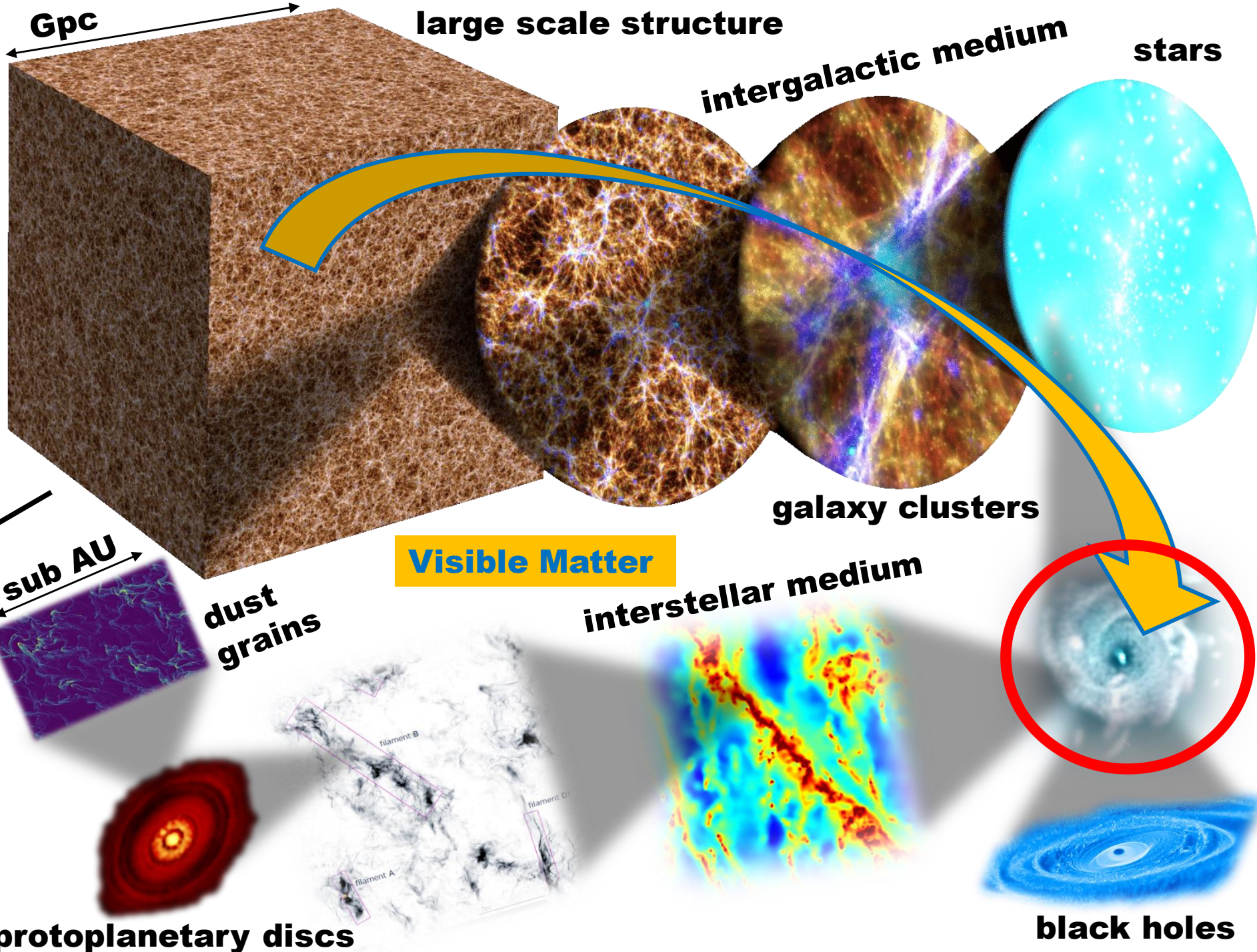
**multi-scale,
multi-physics**

$3 \cdot 10^{22} \text{ km}$



	λ_{mfp}	λ_{Lamor}	λ_{Debye}
electrons	1 kpc	700 km	6 km
protons		29000 km	

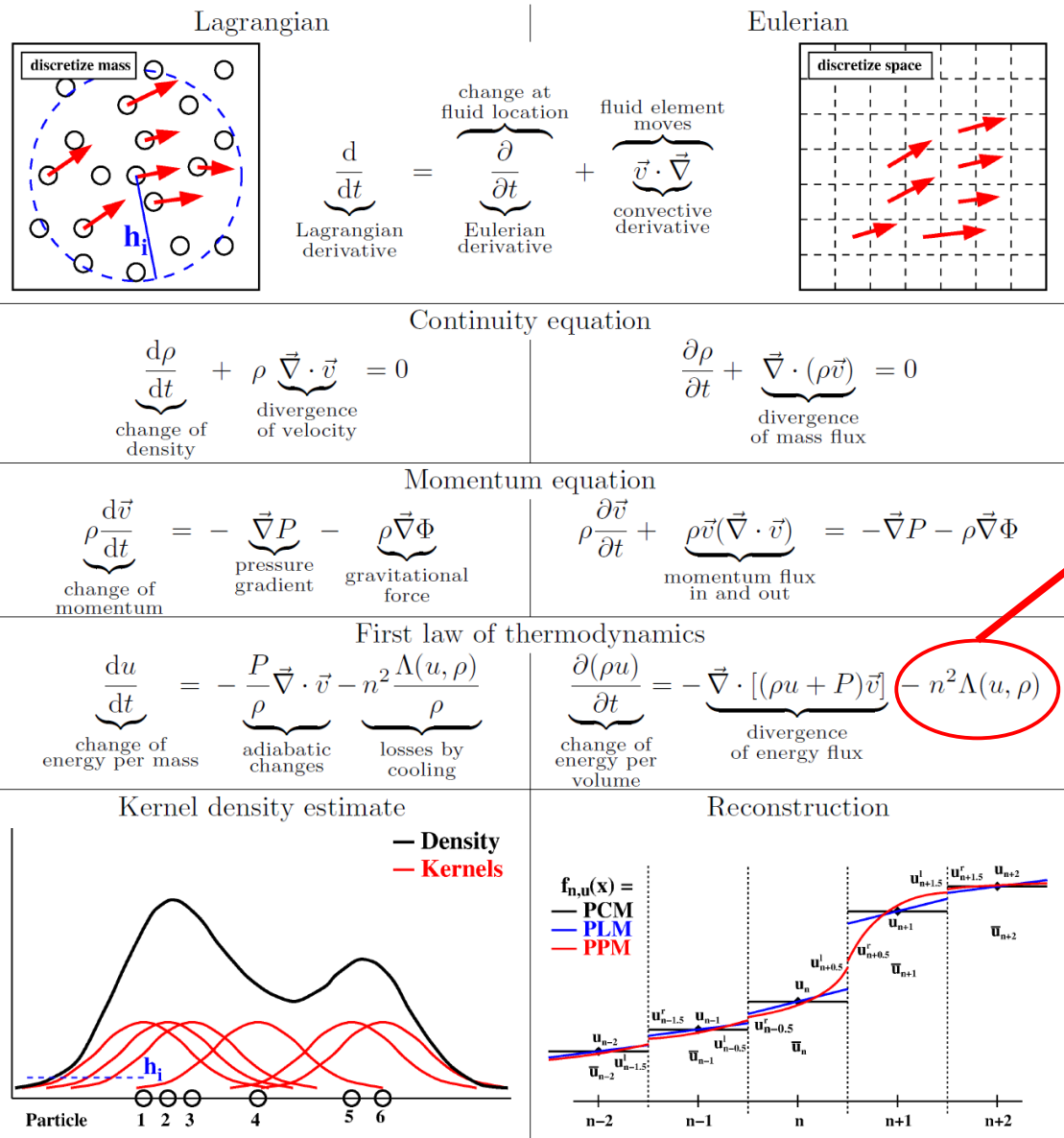
Plasma Physics!



Gpc

Basics: hydro-dynamics for simulations

Ω_{stars}	~ 0.002
Ω_{gas}	~ 0.038
Ω_{dm}	~ 0.267
Ω_{Λ}	~ 0.693



Hydrodynamic methods and sub-resolution models for cosmological simulations

Milena Valentini^{*,†,§} and Klaus Dolag^{*,†,§}

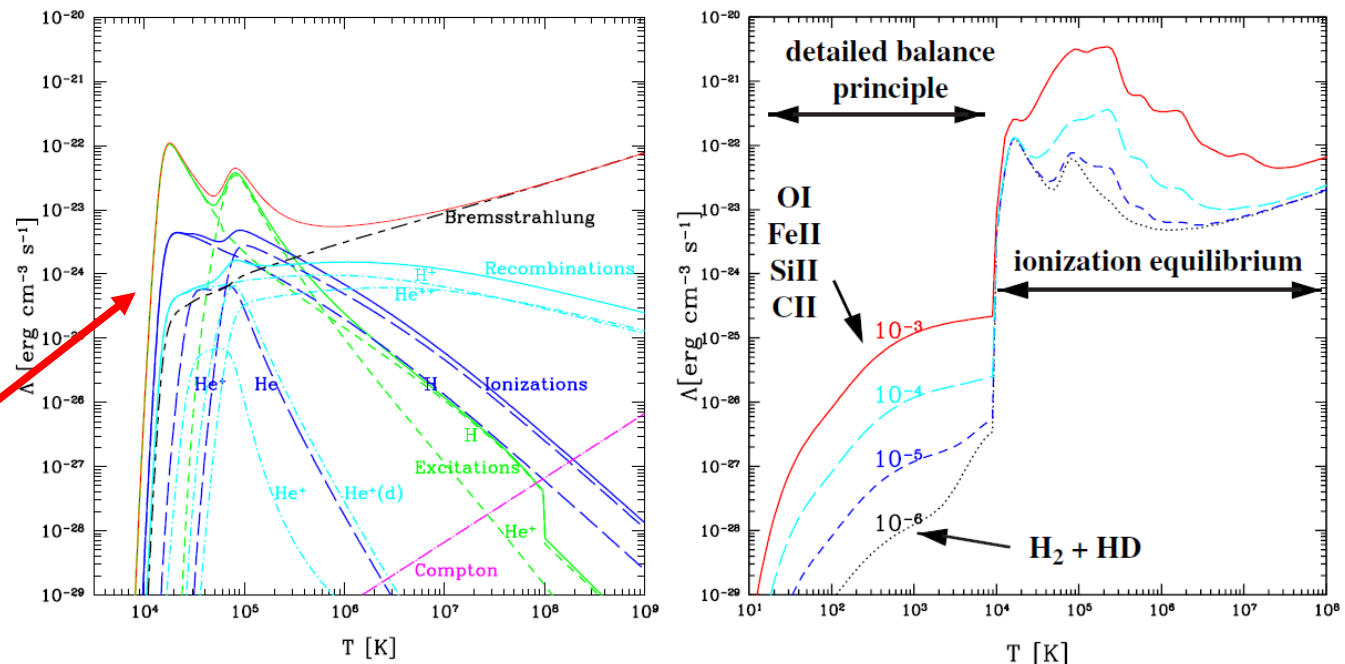


Fig. 3.9. Left panel: The total cooling curve (solid line) and its composition from different processes for a primordial mixture of H and He. Figure taken from [17]. Right panel: The total cooling curve as a function of different metallicity. The part below 10^4 K also takes into account cooling by molecules (e.g., HD and H_2) and metal lines. Figure taken from [122].

- a) Discretize either mass or volume
- b) Solve the Euler equations
- c) Include cooling due to radiation

Fig. 3.2. Comparison of the concept of Lagrangian and Eulerian formulation of hydrodynamics and the resulting set of equations.

Basics: Simulation of star-formation

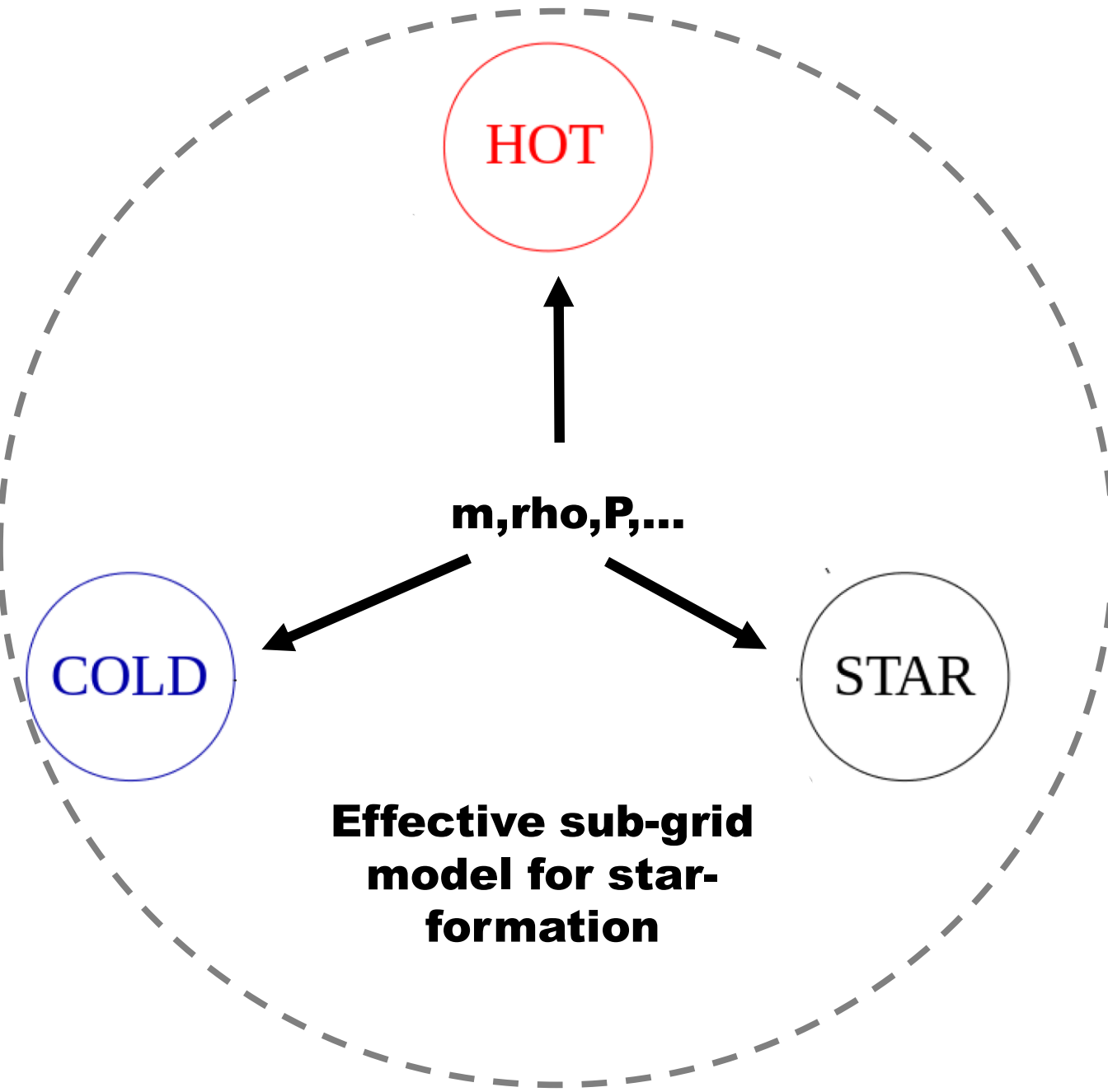
Ω_{stars}	~ 0.002
Ω_{gas}	~ 0.038
Ω_{dm}	~ 0.267
Ω_{Λ}	~ 0.693



Resolution element
 x, v, m, ρ, P, \dots

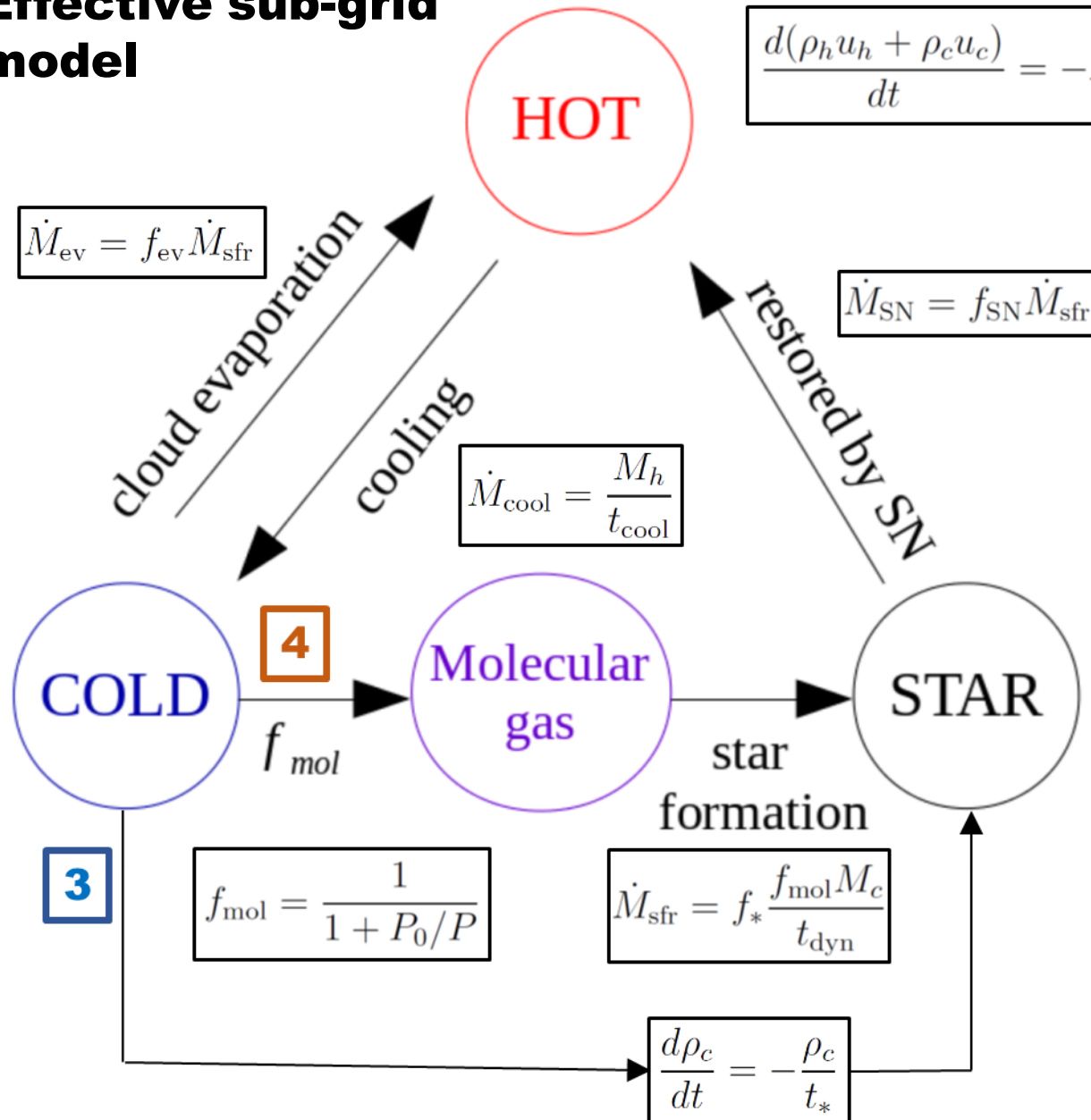
Basics: Simulation of star-formation

Ω_{stars}	~ 0.002
Ω_{gas}	~ 0.038
Ω_{dm}	~ 0.267
Ω_{Λ}	~ 0.693



Basics: Simulation of star-formation

Effective sub-grid model



$$\frac{d(\rho_h u_h + \rho_c u_c)}{dt} = -\Lambda_{net}(\rho_h u_h) + \beta \frac{\rho_c}{t_*} u_{SN} - (1 - \beta) \frac{\rho_c}{t_*} u_c$$

$$\dot{M}_* = \dot{M}_{sfr} - \dot{M}_{SN}$$

$$\dot{M}_c = \dot{M}_{cool} - \dot{M}_{sfr} - \dot{M}_{ev}$$

$$\dot{M}_h = -\dot{M}_{cool} + \dot{M}_{SN} + \dot{M}_{ev}$$

$$\begin{aligned} \Omega_{stars} &\sim 0.002 \\ \Omega_{gas} &\sim 0.038 \\ \Omega_{dm} &\sim 0.267 \\ \Omega_{\Lambda} &\sim 0.693 \end{aligned}$$

System of differential equations
-> Solutions

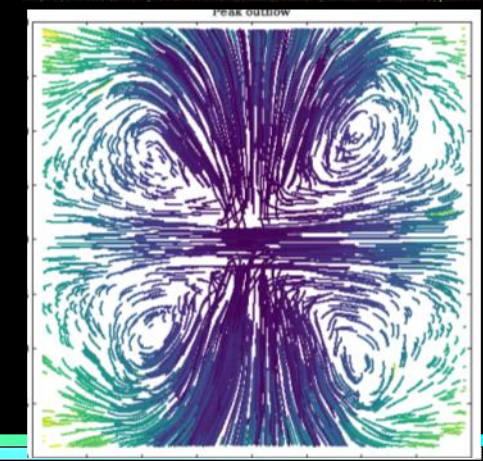
Different Variants:

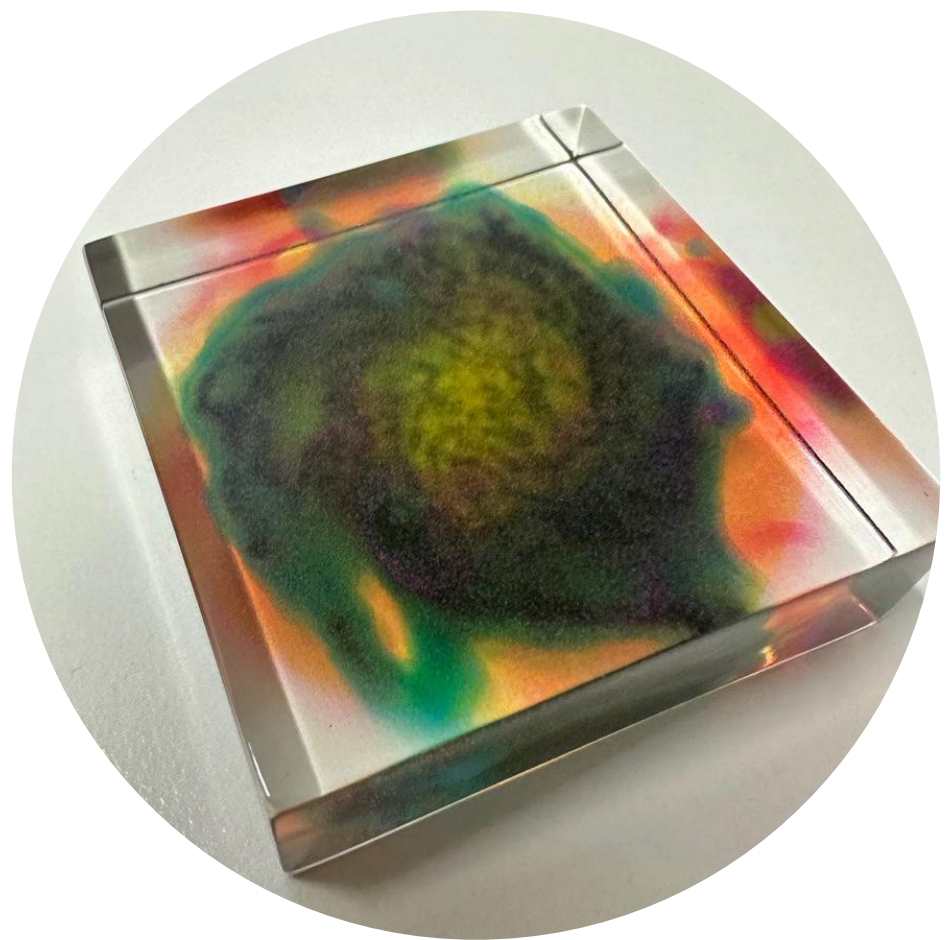
- **3 Phases**
- **4 Phases**
- **Equilibrium solution**
- **Dynamical solution**
- **Empirically motivated**
- **Theoretically motivated**

Extensions:

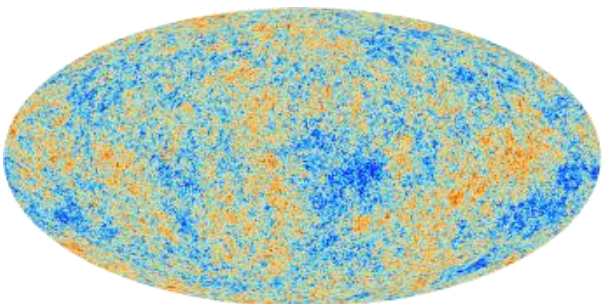
- **Stellar/Chemical Evolution**
- **Kinetic feedback**

Gyr = 0.28
 $z = 15.304$





The Computational Challenge



**multi-scale,
multi-physics**

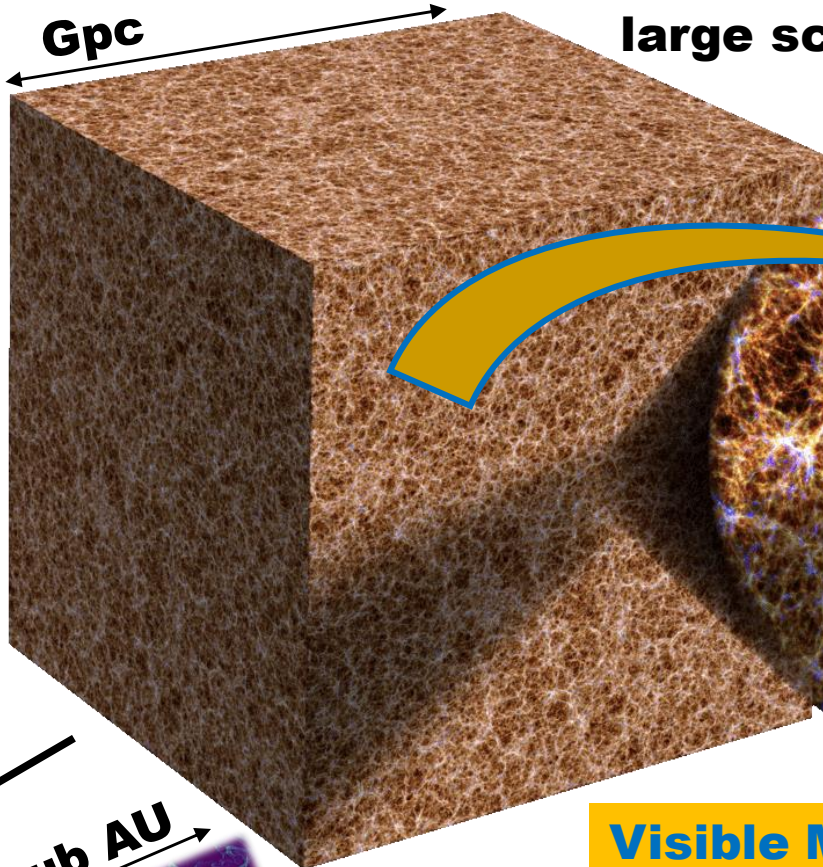
$3 \cdot 10^{22} \text{ km}$



	λ_{mfp}	λ_{Lamor}	λ_{Debye}
electrons	1 kpc	700 km	6 km
protons		29000 km	

Plasma Physics!

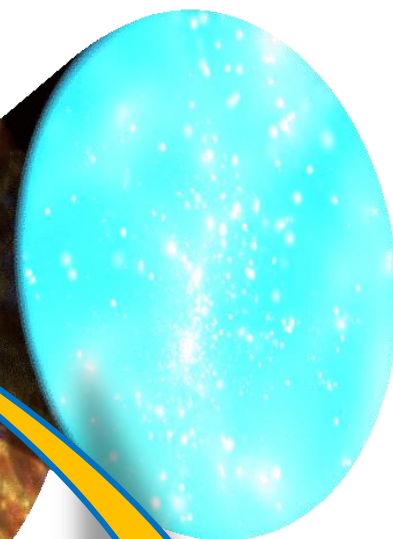
Gpc



large scale structure

intergalactic medium

stars

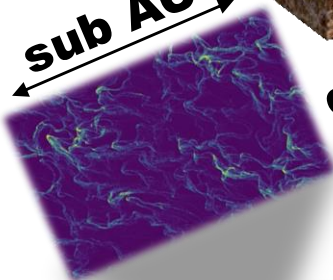


galaxy clusters

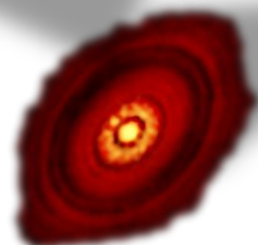
Visible Matter

interstellar medium

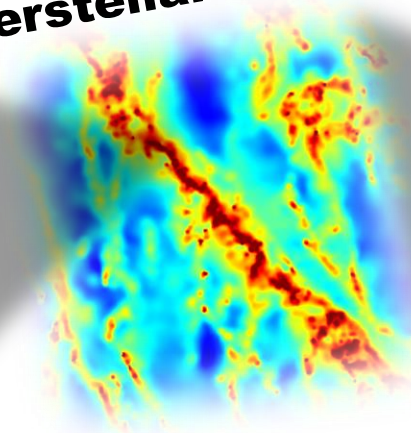
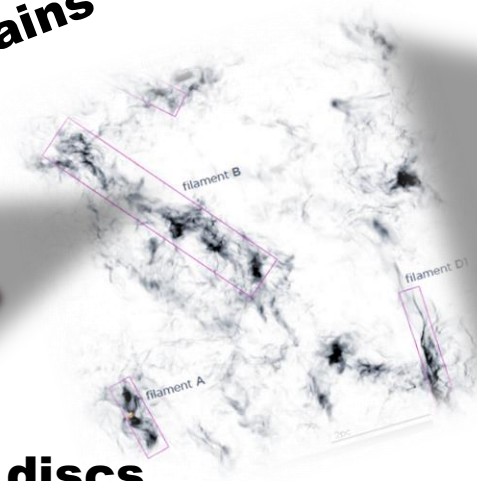
sub AU



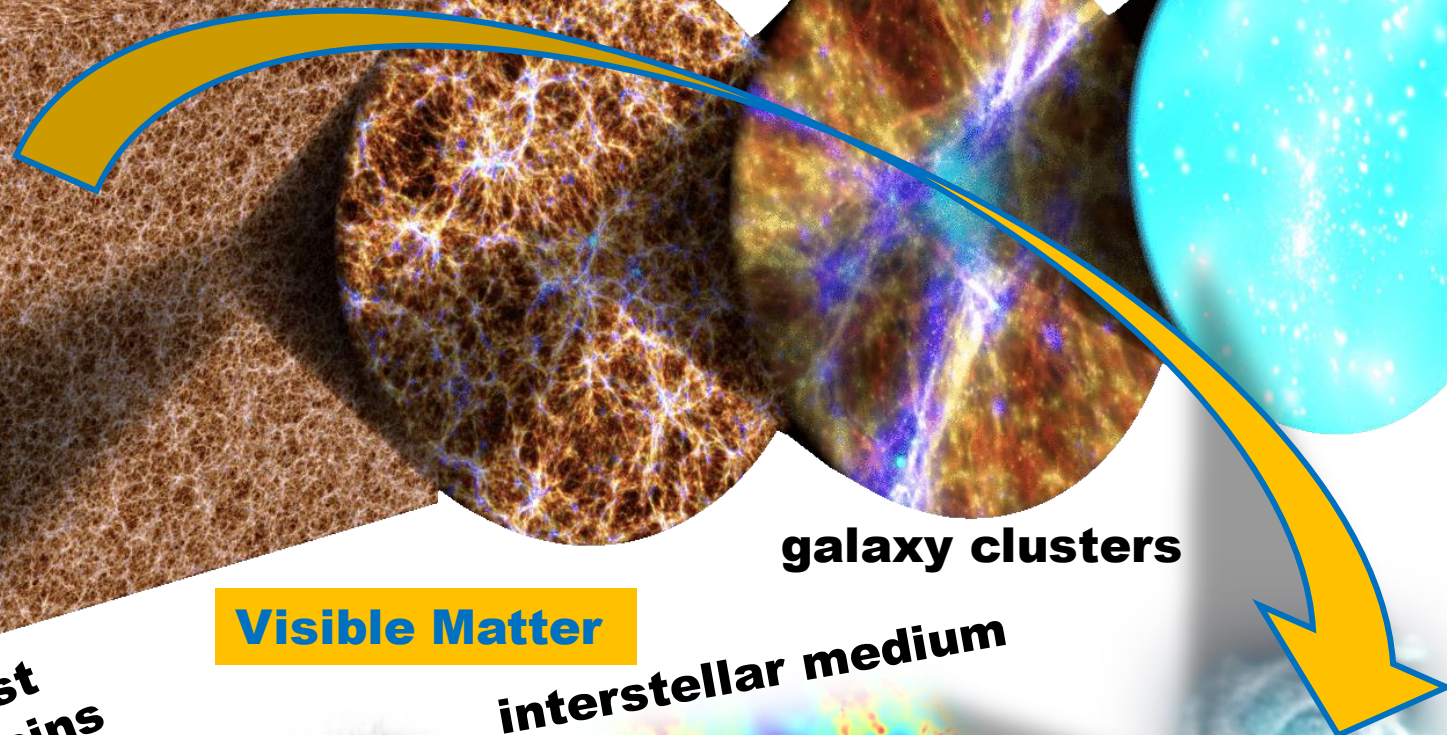
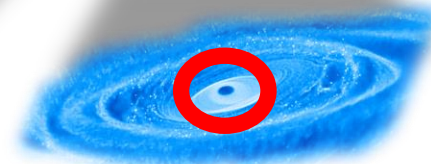
dust grains



protoplanetary discs



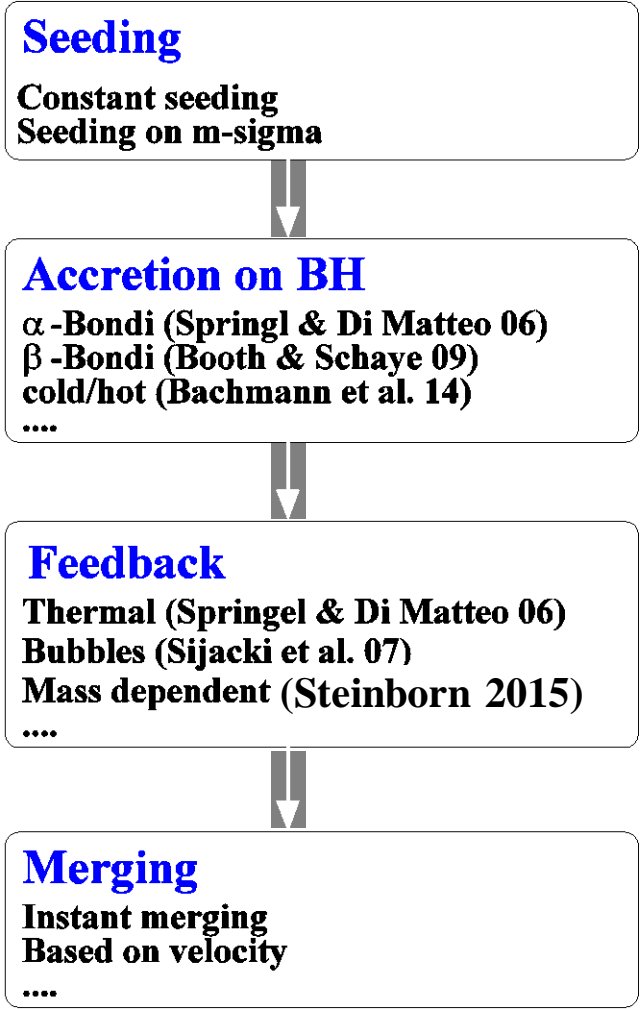
black holes



Basics: Including Black Holes in Simulations

Sub-grid model for handling black holes in cosmological simulations:

Springel & Di Matteo 2006



Growth of Black Hole

$$\dot{M}_B = \alpha \times 4\pi R_B^2 \rho c_s \simeq \frac{4\pi\alpha G^2 M_\bullet^2 \rho}{(c_s^2 + v^2)^{3/2}}$$

gas density

sound speed

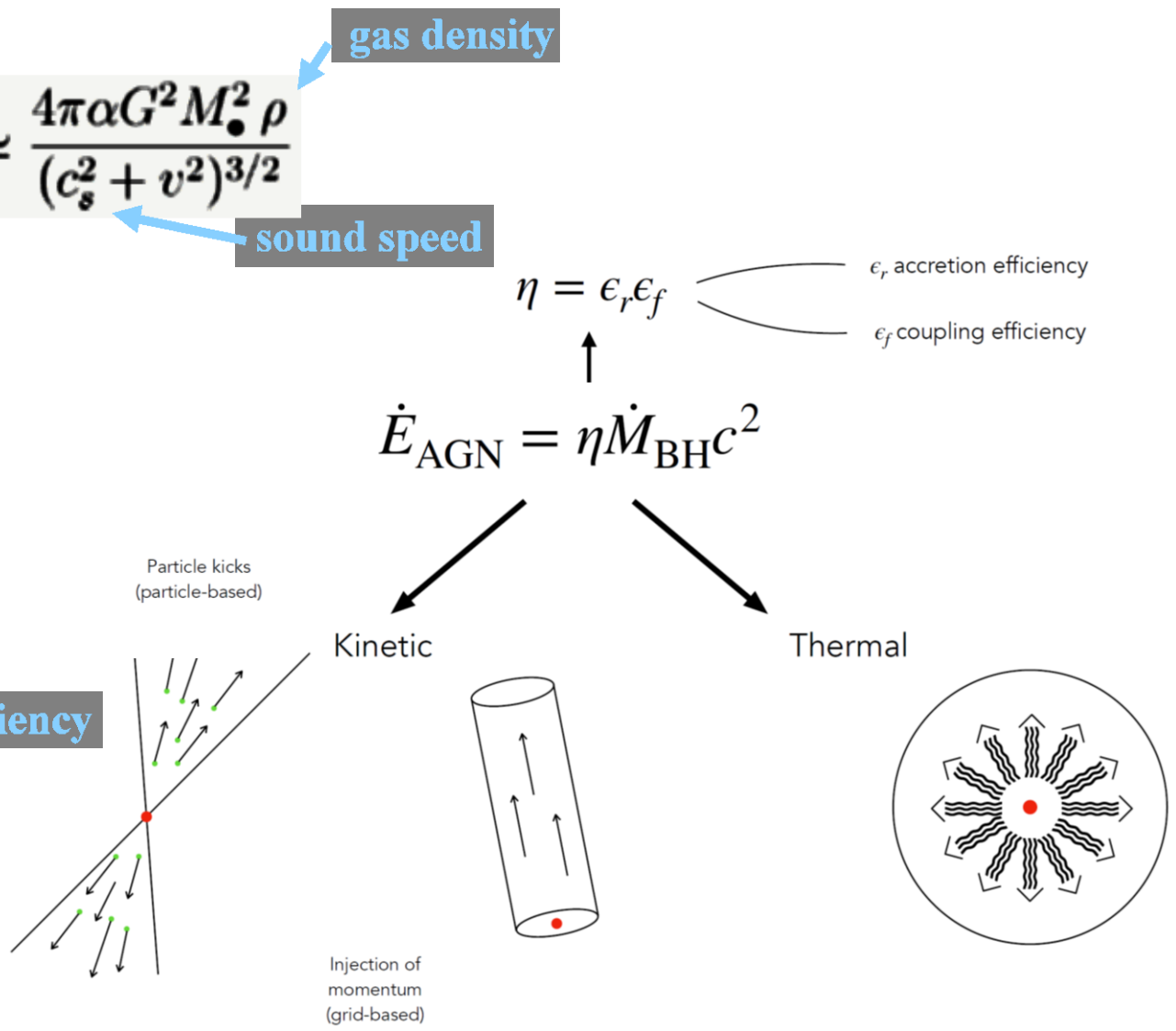
$$\dot{M}_\bullet = \min(\dot{M}_B, \dot{M}_{\text{Edd}})$$

Feedback by Black Holes

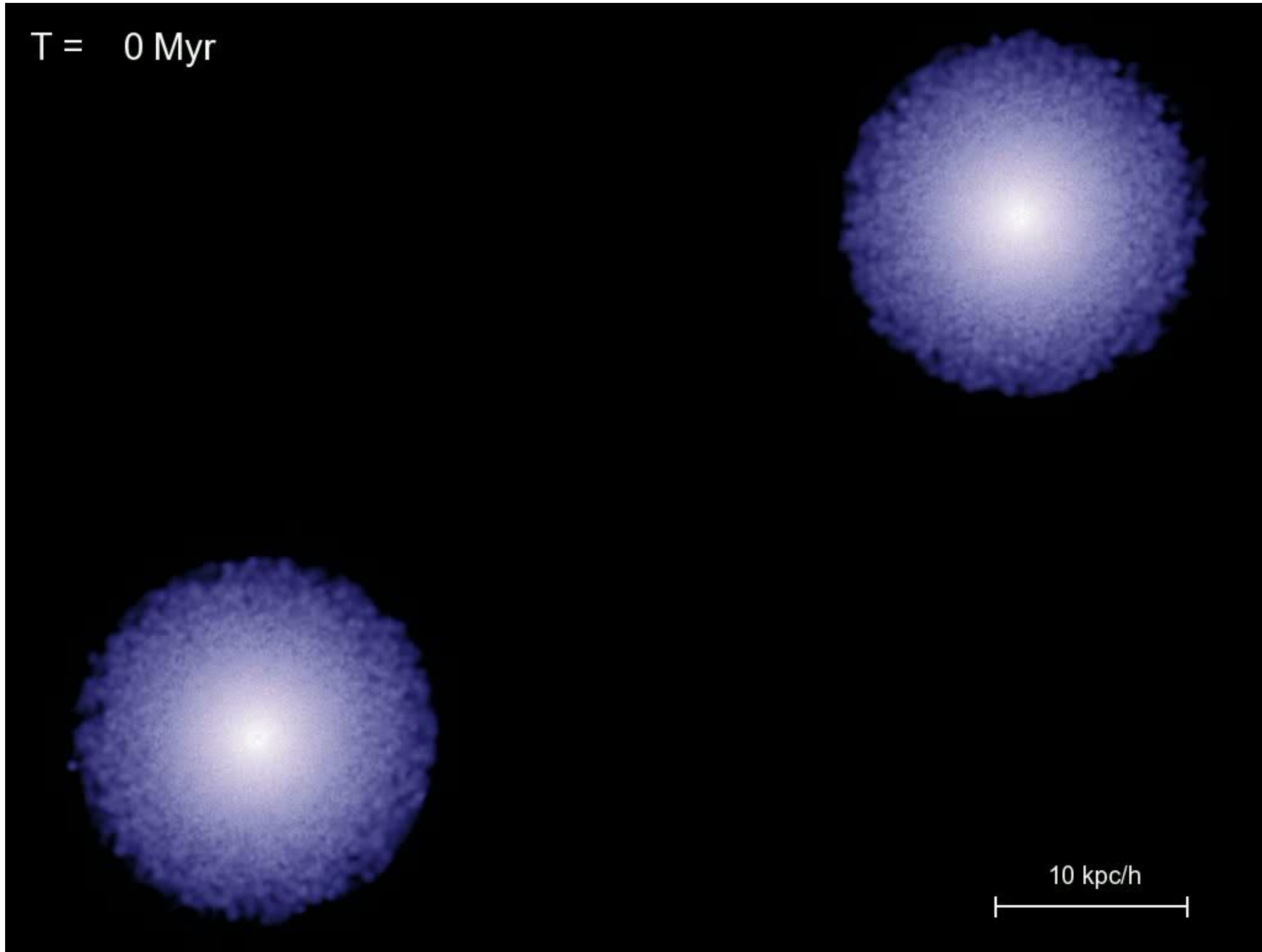
$$L_{\text{bol}} = 0.1 \times \dot{M}_\bullet c^2$$
$$\dot{E}_{\text{feedback}} = f \times L_{\text{bol}}$$

efficiency

Positioning:
Pinning to min. Potential
Free floating



Large impact of Black Holes on galaxy evolution



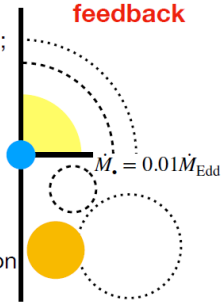
Large impact of Black Holes on galaxy evolution

Magneticum/Slow

BH seeding: halo stellar mass and gas to stellar mass fraction; BH mass at seeding scaled via $M_{\text{BH}}/M_{\text{star}}$ relation

BH feeding: Bondi formula, boosted $\alpha=100$; in some runs, hot and cold gas accretion, $\alpha=10$ for hot, 100 for cold gas

BH dynamics: dynamical friction and boosted dynamical mass

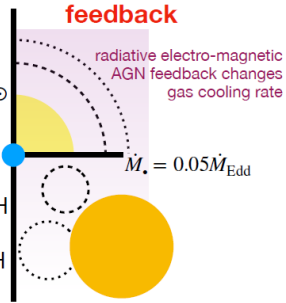


Illustris

BH seeding: halo mass $> 7.1 \times 10^{10} M_{\odot}$
BH mass at seeding: $1.4 \times 10^5 M_{\odot}$

BH feeding: Bondi formula, $\alpha=100$, accretion reduced if low gas pressure surrounding the BH

BH dynamics: repositioning, BH fixed to local potential minimum



Hydrodynamic methods and sub-resolution models for cosmological simulations

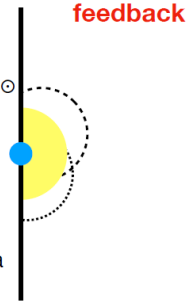
Milena Valentini^{*,†,§} and Klaus Dolag^{*,†,§}

Eagle

BH seeding: halo mass $> 1.5 \times 10^{10} M_{\odot}$
BH mass at seeding: $1.5 \times 10^5 M_{\odot}$

BH feeding: Bondi formula, not boosted, reduced for gas with high angular momentum

BH dynamics: repositioning via pinning on minimum potential

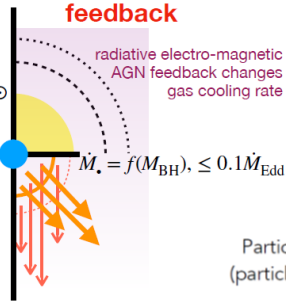


Illustris-TNG

BH seeding: halo mass $> 7.4 \times 10^{10} M_{\odot}$
BH mass at seeding: $1.2 \times 10^6 M_{\odot}$

BH feeding: Bondi formula, unboosted

BH dynamics: repositioning via pinning on minimum potential



AGN Feedback in simulations

$$\dot{E}_{\text{AGN}} = \eta \dot{M}_{\text{BH}} c^2$$

$\eta = \epsilon_r \epsilon_f$

ϵ_r accretion efficiency
 ϵ_f coupling efficiency

Kinetic

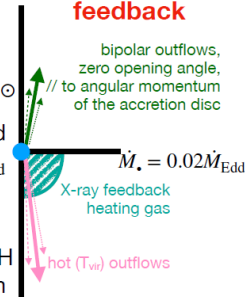
Thermal

Simba

BH seeding: stellar mass in halo $> 10^{9.5} M_{\odot}$
BH mass at seeding: $1.4 \times 10^4 M_{\odot}$

BH feeding: torque-limited cold gas accretion capped to $3 \dot{M}_{\text{Edd}}$ and Eddington limited Bondi accretion for hot gas ($\alpha=0.1$)

BH dynamics: repositioning, BH fixed to local potential minimum

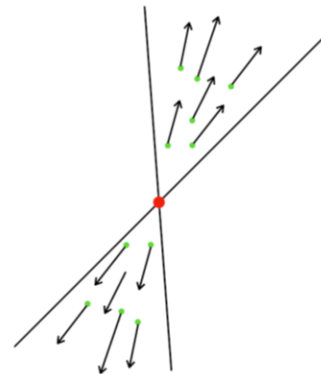
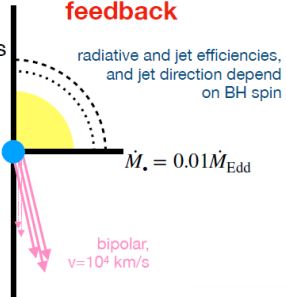


(New)Horizon-AGN

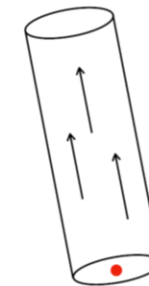
BH seeding: starforming gas, $\sigma > 20-100 \text{ km/s}$
BH mass at seeding: $10^5 M_{\odot}$

BH feeding: Bondi formula, not boosted, Eddington-limited

BH dynamics: drag force of the gas onto BH and enforced mesh refinement around the BH



Injection of momentum (grid-based)



IllustrisTNG

SIMBA

Ramses

CROCODILE

$z = 10.00$

Magneticum

EAGLE

Astrid

Obsidian

Astro Quiz Again !



What happens when you heat water in a micro gravity environment ?

The bubbles get smaller

A

The bubbles don't rise

B

A single bubble forms and rises as fast as it grows

C

No bubbles form

D

Bubbles rise with supersonic speed

E

What happens when you heat water in a micro gravity environment ?

The bubbles get smaller

A

The bubbles don't rise

B

A single bubble forms and rises as fast as it grows

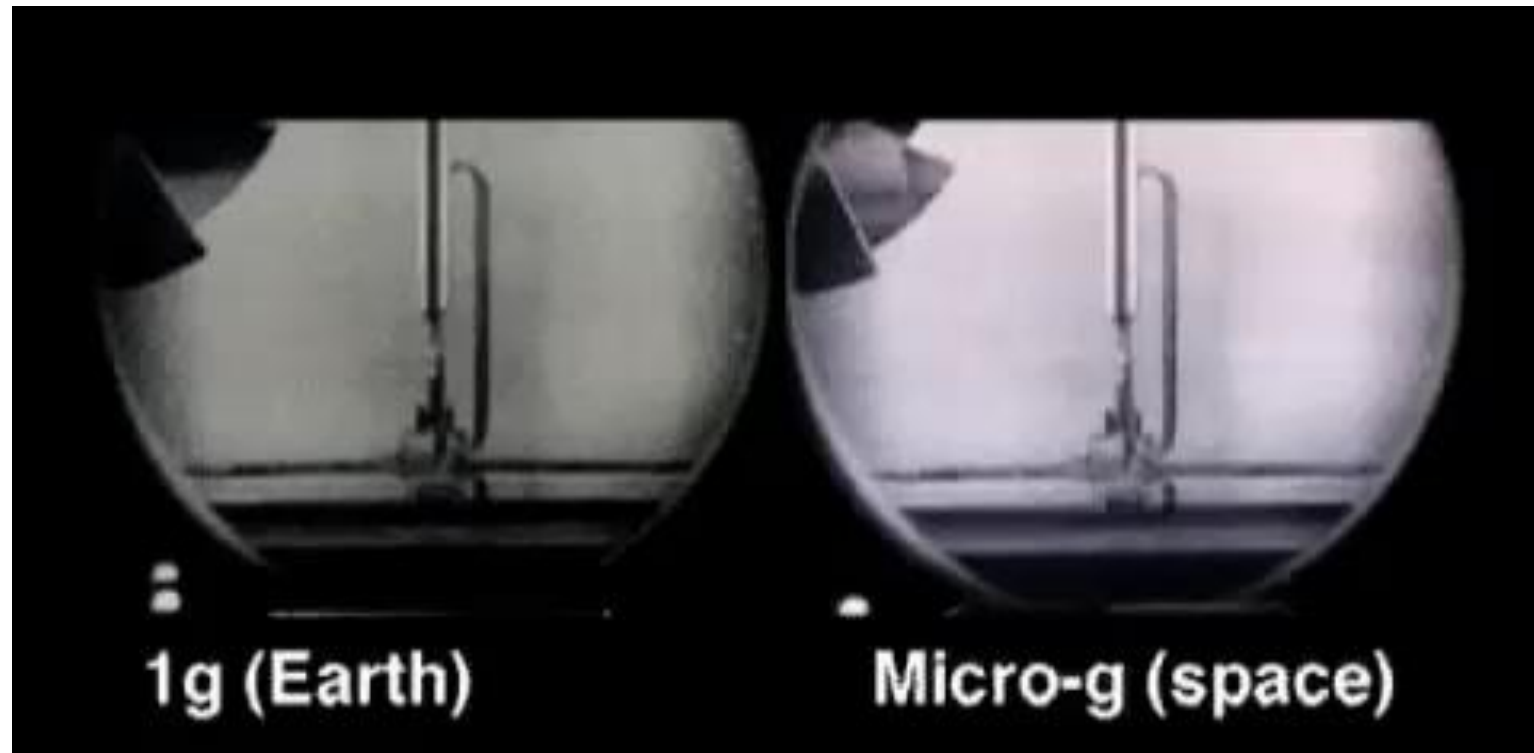
C

No bubbles form

D

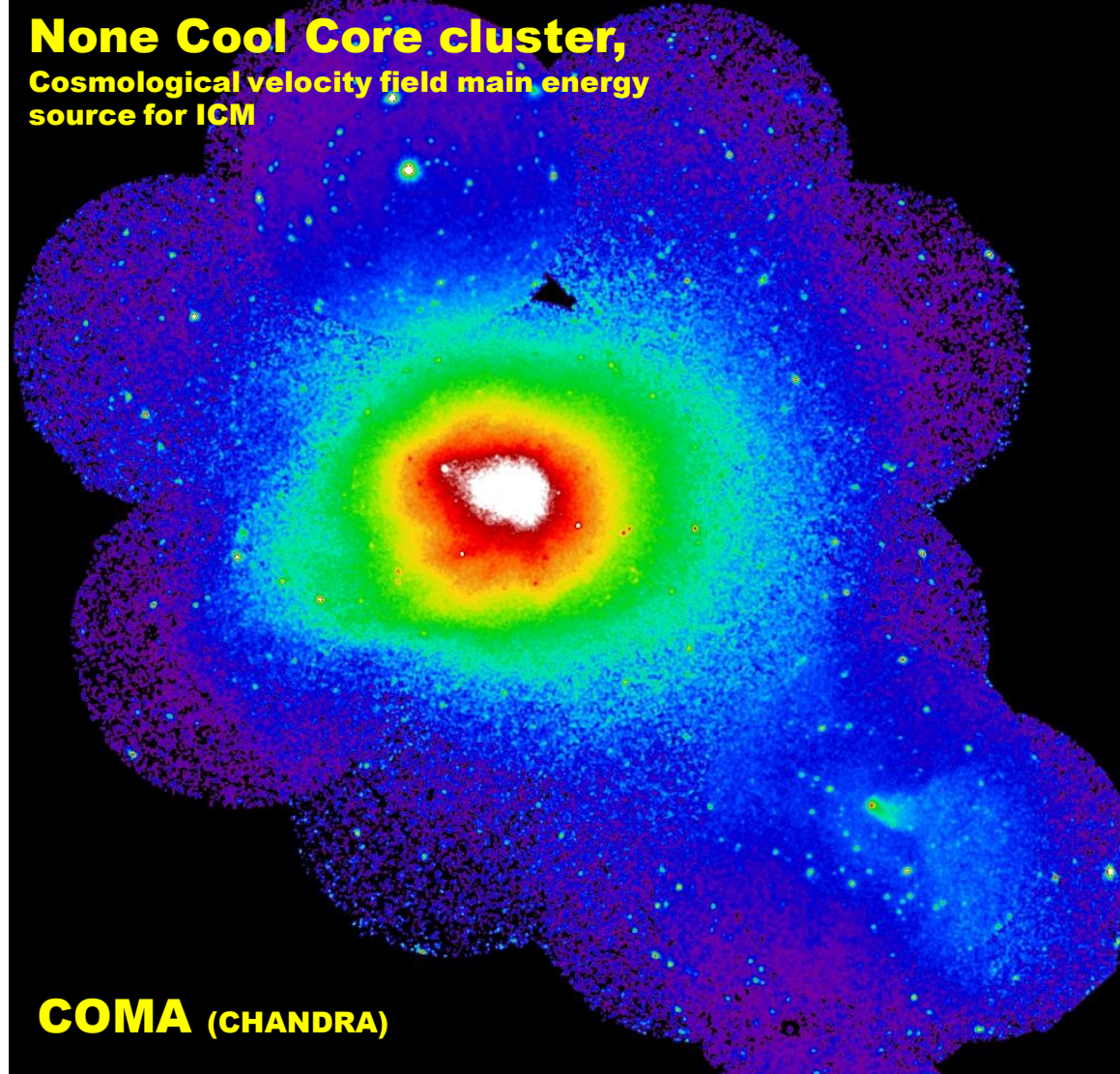
Bubbles rise with supersonic speed

E

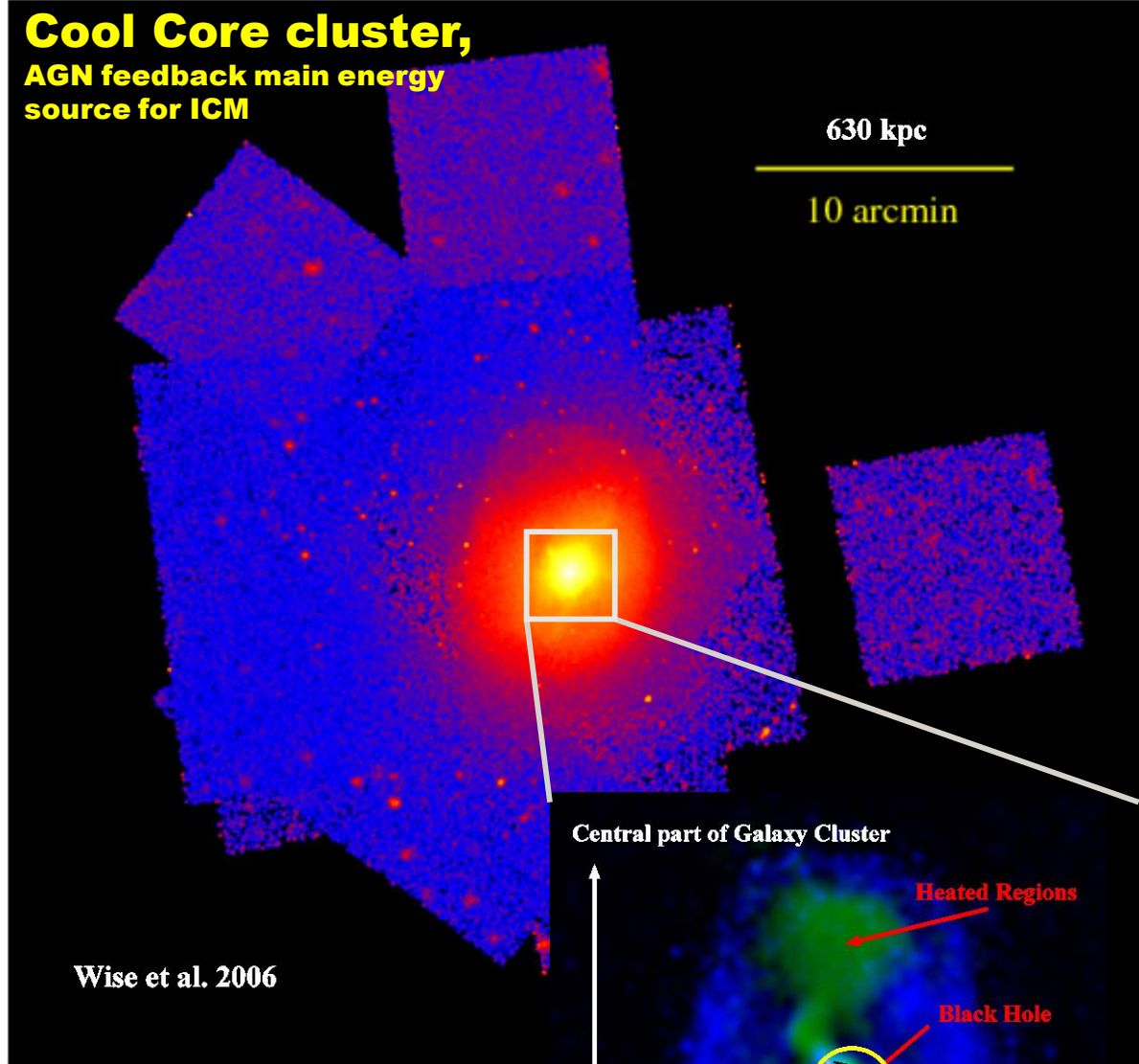


Credits: E. Churazov

None Cool Core cluster,
Cosmological velocity field main energy
source for ICM



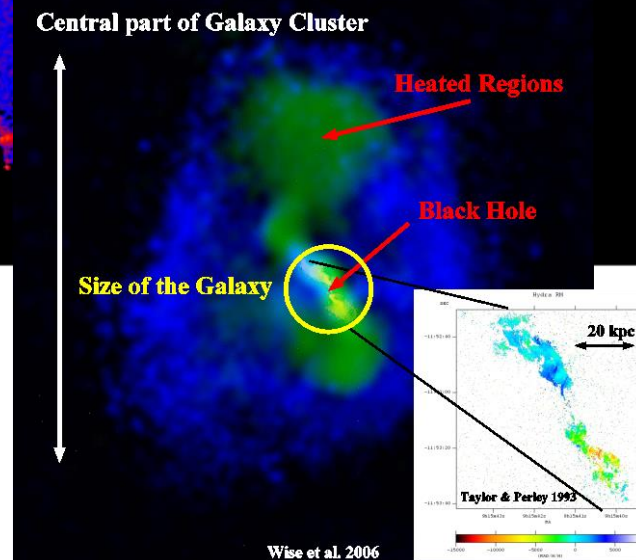
Cool Core cluster,
AGN feedback main energy
source for ICM



HYDRA (Chandra)

CC vs. non CC Clusters

also feature different non thermal
features (active AGN in center)



Large impact of Black Holes on galaxy clusters

$$\text{expansion velocity } v_{\text{exp}} : L_j \gg \frac{g}{g-1} P \dot{V} \gg P 4 \rho R^2 v_{\text{exp}}$$

$$\text{rise velocity } v_{\text{rise}} \gg \sqrt{gR}$$

$$V_{\text{exp}} \gg V_{\text{rise}}$$

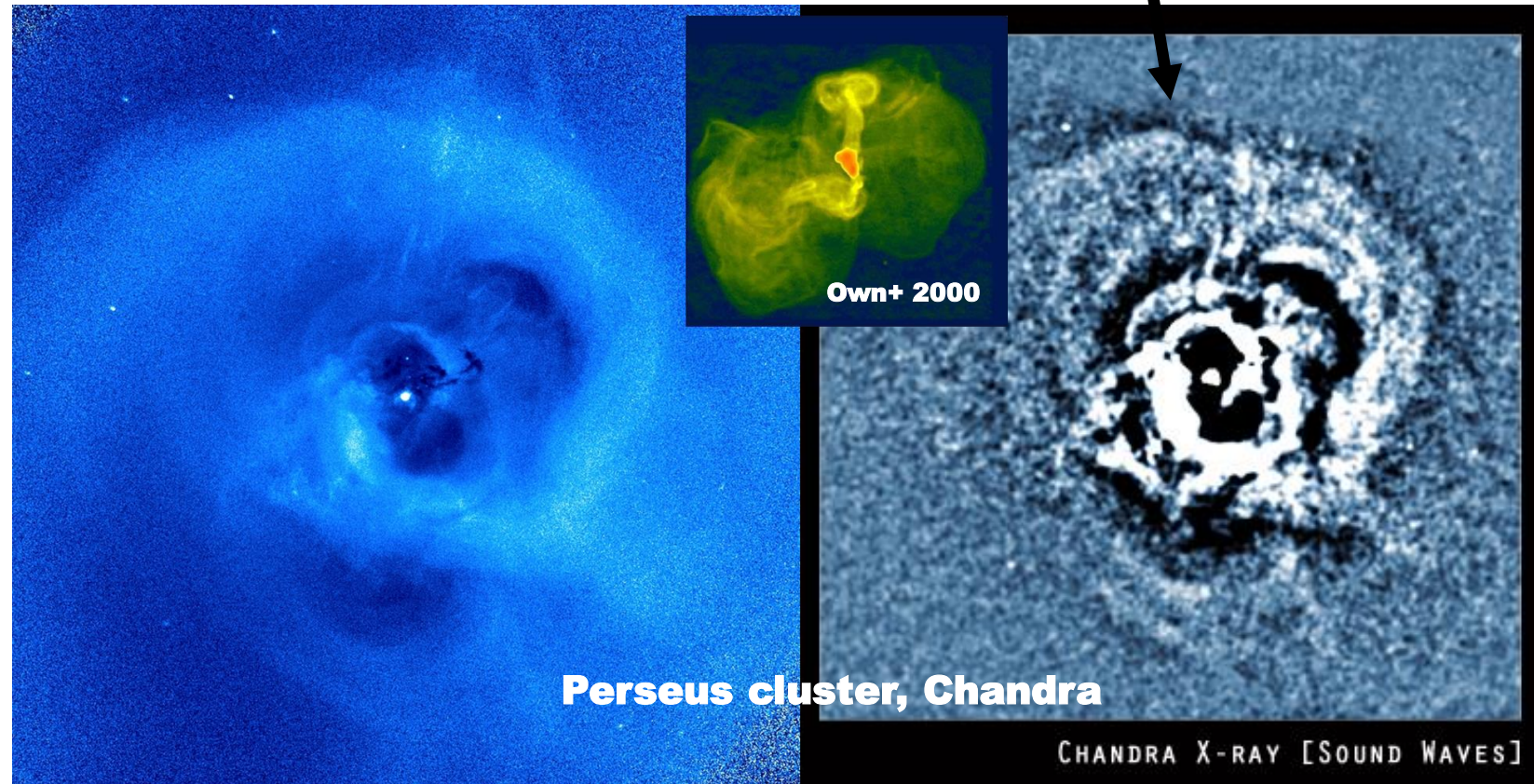
**Allows to measure
energy deposited in
the ICM.**

$$L \gg 10^{45} \text{ erg/s}$$

Churazov et al. 2000

Soundwaves!

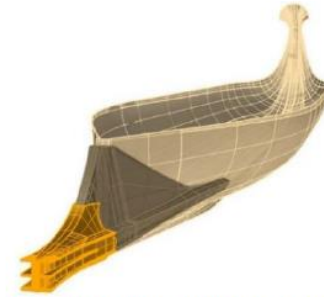
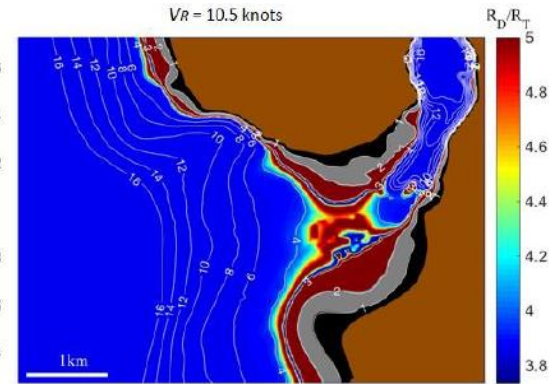
**(This cosmic soundwave is 57
octaves lower than middle-C!)**



Astro Quiz Again !



What do these images show?



The small scale model of the Greek galley

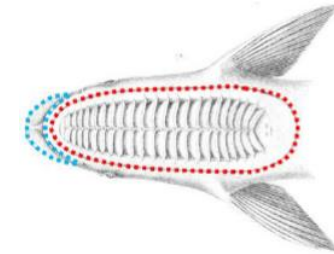
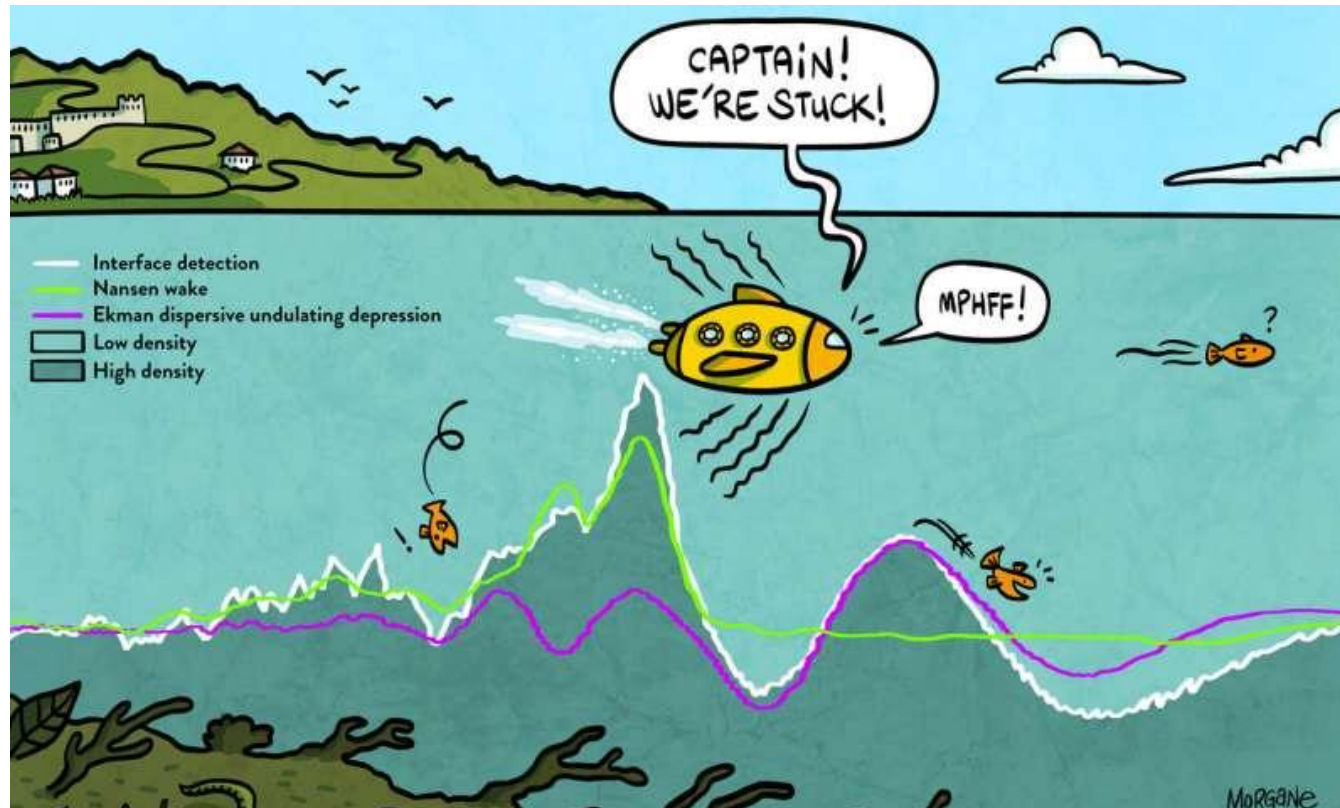
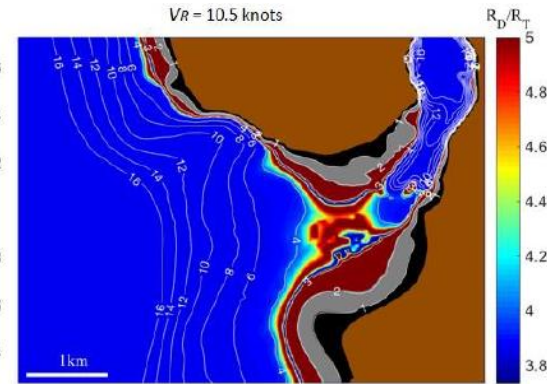


Illustration of *Echeis naucrates*



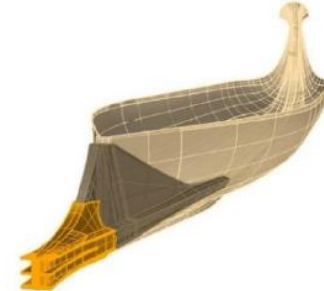
What do these images show?

Cleopatra

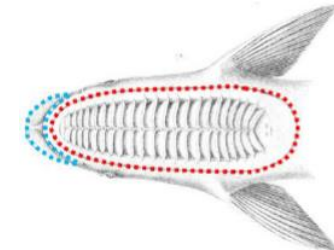


Ambracian Gulf

ancient galley



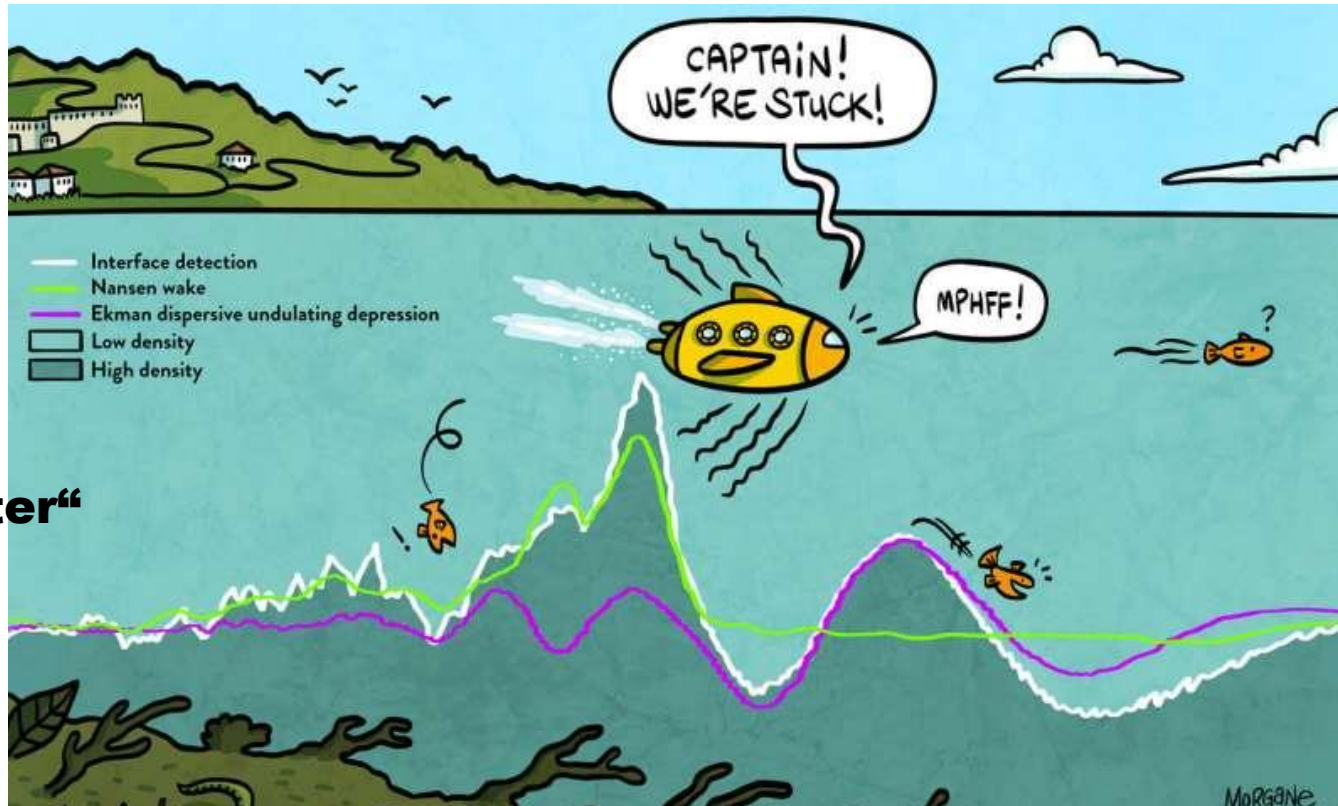
The small scale model of the Greek galley



sucker fish

Illustration of *Echeneis naucrates*

„dead-water“



Octavian



THE NAVAL BATTLE OF ACTIUM AND THE MYTH OF THE SHIP-HOLDER: THE EFFECT OF BATHYMETRY

Johan Fourdrinoy, Clément Caplier, Yann Devaux and Germain Rousseaux, CNRS – Université de Poitiers – ISAE-ENSMA - Institut Pprime, France

Areti Gianni and Ierotheos Zacharias, University of Patras, Greece

Isabelle Jouteur, Université de Poitiers, Forellis France

Paul Martin, Université de Montpellier, France

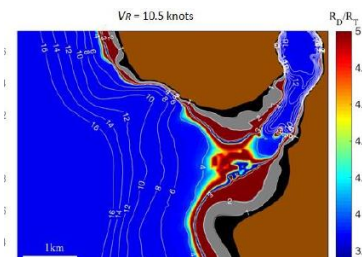
Julien Dambrine, Madalina Petcu and Morgan Pierre, Université de Poitiers, Laboratoire de Mathématiques et Applications, France.

SUMMARY

A myth of antiquity is explained with modern science in the context of an ancient naval battle. A legend was invoked by the admiral Pliny the Elder to explain the defeat of Antony and Cleopatra against Octavian at the naval battle of Actium. A fish, called echeneis or remora, is said to have the power to stop ships or to delay their motion by adhering to the hull. Naturalists have since studied how the fish sucking-disk with its typical pattern of parallel striae sticks to its host. Here we show the pattern of the free surface measured in a towing tank in the wake of an ancient galley is similar to the striae pattern of the fish. We have measured the bathymetry at the mouth of the Ambracian Gulf that influenced the physical environment of the battle. The computations demonstrate the increase of wave resistance of a galley as a function of the draft to the water depth ratio in shallow water corresponding to the appearance of a particular wake pattern: the echeneidian free surface pattern.



VS.

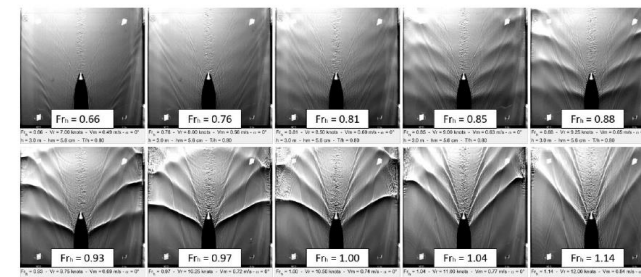


+



The small scale model of the Greek galley

=



≠

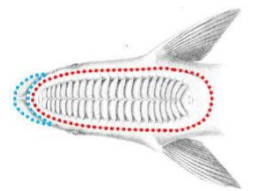


Illustration of Echineis naucrates

5 CONCLUSIONS

For the first time since twenty centuries, we have shown conclusively that the global pattern of the free surface measured in this work with modern and non-intrusive optical methods in the wake of an ancient galley moving in shallow waters is similar to the pattern of striae on the sucking-disk of the echeneis fish. Hence, the Antonian boats have been influenced by a physical echeneis and not a biological one during the battle of Actium. From the analysis of the resistance charts, we have demonstrated that the Antonian fleet was unable to use the ramming tactics because the wave resistance was increased up to ten times compared to the Octavian fleet. By a strange coincidence (or maybe not a hazard?), several centuries later another naval battle at the same location produces the same astonishment for the final result: Preveza battle in 1538, where the Ottoman forces fought against the Christian navy and, to the general surprise, won. The Ottoman fleet under the command of Barbarossa with the smallest boats albeit considered as inferior, prevailed. Another possible explanation for the boats difficulty in manoeuvres is the dead-water phenomenon, which can be encountered, for example, in the Northern fjords where ice melting creates two water layers of different densities, with a sharp interface between fresh and saline water (see

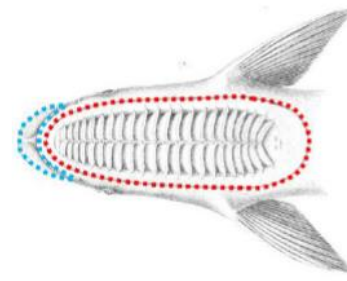


Illustration of *Echeneis naucrates*

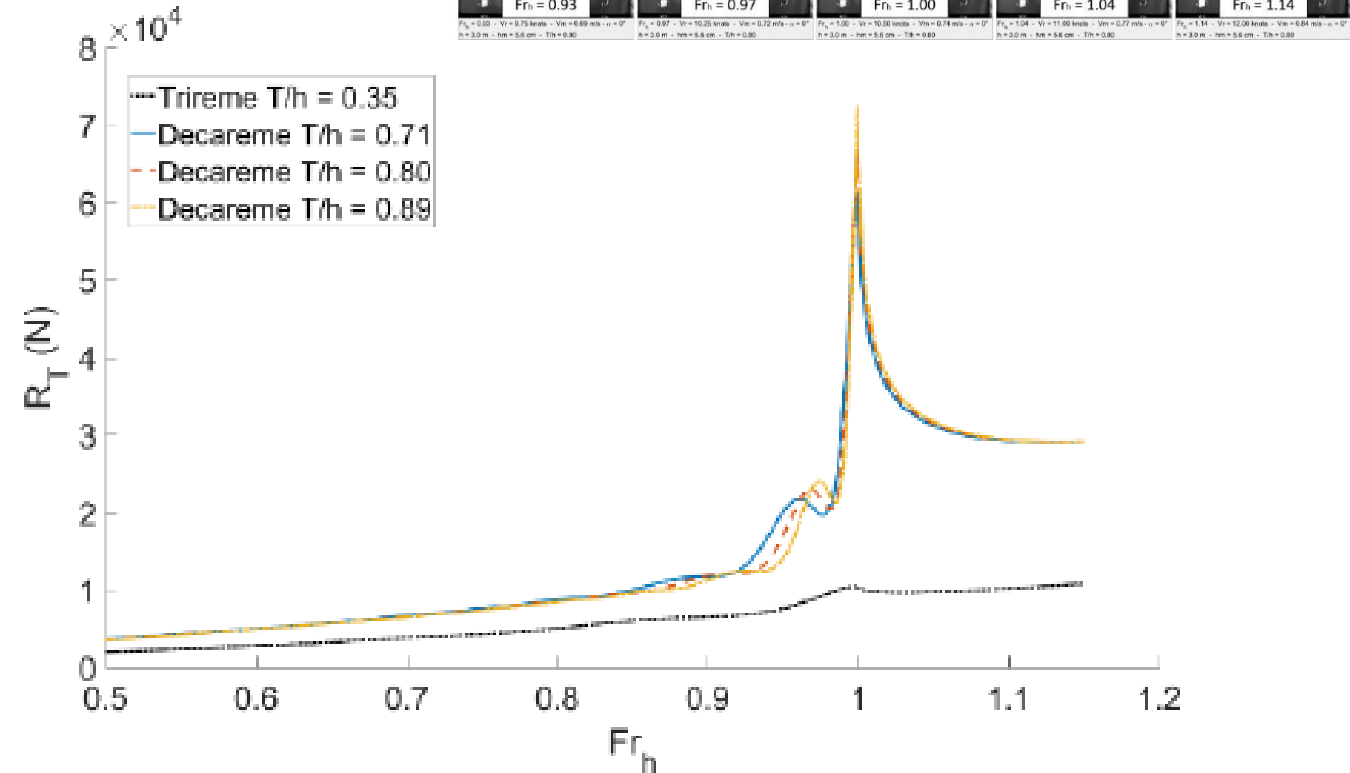


Figure 3. Calculated total resistances, composed by a wave making resistance and a viscous resistance, as a function of Fr_h for a varying ship draft to depth ratio.

The dual nature of the dead-water phenomenology: Nansen versus Ekman wave-making drags

Johan Fourdrinoy^a, Julien Dambrine^b, Madalina Petcu^{b,c,d}, Morgan Pierre^b, and Germain Rousseaux^{a,1}

^aInstitut Pprime, CNRS, Université de Poitiers, Institut supérieur de l'aéronautique et de l'espace–École nationale supérieure de mécanique et d'aérotechnique (ISAE-ENSMA), 86073 Poitiers Cedex 9, France; ^bLaboratoire de Mathématiques et Applications, Université de Poitiers–CNRS, 86073 Poitiers Cedex 9, France; ^cThe Institute of Mathematics of the Romanian Academy, 010702 Bucharest, Romania; and ^dThe Institute of Statistics and Applied Mathematics of the Romanian Academy, 050711 Bucharest, Romania

Edited by Howard A. Stone, Princeton University, Princeton, NJ, and approved June 12, 2020 (received for review December 23, 2019)

A ship encounters a higher drag in a stratified fluid compared to a homogeneous one. Grouped under the same “dead-water” vocabulary, two wave-making resistance phenomena have been historically reported. The first, the Nansen wave-making drag, generates a stationary internal wake which produces a kinematic drag with a noticeable hysteresis. The second, the Ekman wave-making drag, is characterized by velocity oscillations caused by a dynamical resistance whose origin is still unclear. The latter has been justified previously by a periodic emission of nonlinear internal waves. Here we show that these speed variations are due to the generation of an internal dispersive undulating depression produced during the initial acceleration of the ship within a linear regime. The dispersive undulating depression front and its subsequent whelps act as a bumpy treadmill on which the ship would move back and forth. We provide an analytical description of the coupled dynamics of the ship and the wave, which demonstrates the unsteady motion of the ship. Thanks to dynamic calculations substantiated by laboratory experiments, we prove that this oscillating regime is only temporary: the ship will escape the transient Ekman regime while maintaining its propulsion force, reaching the asymptotic Nansen limit. In addition, we show that the lateral confinement, often imposed by experimental setups or in harbors and locks, exacerbates oscillations and modifies the asymptotic speed.

This work is part of a major project¹ investigating why, during the Battle of Actium (31 BC), Cleopatra’s large ships lost when they faced Octavian’s weaker vessels. Might the Bay of Actium, which has all the characteristics of a fjord, have trapped the Queen of Egypt’s fleet in dead water? So now we have another hypothesis to explain this resounding defeat, that in antiquity was attributed to remoras, ‘suckerfish’ attached to their hulls, as the legend goes.

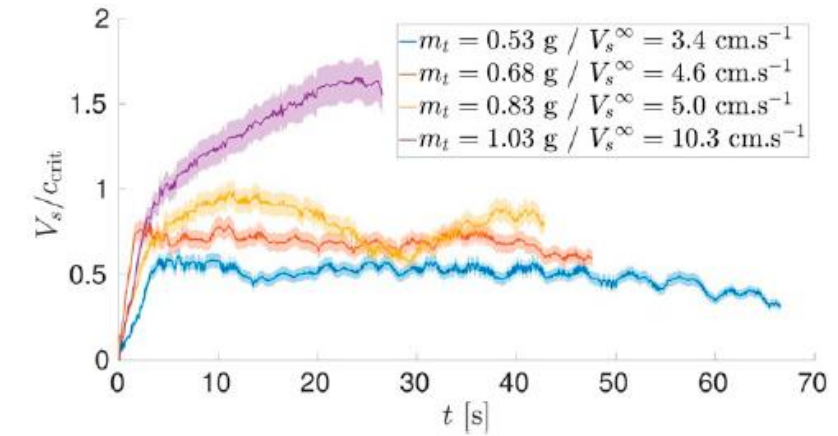
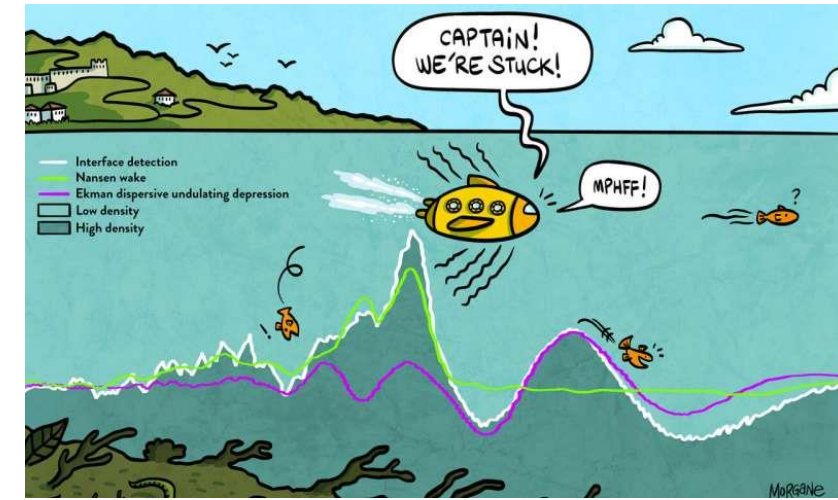
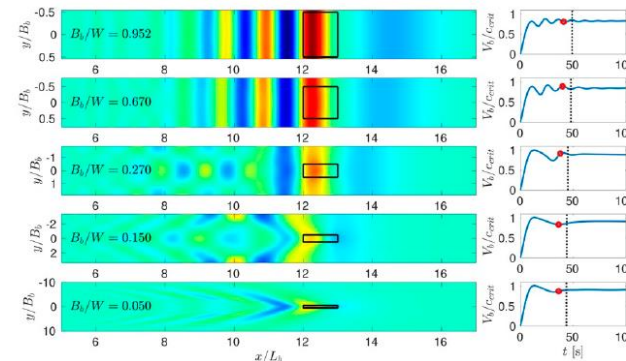


Fig. 1. Time evolutions of the ship speed for different constant towing forces. In yellow (purple), the ship reaches an oscillating (ballistic) regime. Speed error $\Delta V_S = 7.2 \times 10^{-2} V_S + 1.8 \times 10^{-4} \text{ [m} \cdot \text{s}^{-1}]$. Configuration data are given in *SI Appendix, Table S1*.

Do rising bubbles in galaxy clusters drive interna waves?

Generation of Internal Waves by Buoyant Bubbles in Galaxy Clusters and Heating of Intracuster Medium

Congyao Zhang,^{1*} Eugene Churazov,^{1,2} Alexander A. Schekochihin^{3,4}

¹ Max Planck Institute for Astrophysics, Karl-Schwarzschild-Str. 1, D-85741 Garching, Germany

² Space Research Institute (IKI), Profsoyuznaya 84/32, Moscow 117997, Russia

³ Rudolf Peierls Centre for Theoretical Physics, University of Oxford, Oxford OX1 3NP, UK

⁴ Merton College, Oxford OX1 4JD, UK

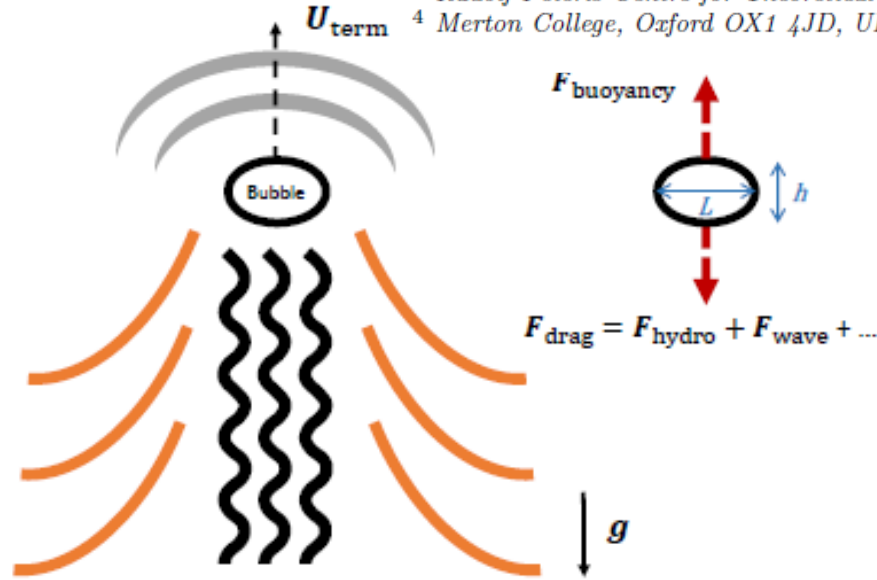


Figure 1. Sketch showing a bubble rising in a stratified medium. The bubble rises at the terminal velocity when the buoyancy force is balanced by the drag force. The gray, black and orange lines show schematically sound waves, turbulence, and internal waves excited by the moving bubble, which all can contribute to the total drag.

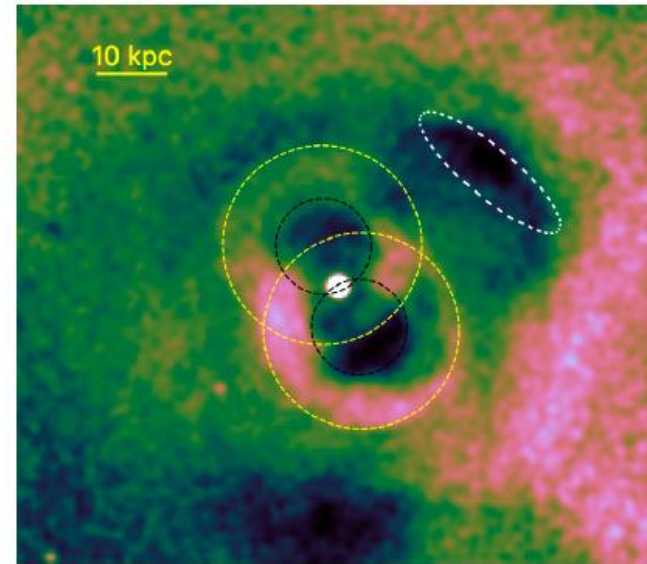


Figure 2. *Chandra* 3.5-7.5 keV band image of the Perseus cluster. The bubbles appear as dark (X-ray dim) regions in this image. “Active” bubbles (radius ~ 7 kpc) are marked with black dashed circles. They are surrounded by quasi-spherical weak shocks (radius ~ 14 kpc), shown by yellow circles. The outer bubble, to the NW from the center, has the “horizontal” and “vertical” (radial) sizes $L \sim 25$ kpc and $h \sim 7$ kpc, respectively. Thus, its aspect ratio is $\epsilon_b = L/h \sim 3.6$. We argue that for such bubbles the effects of stratification dominate in the total drag force.

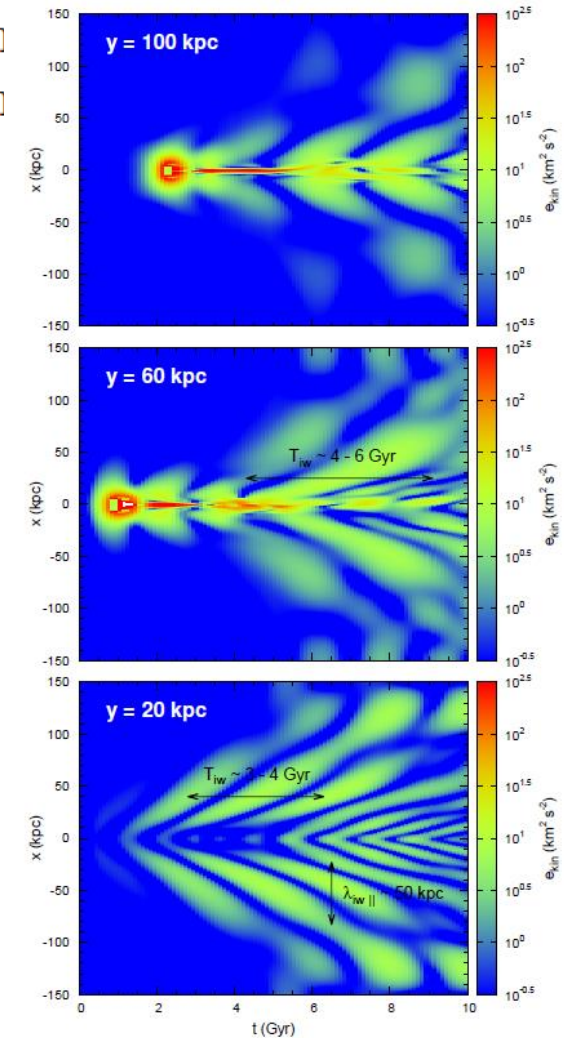
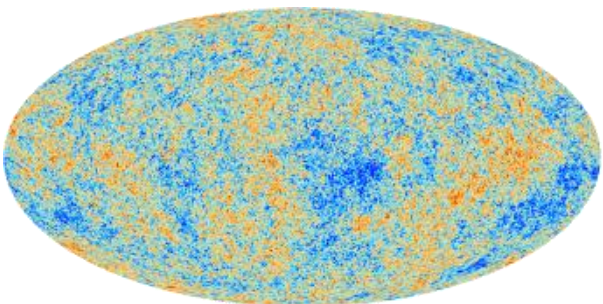


Figure 8. Time evolution of 1D slices of the specific kinetic energy of the gas at $y = 20$ kpc (bottom panel), 60 kpc (middle panel), and 100 kpc (top panel) for the run GE4L12V30. The periodic pattern reveals internal waves propagating outwards (up and down in this plot). The period of internal waves is approximately $T_{iw} \sim 3 - 4$ Gyr at $y = 20$ kpc and $T_{iw} \sim 4 - 6$ Gyr at both $y = 60$ and 100 kpc (marked in the panels, see Section 4.2).

HPC Challenges in Astrophysics

IV) Some HPC aspects

The Computational Challenge



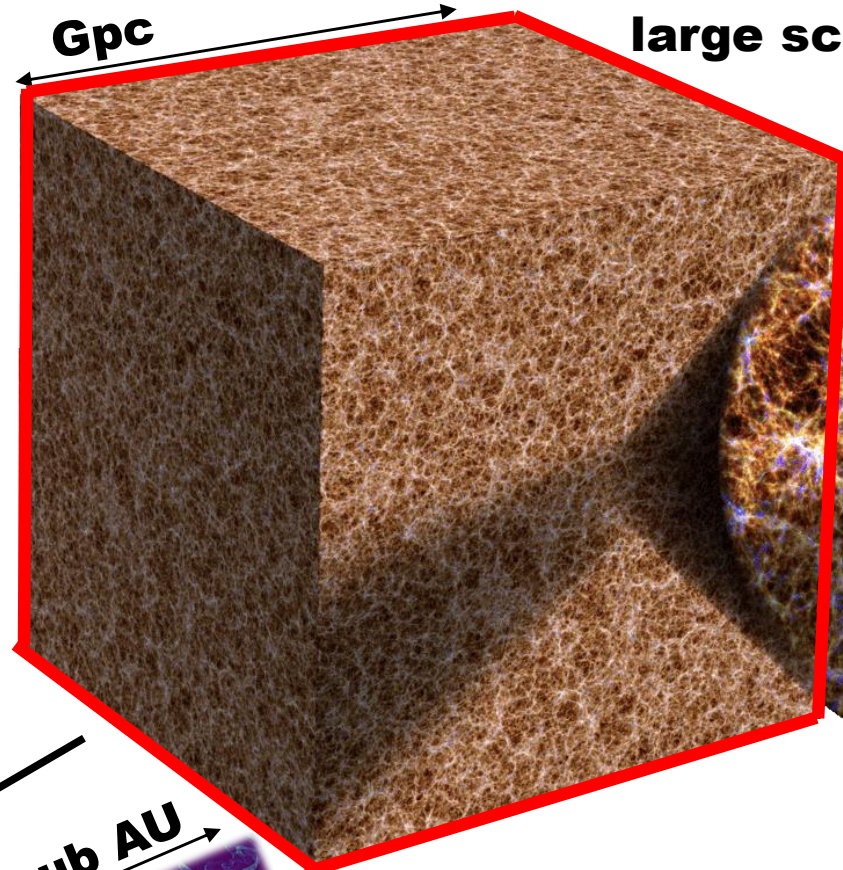
**multi-scale,
multi-physics**

$3 \cdot 10^{22} \text{ km}$

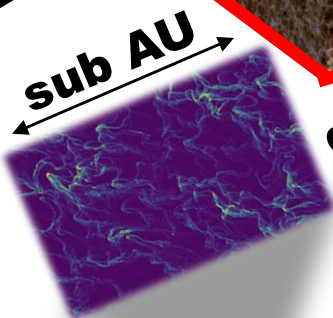


	λ_{mfp}	λ_{Lamor}	λ_{Debye}
electrons	1 kpc	700 km	6 km
protons		29000 km	

Plasma Physics!

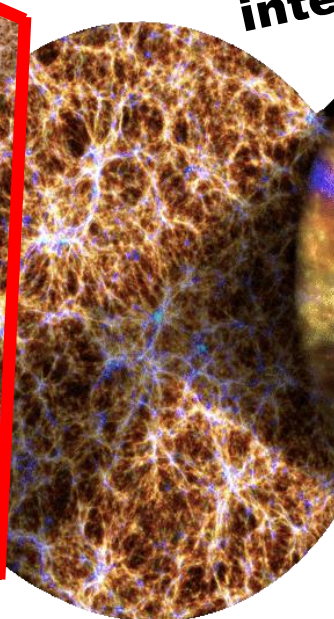
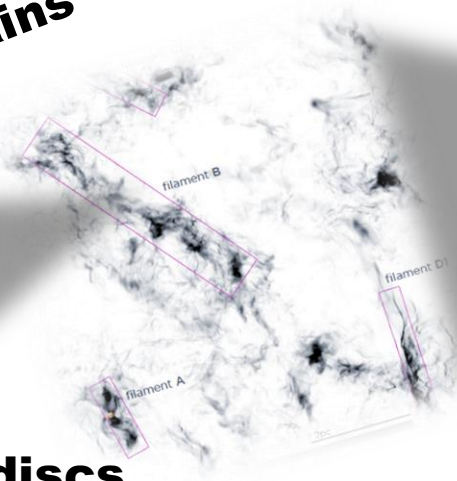
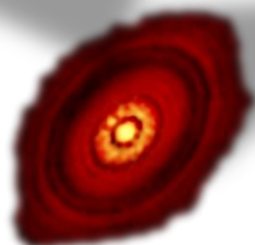


large scale structure



dust grains

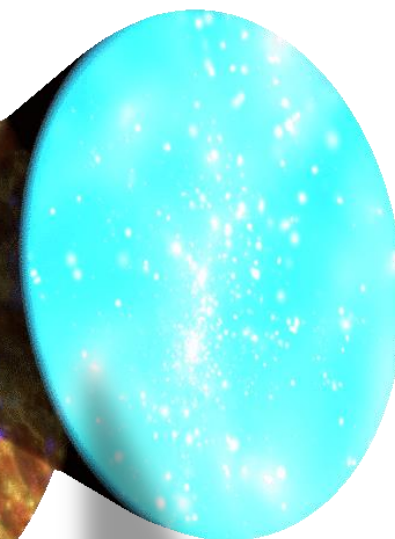
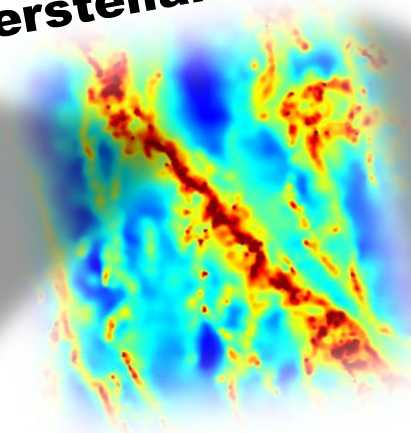
protoplanetary discs



intergalactic medium

galaxy clusters

interstellar medium

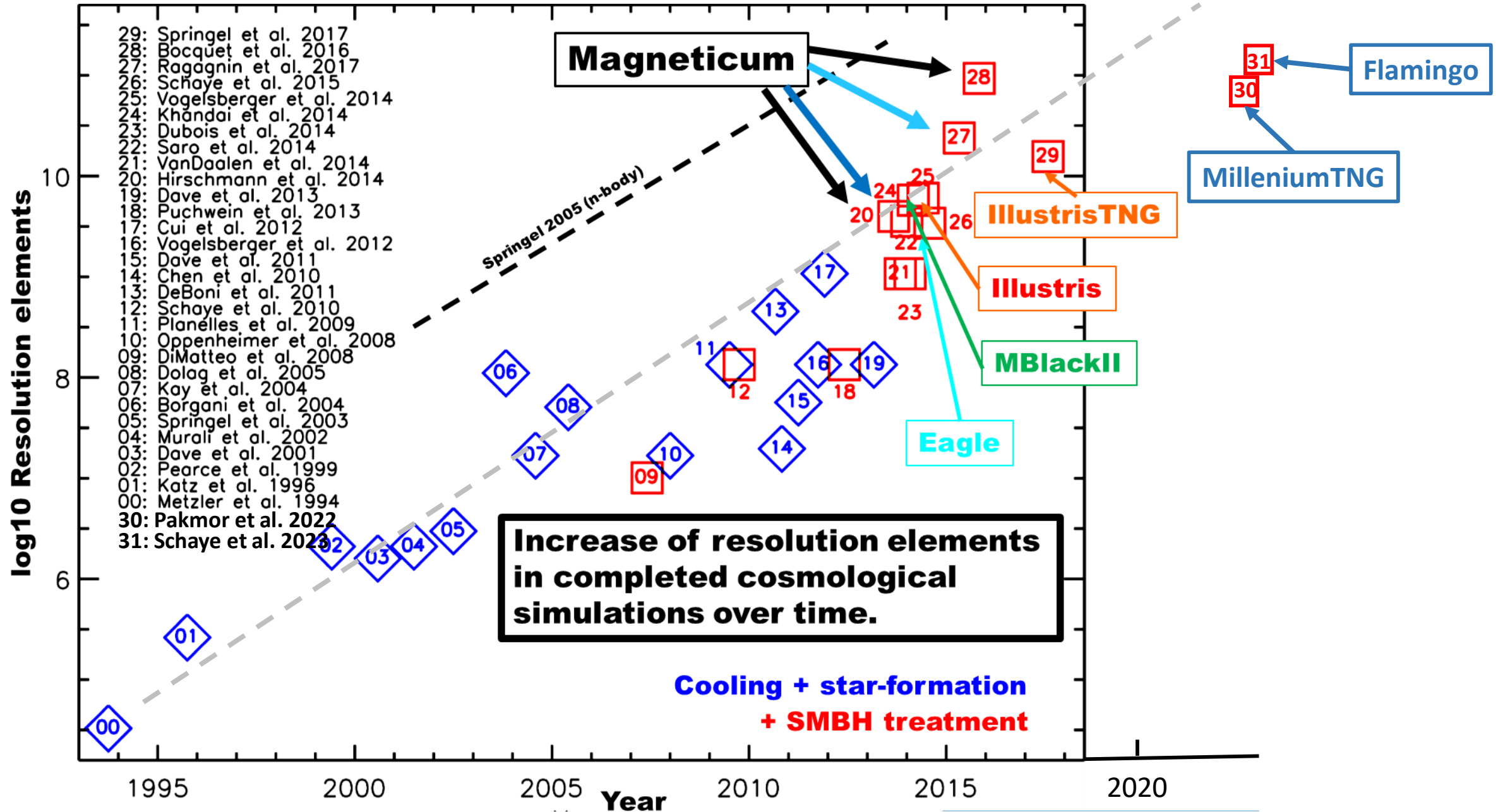


stars

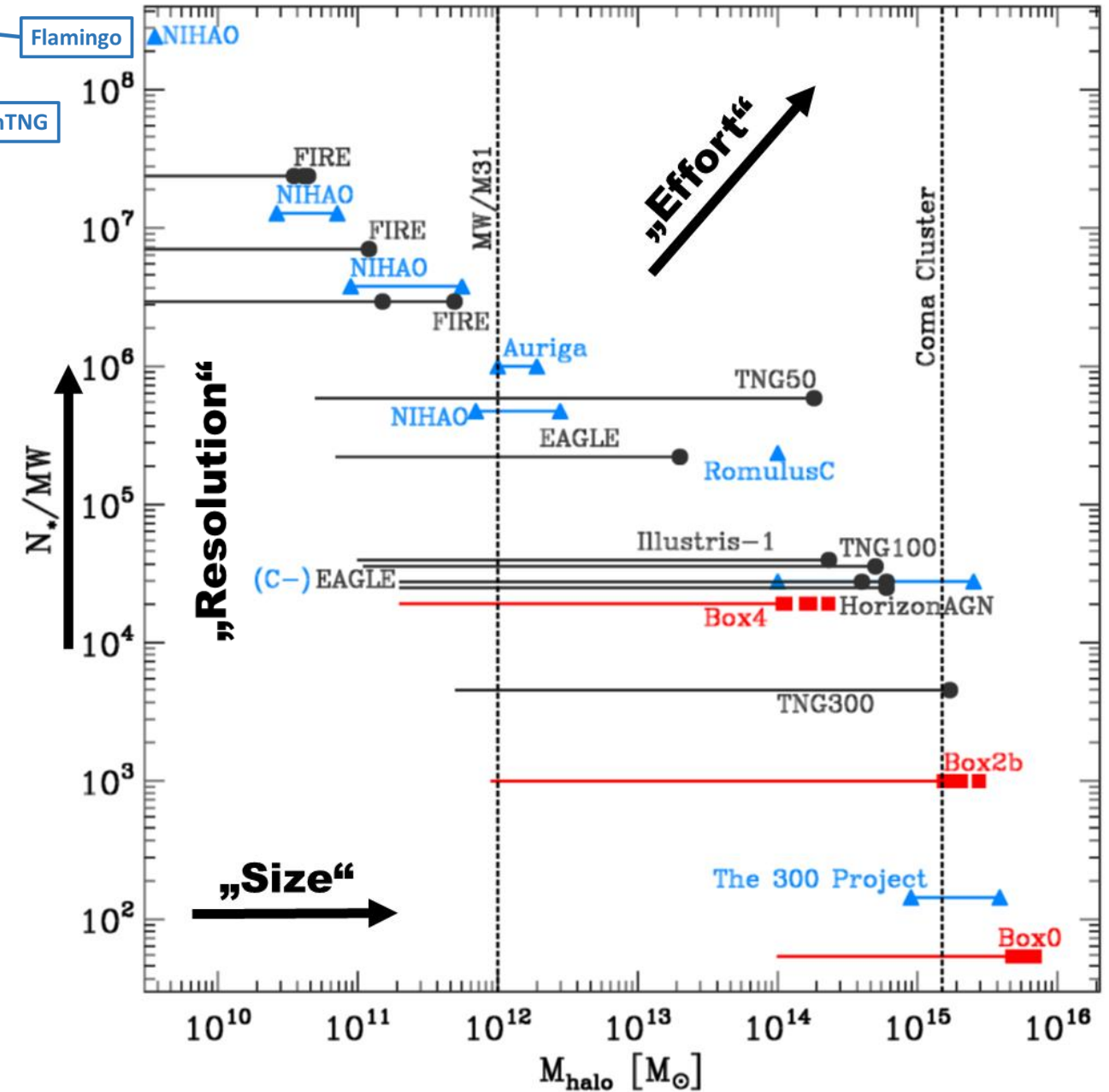
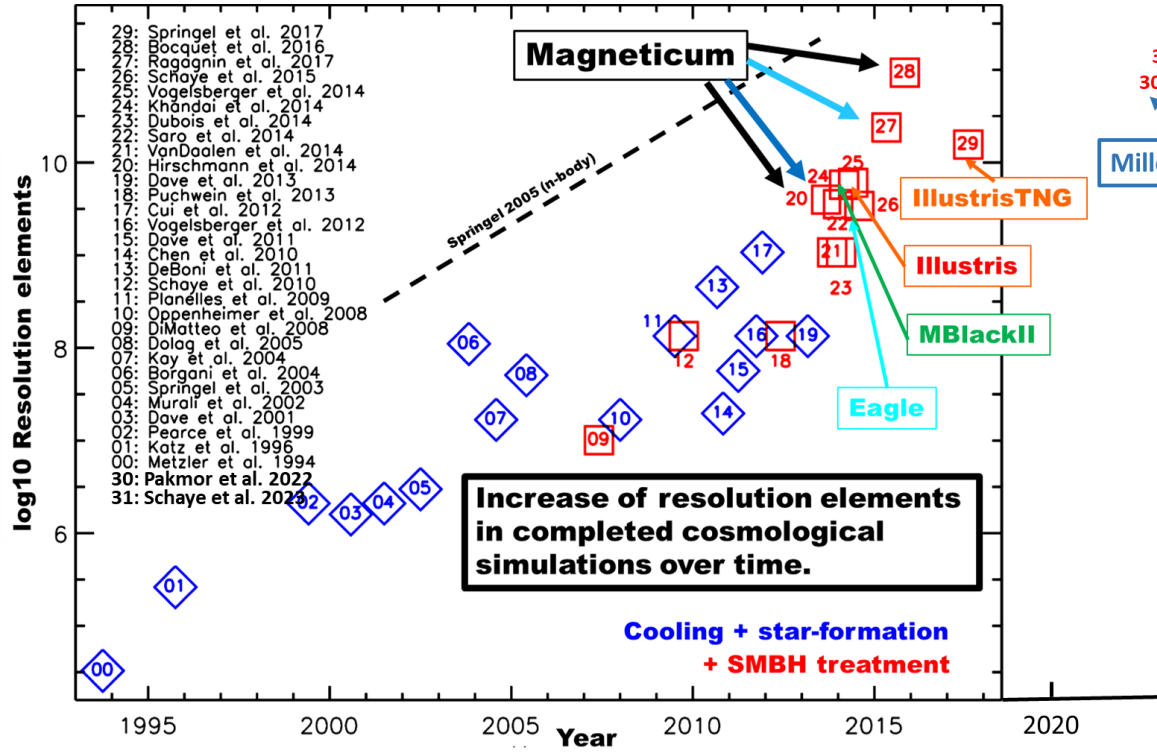
black holes



The Computational Challenge



The Computational Challenge



MAGNETICUM



	Box0	Box1	Box2b	Box2	Box3	Box4
[Mpc/h]	2688	896	640	352	128	48
mr	2×4536^3	2×1526^3	—	2×594^3	2×216^3	2×81^3
hr	—	—	2×2880^3	2×1584^3	2×576^3	2×216^3
uhr	—	—	—	—	$2 \times 1536^3 (z = 2)$	2×576^3

Setup:

$2 \times 4536^3 = 186.659.085.312$ particle

Almost 20 times size of ILLUSTRIS or EAGLE

Full Physics + improved SPH:

200 bytes per DM particle, 456 bytes per GAS particle

Complete SuperMUC Phase II:

$6 \times 512 \times 2 \times 28 = 172032$ tasks

1 MPI task per socket, 28 OpenMP per MPI

68.5 TB for single checkpointing

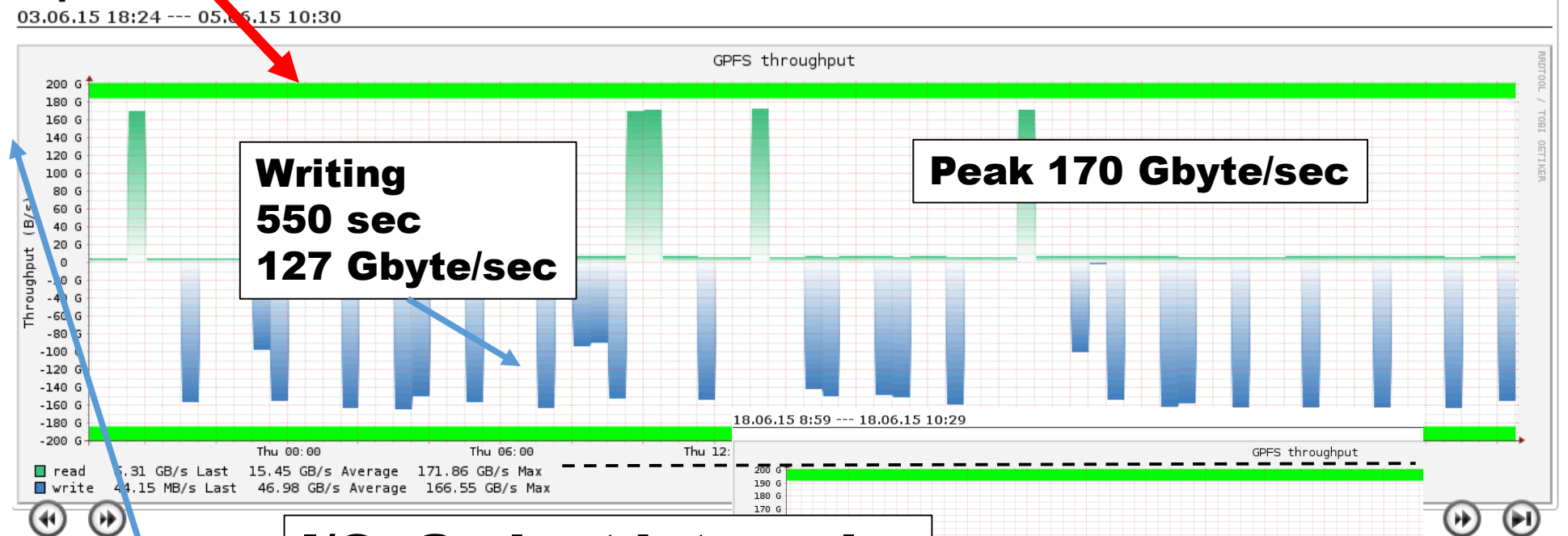
reaching 170 Gbyte/sec, more than 3 Peta byte written

Dying nodes are the main hassle !

12h longest continuous run, checkpoints all 1.5h

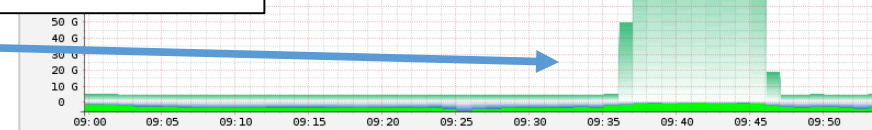
MAGNETICUM

	Box0	Box1	Box2b	Box2	Box3	Box4
[Mpc/h]	2688	896	640	352	128	48
mr	2×4536^3	2×1526^3	—	2×594^3	2×216^3	2×81^3
hr	—	—	2×2880^3	2×1584^3	2×576^3	2×216^3
uhr	—	—	—	—	$2 \times 1536^3 (z=2)$	2×576^3



Reading
460 sec
152 Gbyte/sec

I/O: Gadget internal,
2048 tasks in parallel



The Computational Challenge

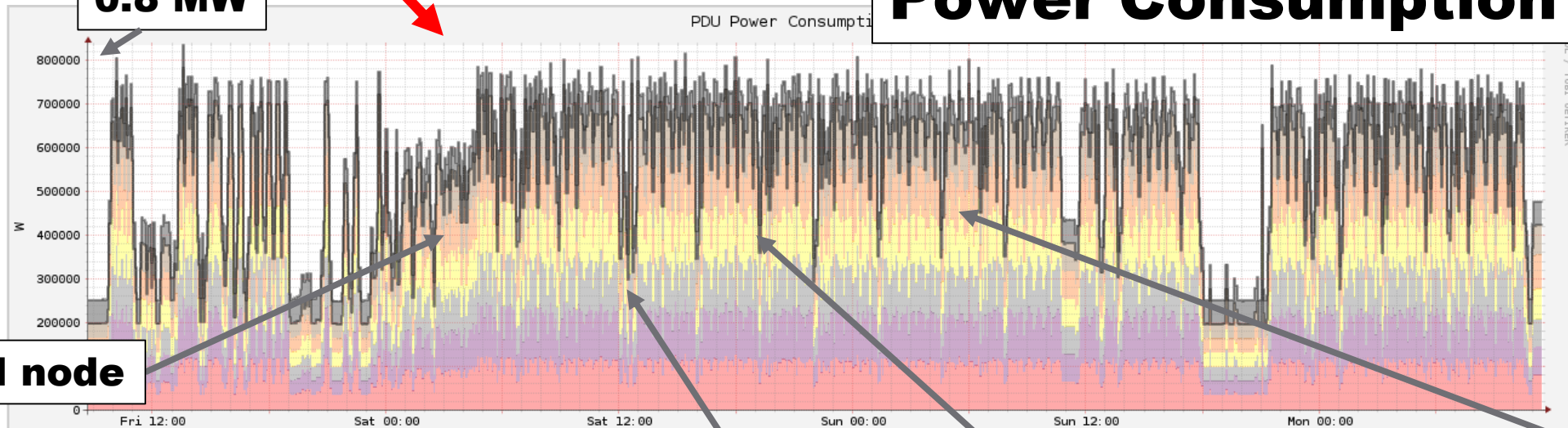
MAGNETICUM



	Box0	Box1	Box2b	Box2	Box3	Box4
[Mpc/h]	2688	896	640	352	128	48
mr	2×4536^3	2×1526^3	—	2×594^3	2×216^3	2×81^3
hr	—	—	2×2880^3	2×1584^3	2×576^3	2×216^3
uhr	—	—	—	—	$2 \times 1536^3 (z=2)$	2×576^3

0.8 MW

Power Consumption



Single bad node

checkpointing

12 h

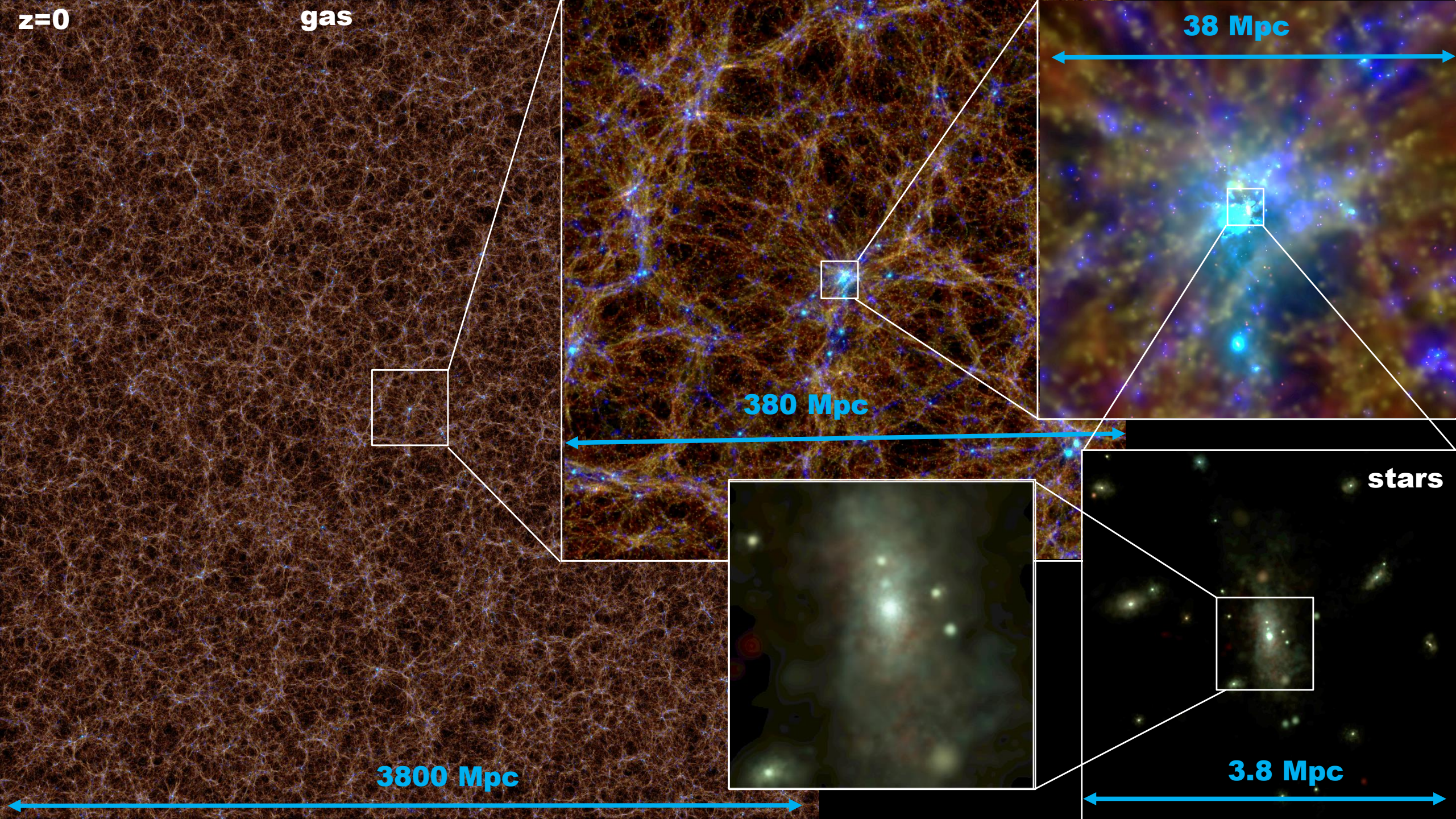
global timestep

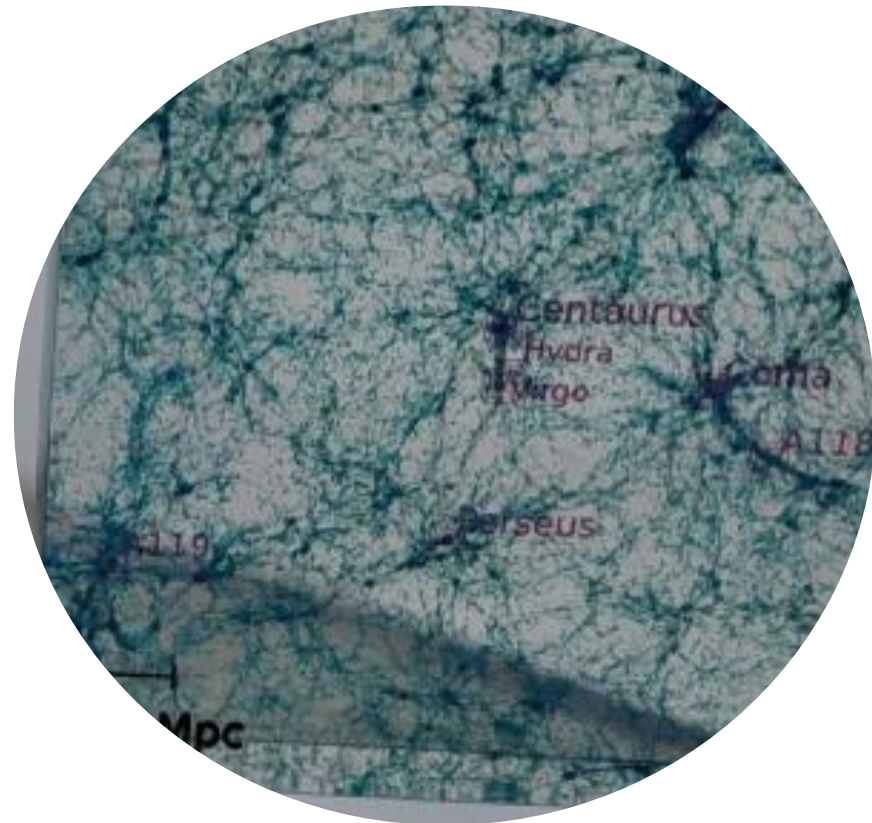
dying nodes

■ i20	79.01 kW Last	89.66 kW Average	129.72 kW Max
■ i21	65.03 kW Last	88.88 kW Average	129.39 kW Max
■ i22	63.08 kW Last	88.95 kW Average	130.15 kW Max
■ i23	69.63 kW Last	89.31 kW Average	130.40 kW Max
■ i24	78.51 kW Last	89.51 kW Average	131.31 kW Max
■ i25	67.61 kW Last	89.18 kW Average	130.03 kW Max
■ io02	52.47 kW Last	54.89 kW Average	64.01 kW Max

Average power consumption in time period (compute): 535.488 kW

Average power consumption in time period (all): 590.375 kW

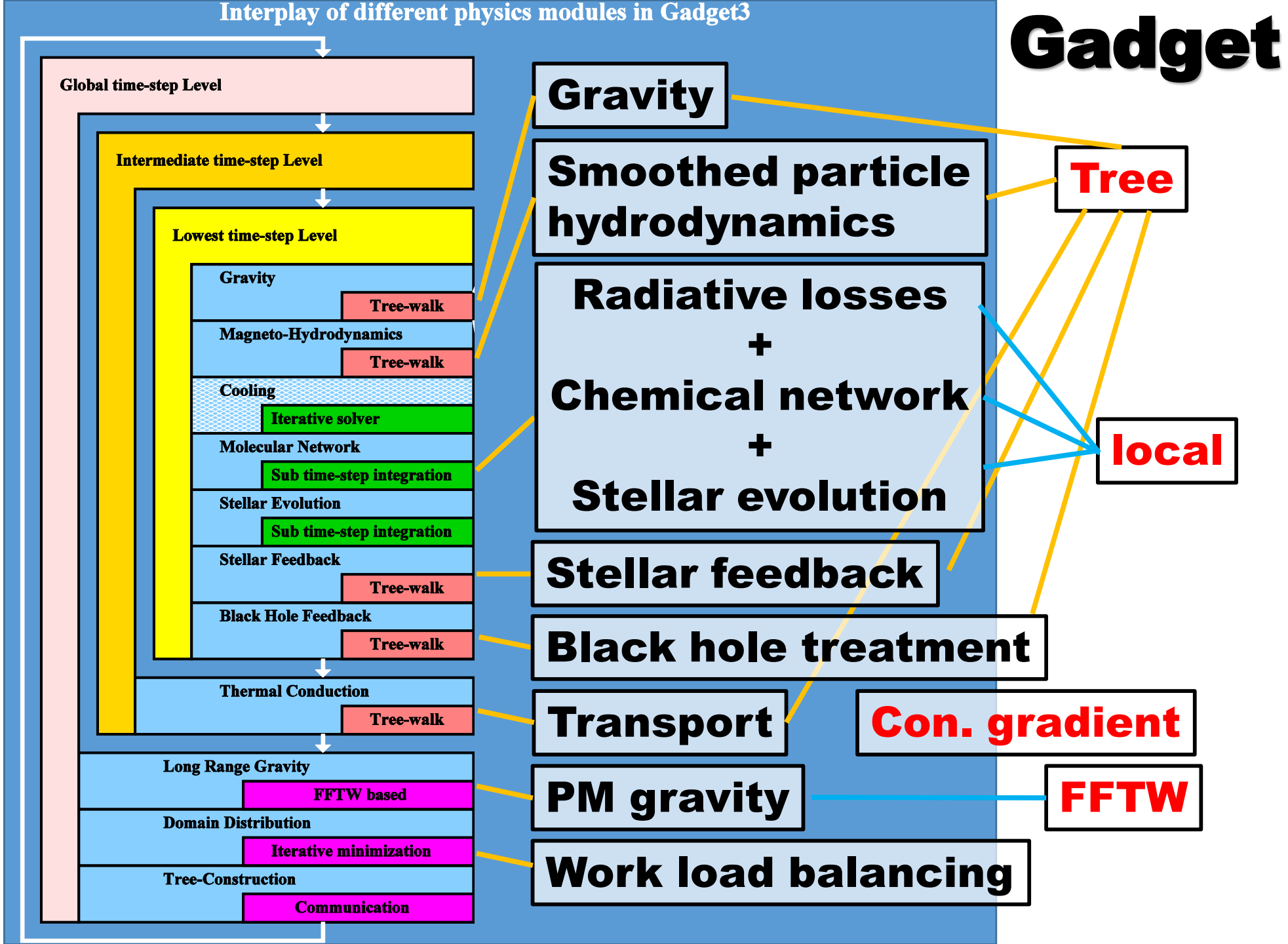




HPC Challenges in Astrophysics

V) Parallelization

Various physical processes on various timescales ...



MPI level

How to count workload?

compute dominated

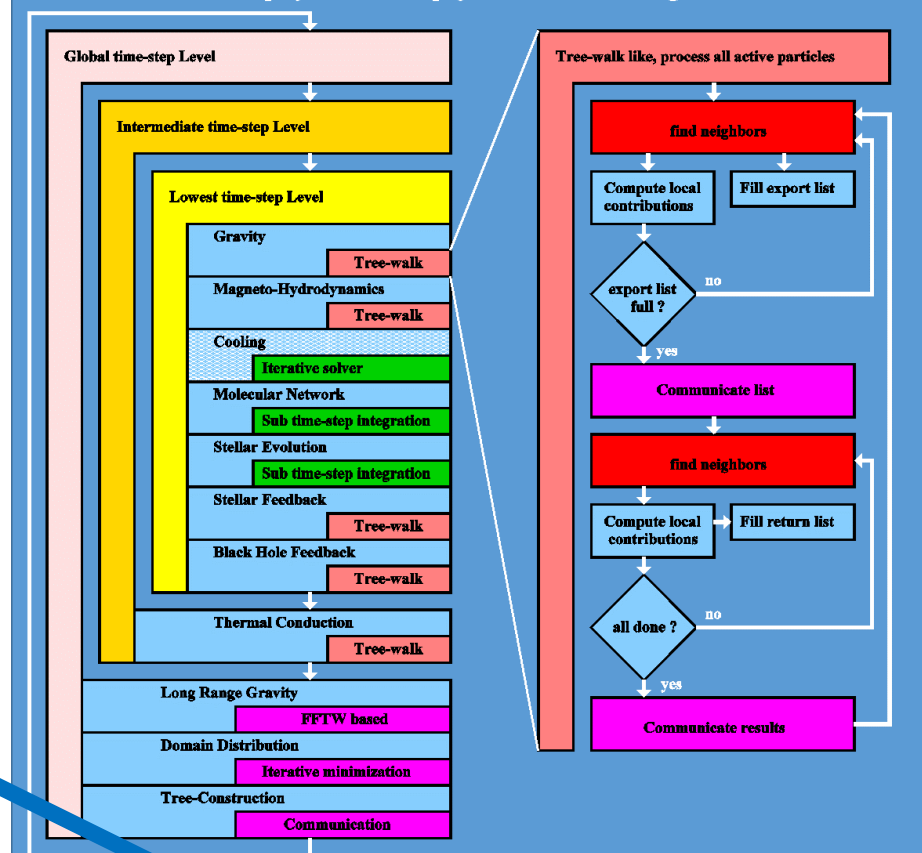
overhead dominated

Sync-Point 35762, Time: 0.354961, Redshift: 1.81721, Systemstep: 5.56636e-06, Dloga: 1.56817e-05

	Occupied timebins:	non-cells	cells	dt	cumulative A D	avg-time	cpu-frac
X bin=20	88467428683	83736416883	0.008029050471	187287803634	< *	712.64	22.0%
X bin=19	4161559798	7573611723	0.004014525236	15083958068	*	219.80	6.8%
X bin=18	689640843	1347123564	0.002007262618	3348786547	*	63.43	3.9%
X bin=17	114047063	493679540	0.001003631309	1312022140		100.57	12.4%
X bin=16	424984562	98886753	0.000501815654	704295537		14.78	3.7%
X bin=15	149882337	22957206	0.000250907827	180424222		24.04	11.9%
X bin=14	1436369	5551598	0.000125453914	7584679		5.78	5.7%
X bin=13	10827	562559	0.000062726957	596712		3.46	6.8%
X bin=12	453	22095	0.000031363478	23326		2.38	9.4%
X bin=11	10	768	0.000015681739	778		2.20	17.4%

PM-Step. Total:		94008990945	93278812689	Sum:	187287803634		

Interplay of different physics modules in Gadget3



Various physical processes on various timescales ...

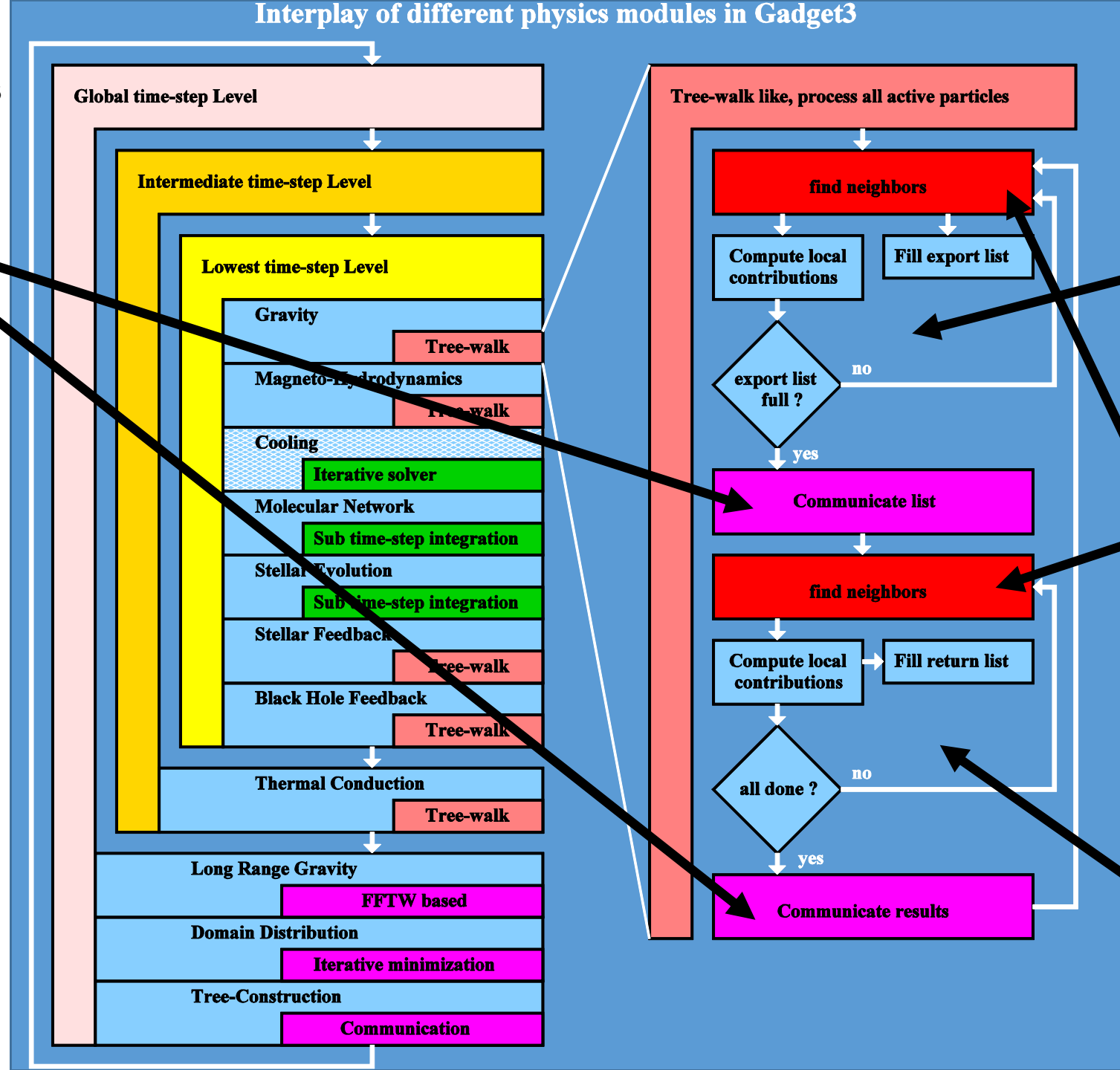
MPI:
Communication needs to be buffered/chopped!

The GPU Challenge

Goal:
 10^5 Cores
+
 10^4 GPUs
+
Physics

OpenACC

Interplay of different physics modules in Gadget3

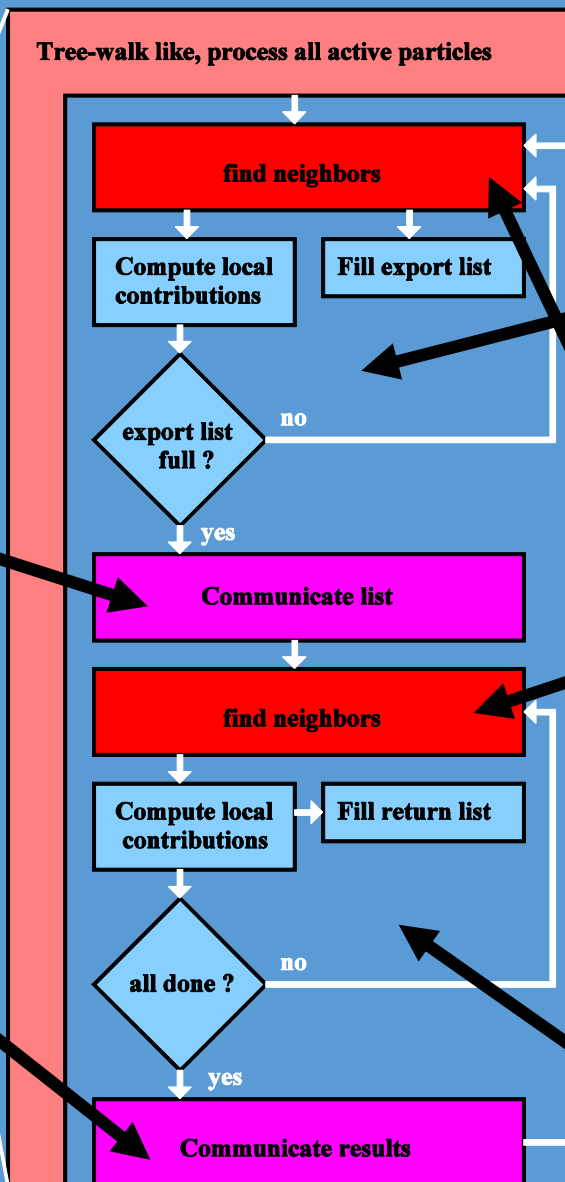


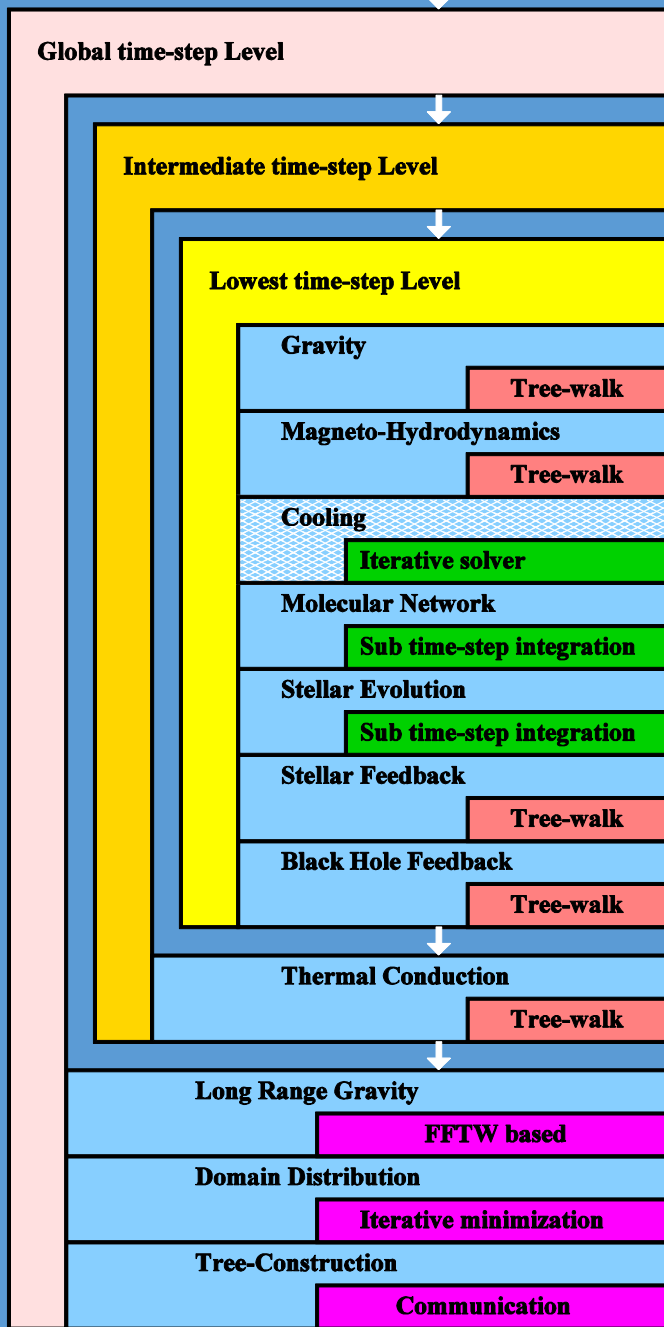
Gadget

Compute local contributions to forces

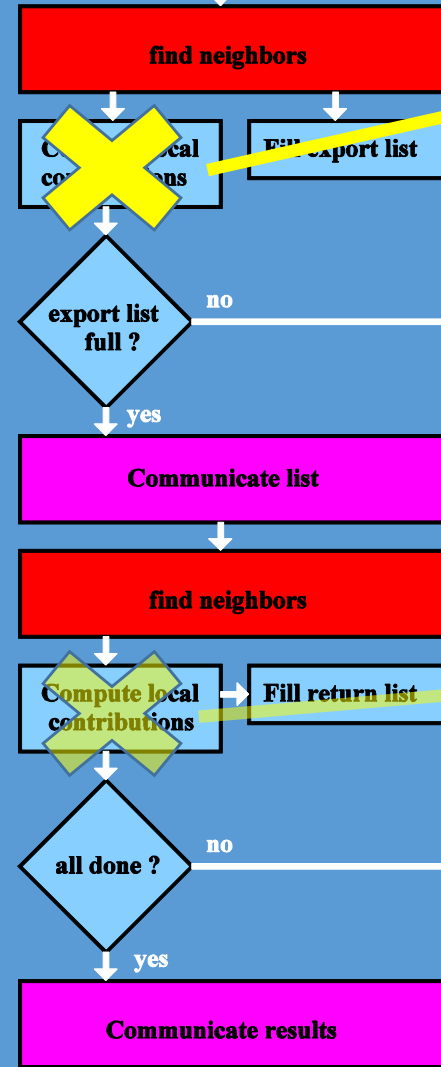
OpenMP
(loop over particles)

Compute contributions for external cells/particles

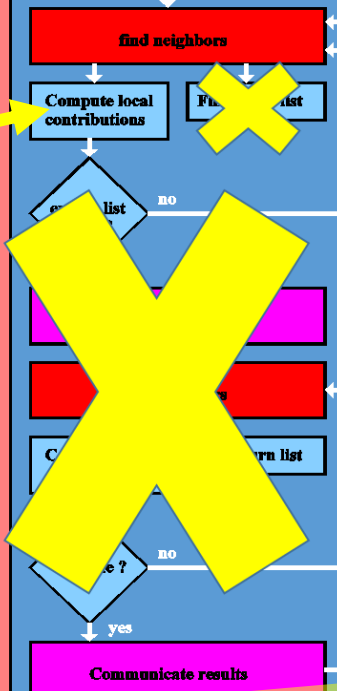




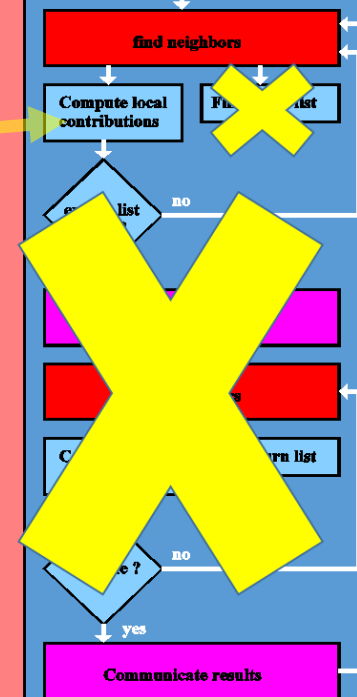
Tree-walk like, process all active particles



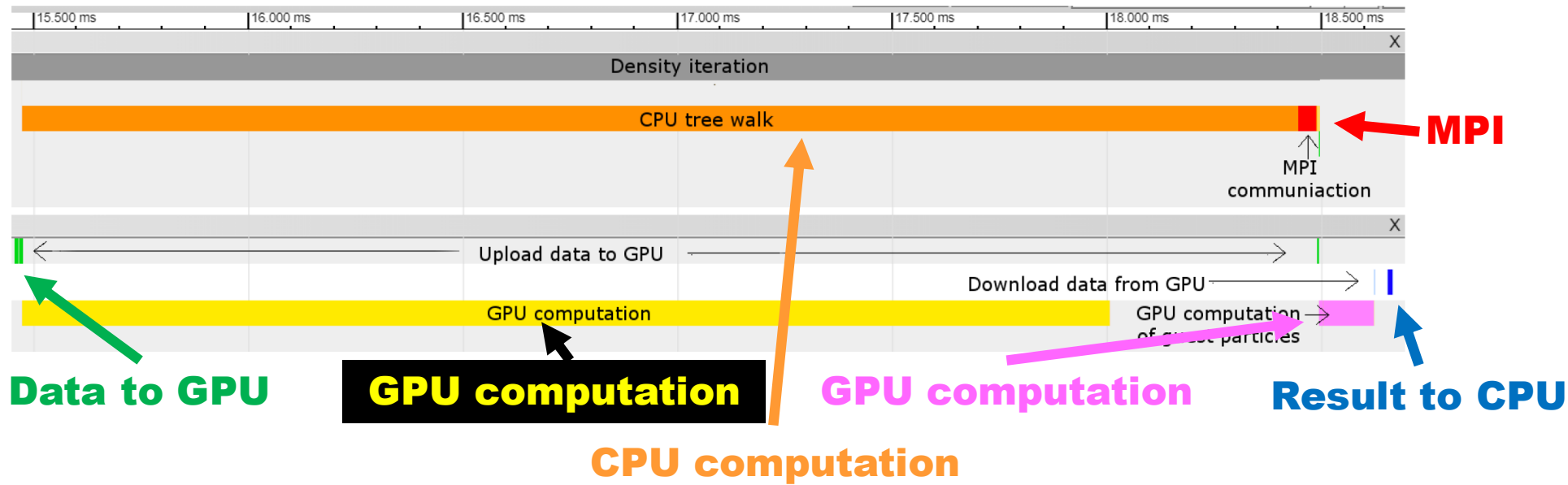
Tree-walk like, process all active particles



Tree-walk like, process all active particles



asynchrones hybrid approach !



256 Nodes with GPUs, 48 Million part/node

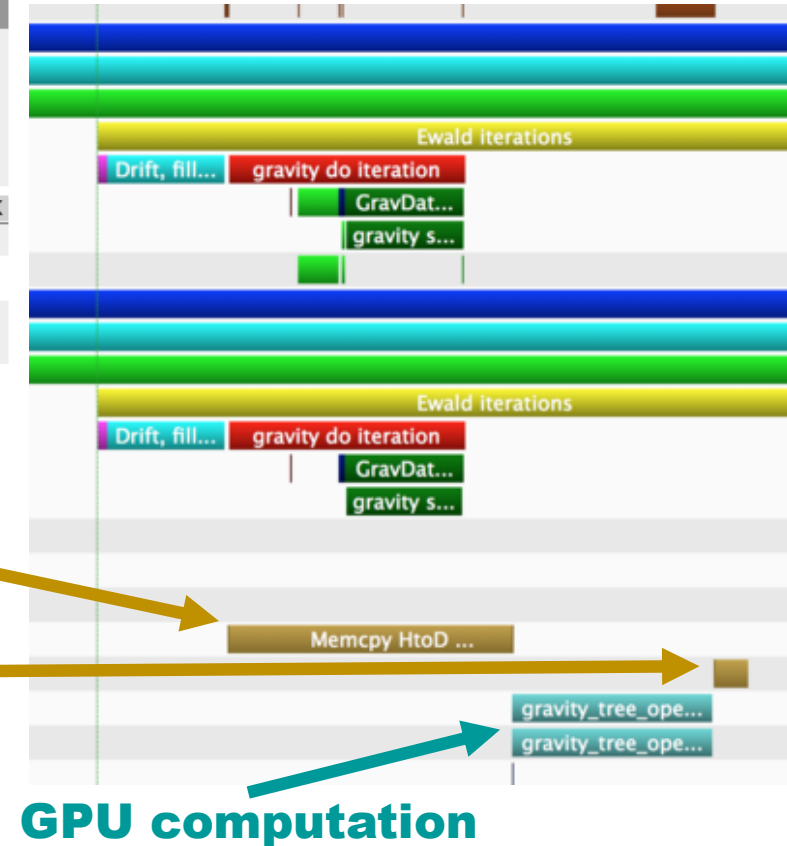
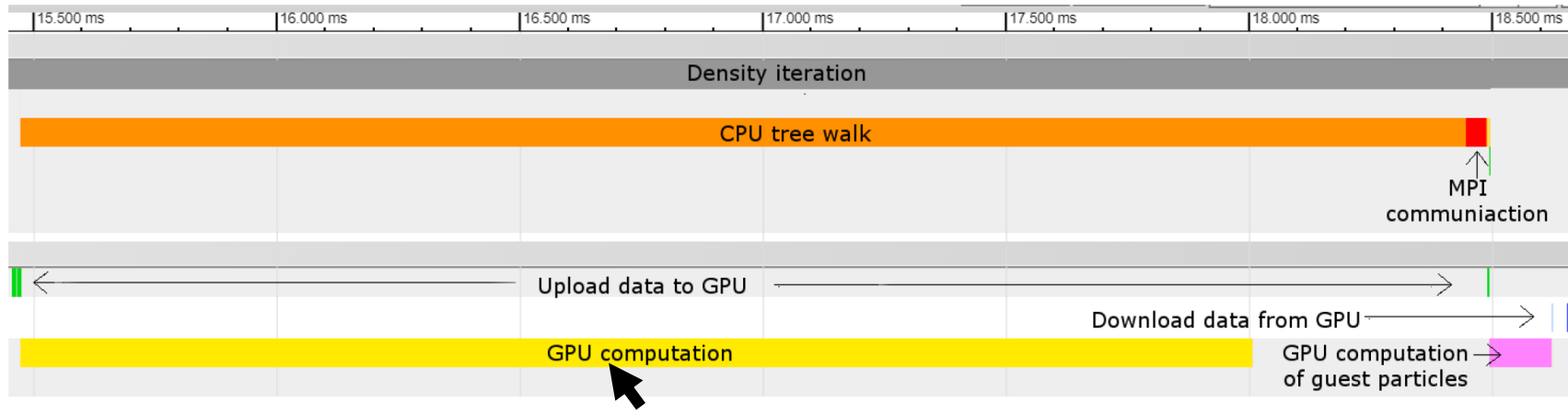
Step 0, Time: 0.0163934, CPUs: 256

	CPU only	GPU hybrid
total	356.60	153.48
treegrav	112.32	44.08
treebuild	17.64	28.08
treewalk	86.22	8.90
pmgrav	52.42	16.92
peano	12.32	4.94

Significant gain !

Performance analysis (see talks by Zhukov/Ernst)

Gadget



Data to GPU

Result to CPU

GPU computation

256 Nodes with GPUs, 48 Million part/node

Step 0, Time: 0.0163934, CPUs: 256

	CPU only	GPU hybrid
total	356.60	153.48
treegrav	112.32	44.08
treebuild	17.64	28.08
treewalk	86.22	8.90
pmgrav	52.42	16.92
peano	12.32	4.94

Sync-Point 778948, Time: 0.304166, Redshift: 2.28768, Systemstep: 7.4529e-08, Dloga: 2.45027e-07

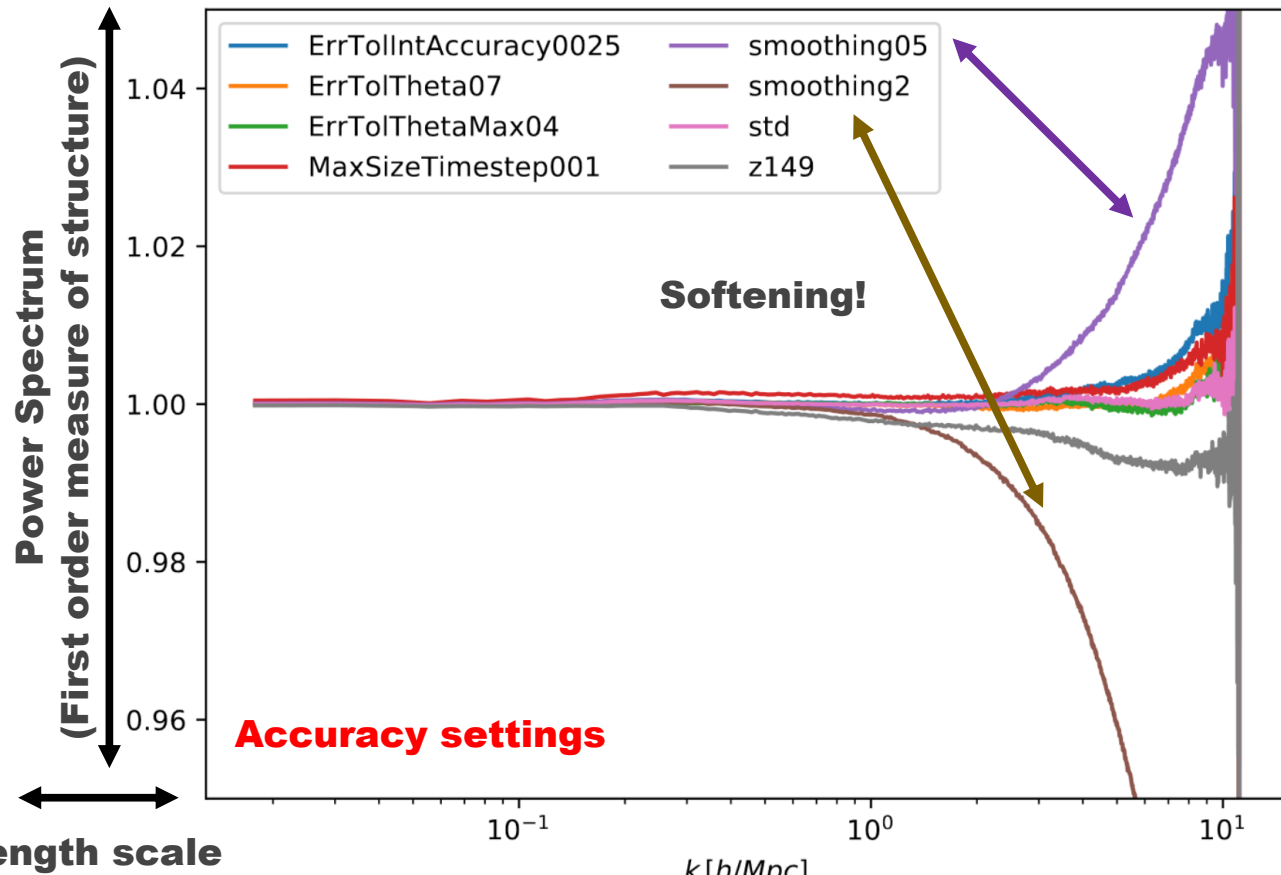
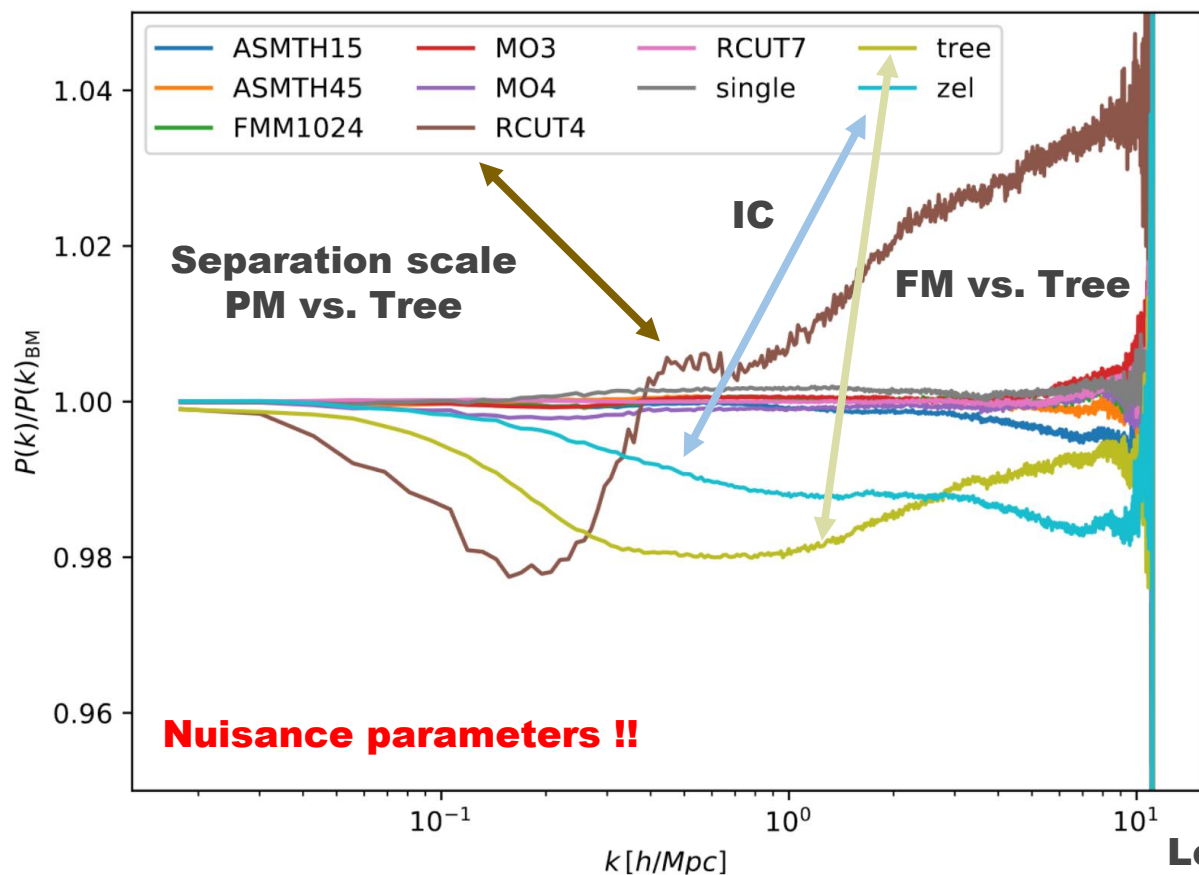
Occupied timebins:	non-cells	cells	dt	cumulative A D	avg-time	cpu-frac
bin=17	3691699971	3369282024	0.001003631309	7765818991 *	595.00	7.8%
bin=16	222244624	113555358	0.000501815654	704836996 *	324.98	4.3%
bin=15	192638063	55376259	0.000250907827	369037014 *	260.81	6.9%
X bin=14	62615764	27335556	0.000125453914	121022692 < *	273.60	14.4%
X bin=13	9092395	13188845	0.000062726957	31071372	130.15	13.7%
X bin=12	1478314	4993371	0.000031363478	8790132	68.56	14.4%
X bin=11	202915	1571775	0.000015681739	2318447	31.35	13.2%
X bin=10	627	426009	0.000007840870	543757	1.60	1.3%
X bin= 9	144	98760	0.000003920435	117121	1.16	1.9%
X bin= 8	21	14971	0.000001960217	18217	0.95	3.2%
X bin= 7	1	2800	0.000000980109	3225	0.60	4.1%
X bin= 6	1	414	0.000000490054	424	0.39	5.2%
X bin= 5	0	9	0.000000245027	9	0.35	9.5%
Total active:	73390182	47632510	Sum:	121022692		

HPC Challenges in Astrophysics

VI) Basic precision

Now „High-Precision Cosmology“ era, need to reach % precision !

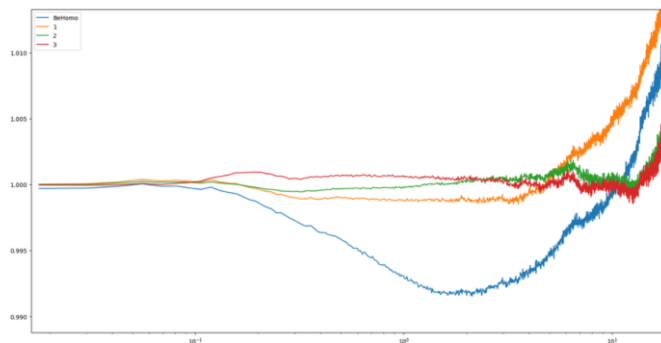
How good do we understand Dark Matter only simulations ?



G4 Tests

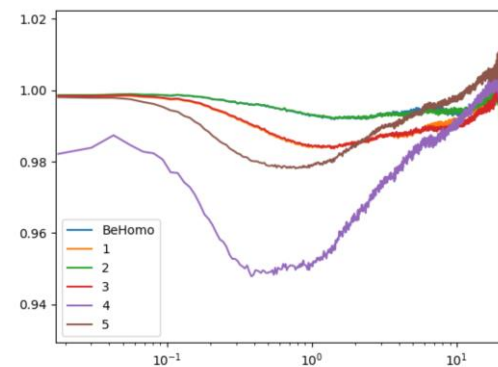
Name	# ASMTH	# RCUT	# PM	# Box
BeHomo	1.25	4.5	1024	500
Benchmark	3	6	512	500
config1	1.25	6	1024	500
config2	2.5	6	512	500
config3	5	6	512	500

COUNT 5



G5 Tests

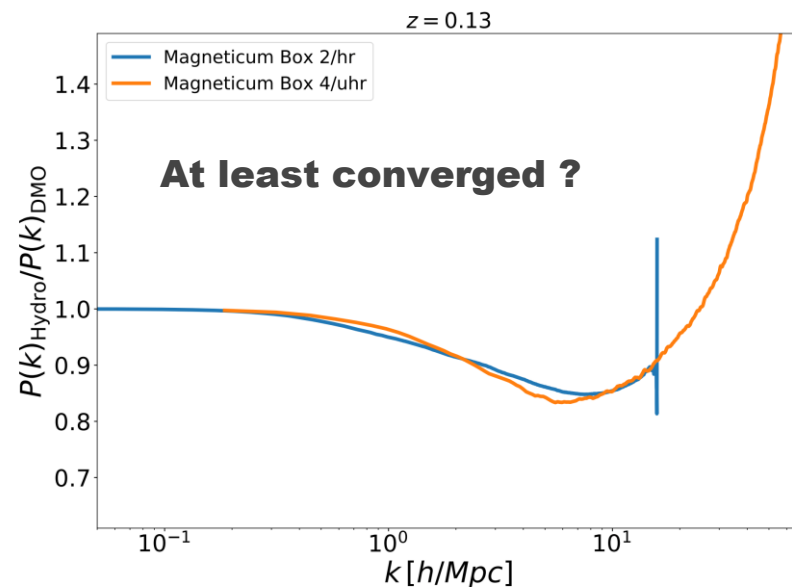
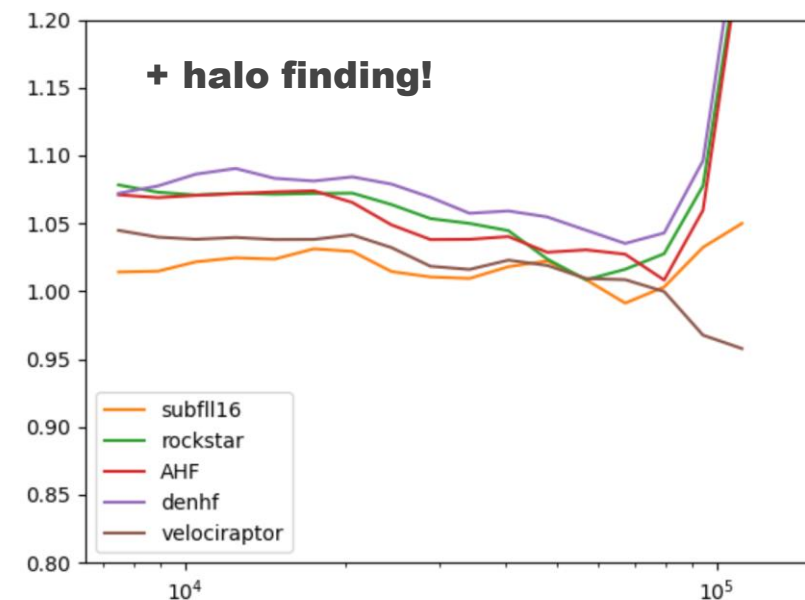
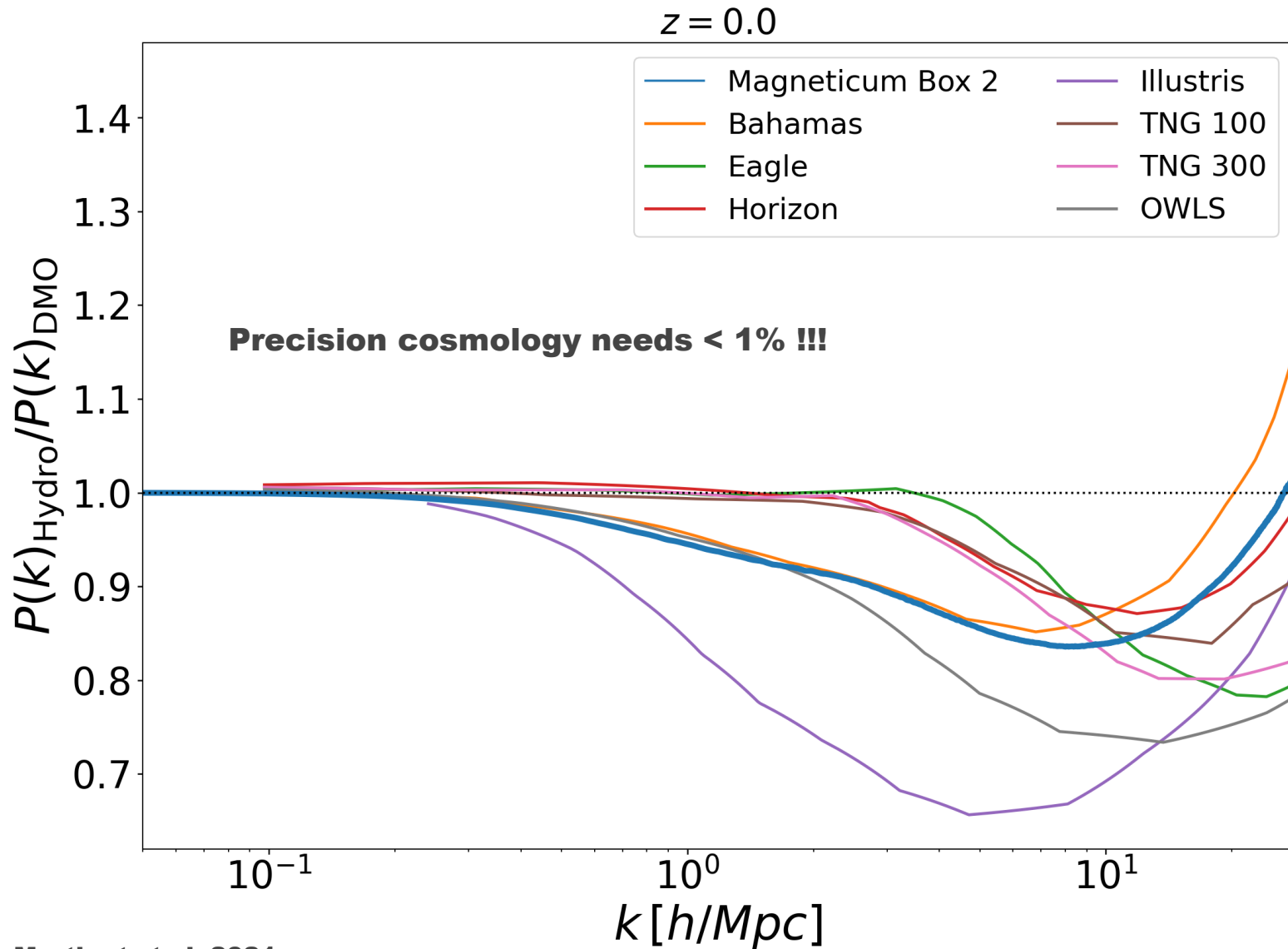
Name	# ASMTH	# RCUT	# PM	# Box
BeHomo	1.25	4.5	1024	500
config1	2.5	4.5	1024	500
config2	1.25	6	1024	500
config3	2.5	6	1024	500
config4	5	3	1024	500
config5	5	4.5	1024	500



Now „High-Precision Cosmology“ era, need to reach % precision !

Dark Matter only vs. hydro dynamical simulation

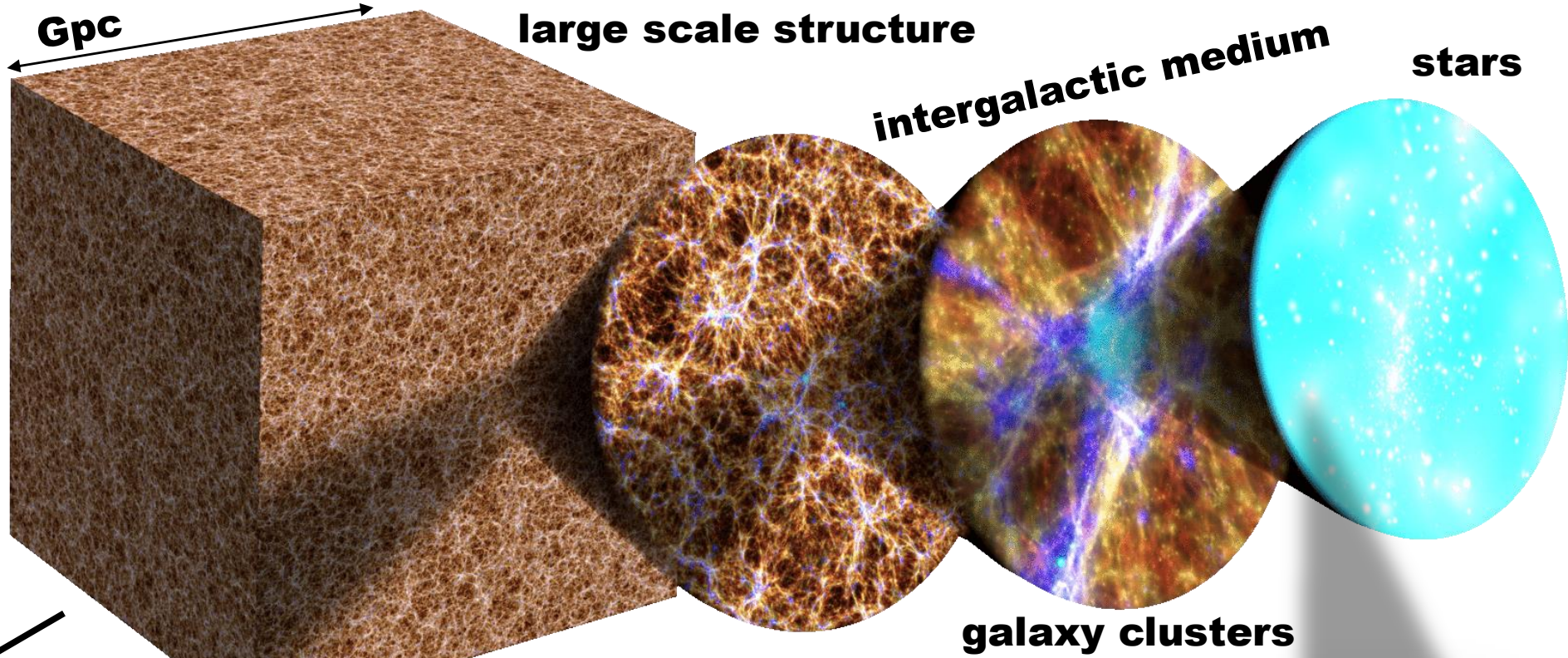
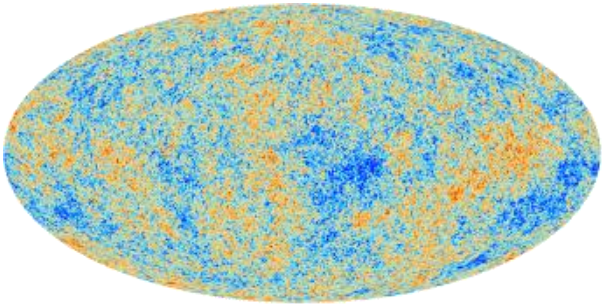
Do we understand our “astrophysics” ?



HPC Challenges in Astrophysics

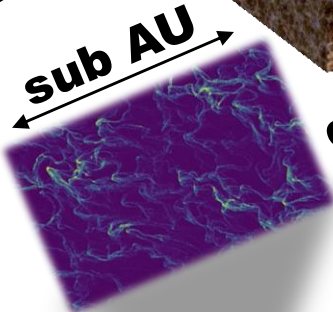
VII) Extra Physics

The Computational Challenge



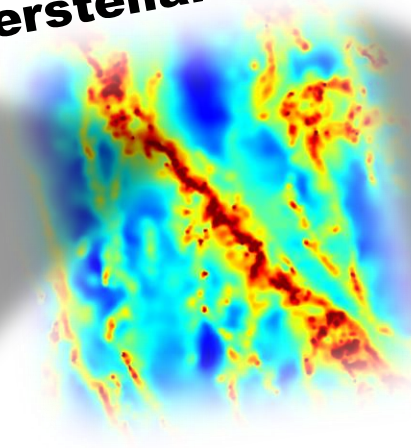
**multi-scale,
multi-physics**

$3 \cdot 10^{22} \text{ km}$

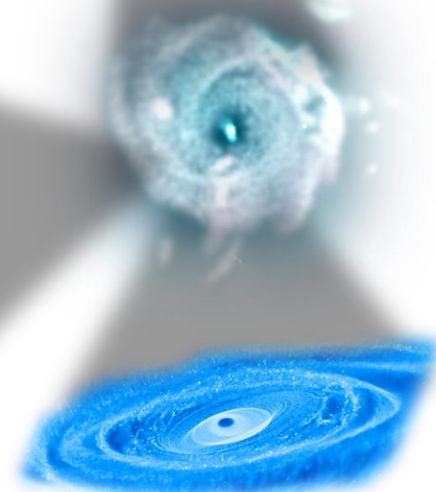


**dust
grains**

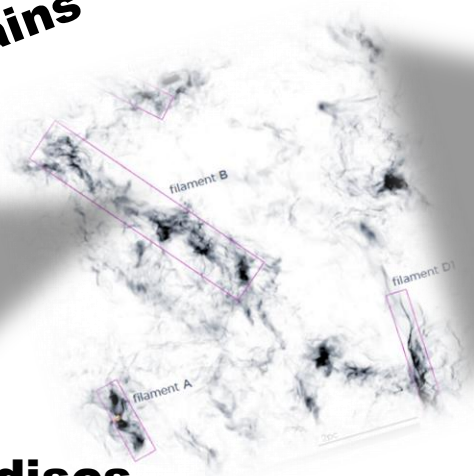
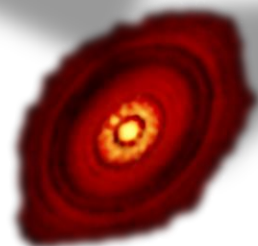
interstellar medium



black holes



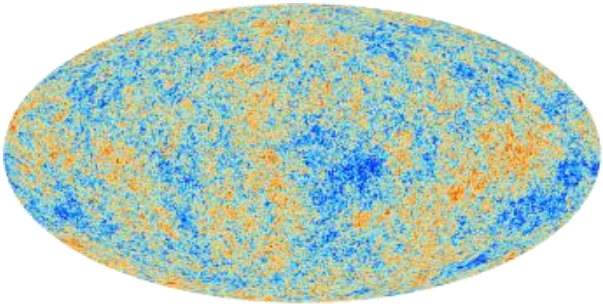
protoplanetary discs



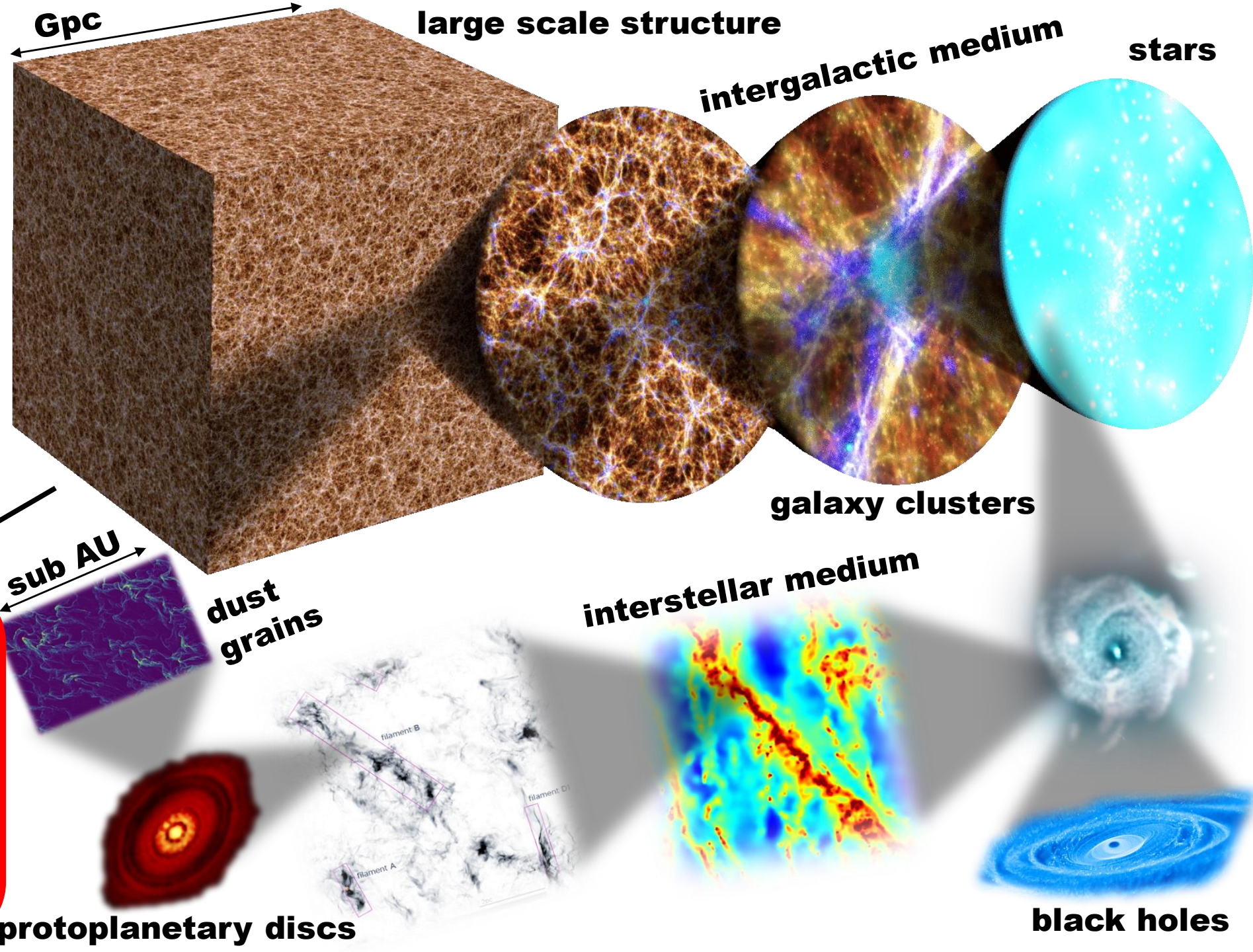
	λ_{mfp}	λ_{Lamor}	λ_{Debye}
electrons	1 kpc	700 km	6 km
protons		29000 km	

Plasma Physics!

The Computational Challenge



**multi-scale,
multi-physics**



$3 \cdot 10^{22} \text{ km}$



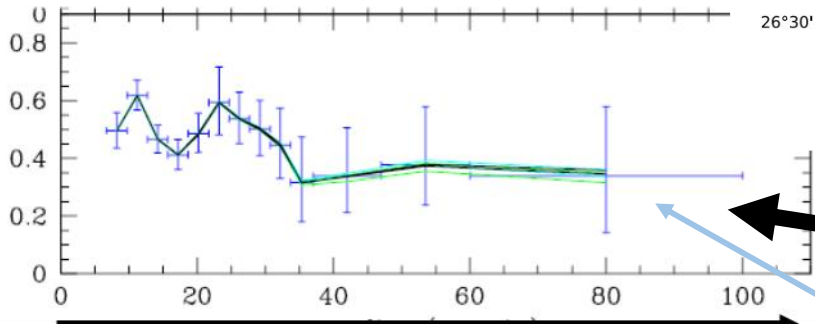
	λ_{mfp}	λ_{Lamor}	λ_{Debye}
electrons	1 kpc	700 km	6 km
protons		29000 km	

Plasma Physics!

ICM is the hot Atmosphere of Massive Galaxies

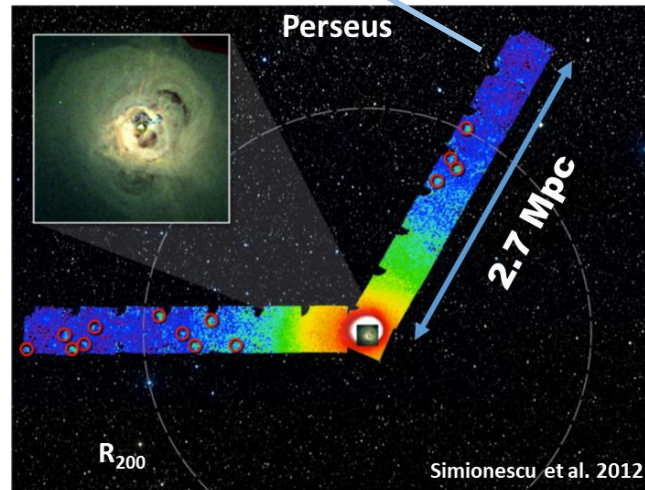
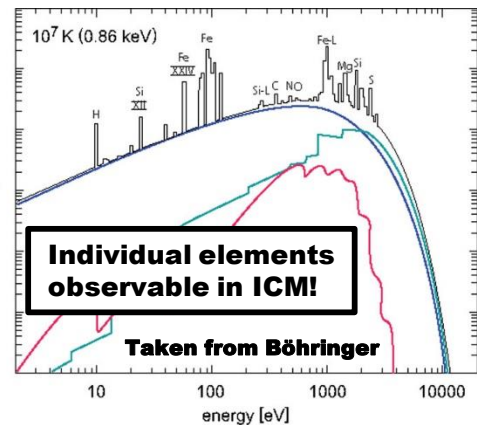
- ❑ Measured in large details
X-ray (temperature, velocities)
SZ (pressure)
- ❑ Non-thermal components
give additional insights
(magnetic fields, CRs)
- ❑ Closed system
(chemical imprint)

Metallicity [Solar]

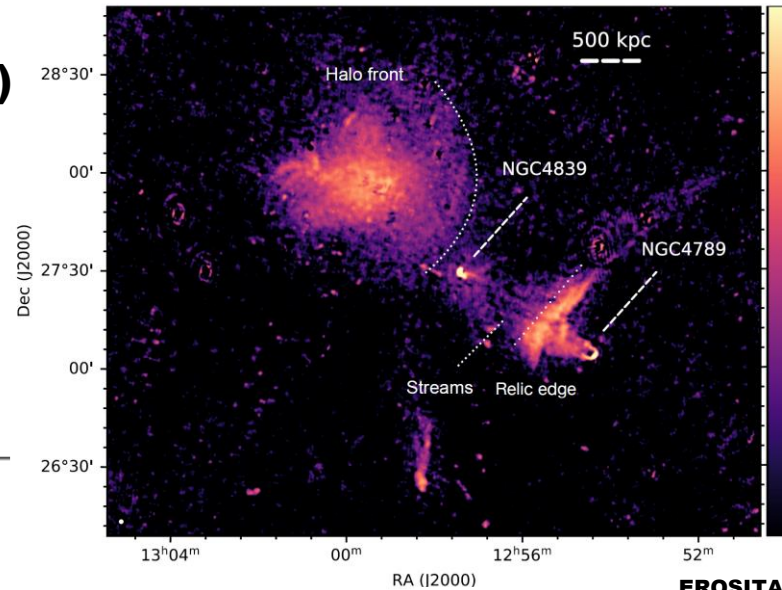


Radius

All ICM within R_{vir}
contains at least
10% stellar debris!

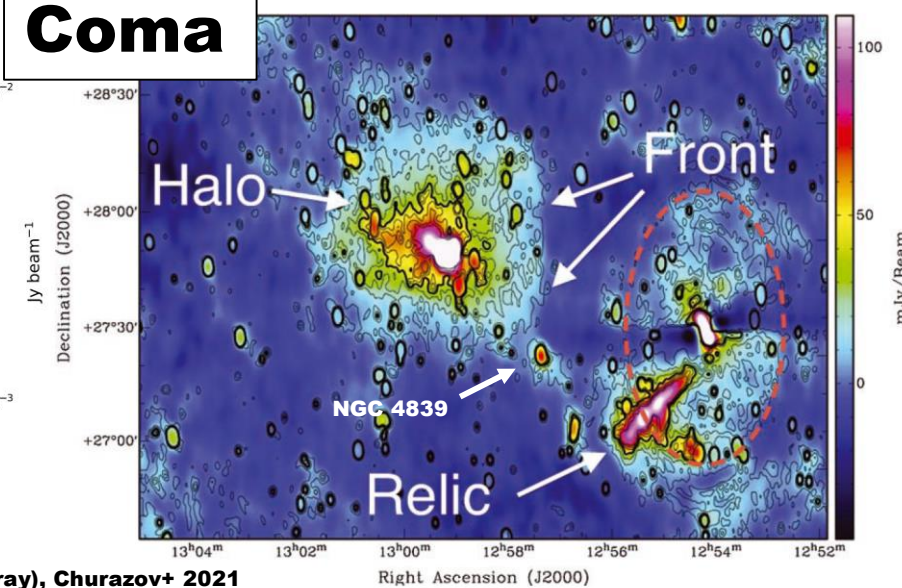


LOFAR (144 MHz), Bonafede+ 2020

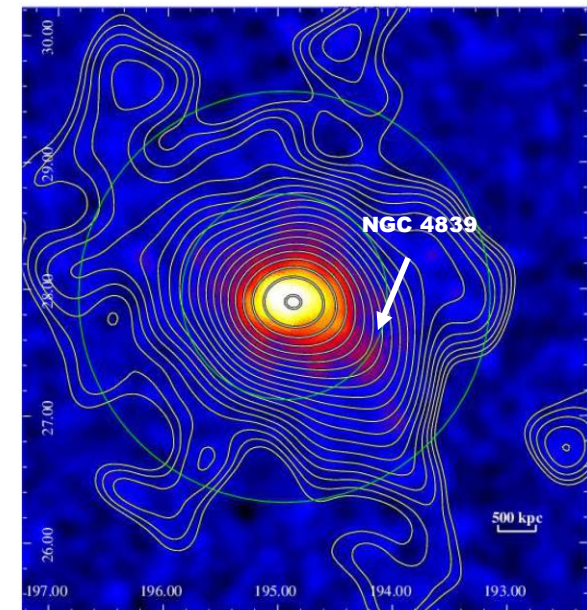
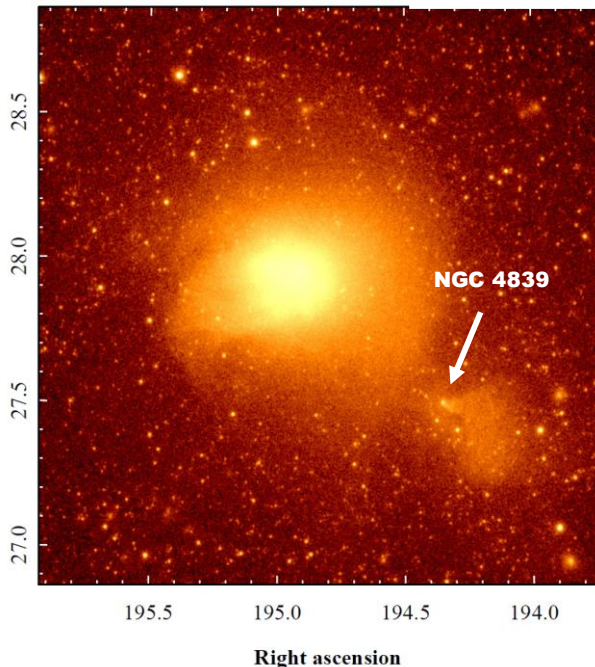


Coma

GMRT (352 MHz), Brown+ 2011



EROSITA (X-ray), Churazov+ 2021



PLANCK (SZ), Planck 2012

Example: Cosmic Rays (e.g. high energy articles)

Short cooling time of CRe:

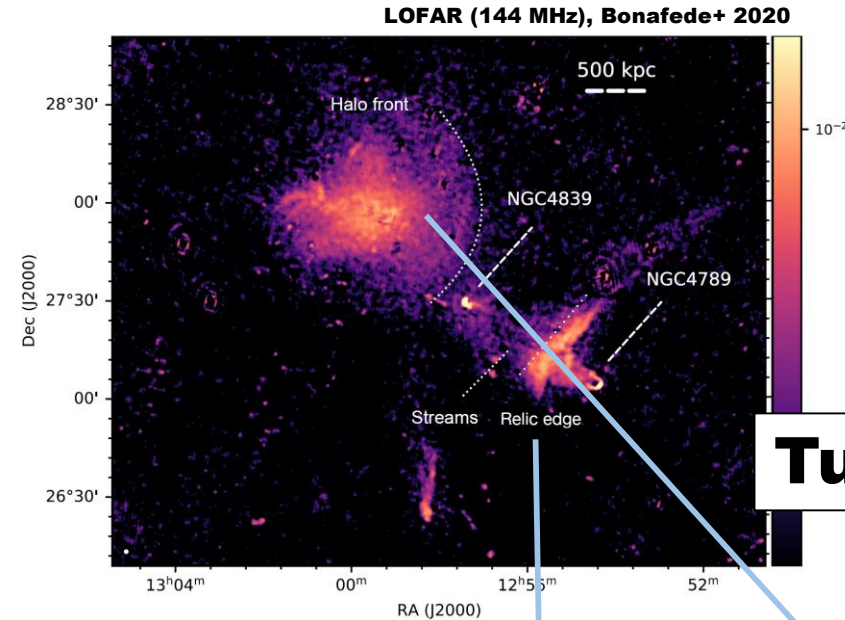
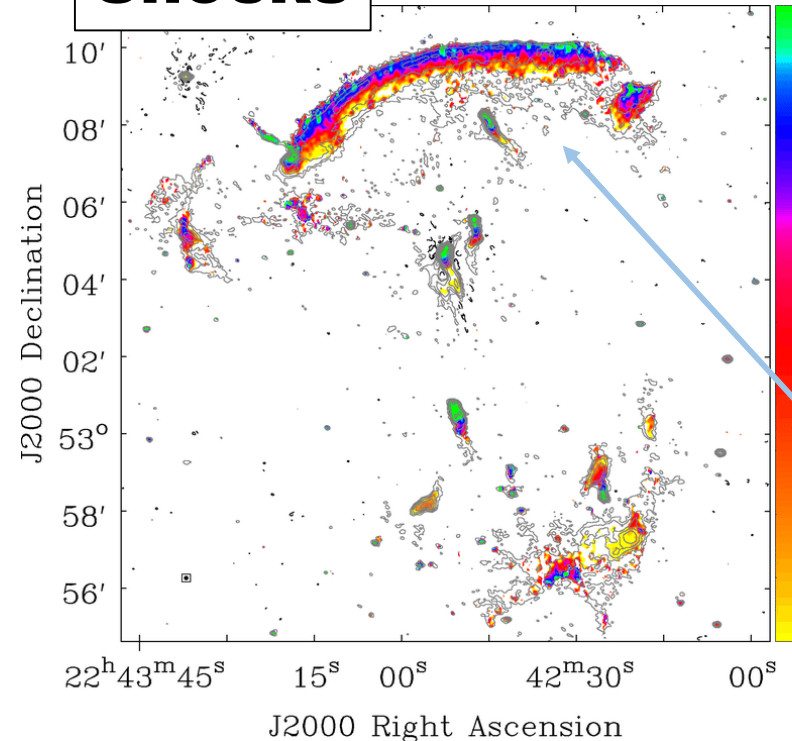
- ❑ test shocks on 10th of kpc
- ❑ test turbulence (re-acceleration)

Long cooling time of CRp:

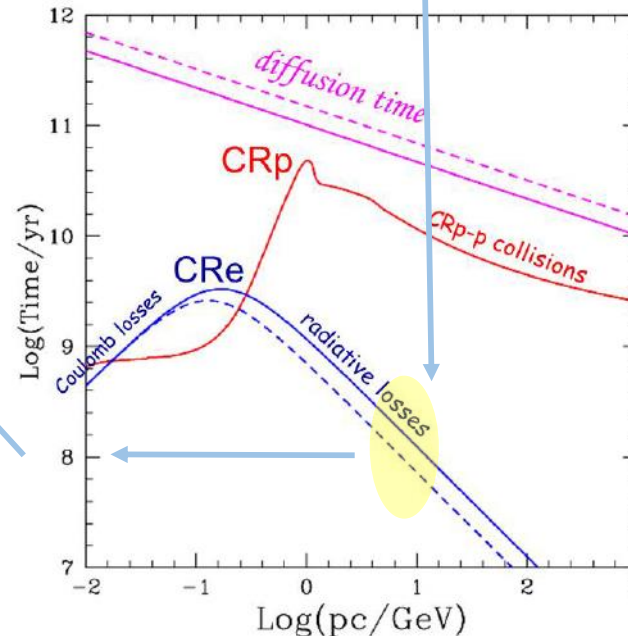
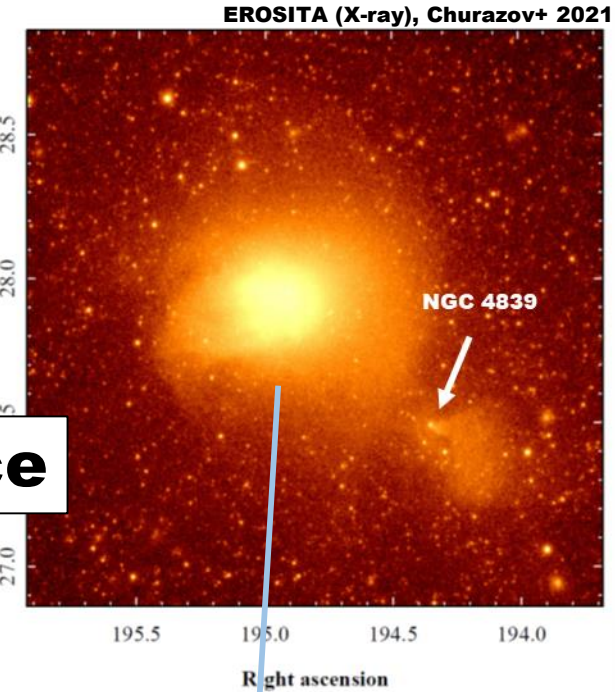
- ❑ can be dynamically important

Both couple to B-Field

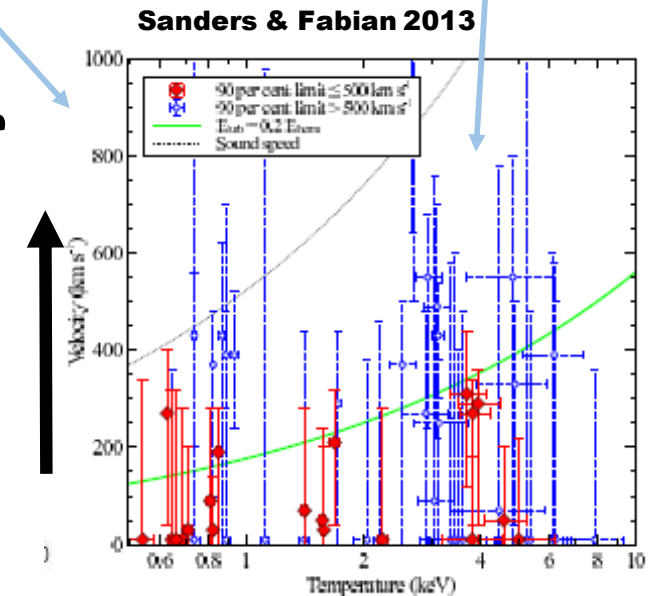
Shocks



Turbulence



Turbulent Velocity

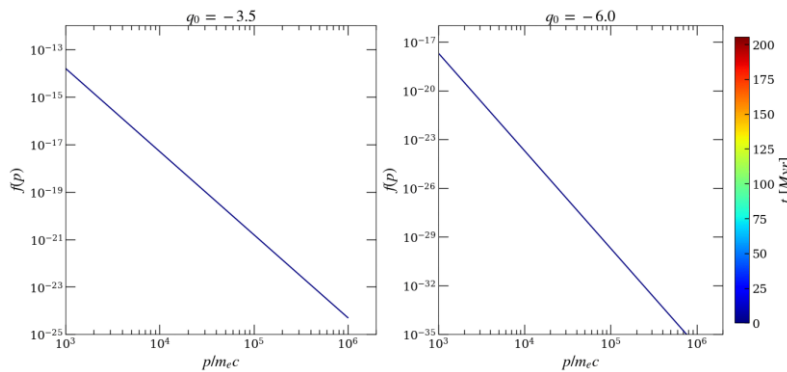


Adding a Fokker-Planck solver for CRs to the gas

$$\frac{\partial f}{\partial t} + \underbrace{\mathbf{u} \cdot \nabla f}_{\text{spatial convection}} - \underbrace{\nabla (\kappa \nabla f)}_{\text{spatial diffusion}} =$$
$$\underbrace{\frac{1}{3} (\nabla \cdot \mathbf{u}) p \frac{\partial f}{\partial p}}_{\text{momentum convection}} + \underbrace{\frac{1}{p^2} \frac{\partial}{\partial p} \left(p^2 \left[b_\ell f + D_p \frac{\partial f}{\partial p} \right] \right)}_{\text{momentum diffusion + continuous losses}} - \underbrace{\frac{f(p, \mathbf{x}, t)}{t_c(p, \mathbf{x})}}_{\text{catastrophic losses}} + \underbrace{j(p, \mathbf{x})}_{\text{source term}}$$

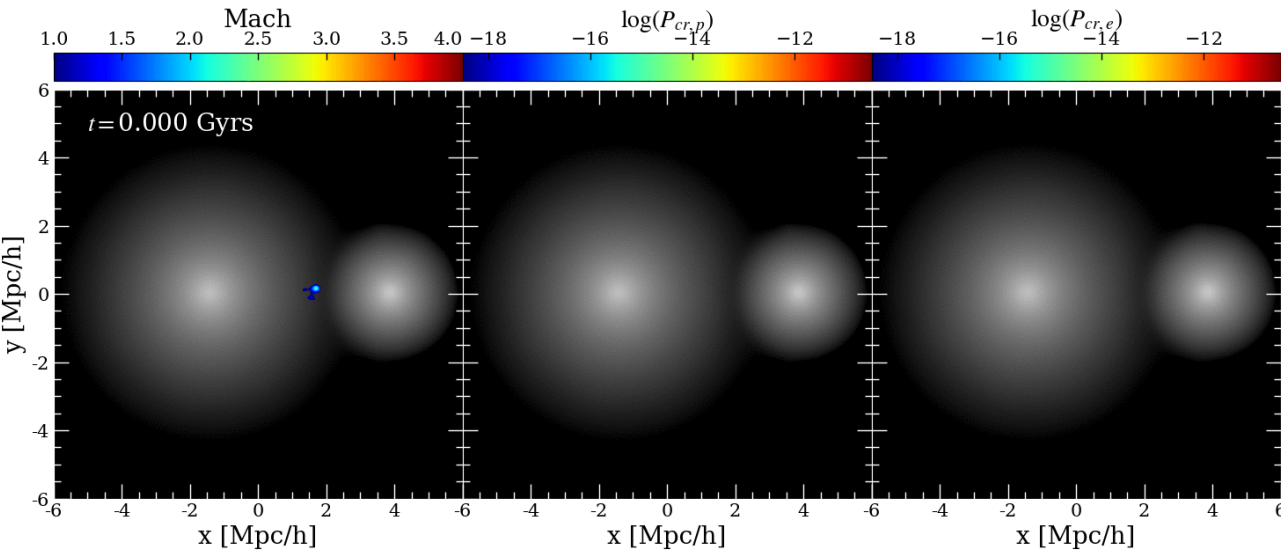
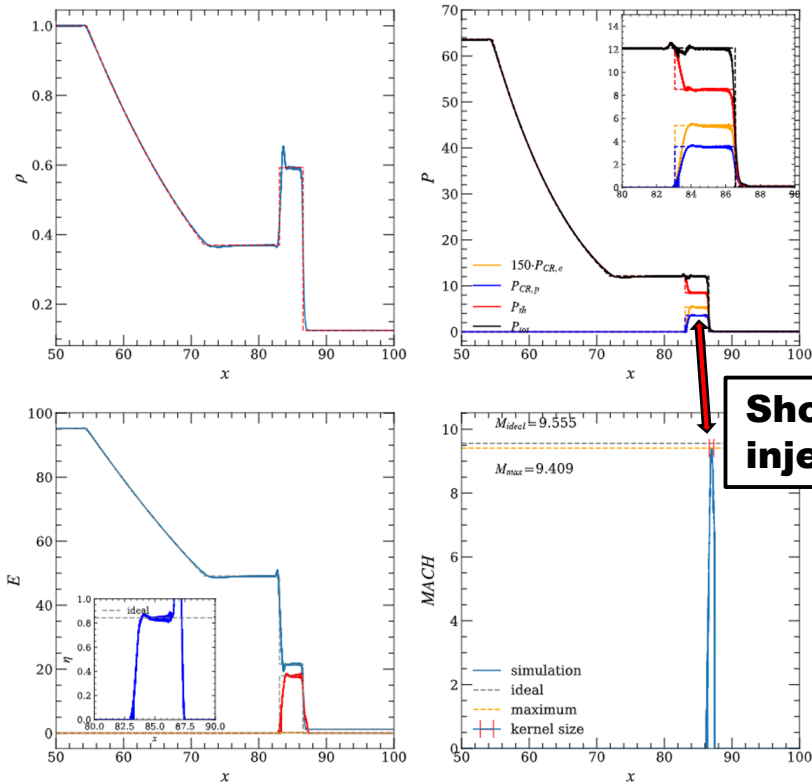
- Shocks
- SFR
- AGN

Cooling of CRe

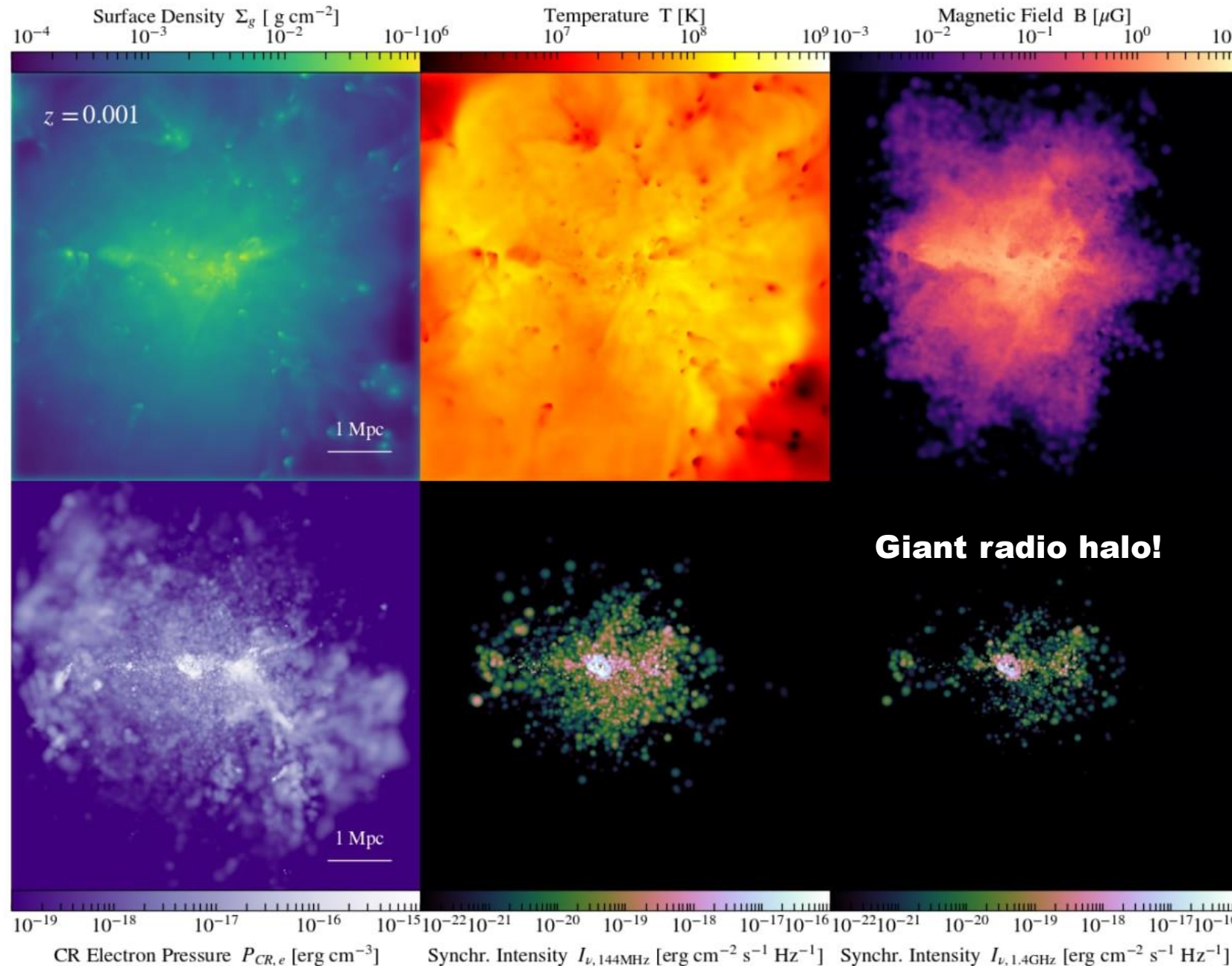


Every resolution element in a simulation has to additionally evolve a sampled distribution function of CR(e,p)!

Shock injection



SLOW: 3072³ cosmological simulation with MHD+CR (60 Mio CPUh!)



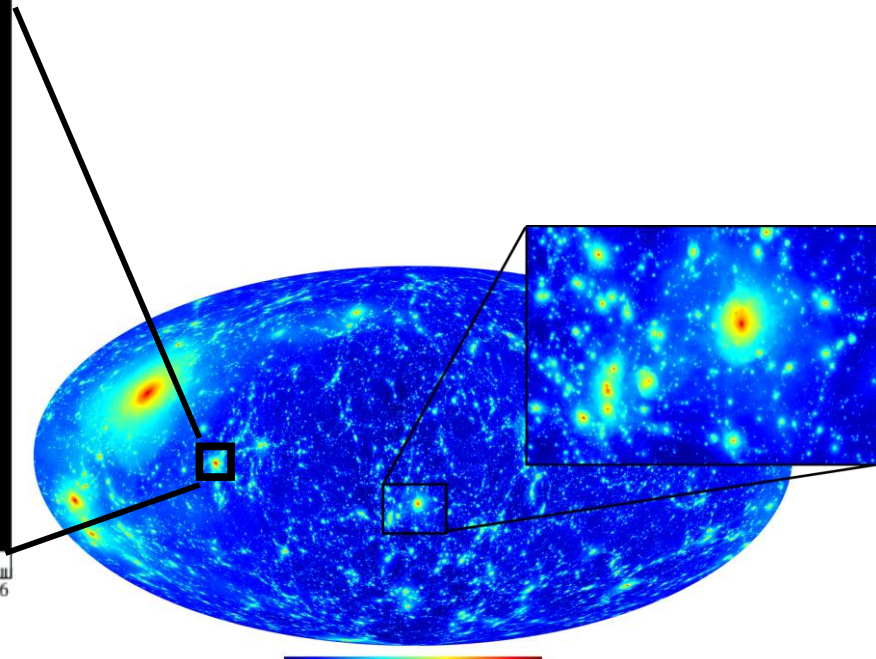
3072³ resolution elements
2.9·10¹⁰ particles, each 2.5kb

24 bins CRe, 8 bins CRp
63592 time steps

→ 5.2·10¹³ times solved Fokker-Planck EQ

3072 Nodes, 48 cores
(=147456 threads, e.g. halve SuperMUC-NG)

Giant radio halo!

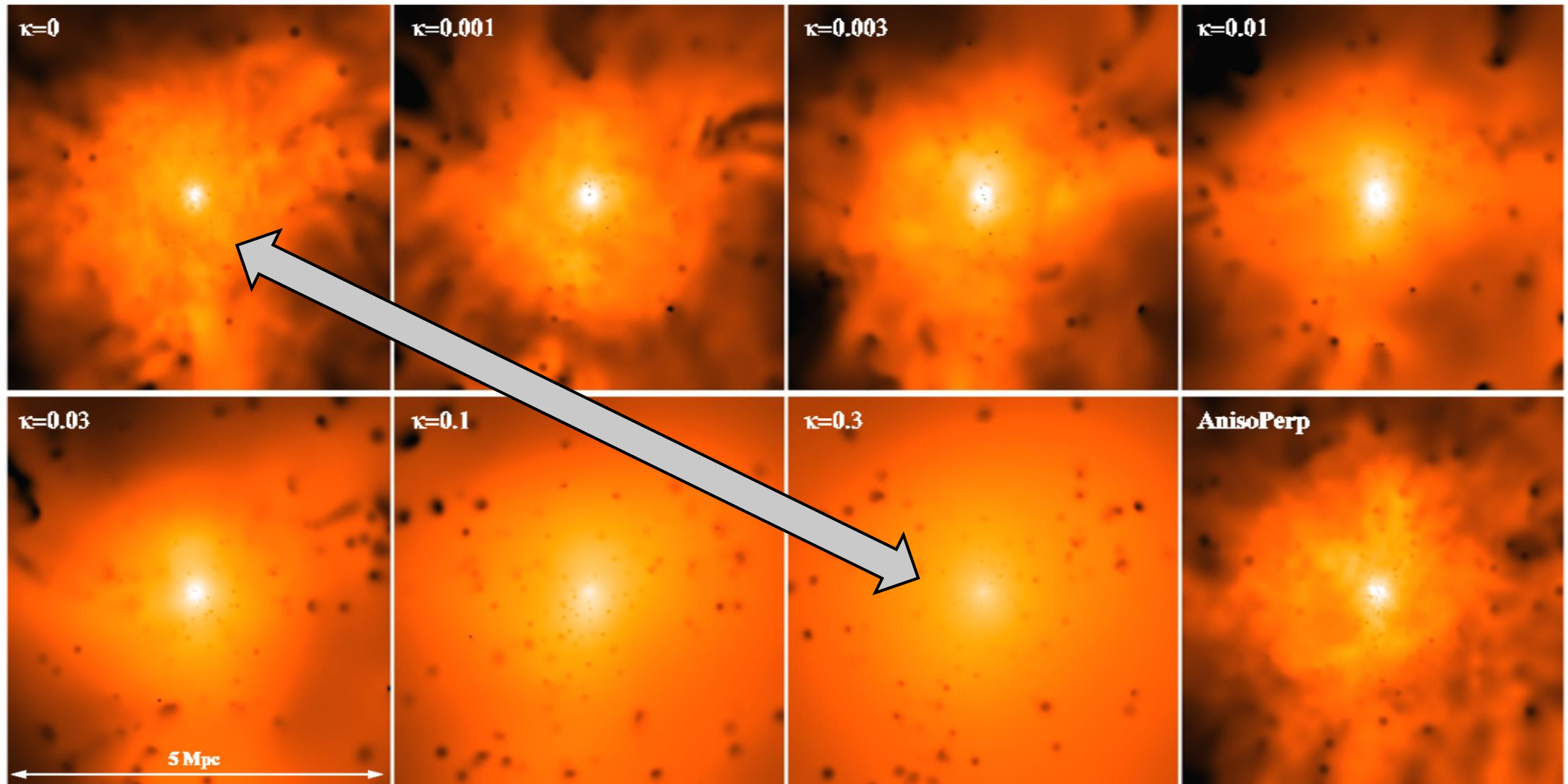


$$\kappa = 1.31 n_e \lambda_e k \left(\frac{k T_e}{m_e} \right)^{1/2}$$

$$\approx 4.6 \times 10^{13} \left(\frac{T_e}{10^8 \text{ K}} \right)^{5/2} \left(\frac{\ln \Lambda}{40} \right)^{-1} \text{ ergs s}^{-1} \text{ cm}^{-1} \text{ K}^{-1}.$$

Effect of heat transport

**ICM temperature maps for simulations
varying thermal conduction**



mach number

size of galaxies

Effect of viscosity

$$Re \approx 3M \left(\frac{l}{\lambda_i} \right)$$

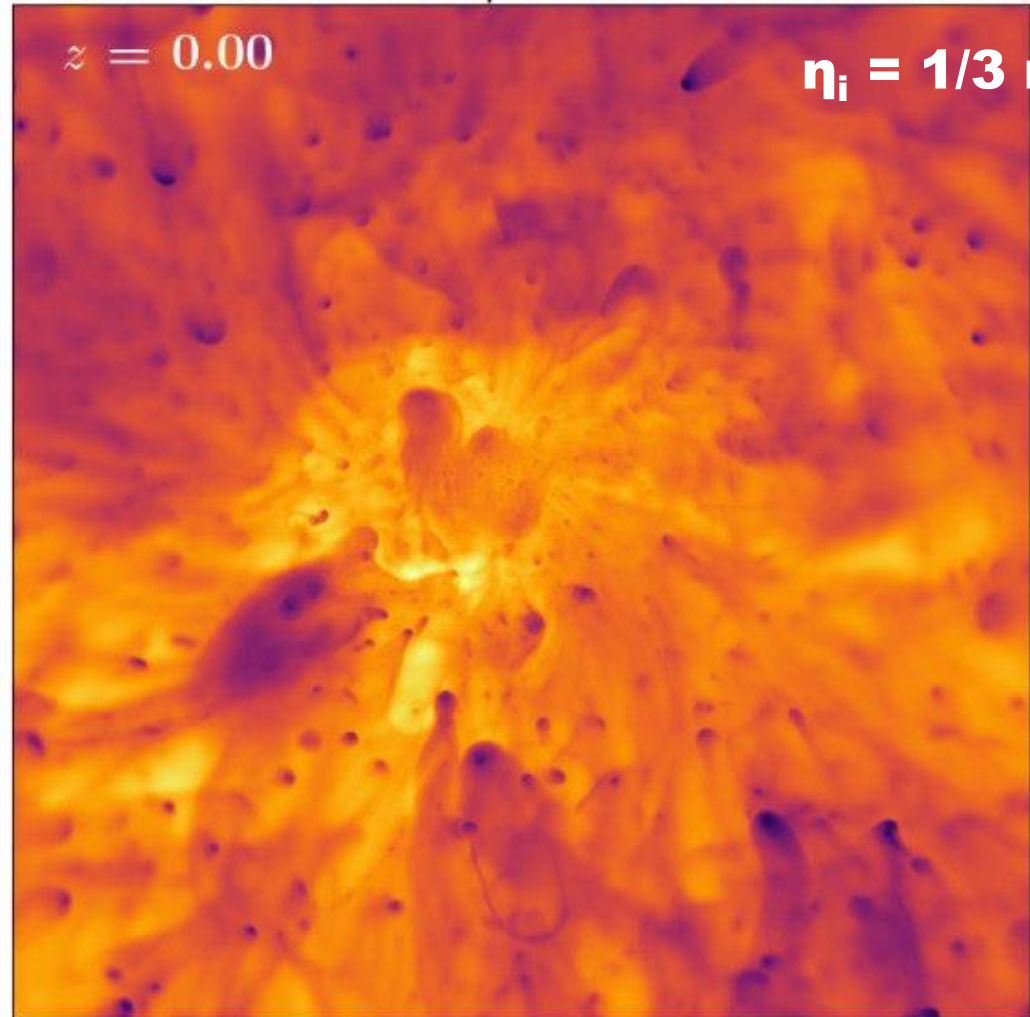
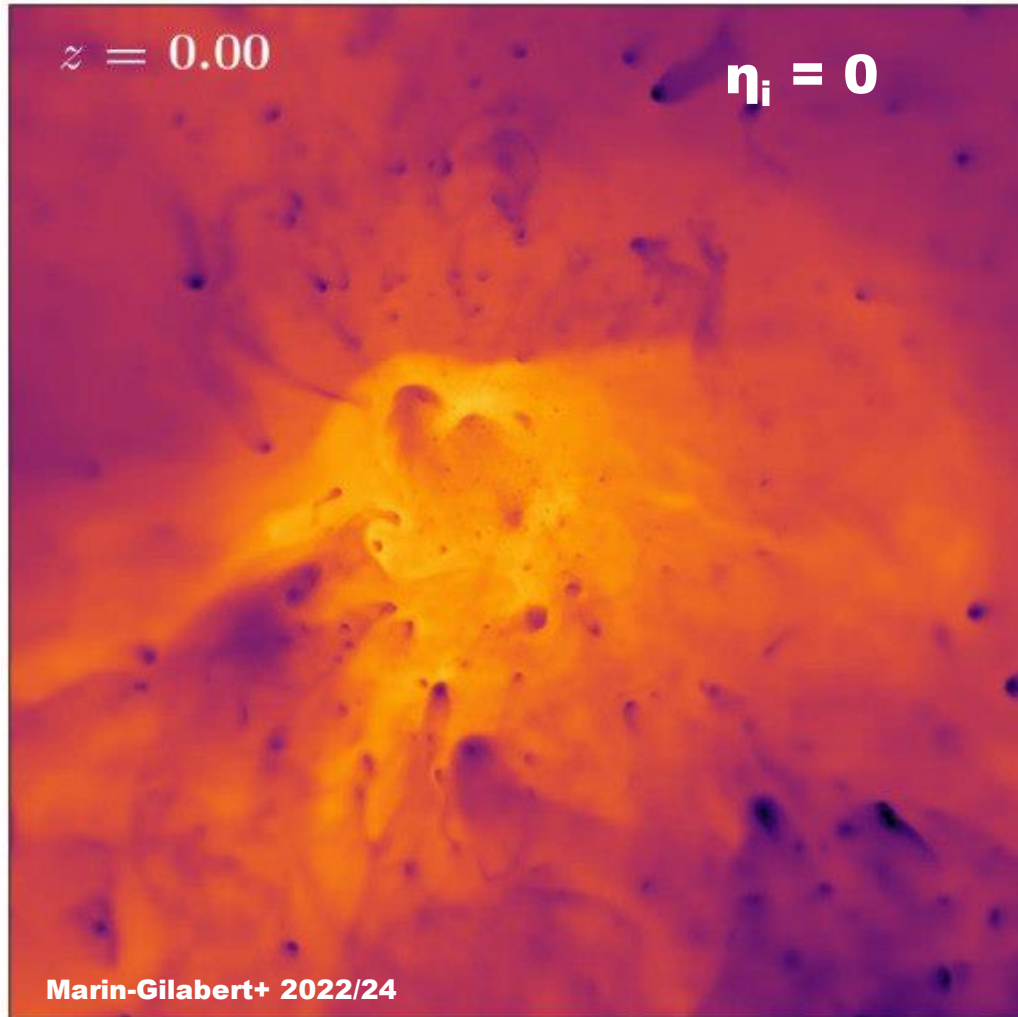
$$l \sim \lambda_i !!!$$

ion mean free path: $\lambda_e = \lambda_i \approx 23 \text{ kpc} \left(\frac{T_g}{10^8 \text{ K}} \right)^2 \left(\frac{n_e}{10^{-3} \text{ cm}^{-3}} \right)^{-1}$

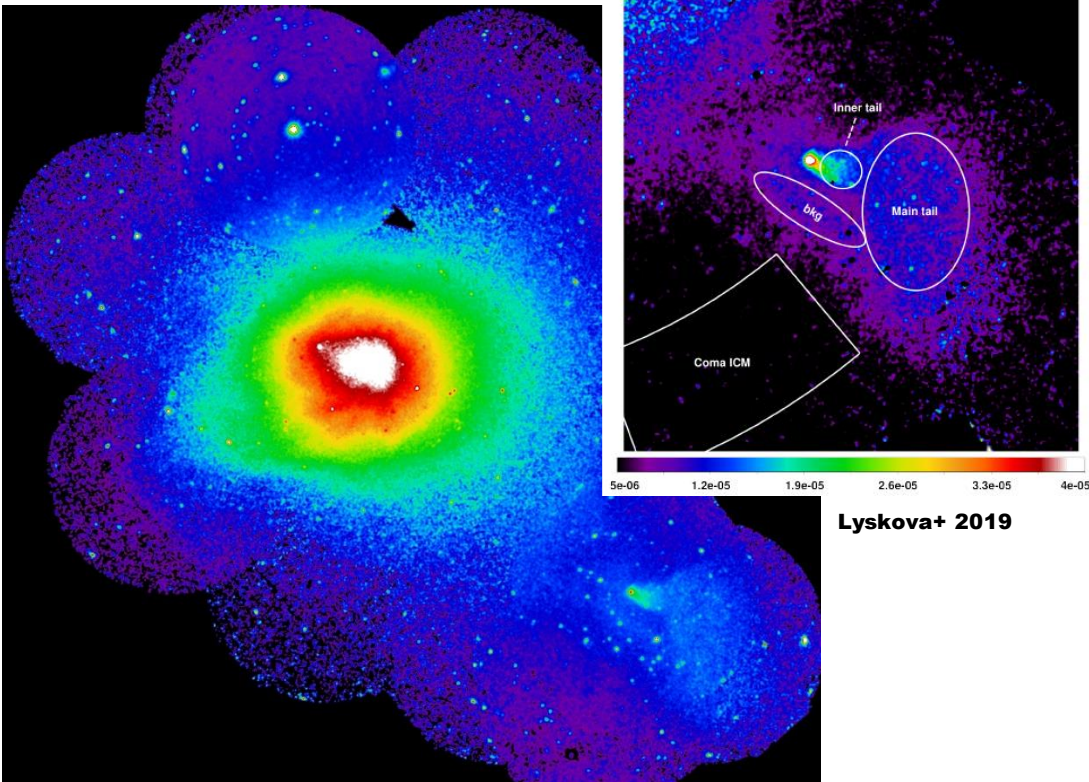
Ideal xz

ICM density maps for simulations
Without (left) and with (right) viscosity

$$\eta \approx \frac{1}{3} m_i n_i \langle v_i \rangle_{rms} \lambda_i$$
$$\approx 5500 \text{ gm cm}^{-1} \text{ s}^{-1} \left(\frac{T_e}{10^8 \text{ K}} \right)^{5/2} \left(\frac{\ln \Lambda}{40} \right)^{-1}$$

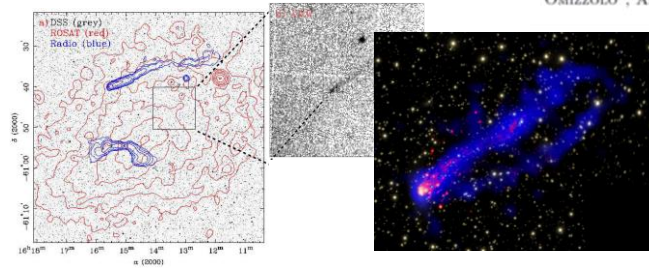


Interactions with the ICM (mixing, conduction, viscosity?)



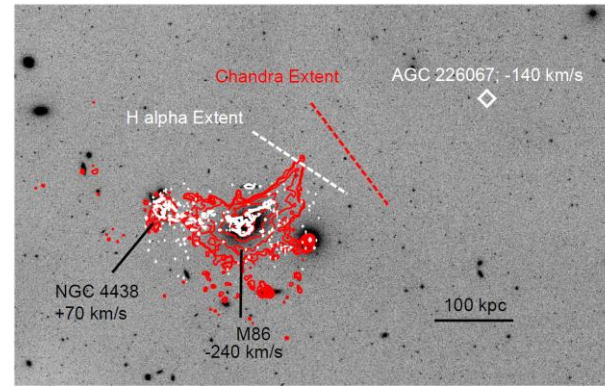
A 70 Kiloparsec X-Ray Tail in the Cluster A3627

Sun, M.; Jones, C.; Forman, W.; Nulsen, P. E. J.; Donahue, M.; Voit, G. M.



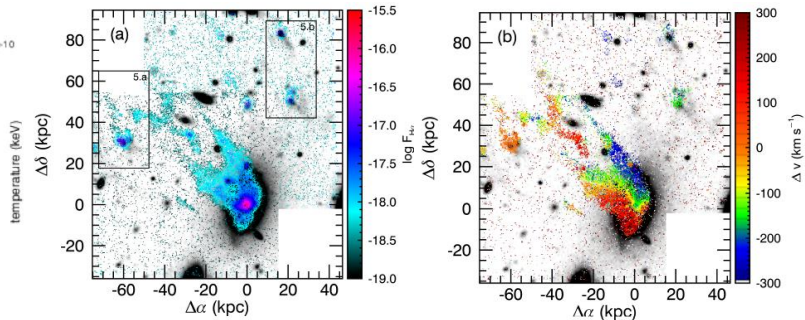
HUBBLE SPACE TELESCOPE IMAGING OF THE ULTRA-COMPACT HIGH VELOCITY CLOUD AGC 226067: A STRIPPED REMNANT IN THE VIRGO CLUSTER

D. J. SAND,¹ A. C. SETH,² D. CRNOJEVIĆ,¹ K. SPEKENS,² J. STRADER,² E. A. K. ADAMS,² N. CALDWELL,² P. GUHATHAKURTA,² J. KENNEY,² S. RANDALL,² J. D. SIMON,² E. TOLOBA,¹⁰ B. WILLMAN^{1,12}



DISCOVERY OF RAM PRESSURE STRIPPED GAS AROUND AN ELLIPTICAL GALAXY IN ABELL 2670

YUN-KYONG SHEEN,¹ RORY SMITH,² YARA JAFFÉ,³ MINJIN KIM,¹ SUKYOUNG K. YI,² PIERRE-ALAIN DUC,⁴ JULIE NANTAIS,⁵ GRAEME CANDLISH,⁶ RICARDO DEMARCO,⁷ AND EZEQUEL TREISTER⁸



GASP I: GAS STRIPPING PHENOMENA IN GALAXIES WITH MUSE

BIANCA M. POGGIANTI¹, ALESSIA MORETTI¹, MARCO GULLIEUSZIK¹, JACOPO FRITZ², YARA JAFFÉ³, DANIELA BETTONI¹, GIOVANNI FASANO¹, CALLUM BELLHOUSE^{4,3}, GEORGE HAU³, BENEDETTA VULCANI^{5,1}, ANDREA BIVIANO⁶, ALESSANDRO UMIZZOLO⁷, ANGELA PACCAGNELLA^{8,1}, MAURO D'ONOFRIO⁹, ANTONIO CAVA⁹, Y.-K. SHEEN¹⁰, WARRICK COUCH¹¹, MATT OWERS^{12,11}

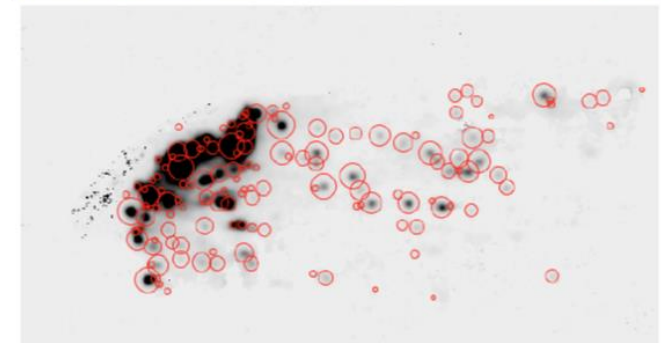
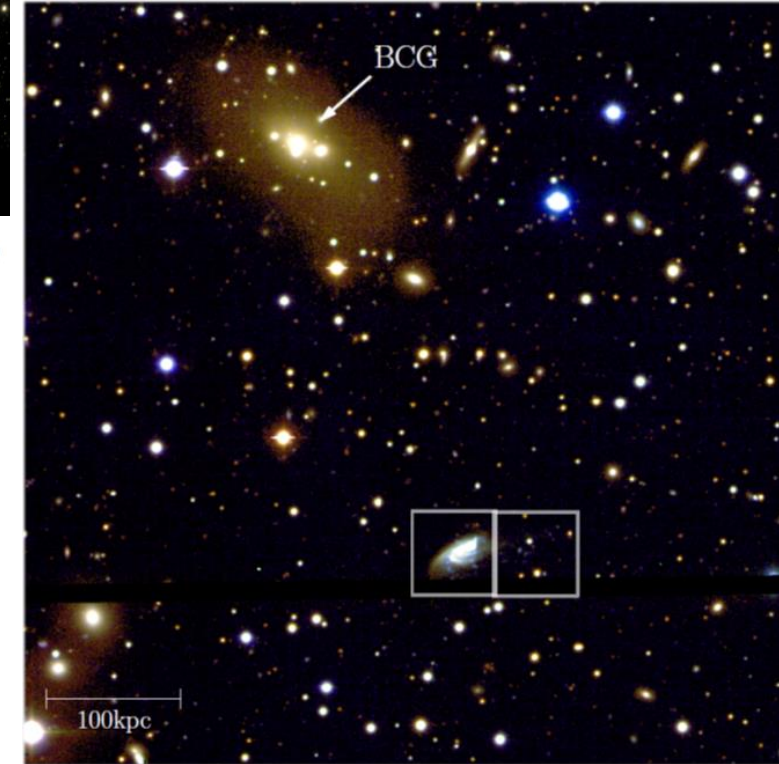


Figure 12. H α flux map (black) with H α knots as red circles.

HPC Challenges in Astrophysics

VIII) ML for extra physics

Cooling function nowadays has high dimensional parameter space

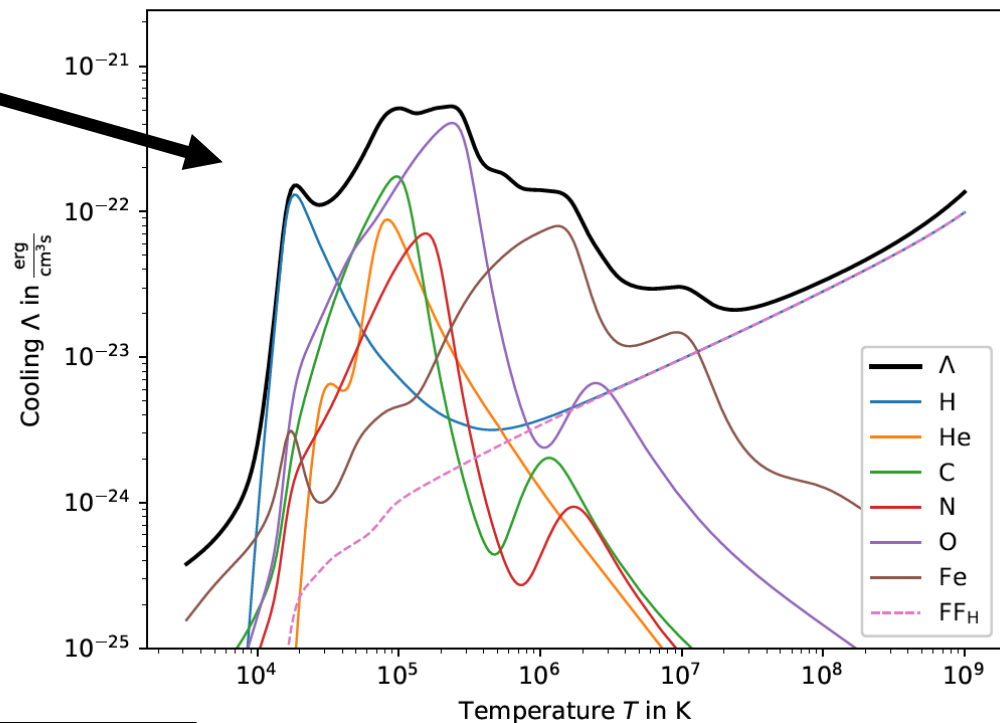
$$\frac{du}{dt} = -\frac{P}{\rho} \nabla \cdot \vec{v} + \underbrace{H - \Lambda}_{\text{tabulated}}$$

Spectral synthesis code \rightarrow tabulate

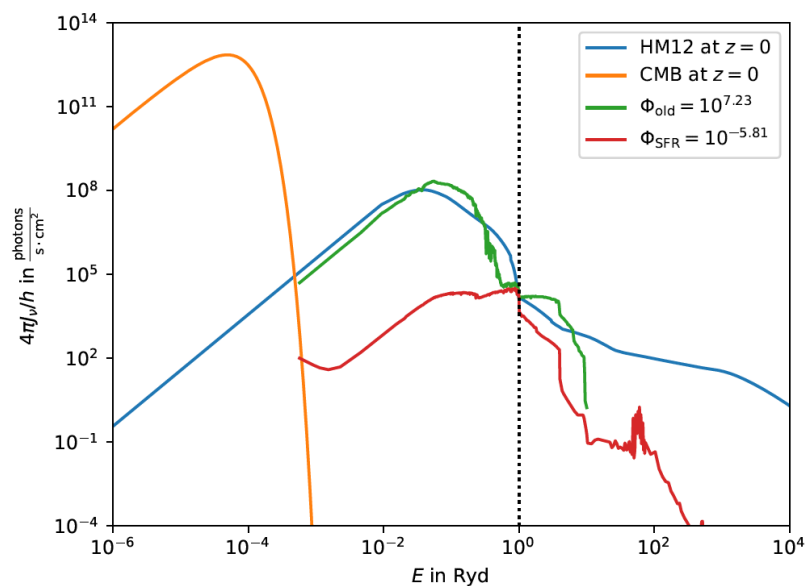
$$H(\Phi_{\text{UVB}}(z), n_{\text{H}}, T, \{Z\}, \{\Phi_{\text{local } 1}, \Phi_{\text{local } 2}, \dots\})$$

$$\Lambda(\Phi_{\text{UVB}}(z), n_{\text{H}}, T, \{Z\}, \{\Phi_{\text{local } 1}, \Phi_{\text{local } 2}, \dots\})$$

\rightarrow interpolate on-the-fly



- a) Direct computation (much too expensive)**
- b) Cartesian sampling (too much data)**



Cooling function nowadays has high dimensional parameter space

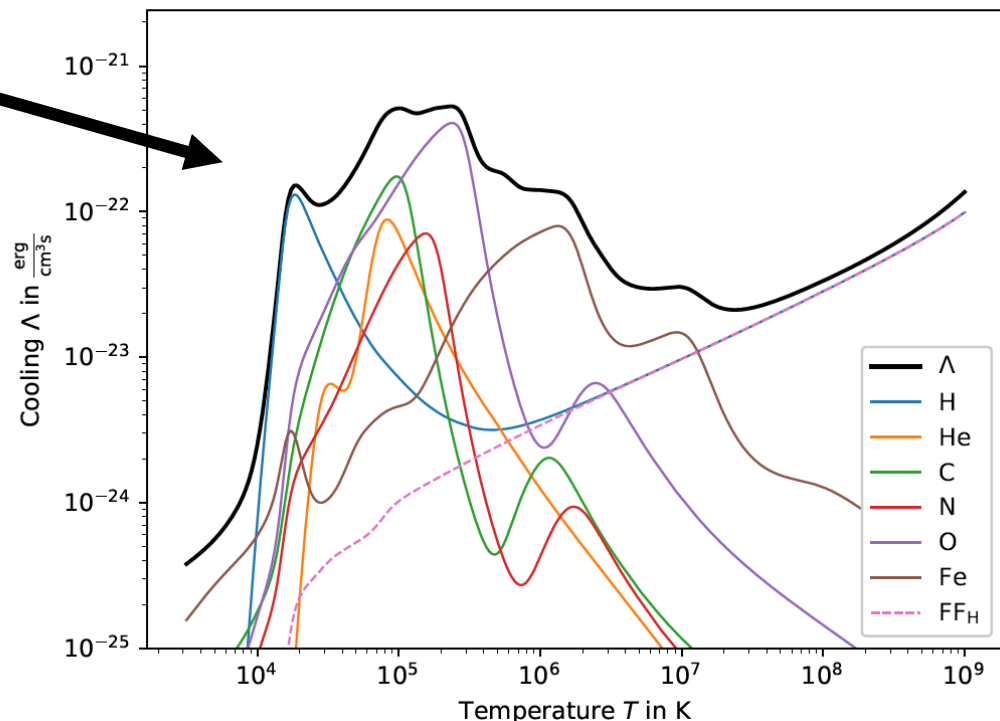
$$\frac{du}{dt} = -\frac{P}{\rho} \nabla \cdot \vec{v} + \underbrace{H - \Lambda}_{\text{cooling function}}$$

Spectral synthesis code → tabulate

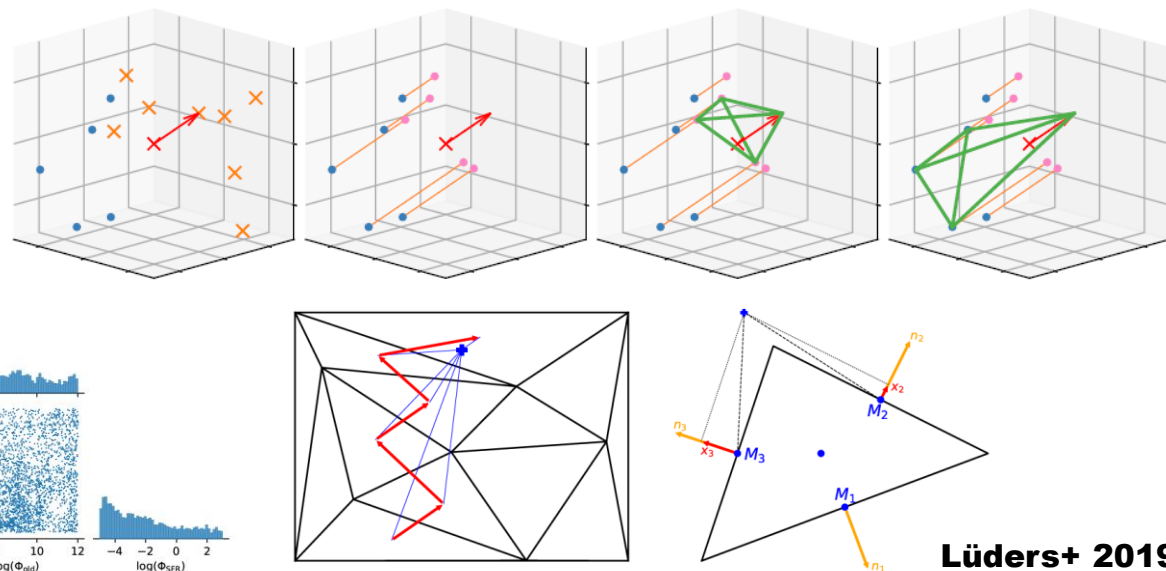
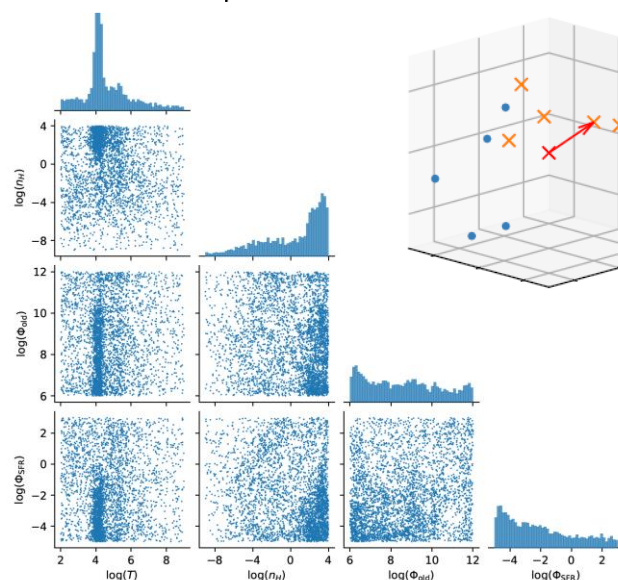
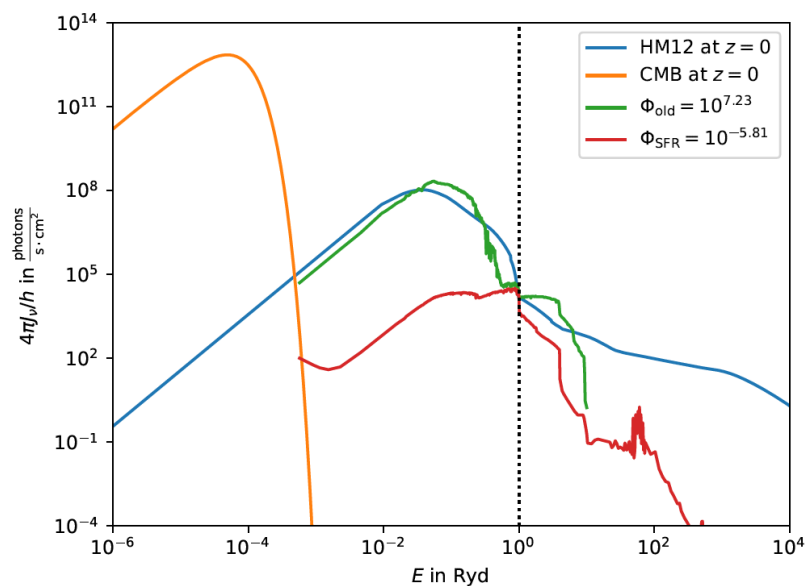
$$H(\Phi_{\text{UVB}}(z), n_{\text{H}}, T, \{Z\}, \{\Phi_{\text{local } 1}, \Phi_{\text{local } 2}, \dots\})$$

$$\Lambda(\Phi_{\text{UVB}}(z), n_{\text{H}}, T, \{Z\}, \{\Phi_{\text{local } 1}, \Phi_{\text{local } 2}, \dots\})$$

→ interpolate on-the-fly



- a) Direct computation (much too expensive)**
- b) Cartesian sampling (too much data)**
- c) Unstructured sampling (complex re-construction and interpolation)**



Cooling function nowadays has high dimensional parameter space

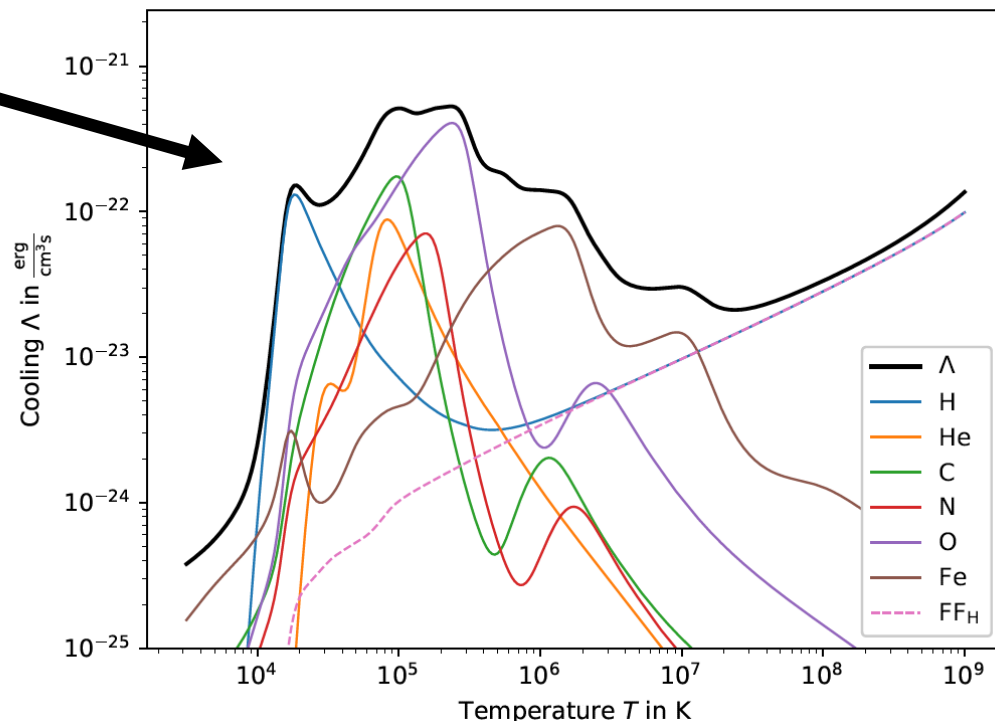
$$\frac{du}{dt} = -\frac{P}{\rho} \nabla \cdot \vec{v} + \underbrace{H - \Lambda}_{\text{Cooling function}}$$

Spectral synthesis code \rightarrow tabulate

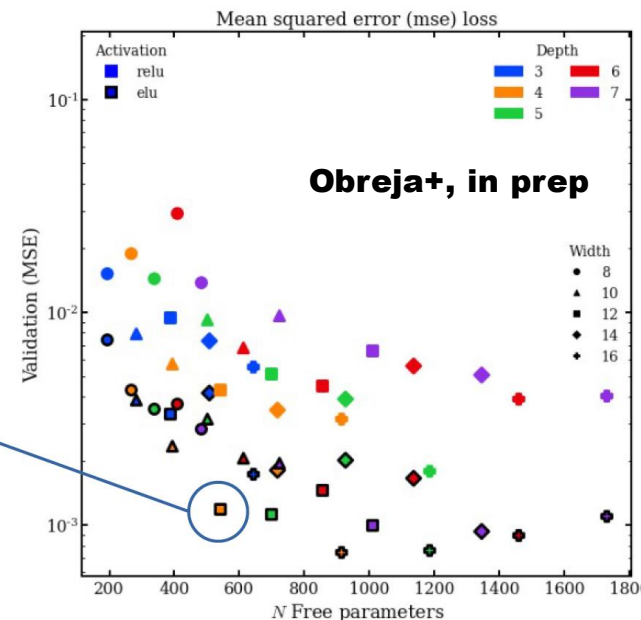
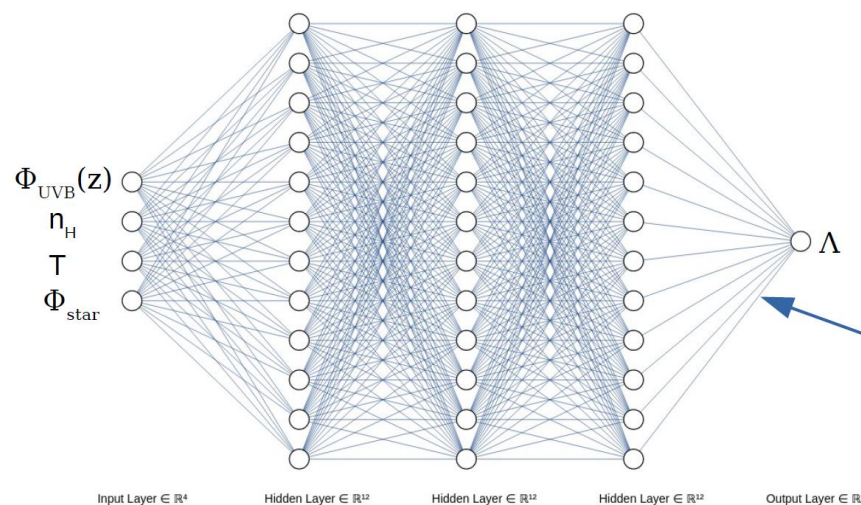
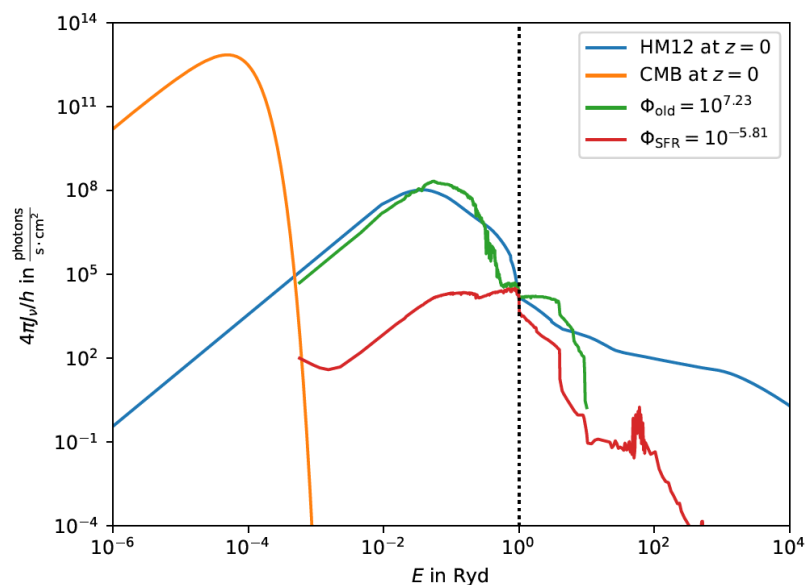
$$H(\Phi_{\text{UVB}}(z), n_{\text{H}}, T, \{Z\}, \{\Phi_{\text{local } 1}, \Phi_{\text{local } 2}, \dots\})$$

$$\Lambda(\Phi_{\text{UVB}}(z), n_{\text{H}}, T, \{Z\}, \{\Phi_{\text{local } 1}, \Phi_{\text{local } 2}, \dots\})$$

\rightarrow interpolate on-the-fly



- a) **Direct computation**
(much too expensive)
- b) **Cartesian sampling**
(too much data)
- c) **Unstructured sampling**
(complex re-construction and interpolation)
- d) **Machine learning**
(better precision, lower memory footprint)



HPC Challenges in Astrophysics

IX) Post-processing

Single simulation output 20TB → post processing has to be HPC ready

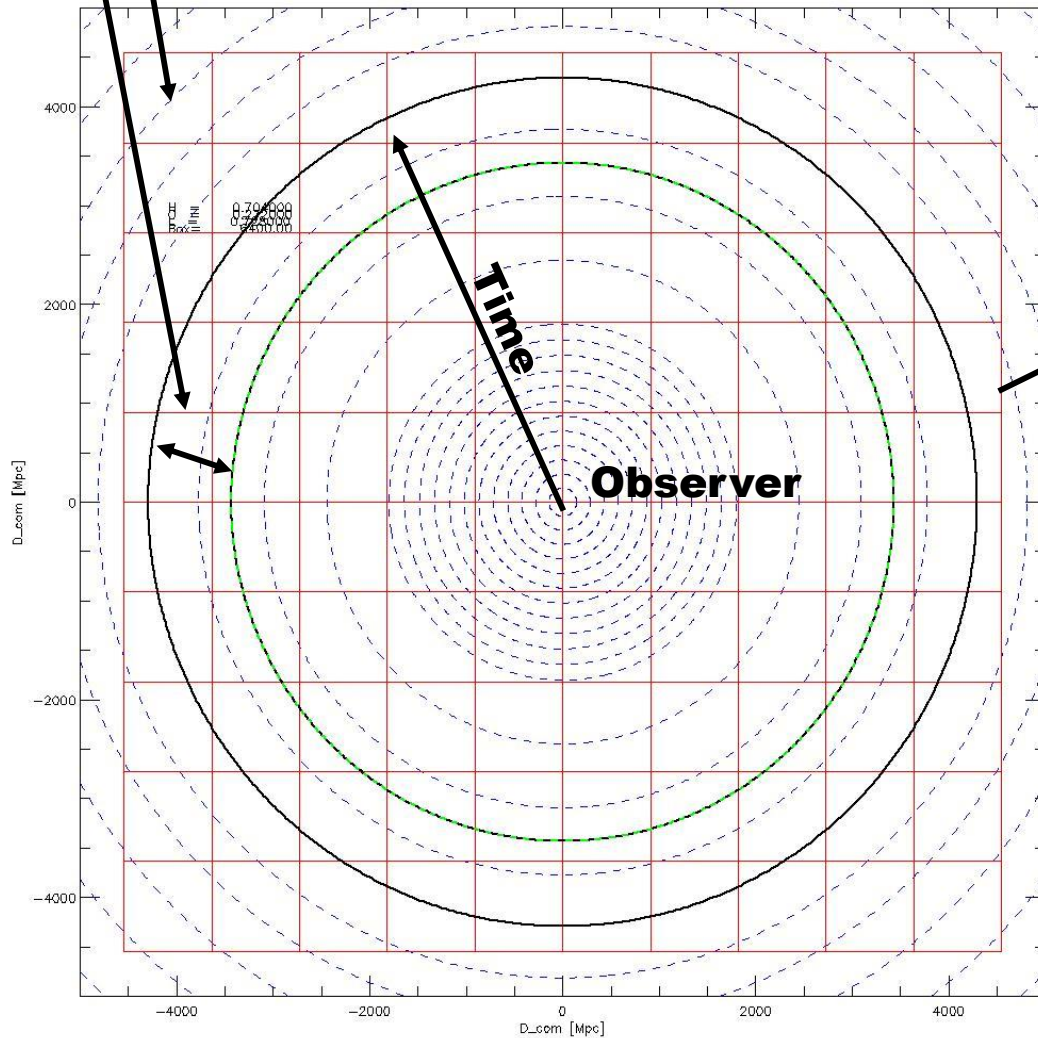
Shell $z = 1.2 - 1.44$

Box2b/hr (4.8TB per snapshot)

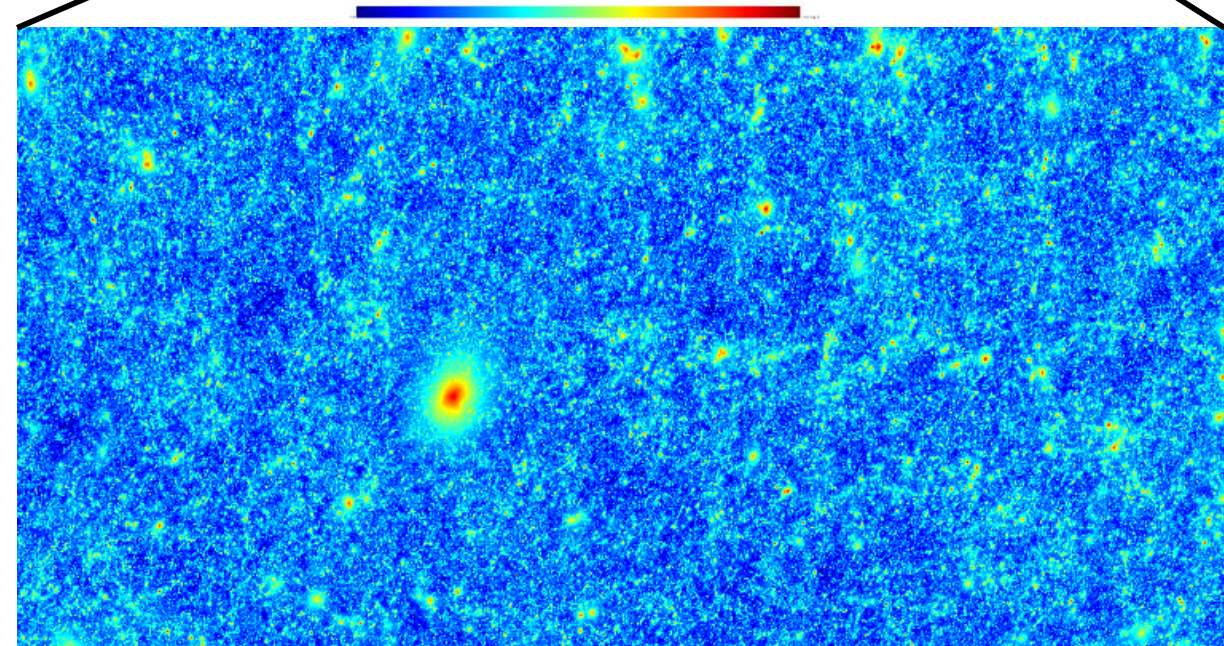
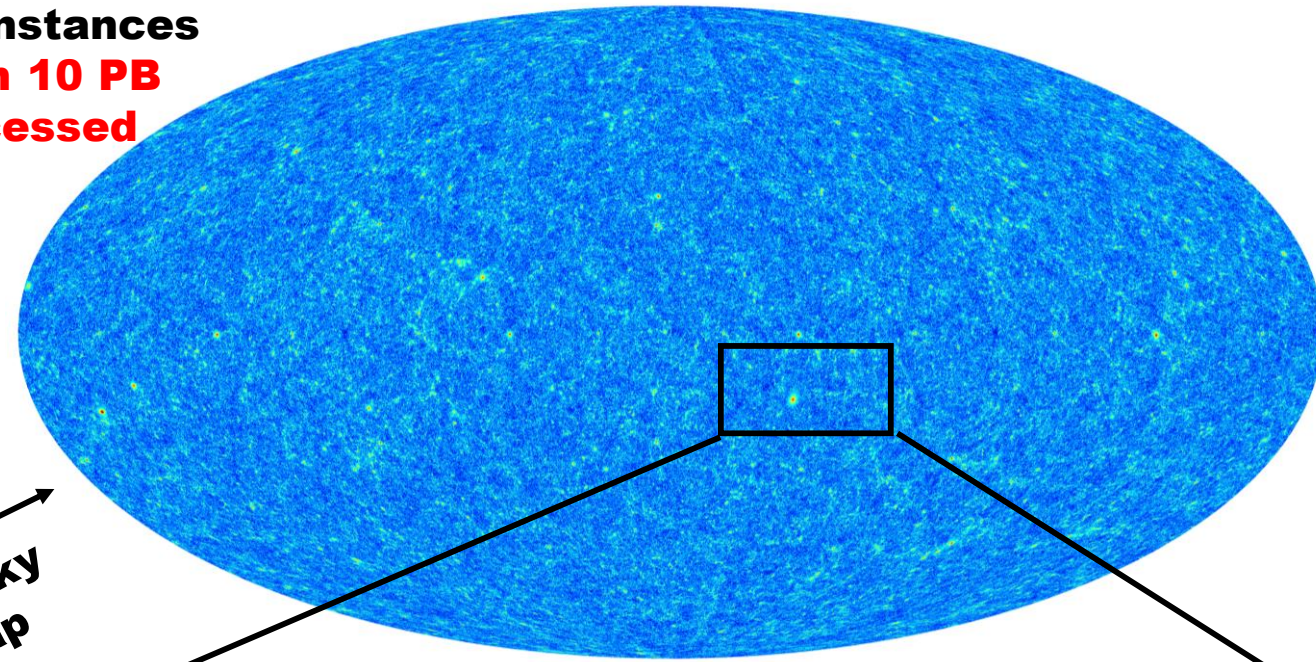
1000x replicated to fill full sky

Many time instances

→ **more than 10 PB**
of data processed



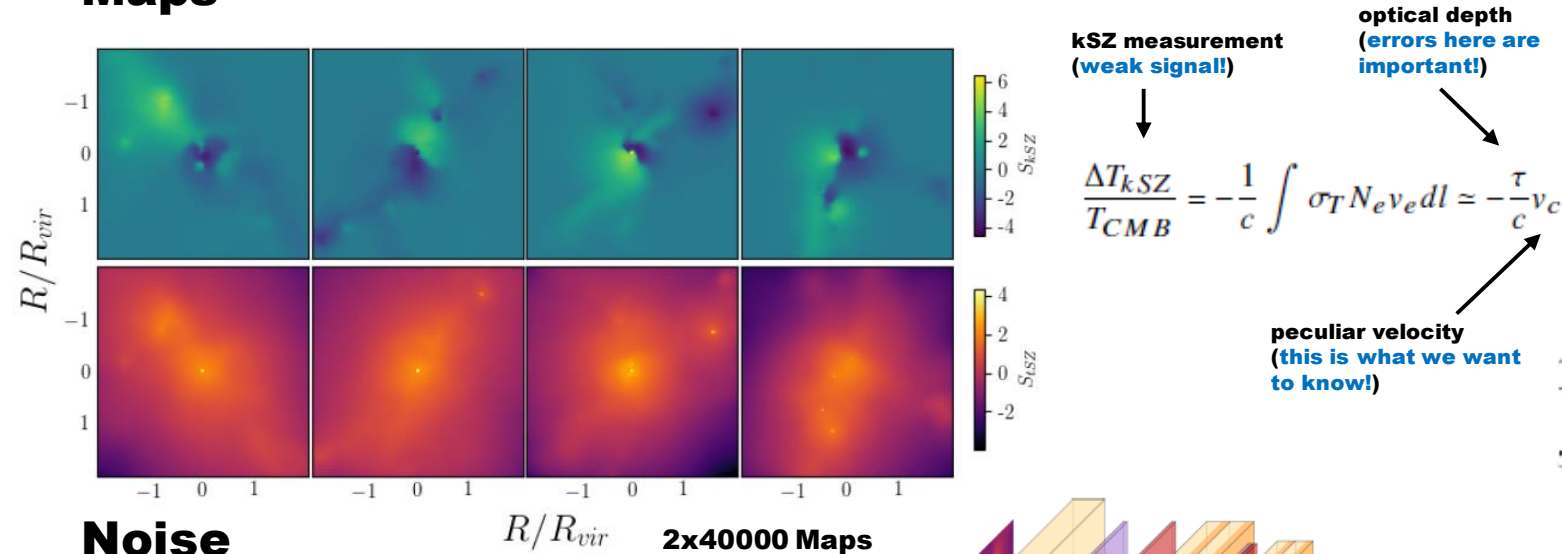
Full sky
map



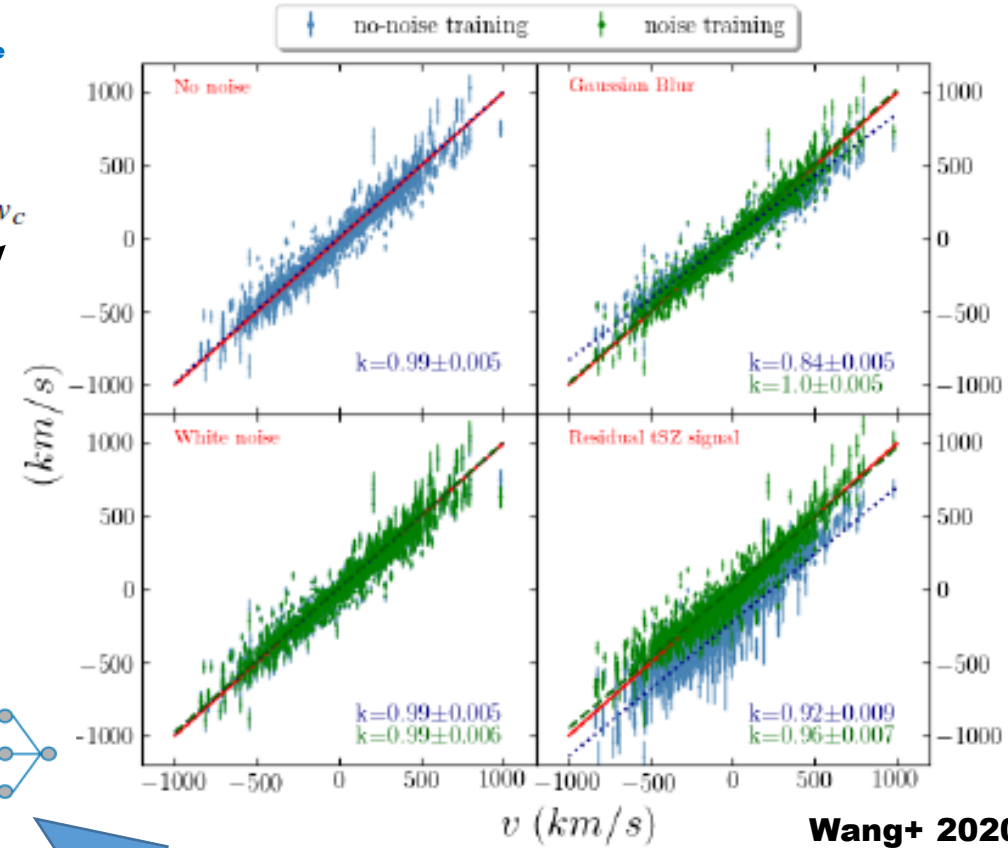
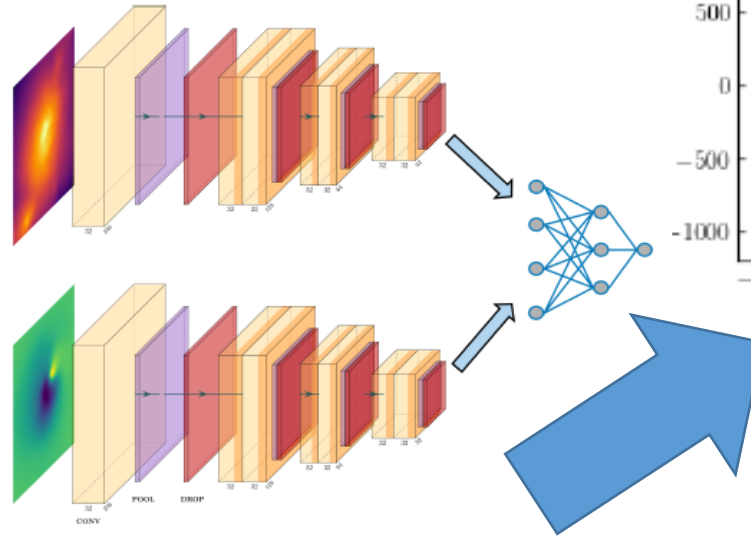
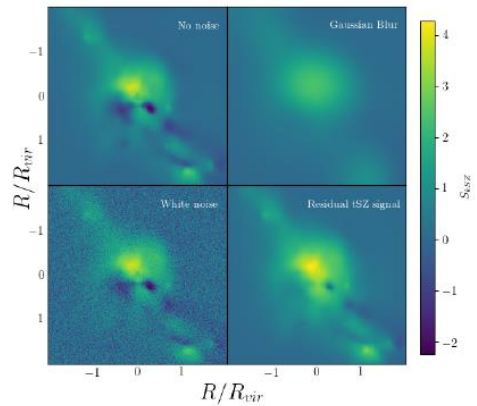
ML is often used to improve analysis of data.

Example: Using Deep Neural Networks

Maps



Noise

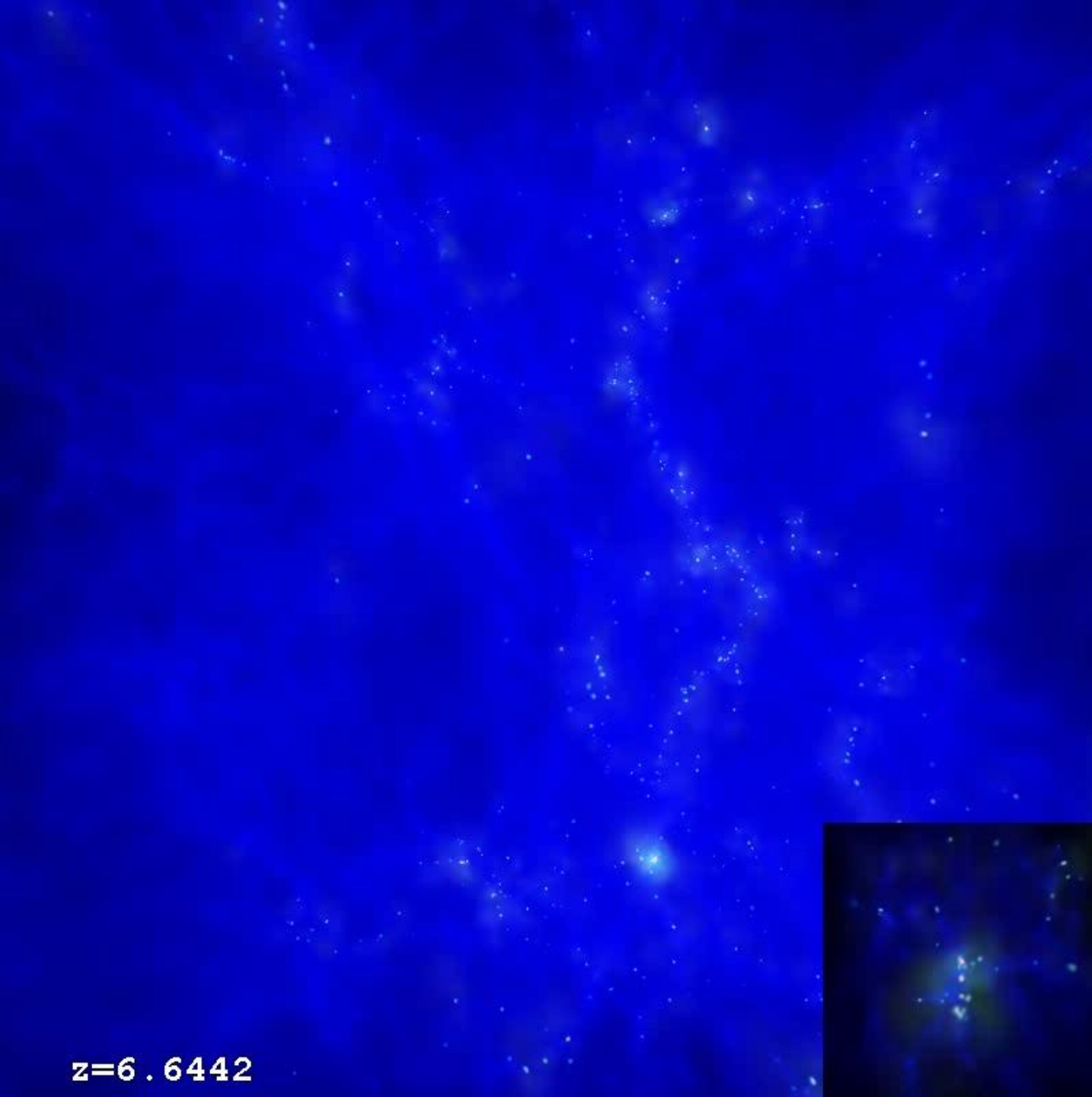


Wang+ 2020

Predicted v from kSZ Maps

**tSZ/kSZ maps
from Magneticum**

The true value of „v“ is deeply convolved in the combination of two observables, ML helps to extract it properly from mock observations.



$z=6.6442$

THE ASTROPHYSICAL JOURNAL

AN INTERNATIONAL REVIEW OF SPECTROSCOPY AND
ASTRONOMICAL PHYSICS

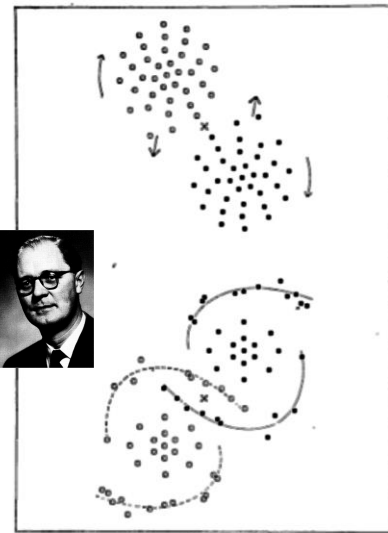
VOLUME 94

NOVEMBER 1941

NUMBER 3

ON THE CLUSTERING TENDENCIES AMONG THE NEBULAE II. A STUDY OF ENCOUNTERS BETWEEN LABORATORY MODELS OF STELLAR SYSTEMS BY A NEW INTEGRATION PROCEDURE

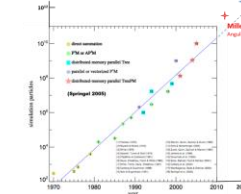
ERIK HOLMBERG



Z3, 1941-1943 (Germany)
5 Berechnungen pro Sekunde



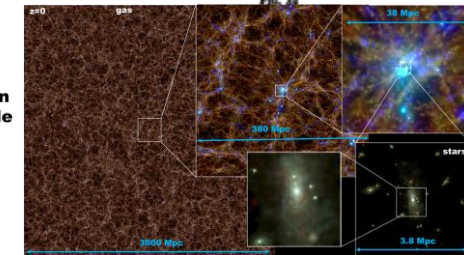
SuperMUC, 2013- (München)
3 Petaflops ($3 \cdot 10^{15}$ pro Sekunde)



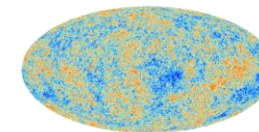
**Moore's Gesetz: Anzahl der Transistoren
(e.g. Berechnungen) verdoppelt sich alle
1.5 Jahre.**

Z3 - SuperMUC: 1.4 Jahre

N-Teilchen (1970-2010): 1.3 Jahre



The Computational Challenge



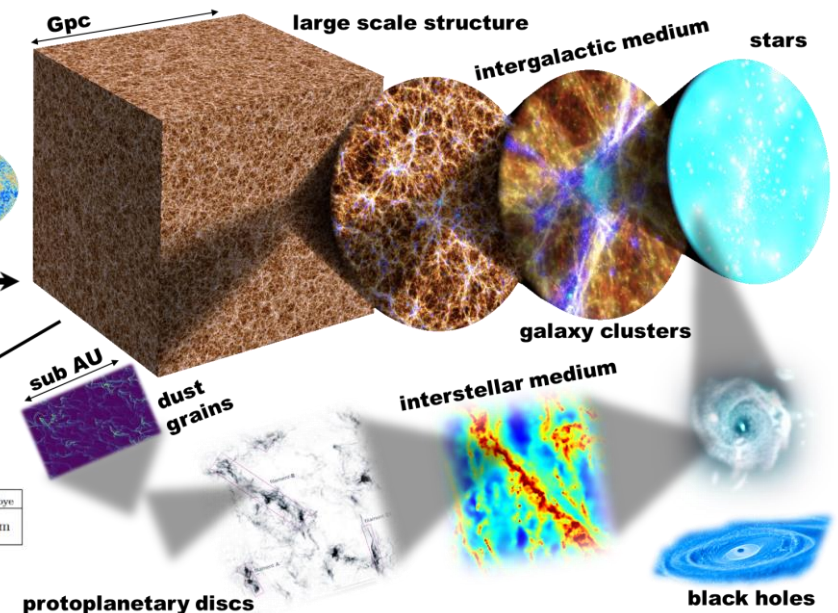
**multi-scale,
multi-physics**

$3 \cdot 10^{22}$ km



	λ_{mfp}	λ_{Lamor}	λ_{Debye}
electrons	1 kpc	700 km	29000 km
protons			6 km

Plasma Physics!



protoplanetary discs

black holes